COMPREHENSIVE ASSESSMENT OF A SOLAR-ASSISTED HEAT PUMP DRYER INTEGRATED WITH THERMAL ENERGY STORAGE MATERIALS: PERFORMANCE, TECHNO-ECONOMIC VIABILITY, AND LIFE CYCLE ANALYSIS

Aldé Belgard Tchicaya Loemba

A Dissertation Submitted in Partial Fulfillment of the Requirements for the Degree of Doctor of Philosophy in Material Sciences and Engineering of the Nelson Mandela African Institution of Science and Technology

Arusha, Tanzania

August, 2024

ABSTRACT

Appropriate drying methods are essential for preserving nutrients in agricultural products. In most developing countries, open sun drying is the traditional method for drying agricultural products. Nevertheless, there are several risks associated with this method for agricultural products, such as microbial contamination, deterioration of quality, and animal loss. Because drying parameters can be easily controlled and the quality of the dried products is preserved, heat pump drying has recently been found to be an effective drying technique for agricultural products. Heat pump dryers are currently used in conjunction with solar drying systems to improve drying and thermal performance. However, in developing countries, particularly Sub-Saharan Africa, these devices are still in their infancy. The few reported heat pump dryers in Africa are made from locally available materials to keep them affordable, but very little is known about their techno-economic analysis and life cycle assessment. In addition, more works need to be done to maximize this device's efficiency, because using solar-assisted heat pump dryers in non-sunny weather, or particularly at night, is difficult because solar is intermittent. This study therefore focused on designing, manufacturing, and investigating the performance, techno-economic viability, and life cycle analysis of a solar-assisted heat pump dryer integrated with thermal energy storage materials for drying agricultural products. Experiments were carried out to dry tomatoes, moringa *oleifera* leaves, and cavendish bananas. Along with proximate, mineral, and vitamin analyses, the study also included performance, techno-economic and life cycle analysis of the proposed dryer. Results showed that the proposed dryer is an effective method to preserve nutrients of the dried products. Furthermore, the developed dryer showed good efficiency and demonstrated a noticeable decrease in the moisture content of the agricultural products tested. The dryer's low energy consumption was proven by the coefficient of performance ranging from 2.54 to 3.69. Concurrently, the drying rate varied from 0.16 to 0.24%.min^{-1}. The average dryer efficiency ranges from 12.52 to 23.23%, and the highest dryer efficiency was 80.69%. The highest dryer efficiency that was attained is higher than the 72% that is typically documented in the literature. Furthermore, the results showed that the dried products contained significantly higher concentrations of proximate parameters and minerals than the fresh ones, as evidenced by a p-value less than 0.05. In addition, interesting economic indicators were found by the techno-economic analysis, with a 1.5-year payback period and a 65% return on investment. This demonstrates that the investment in the proposed dryer can

be recovered in a relatively short period of time. Results of the life cycle assessment revealed that the drying process using the proposed dryer has less environmental effects. These findings are consistent with previous research. Thus, the proposed solar-assisted heat pump dryer integrated with thermal energy storage system is a successful method to dry agricultural products. The findings highlight the significance of using thermal energy storage materials to improve both the efficiency and performance of solar-assisted heat pump dryers in agricultural product drying. Therefore, the proposed dryer is recommended for drying agricultural products.

DECLARATION

I, Aldé Belgard Tchicaya Loemba, hereby declare that no part of the content provided in this dissertation has been used to obtain any other institution's qualification.

Aldé Belgard Tchicaya Loemba		10-10-2024
Candidate name	**Signature**	**Date**

This dissertation has been developed and submitted with our approval as the university supervisors.

Prof. Thomas Kivevele		10-10-2024
Name of Supervisor 1	**Signature**	**Date**

Dr. Baraka Kichonge		10-10-2024
Name of Supervisor 1	**Signature**	**Date**

COPYRIGHT

CERTIFICATION

The undersigned certify that, they have read and found this dissertation titled, "Comprehensive Assessment Of A Solar-Assisted Heat Pump Dryer Integrated With Thermal Energy Storage Materials: Performance, Techno-Economic Viability, And Life Cycle Analysis" qualify for acceptance by the Nelson Mandela African Institution of Science and Technology (NM-AIST) , in partial fulfillment of the requirements for the degree of Doctor of Philosophy in Materials Science and Engineering of the Nelson Mandela African Institution of Science and Technology.

Prof. Thomas Kivevele		10-10-2024
Name of Supervisor 1	**Signature**	**Date**

Dr. Baraka Kichonge		10-10-2024
Name of Supervisor 1	**Signature**	**Date**

ACKNOWLEDGMENT

The completion of this thesis was made ossible by the guidance, mentorship, technical and material support of my supervisors, Prof. Thomas Kivevele of the Nelson Mandela African Institution of Science and Technology (NM-AIST), and Dr. Baraka Kichonge of the NM-AIST and Arusha Technical College (ATC).

I also received useful academic inputs from Dr. Mwemezi Rwiza, as well as students, staff and lecturers of the NM-AIST.

The work was made possible by funding from the Regional Scholarship and Innovation Fund (RSIF), which covered my research and study expenses as well as my stipend. Through competitively selected African universities partnered with international universities, RSIF provides African countries with a unique opportunity to train new PhD students in high-quality PhD programs in applied sciences, engineering, and technology at an affordable cost. RSIF fosters partnerships between universities and domestic and international firms to find solutions to local challenges, thereby going beyond doctoral training in order to systematically nurture research capacity. The RSIF is the flagship programme of the Partnership for Skills in Applied Sciences, Engineering and Technology (PASET), an Africa-led, World Bank-affiliated initiative.

I am also grateful for the funding provided by the RSIF project "Solar-assisted heat pump dryer with energy storage for drying biomaterials (SOHEADS)" with Grant reference no. RSIF/RA/001.

Finally, I thank all the staff of Arusha Technical College (ATC), especially Mr. Gelion Mgaya, mechanical workshop manager and lecturer in the Department of Mechanical Engineering, for contributing ideas to this work.

DEDICATION

I dedicate this work to my entire family.

TABLE OF CONTENTS

LIST OF TABLES

LIST OF FIGURES

LIST OF APPENDICES

LIST OF ABBREVIATIONS AND SYMBOLS

$	American dollars
%	Percentage
°C	Degree Celsius
Cond	Condenser
COP	Coefficient of performance
C_p	Specific heat
db	Dry basis
F	Final
H	Hour
I	Initial
kJ	Kilojoule
kW	Kilowatt
kWh	Kilowatt-hour
m	Meter
$\dot{m}$	Mass flow rate
MC	Moisture content
min	Minute
M_w	Mass of water removed
Q	Heating capacity
RH_a	Relative humidity of the ambient air
RH_{in}	Relative humidity at the drying chamber's inlet
RH_{out}	Relative humidity at the drying chamber's outlet
S	Surface
s	Second
SAHPD	Solar-assisted heat pump dryer
t	Time
T_a	Temperature of the ambient air
TES	Thermal energy storage
T_{in}	Drying chamber’s inlet temperature
T_{out}	Drying chamber’s outlet temperature
V	Velocity
W	Watt
wb	Wet basis
ρ	Density

CHAPTER ONE

INTRODUCTION

1.1 Background of the problem

The rise in food needs is a direct result of the demographic growth that has been seen in every nation on earth. So, providing fair access to food within families is one of the current challenges facing governments, especially in sub-Saharan Africa, in meeting the needs of the populace. For many countries, population well-being is more important than any other issue. Unfortunately, it is always difficult to meet all of the population's needs, even the most basic ones, due to obstacles such as a lack of financial resources and mismanagement. Despite having abundant natural resources, Sub-Saharan African countries are unable to use them to create wealth and combat poverty. Although many countries are still proposing solutions to enhance good governance and efficiently manage natural resources for development, these efforts are insignificant in terms of permanently resolving these significant issues.

Health, food, and energy needs are central to populations' basic needs (Rasskazova *et al.*, 2016). Among all of the needs mentioned, energy remains a significant issue because, in poor and developing countries, access to energy in general is sometimes regarded as a luxury that the average citizen cannot afford. This significantly impedes development and creates a terrible social divide. Furthermore, the majority of the energy used is derived from fossil resources, which will eventually deplete. For instance, energy is still considered a luxury in Africa since it is costly and not always available. Furthermore, there are sporadic issues with the energy supply. A number of nations are initiating efforts to promote alternative energy sources in order to tackle this ongoing issue. However, without the support of scientists, engineers, and technicians, government efforts will not be very effective. It is worth mentioning that numerous researchers have recently implemented various solutions in Africa that assist not only countries but also populations in improving their living conditions through the implementation of less expensive and more suited energy systems.

Several scientific studies show that Africa is interested in exploring new energy sources. As a result, we are seeing the development of multiple energy systems related to wind, biomass, and solar energy. However, there is still more work to be done in this area (Montaigne, 2019). Solar water heaters, dryers, lights, ovens, and many other devices are examples of these systems.

This present work is focused on heat pump dryers with the goal of contributing to the battle against agricultural product waste, which is prevalent in many African countries, particularly during post-harvest periods, where more than 40% is wasted. Heat pumps are efficient heating and cooling generation systems. They are normal refrigeration systems comprising a thermal expansion valve, condenser, evaporator and compressor (Goh *et al.*, 2011). Heat pump dryers have been studied extensively around the world for drying applications in which the heat rejected from the condenser is used to dry agricultural products such as fruits and vegetables. The majority of the studies in the open literature focused on improving the performance of these systems. Today, there are several types of heat pump dryers, but their main components are the same (Grassi, 2018). Drying fruits, vegetables, and herbal remedies with heat pump dryers is a useful approach (Fayose & Huan, 2016).

Heat pump dryers are currently being integrated with solar energy systems to improve their drying and thermal performance, giving rise to the term solar-assisted heat pump dryer. Solar-assisted heat pump dryers are easy-to-design devices for drying food using solar energy (Yahya, 2016). In the sub-Saharan region, it has been noted that a lot of work has been done in both the design, construction and performance of solar-assisted heat pump dryers, but much remains to be done to optimize the efficiency of this device, which is commonly reported in the literature to range between 5 and 72% (Badiei *et al.*, 2020; Loemba *et al.*, 2022).

Furthermore, heat pump dryers manufactured in Africa are constructed with locally available materials to reduce costs. However, their techno-economic analysis and life cycle evaluation are mostly unknown. Additionally, to improve the efficiency of a solar-assisted heat pump dryer, energy storage materials can be integrated to complement the intermittency of solar energy. The comparison of the performance of solar dryer integrated with sensible heat storage material, phase change material, without thermal storage and traditional shade drying has been done (Bhardwaj *et al.,* 2019). The results showed that the drying rate of the dryer with heat storage systems was almost double as compared to the one with no use of thermal storage medium and traditional shade drying. However, to the best of my knowledge, the performance of solar-assisted heat pump integrated with thermal energy storage system for drying agricultural products (fruits and vegetables) has not been reported yet in the open literature. Moreover, no studies have been found using soapstone as storage medium in heat pump dryers. Soapstone was selected in this study because it is a locally available material in Tanzania, and it has good performance in terms of thermal capacity, conductivity, and absorption, resulting

in good heat storage and transmission. Additionally, soapstone has good chemical stability at higher temperatures and mechanical strength (Kakoko *et al.*, 2023).

Therefore, this study proposes a solar-assisted heat pump dryer integrated with thermal energy storage materials (soapstone). Furthermore, the techno-economic analysis was conducted because the majority of the work on solar-assisted heat pump dryers developed so far in the sub-Sahara region does not address this issue (Daghigh *et al.*, 2010). The study also carried-out life cycle analysis of the developed dryer, which is an essential aspect that has been neglected in the majority of published research works on solar-assisted heat pump dryers. The study also examines the nutritional composition of agricultural products dried using the proposed dryer.

1.2 Statement of the problem

Heat pump dryers can dry agricultural products using the heat rejected by the condenser, allowing them to be stored for longer periods. In developed countries, these devices are becoming more advanced and popular. However, in developing countries, particularly Sub-Saharan Africa, these devices are still in their infancy. The few reported heat pump dryers in Africa are made from locally available materials to keep them affordable. However, very little is known about their techno-economic analysis and life cycle assessment. Conducting a comprehensive techno-economic and life cycle assessment is crucial to ensure the dryer is both cost-effective and environmentally friendly, even if it is made from locally available materials. Furthermore, the use of passive solar dryers, which are most common in Sub-Saharan Africa, is limited because drying with passive solar dryers requires sunlight. This issue could be solved by connecting a solar-assisted heat pump dryer to a thermal energy storage system. The system would be capable of operating in cloudy, evening, and nighttime conditions. As a result, soapstone was chosen as a thermal energy storage material in this study because it is readily available in Tanzania and has good heat storage and transmission properties. Furthermore, no research has been found in the literature on the integration of soapstone in a solar-assisted heat pump dryer.

1.3 Rationale of the study

Drying has long been used in every region of the globe to preserve food and medicinal plants. Drying is primarily understood to be the reduction of plant moisture content with the objective of inhibiting enzyme and microbiological activity and, as a result, extending shelf life

(Jayaraman *et al.*, 2020; Mothibe *et al.*, 2011). However, the presence of water in agricultural products is regarded as the most significant challenge to their preservation. Water is an important component that, through its moisture content, determines the physical and chemical properties of aromatic and medicinal plants. The water content of agricultural products like fruits, herbs, and vegetables can be reduced or removed using drying method to facilitate their preservation (Sagar *et al.*, 2010). These agricultural products can be then consumed out of season once they have been preserved because agricultural products are not typically available throughout the year in most countries. Drying as well reduces the weight and volume of agricultural products, which is advantageous for transportation and storage (Barbosa *et al.,* 2017).

Another important factor is that drying reduces postharvest losses, which are a major issue in many countries, particularly in Sub-Saharan Africa. In low- and middle-income countries, perishable horticultural crop post-harvest losses range from 38 to 80% (Balana *et al.*, 2022; Jarman *et al.*, 2023; Teferra, 2022). In order, to get high quality dried products, the drying method must be carefully selected. Tray dryers, open sun dryers, vacuum dryers, and microwave dryers are frequently used in Africa and other parts of the world to dry agricultural products (Rocha *et al.*, 2011). The main concern is that, these drying methods do not effectively retain phytochemical qualities, nutritional value, or color of the dried product. Another alternative method is heat pump drying, which controls the drying process and help in preserving phytochemicals, nutrients, and color properties. Heat pumps are normal refrigeration systems comprising a thermal expansion valve, condenser, evaporator, and compressor (Fan *et al.,* 2021; Goh *et al.,* 2011; Jabari *et al.,* 2018). Heat pumps are currently used in conjunction with solar drying systems to improve drying and thermal performance. It has been reported that some works have been done in the sub-Saharan region on solar-assisted heat pump dryer. However, additional works need to be done to maximize this device's efficiency, because using solar-assisted heat pump dryers in non-sunny weather, or particularly at night, is impossible because solar is intermittent (Loemba *et al.*, 2022; Yahya *et al.*, 2018; Muhammad *et al.*, 2016). In this regard, this study therefore aimed to propose a new solar-assisted heat pump dryer integrated with an energy storage system using soapstone as storage material.

1.4 Research objectives

1.4.1 General objectives

The main objective of this study was to comprehensively assess the performance, techno-economic viability, and life cycle analysis of a solar-assisted heat pump dryer integrated with thermal energy storage materials for drying agricultural products

1.4.2 Specific objectives

The specific objectives of this work were:

(i) To manufacture and test a solar-assisted heat pump dryer integrated with thermal energy storage system.

(ii) To carry out thermodynamic analysis of the developed dryer (system performance) and evaluate the factors affecting the energy efficiency for system optimization.

(iii) To assess the quality of dried products (fruits and vegetables).

(iv) To conduct a techno-economic and a life cycle analysis of the developed dryer.

1.5 Research questions

The research questions of the study were:

(i) What are the most important design factors to consider for drying agricultural products with this novel solar-assisted heat pump dryer integrated with thermal energy storage to maximize moisture reduction?

(ii) Does the solar-assisted heat pump dryer integrated with thermal energy storage system meet users' expectations in terms of technical performance?

(iii) What is the effect of using the solar-assisted heat pump dryer integrated with an energy storage system on the drying performance and nutritional content of the dried products?

(iv) What is the economic feasibility and environmental impact of the solar-assisted heat pump dryer integrated with thermal energy storage system?

1.6 Significance of the study

The study's findings offer valuable information for designing and manufacturing a solar-assisted heat pump dryer which incorporates thermal energy storage with soapstone as the storage material. The results promote the use of readily available, locally sourced materials, which are more affordable for the manufacture of heat pump dryers. Evaluating the thermal performance of the proposed dryer could lead to a better understanding of its operation and inspire research into alternative thermal energy storage options to improve heat pump dryer efficiency. The proposed dryer may be attractive to investors due to the life cycle assessment results and positive economic analysis indicators like the short payback period and high return on investment. As a whole, the results could act as a useful guide and encourage users to dry agricultural products with the recommended dryer.

1.7 Delineation of the study

The goal of this study was to design, manufacture and experimental investigate a novel solar-assisted heat pump dryer integrated with thermal energy storage utilizing soapstone as storage material. Furthermore, this study evaluated the thermal performance of the proposed dryer, and conducted a techno-economic and life cycle analysis. In addition, the study provided insights into the changes in nutrient composition that occur during the drying process.

CHAPTER TWO

LITERATURE STUDY

2.1 Advancements in heat pump dryers

Several research have demonstrated the usefulness of heat pump dryers for drying food and the importance of choosing drying as an optimal food preservation method (Budžaki *et al.*, 2019; Mahiuddin *et al.*, 2018; Menon *et. al.,* 2020; Tuncer *et al.*, 2019). Heat pumps continue to be a major focus of research on the drying of agricultural products, this is why new heat pump dryer technologies are constantly being developed. The use of heat pump dryers for drying is becoming more widespread throughout the world (Hnin *et al.*, 2018; Qu *et al.*, 2021).

When it comes to achieving their needs for drying fruits, consumers faces challenges that heat pump dryer technologies help to address.

The performance of heat pump dryers varies based on technology and, occasionally, weather conditions. Several parameters can be used to evaluate the effectiveness of these various heat pump dryer technologies. These parameters can be divided into two categories. The moisture content, the velocity, and the drying time are the three main kinetic parameters that we consider first. Conversely, the energy parameters comprise the primary parameters like the coefficient of performance and the specific moisture extraction rate (Taşeri *et al.*, 2018).

The three most recent heat pump dryer types that have been studied are hybrid, ground source, and air source.

2.1.1 Air source heat pump dryer

The air heat pump dryer is better than many other drying techniques since it uses less energy and costs less money. A number of new air source heat pump dryer designs have recently appeared in a number of publications. The efficiency of air source heat pump dryers for drying agricultural products is increased by all of these creative designs, and the system yields satisfactory results regardless of the dried product (Budžaki *et al.*, 2019).

An air source heat pump dryer was suggested to dry garlic (Liu *et al.*, 2018). The results show that during the summer, open type heat pump dryers' specific moisture extraction rate increased and their moisture extraction rate decreased due to the high ambient air temperature and

humidity. Throughout the winter, however, the low ambient temperature and humidity increased the rate of moisture extraction while reducing the specific rate of moisture extraction. The closed type heat pump dryer's maximum specific moisture extraction rate was achieved when the bypass air rate attained 0.4. The rate of moisture extraction reduced as the bypass air rate rose. Another study by Shen *et al.* (2017) proposed an air source heat pump dryer incorporating cascade and single modes for drying. The study's findings showed that the single mode's coefficient of performance was greater. An enclosed fixed-frequency air source heat pump dryer was proposed by Liu *et al.* (2017). The results showed that altering air flow ratios through an air bypass duct enhanced system performance.

A small heat pump dryer was fabricated by Singh *et al.* (2020b). In the present investigation, different agricultural products were dried. The system operated in two different drying modes: closed and open modes. The results showed that the total energy consumption for potato chips was 3.564 and 3.51 kWh, and for banana it was 3.3 and 2.41 kWh in the open and closed systems. While the open mode showed a higher coefficient of performance, the closed mode had a higher specific moisture extraction rate. Furthermore, the closed mode exhibited the highest total energy destruction for the drying process of bananas and potato. Figure 1 displays the air source heat pump dryer's schematic diagram.

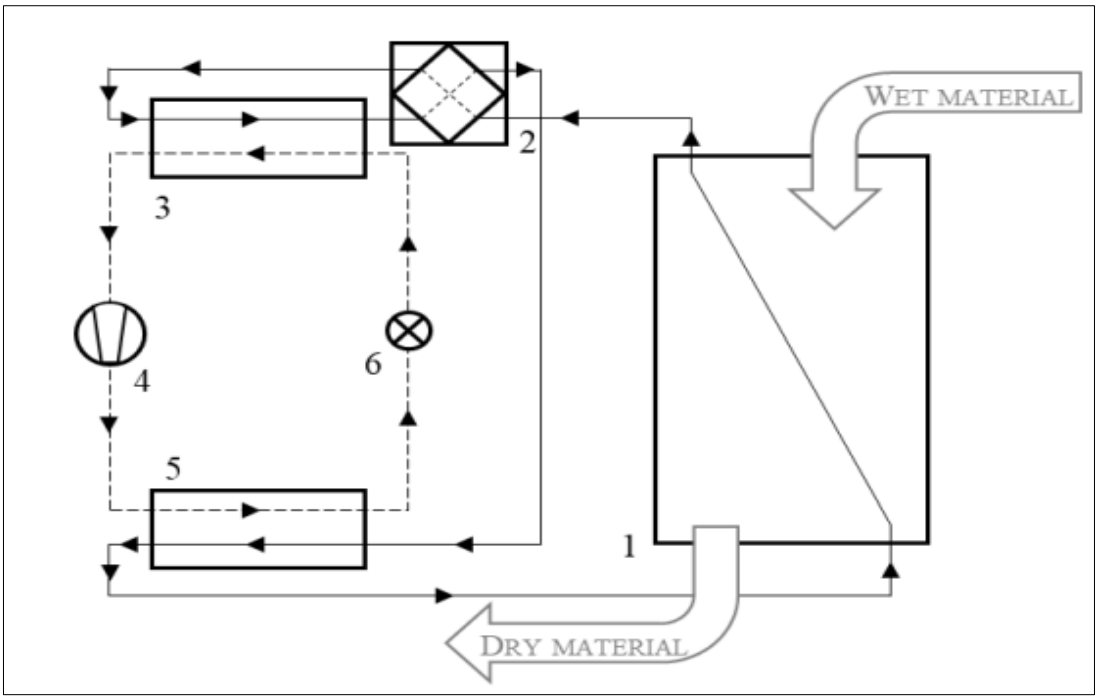

1 drying chamber, 2 heat recovery unit, 3 evaporator, 4 compressor, 5 condenser, 6 expansion

Figure 1: Air source heat pump dryer's schematic diagram (Budžaki *et al.*, 2019)

2.1.2 Ground source heat pump dryer

Even though ground source heat pump dryers are among the most effective kinds of heat pump dryers, they have not received much attention in food drying applications.

A ground source heat pump dryer was designed by Wu *et al.* (2021). The findings showed that when the drying temperature was between 40 and 60 °C, the coefficient of performance varied from 3.2 to 5.2. Furthermore, for ambient temperatures of 20 °C, the highest and lowest specific moisture extraction rates were 4.4 and 1.4, respectively, and for ambient temperatures of -10 °C, the highest and lowest specific moisture extraction rates were 2.6 and 1.1, respectively. Figure 2 shows the ground source heat pump dryer's schematic diagram.

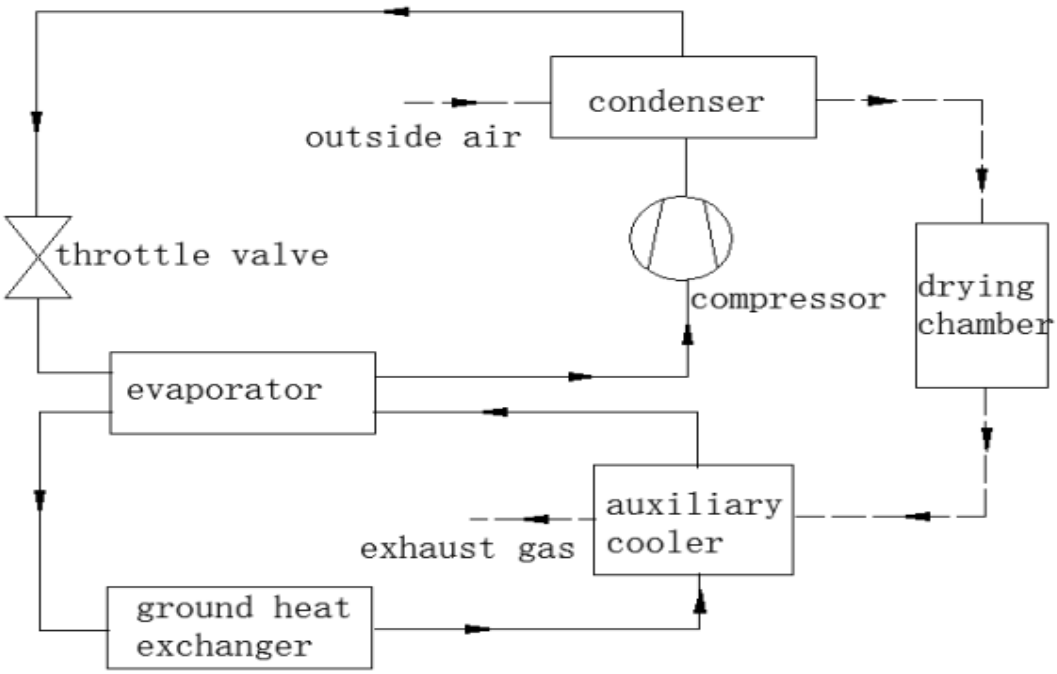

Figure 2: Ground source heat pump dryer's schematic diagram (Wu *et al.*, 2021)

2.1.3 Hybrid heat pump dryer

Recent investigations on hybrid heat pump dryers have focused on the use of heat pumps in conjunction with solar energy to assist in the drying process. Consequently, there has been a lot of interest in solar-infrared and solar-assisted heat pump dryer technologies. However, other technologies are not excluded either, as multiple studies have demonstrated the effectiveness of combining waste heat recovery, photovoltaic, Coulomb force, radiofrequency, ultrasound, and radiofrequency with heat pumps. Figure 3 illustrates the different types of hybrid heat pump dryers that are examined in this section. More in-depth research and examples of effective implementation are also provided in this section.

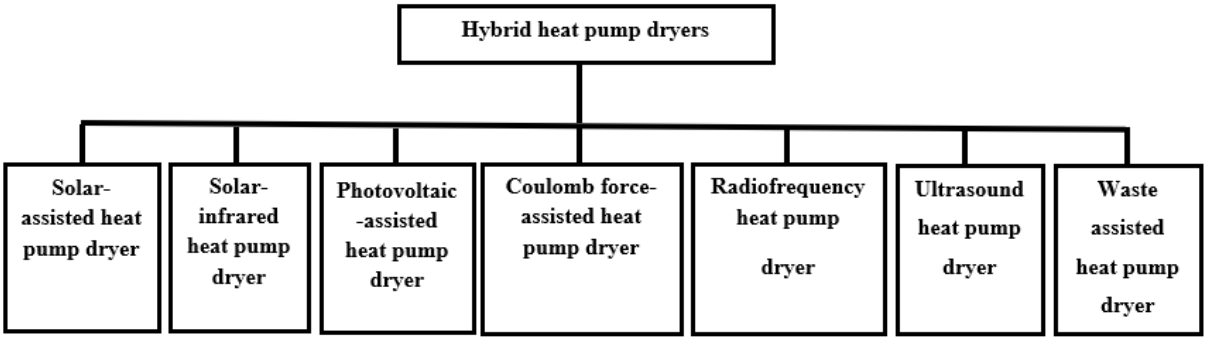

Figure 3: Hybrid heat pump dryers

(i) Solar-assisted heat pump dryer

The effectiveness of solar-assisted heat pump dryers for drying agricultural products has been demonstrated by multiple studies worldwide, leading to an increasing interest in these dryers. It has been discovered that solar-assisted heat pump dryers are efficient in cutting down on drying time and energy usage. A solar-assisted heat pump dryer was proposed by Xu *et al.* (2021) for drying mushroom. The findings showed that the proposed dryer worked effectively. Moreover, the rate of energy savings may rise to 37.96%. Solar-assisted heat pump drying was recommended to dry pumpkins (Dai & Deng, 2021). Compared to a conventional heat pump dryer, the suggested dryer showed good results in reducing energy consumption and drying time by 40%. A solar-assisted heat pump dryer was also developed by Hu *et al.* (2020) for drying wolfberry. It was discovered that the power usage was lower compared to a heat pump dryer used alone. Moreover, the power usage during the summer drying process was 9.1 kWh lower than that of the autumn drying procedure. A solar dryer with an expansion heat pump system was designed by Hao *et al.* (2021). Lemon was employed as a drying material. The findings showed that following seven hours of drying, the moisture content curve seemed to be constant. On the other hand, the system's precise moisture extraction ratio was 0.85 kg/kWh. Furthermore, the drying chamber's temperature and the coefficient of performance were significantly impacted by the intensity of solar radiation. To dry misai kucing leaves, a solar-assisted heat pump drying system was used by (Gan *et al.*, 2017). When compared to the conventional solar dryer, the system showed a four-hour reduction in drying time.

Solar-assisted heat pump dryers are also effective when paired with a thermal recovery unit or storage system. In Ismaeel and Yumrutas (2020), the efficiency of an underground storage system, a solar heat pump drying system, and a heat recovery system was studied by the authors. By comparison with non-heat recovery systems, an annual energy savings of 21% was

found. Finally, to dry mango, a solar-assisted heat pump dryer with secondary heat recovery was investigated by Wang *et al.* (2019). It was discovered that the solar mode was more energy-efficient than the heat pump mode, saving 3.5 kWh. A study by Singh *et al.* (2021) has also shown that, in general, solar-assisted heat pump dryers perform well by achieving higher energy and drying efficiency. A solar-assisted heat pump dryer's schematic diagram is displayed in Fig. 4.

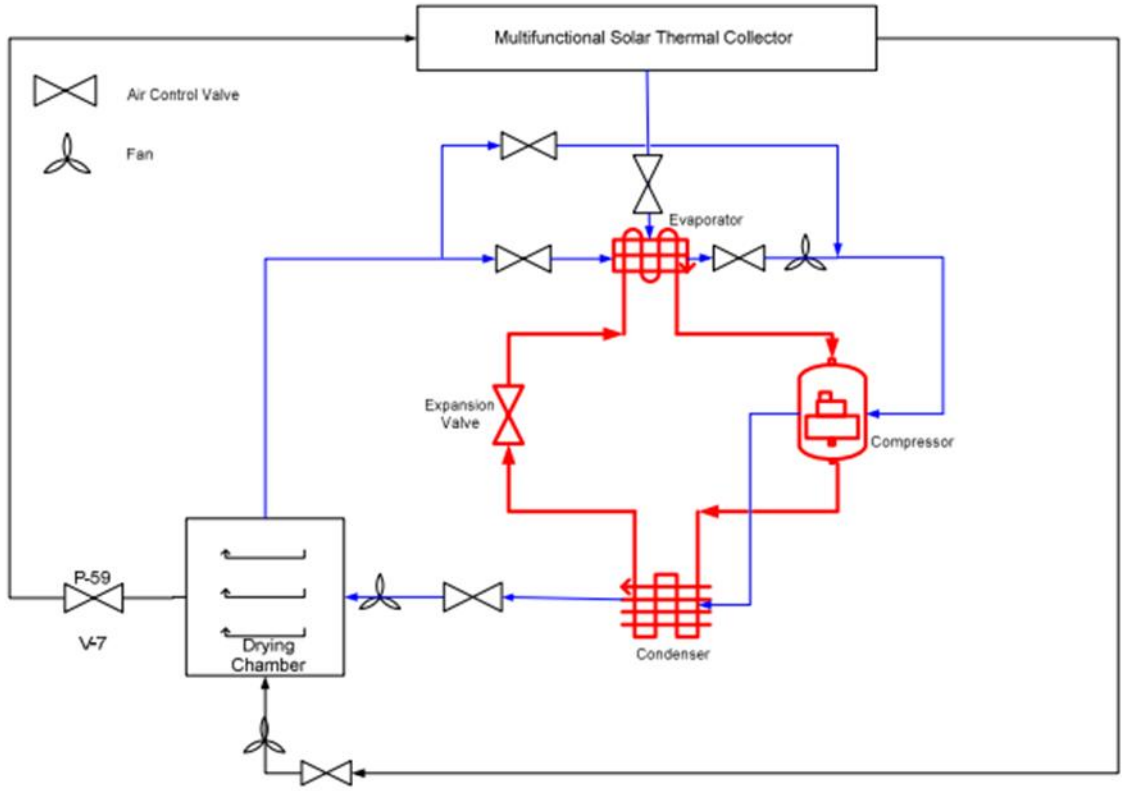

Figure 4: Solar-assisted heat pump dryer's schematic diagram (Majid *et al.*, 2009)

(ii) Solar-infrared assisted heat pump dryer

Very little attention has been paid to the solar-infrared assisted heat pump dryer. For drying banana, a solar-infrared assisted heat pump dryer was investigated by Singh *et al.* (2020c). Different operational modes of the system were compared. Results showed that the conventional heat pump dryer produced the lowest average moisture extraction rate, while the solar-infrared assisted heat pump dryer produced the highest. Infrared-assisted heat pump drying produced the lowest specific moisture extraction rate, while solar-assisted heat pump drying produced the highest.

An infrared-assisted heat pump dryer was also investigated by Ha and Tung (2021) to dry lime slices. The drying air velocity used in the experiments was 1.2 m/s, and the drying capacity was 1.2 kg/batch. The findings showed that using 3 mm thick lime slices; a drying chamber temperature of 42.5 or 45 °C, and a radiation intensity of 110 to 300 W/m^2, a good drying range was achieved.

A study by Song *et al.* (2018), stated that heat pump drying combined with far-infrared radiation could be used to efficiently dry yam chips. Furthermore, results of the study revealed that increasing the power supplied to the far-infrared radiation heaters significantly reduced energy consumption. The work carried out by Aktaş *et al.* (2017) also demonstrated the efficiency of heat pump and an infrared heater. A solar-infrared heat pump dryer's schematic diagram is displayed in Figure 5.

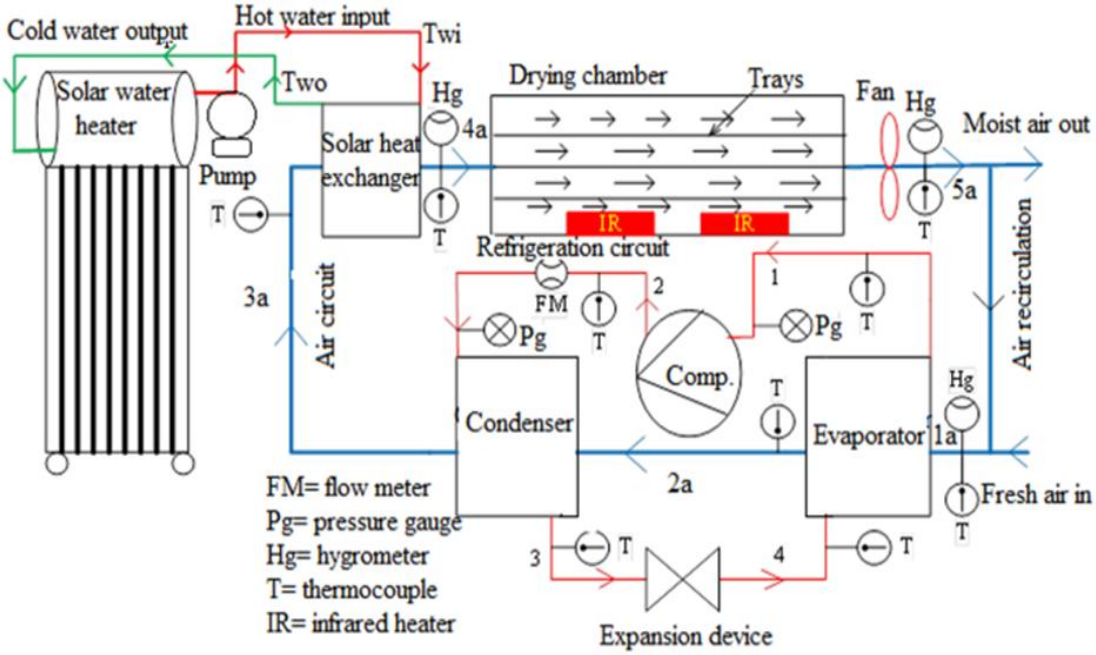

Figure 5: Solar-infrared heat pump dryer's schematic diagram (Singh *et al.*, 2020c)

(iii) Photovoltaic-assisted heat pump dryer

Though little is known about photovoltaics combined with heat pump dryers, the research conducted by Koşan *et al.* (2020), has enabled the comprehension that the integration of a heat pump dryer and photovoltaic system can yield superior outcomes and attain performance comparable to that of alternative drying systems. A heat pump, a photovoltaic system, and drying chamber are typically included in the experimental device for this type of dryer (Koşan *et al.*, 2020). In addition to performing better than other heat pump dryers, the photovoltaic-

assisted heat pump dryer produces excellent results. This is exemplified by the dryer developed by Candan *et al.* (2021).

Results showed that this system could achieve a specific humidity extraction rate of an average of 0.45 kg/kWh, making it one of the most efficient hybrid heat pump dryers.

A simulation was used to develop a solar heat pump dryer that ran solely on photovoltaic panels (Houhou *et al.*, 2017). The results of simulations conducted at varying temperatures indicated that temperature of the drying air was a more significant parameter than velocity, since when the drying temperature increased from 45 to 55 °C, the product moisture content reduced from 0.75 kg/kg to 0.3 kg/kg. The heat pump dryer's symbolic diagram for photovoltaic/thermal assistance is displayed in Fig. 6.

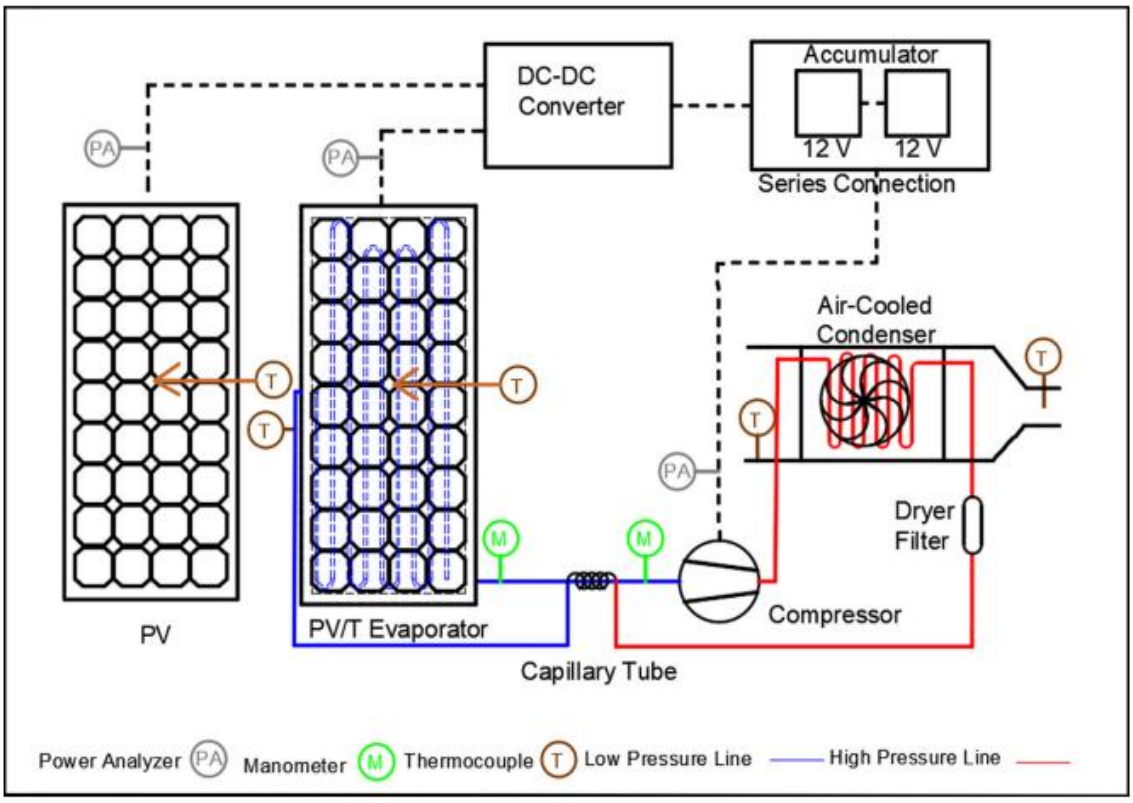

Figure 6: Photovoltaic assisted heat pump dryer's schematic diagram (Koşan *et al.*, 2020)

(iv) Coulomb force-assisted heat pump dryer

Heat pump dryer and a high voltage wire mesh are the two primary parts of this system. The Coulomb force is produced when the product is positioned near a low-frequency and high-

voltage mesh. The resultant force causes the product's moisture diffusion to increase. The heat pump dryer's airflow then dries the product.

To dry lemon, Lee *et al.* (2021) developed a coulomb force-assisted heat pump dryer. In comparison to utilizing a heat pump dryer alone for drying lemon slices, there was a 26% increase in both the effective moisture diffusivity and drying rate. In another study, Lee *et al.* (2015) dried lemon in an oven and a coulomb force-assisted heat pump dryer. A high drying rate was observed during oven drying at different temperatures as the drying temperature rose. Figure 7 shows the Coulomb force-assisted heat pump dryer's schematic diagram.

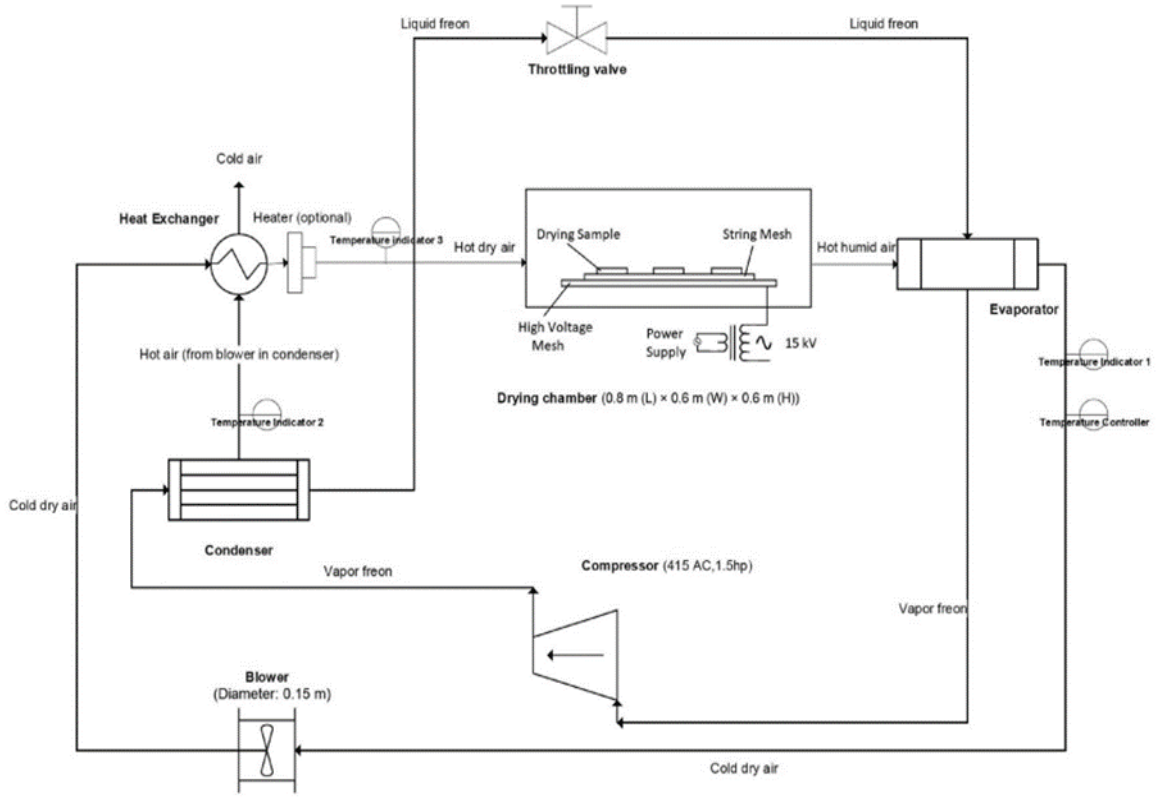

Figure 7: Coulomb force-assisted heat pump dryer's schematic diagram (Lee *et al.*, 2021

(v) Radio frequency heat pump dryer

A radio frequency heat pump dryer can be used to dry food and agricultural products (Alfaifi *et al.*, 2016; Hay *et al.*, 2018; Mao *et al.*, 2021; Zhou & Wang, 2019; Zhou *et al.*, 2018). Because of its deep penetration, quick and volumetric heating, and moisture self-balancing qualities, radio frequency drying is appealing. To maximize energy efficiency and product quality, radio frequency drying technologies are combined with heat pump drying to create radio frequency drying and radio frequency heating. In spite of this heat pump dryer's efficiency, there aren't many recent studies on the subject.

To dry Ganoderma lucidum, a heat pump dryer and radio frequency technology was combined by Hay *et al.* (2019). The results showed that drying air temperature and radio frequency power increases significantly boosted the drying rate. Additionally, the drying air velocity did not alter the drying rate, and the drying time was shortened by increasing radio frequency power.

A radiofrequency assisted heat pump dryer was investigated by Kien *et al.* (2021) to dry Ganoderma lucidum. The results showed that the drying rate increased with increasing radio frequency power and drying air temperature, but decreased with increasing drying air velocity. The radio frequency heat pump dryer's schematic diagram is shown in Fig. 8.

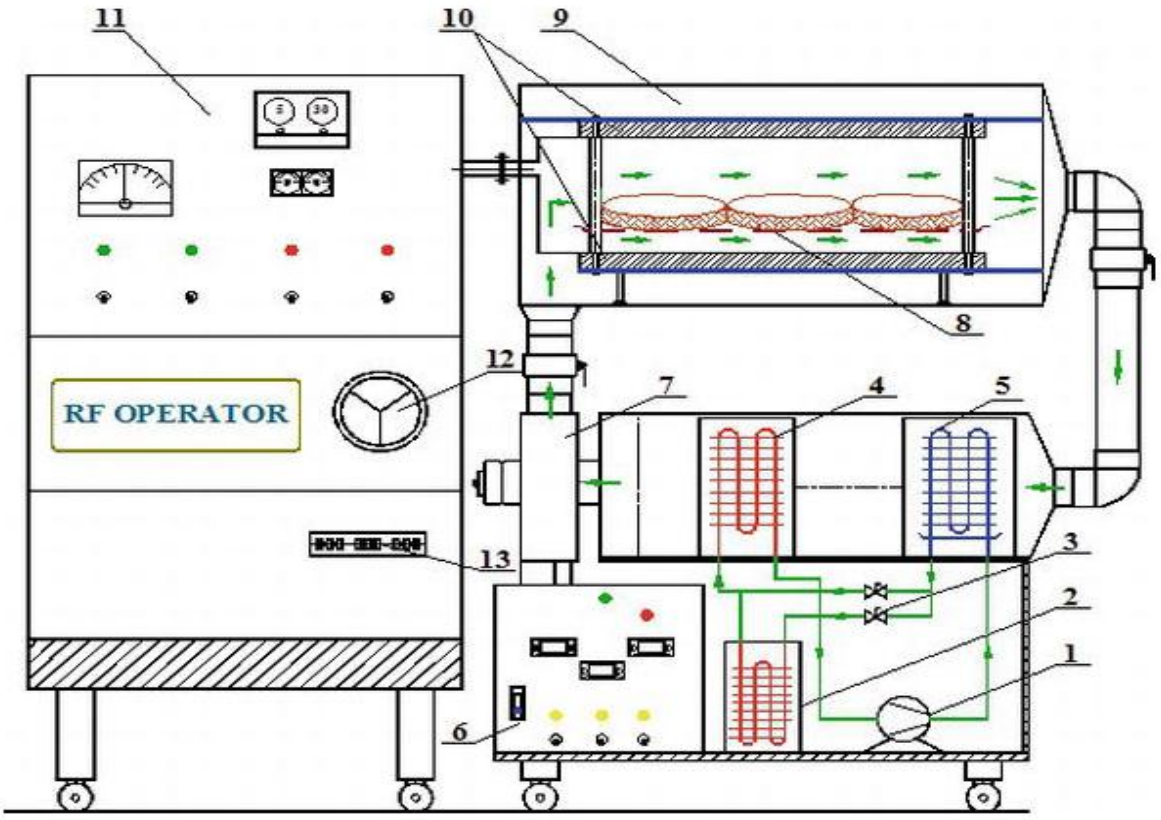

RF-assisted heat pump dryer model. (1) compressor, (2) sub-condenser, (3) valve, (4) condenser, (5) evaporator, (6) heat pump controller, (7) air fan, (8) drying tray, (9) drying chamber, (10) RF electrodes, (11) RF operating controller, (12) operating current intensity controller, (13) unit of supplying the operating voltage.

Figure 8: Radio frequency heat pump dryer's schematic diagram (Hay *et al.*, 2019)

(vi) Ultrasound-assisted heat pump dryer

The most promising drying technique is the heat pump dryer with ultrasound assistance. In order to prevent the deterioration of seed quality and the high energy consumption associated with continuous ultrasound application, the viability of ultrasound-assisted heat pump intermittent drying was investigated by Zongyu (2020). The findings demonstrated that although intermittent drying was essential for reducing energy usage, its impact on seed germination was not as positive as expected. Using the response surface methodology, it was also determined that the optimal drying parameters were 102.80 W ultrasound power, 37.10 °C, and 0.59 intermittency ratio.

The impact of ultrasonic factors and drying temperature on the kinetics of pea seed drying was investigated by Zhao *et al.* (2018). The findings showed that ultrasonic treatment and high temperature significantly improved the kinetics of pea seed drying, shortening the drying period and raising the diffusion coefficient.

Experiments were conducted by Liu (2019) to dry kiwifruit. The results showed that drying time was shortened and the rate of dehydration was greatly increased by this technology. The ultrasound-assisted heat pump dryer is seen in Fig. 9.

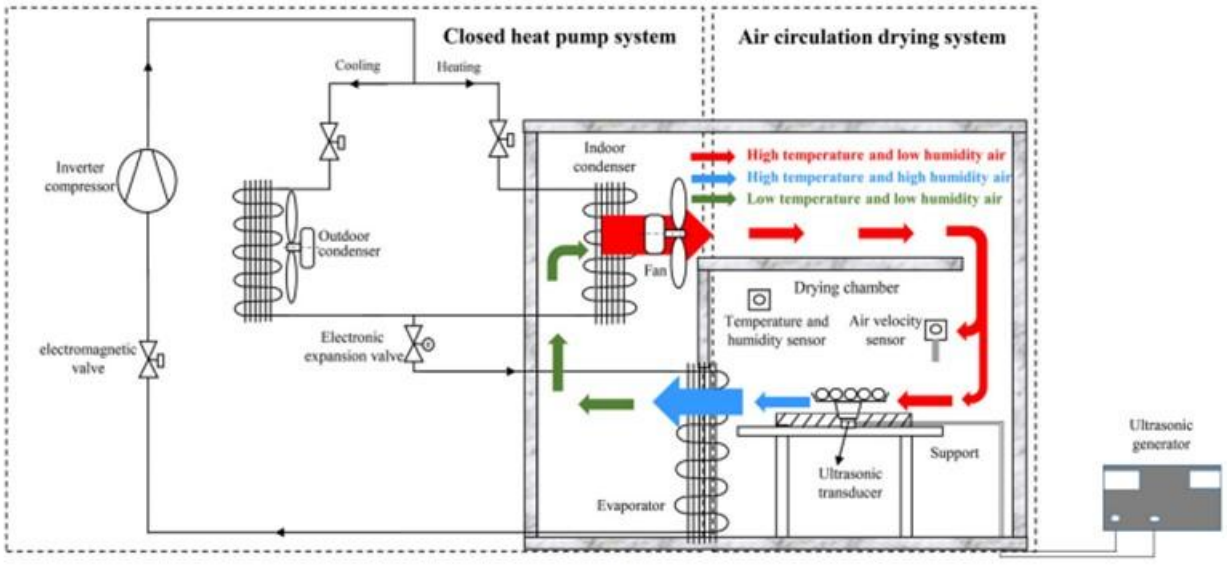

Figure 9: Ultrasound-assisted heat pump dryer's schematic diagram (Zongyu-Yang *et al.*, 2020)

(vii) Waste heat-assisted heat pump dryer

An intriguing substitute for drying agricultural products is to use waste heat recovery from different primary engines to support heat pump dryers, even though there isn't enough data to confirm the efficacy of this type of dryer.

The research carried out by Singh *et al.* (2020a) provided some insight into this innovative design of heat pump dryer by creating a waste-assisted heat pump dryer for drying radish chips using waste heat recovery from diesel engine exhaust. The waste-assisted heat pump dryer decreased the total moisture content of radish from 93.5 to 10.5% in the shortest amount of time. The heat pump dryer on its own demonstrated a higher coefficient of performance in comparison to a waste-assisted heat pump dryer, which in turn demonstrated a higher specific moisture extraction rate. A schematic diagram of a waste-assisted heat pump dryer can be found in Fig. 10.

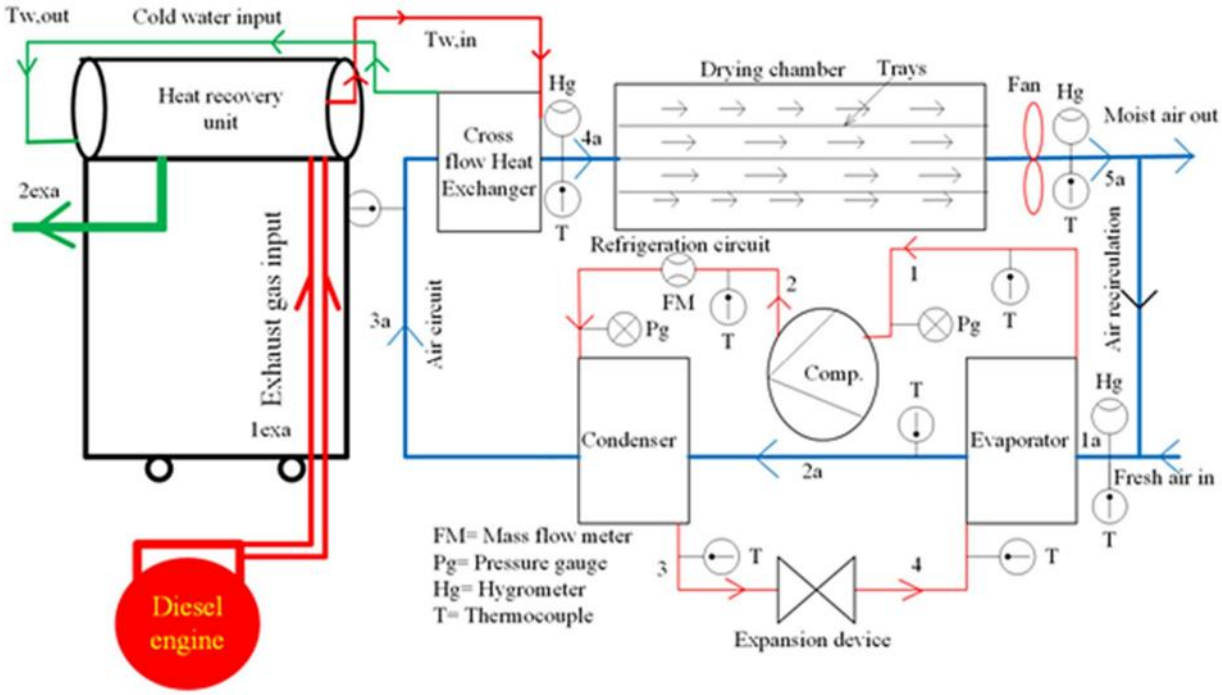

Figure 10: Waste-assisted heat pump dryer's schematic diagram (Singh *et al.*, 2020a)

2.2 Summary of the research's findings about heat pump dryer performance

Table 1 lists the performance parameters for energy and drying kinetic analysis of the various heat pump dryer types that have been previously discussed as being the most researched. It is true that a lot of researchers are interested in heat pumps worldwide, but the majority of recent

studies in this area have been conducted in China since all of the current types of heat pumps have been studied there.

It should be noted that, out of all the parameters examined, the drying time, moisture content, coefficient of performance and specific moisture extraction rate have received the greatest attention. The majority of the results that were looked at showed that air velocity is positively correlated with coefficient of performance, but air temperature and mass are inversely correlated. On the other hand, drying times are shortened by raising air velocity and temperature and prolonged by increasing mass. Conversely, the specific moisture extraction rate increases with air temperature but decreases with air velocity and mass.

Based on the results shown in Table 1, the solar-assisted heat pump dryer combined with heat recovery achieved the highest specific moisture extraction rate of 9.25. All the types of heat pump dryers presented, produce excellent results overall, according to the analysis of all the parameters shown in Table 1. This is especially true when it comes to decreasing the weight of the dried agricultural products and the moisture content in a shorter amount of time than traditional dryers. The heat pump dryers' efficiency was further illustrated by the table's results, which indicated that the photovoltaic-assisted heat pump dryer had the highest coefficient of performance value (5.338) and the solar-assisted heat pump dryer had the lowest.

Unfortunately, because studies have been done on various climatic conditions and specific agricultural products, it is challenging to compare all these types of heat pump dryers shown in Table 1. In fact, the performance of heat pump dryers is significantly influenced by the surrounding temperature, not to mention the various seasons. As such, environmental factors have a direct effect on heat pump dryers. Environmental factors also affect the drying time, the coefficient of performance, and the specific moisture extraction rate.

The drying time, the coefficient of performance, and the specific moisture extraction rate are also significantly impacted by the type of agricultural product because the parameters change based on the moisture content of the dried goods. As can be seen from Table 1, the type of heat pump dryers used also has a significant impact on the drying time, the coefficient of performance, and the specific moisture extraction rate. Depending on how the heat pump dryer is operated, Table 1's results can be analyzed to determine how much the drying time decreases. The study by Wang *et al.* (2019), illustrated this by drying 80 kg of mango using two different operation modes. Heat pump dryer mode produced a drying time of 14 hours, according to the

results, whereas the solar-assisted heat pump dryer produced a drying time of 16.3 hours. Similar results were achieved by Singh *et al.* (2020c), by employing five distinct drying modes to dry bananas. Using the solar-infrared heat pump dryer, the banana chips took 180 minutes to dry; while using the solar-assisted heat pump dryer, it took 225 minutes. Additionally, Table 1 demonstrated that rocks, such as soapstone, have never been used in research on solar-assisted heat pump dryers as a thermal energy storage material for drying processes. This topic should be emphasized in future work.

Table 1: Results of performance analysis from earlier research

Authors	Drying system	Country	Drying temperature (°C)	Final moisture Content	Initial weight (kg)	Product dried	Thickness (mm)	Velocity (m/s)	SMER (kg/kWh)	COP	Drying Time
HYBRID HEAT PUMP DRYER											
Xu *et al.* (2021)	SAHPD in various modes:										
	ISDS mode	China	50	50%	3	Mushroom	NA	NA	3.56	NA	6h
	ICHPDS mode	China	60, 55 and 50	NA	1.5, 2 and 2.5	Mushroom	NA	1.5, 2.5 and 3.5	**a)** 0.163, 0.184 and 0.168 respectively at 1.5, 2.5 and 3.5 m/s. **b)** 0.156, 0.168 and 0.158 respectively at 1.5, 2 and 2.5 kg **c)** 0.184, 0.178 and 0.184 respectively at 50, 55 and 60°C	**a)** 2.11, 2.96 and 3.35 respectively at 1.5, 2.5 and 3.5 m/s. **b)** 3.35, 3.35 and 2.86, respectively at 1.5, 2 and 2.5 kg **c)** 2.96, 2.51 and 2.43 respectively at 50, 55 and 60°C	**a)** 20, 17 and 17h respectively at 1.5, 2.5 and 3.5 m/s. **b)** 15, 17 and 19h respectively at 1.5, 2 and 2.5 kg. **c)** 13, 15 and 17h respectively at 60, 55 and 50°C
	SAHPD in open mode	China	59.17	NA	2	Mushroom	NA	3.5	0.225	3.08	12h

Authors	Drying system	Country	Drying temperature (°C)	Final moisture Content	Initial weight (kg)	Product dried	Thickness (mm)	Velocity (m/s)	SMER (kg/kWh)	COP	Drying Time
	SAHPD in closed mode	China	62.38	NA	2	Mushroom	NA	3.5	0.27	2.68	9h
	SAHPD in semi-open mode	China	60.83	NA	2	Mushroom	NA	3.5	0.23	3.20	12h
Hu *et al.* (2020)	SAHPD	China	40 to 70	12%	50	Wolfberry	NA	1	NA	NA	59 h at 40 °C and 8h at 70 °C
Hao *et al.* (2021)	SAHPD	China	51.8 (maximum)	0.54 (g water/ g dry)	0.4	Lemon	3	NA	0.856	3.63 (maximum)	7h
Gan *et al.* (2017)	SAHPD	Malaysia	33.1	10%-12%	0.01	Misai kucing leaves	NA	6.5	NA	NA	39.8h
Dai and Deng (2021)	SAHPD	China	67.40	0.95 ± 0.05 (g/g dry basis)	NA	Pumpkin slice	4	NA	0.95	NA	7h34min
Ismaeel and Yumrutas (2020)	SAHPD with storage and HRU	Turkey	60	10%	NA	Wheat	NA	NA	9.25	5.28	NA
Wang *et*	SAHPD with heat recovery unit in two modes:										

Authors	Drying system	Country	Drying temperature (°C)	Final moisture Content	Initial weight (kg)	Product dried	Thickness (mm)	Velocity (m/s)	SMER (kg/kWh)	COP	Drying Time
al. (2019)	HPD	China	45	0.25 dry basis	80	Mango	NA	NA	1.82	3.48	14h
	SAHPD	China	45	0.25 dry basis	80	Mango	NA	NA	2.05	3.69	16.3h
Singh *et al.* (2020c)	SIAHPD in various modes:										
	SIAHPD	India	65.7	11.5%	NA	Banana chips	2	0.8	1.351	1.94	180 min
	SAHPD	India	65.7	11.5%	NA	Banana chips	2	0.8	1.45	2.04	225 min
	IAHPD	India	50.54	11.5%	NA	Banana chips	2	0.8	0.968	2.303	225 min
	HPD	India	50.25	11.5%	NA	Banana chips	2	0.8	0.975	2.618	345 min
Ha and Tung (2021)	SIAHPD	Viet Nam	42.5 – 45	13%	1.2	lime slices	3	1.2	NA	NA	10h
Aktaş *et al.* (2017)	SIAHPD	Turkey	45	0.14 g water/g dry basis	1	Carrot	1.5	0.5	NA	4.39	410 min
Candan *et al.* (2021)	PVAHPD	Turkey	31.27	NA	2.5	Banana chips	4	2.77	0.45	5.338	50 min

Authors	Drying system	Country	Drying temperature (°C)	Final moisture Content	Initial weight (kg)	Product dried	Thickness (mm)	Velocity (m/s)	SMER (kg/kWh)	COP	Drying Time
Houhou *et al.* (2017)	PVAHPD	China	45 – 55	0.3 Kg/Kg	10	NA	NA	1-3	NA	NA	NA
Lee *et al.* (2021)	CFAHPD	Malaysia	21-23	NA	NA	Lemon slices	2.5-3.5	1 - 1.2	NA	NA	101.40 h± 1.97
Hay *et al.* (2019)	RFAHPD	Vietnam	45	13% Wet basis	20	Ganoderma lucidum	15	1.2	NA	NA	400-600 min
Kien *et al.* (2021)	RFAHPD	Viet Nam	47	NA	NA	Ganoderma lucidum	NA	1.53	NA	NA	409 min
Zongyu-Yang *et al.* (2020)	UAHPD	China	105 ± 1	14.5 g/g dry basis	0.07	Adzuki bean seeds	6.40 ± 0.15	0.7	NA	NA	24 h
Zhao *et al.* (2018)	UAHPD	China	40	0.0532 dry basis	0.09	Pea seed	NA	0.7	NA	NA	12h
Liu *et al.* (2019)	UAHPD	China	30 and 40	0.2-0.3 g/g dry basis	0.08	Kiwifruit	5	1	NA	NA	450 min at 30℃ and 390 min at 40℃
Singh *et al.* (2020a)	WHR-HPD	India	65°C - 70°C	10.5%	5	Radish	2	0.5 to 2.5	1.39, 1.6436, 2.158, and 2.4 kg/kWh, respectively for	5.34, 4.25, 5.18, and 3.48 respectively for the open-loop	135 min

Authors	Drying system	Country	Drying temperature (°C)	Final moisture Content	Initial weight (kg)	Product dried	Thickness (mm)	Velocity (m/s)	SMER (kg/kWh)	COP	Drying Time
									the open-loop simple-HPD, closed-loop simple-HPD, open-loop WHR-HPD, and closed-loop WHR- HPD.	simple-HPD, closed-loop simple-HPD, open-loop WHR-HPD, and closed-loop WHR-HPD.	
GROUND SOURCE HEAT PUMP DRYER											
Wu *et al.* (2021)	Open - circuit GSHPD	China	40 – 60	NA	NA	NA	NA	NA	4.4 (highest)	3.2-5.2	NA
AIR SOURCE HEAT PUMP DRYER											
Liu *et al.* (2018)	ASHPD	China	50	10% wet basis	15	Garlic slices	3	1	1.136 ± 0.001	NA	270-300 min
Shen *et al.* (2017)	ASHPD	China	70	NA	NA	NA	NA	NA	NA	2.6 (Highest)	NA
Liu *et al.* (2017)	ASHPD	China	30, 35and 40	20%	0.5	Carrot	3	1	NA	NA	315 min at 30°C; 294 min at 35°C and 281 min at 40°C
Singh *et al.* (2020e)	ASHPD	India	50.5 and 50.4 respectively for drying banana and	11.6% and 11.5% for	4 kg of Banana and Potato	Banana and Potato	2	6	1.248 and 1.0498 respectively for drying banana and potato in the	3.09 and 2.85 respectively for drying banana and potato in the	220 and 320 min respectively for drying banana and potato in the

Authors	Drying system	Country	Drying temperature (°C)	Final moisture Content	Initial weight (kg)	Product dried	Thickness (mm)	Velocity (m/s)	SMER (kg/kWh)	COP	Drying Time
			potato in the closed system.	banana and potato.					closed system.	closed system.	closed system.
			41.4 and 40.8 respectively for drying banana and potato in the open system.						0.924 and 0.981respectively for drying banana and potato in the open system.	3.89 and 3.93 respectively for drying banana and potato in the open system.	300 and 370 min respectively for drying banana and potato in the open system.

2.3 Significance of heat pump dryers in preserving nutrients

The ability of heat pump dryers to preserve product quality is just as important to consumers as efficiency when it comes to the adequate or ideal drying of agricultural products. The literature emphasizes both the nutritional qualities of drying materials and their color.

Table 2 summarizes recent published research results on the nutritional content of dried agricultural products when using heat pump dryers. This table illustrates how much work is required to fully investigate these nutritional parameters.

However, this table shows that particular attention is given to dried agricultural products to demonstrate whether they have maintained all of their properties after drying. Recent studies on heat pump dryers frequently evaluate nutritional parameters such as, vitamin C, beta-carotene, phycocyanins, polysaccharides and total phenol content (Costa *et al.*, 2016; Dai & Deng, 2021; Hay *et al.*, 2019; Lee *et al.*, 2021; Li *et al.*, 2019; Liu *et al.*, 2019; Tuncer *et al.*, 2019). These bioactive nutrients are sensitive to heat, so they are regularly evaluated to ensure the quality of dried products (Yitayew & Fenta, 2021).

2.3.1 Beta-carotenes

When ingested by humans, two molecules of vitamin A are produced from one beta-carotene molecule. This is why it is sometimes referred to as provitamin A (Chen *et al.*, 2021; Naikwade, 2015).

Therefore, it's essential to minimize beta-carotenoid loss during drying. The pumpkin was dried using a solar-assisted heat pump dryer, which produced good results in minimizing beta-carotene content losses. The dried sample's beta-carotene content was 10.202 mg/g (Dai & Deng, 2021). The solar-assisted heat pump dryer made by Şevik (2014), gave also good results. The results of this study showed that the amount of beta-carotene in dried products did not significantly decrease. Kaffir lime leaves was dried by Sanpang and Tanongkankit (2022) with a heat pump dryer. At 55 degrees Celsius, the dried samples showed the highest beta-carotene content of kaffir leaves, 1.66 mg/g. However, at 45 and 50 degrees Celsius, respectively, the beta-carotene values were 1.17 and 1.28.

2.3.2 Vitamin C and phenols content

Fruits and vegetables contain the majority of vitamin C, which is commonly used to determine their nutritional value. In fact, because of its extreme sensitivity to a wide range of physicochemical factors, such as temperature, pH, oxygen, enzymes, light and catalysts, it serves as a singular eyewitness to the extent of any degradation that may have happened during processing. Excessive heat or an extended drying period may cause vitamin C to be lost during the process (Catherine, 2016; Li *et al.*, 2019; Zhou *et al.*, 2018).

Nevertheless, total phenol content, or TPC, is a secondary metabolite that emerges on its own during soaking and germination, and phenolic compounds have antioxidant properties (Gao *et al.*, 2020; Niroula *et al.*, 2019; Zhang *et al.*, 2019).

In order to improve the drying quality of agricultural products, Lee *et al.* (2021) proposed a Coulomb force-assisted heat pump dryer. The majority of the vitamin C and total phenolic content in the dried lemon were retained by this dryer, according to the results. The amount of vitamin C was discovered to be 2.5–93.2% greater than in oven-dried samples. Another study by Liu *et al.* (2019), showed that using contact ultrasound in a pump dryer for drying kiwi fruit raised the overall phenolic content and vitamin C content. In addition, the results showed that increasing the ultrasonic power from 0 to 48 W at 30 °C improved the total phenolic content values from 220.51 to 240.58 mg/100 g. At 40 °C, the vitamin C content increased by 11.1 and 20.3%, respectively, when the ultrasonic power was increased from 0 W to 24 and 48 W. Kaffir leaves were dried by Sanpang and Tanongkankit (2022). Before drying, Kaffir leaves had a total phenolic content of 43.03 mg/g GAE; however, following drying, the amounts were 14.56, 17.34, and 16.71 mg/g GAE at 45, 50, and 55 °C, respectively.

2.3.3 Phycocyanins

Phycocyanins are bioactive compounds possessing anti-inflammatory, anti-cancer, and antioxidant characteristics. Thus, it's imperative to make sure that the drying process doesn't alter the characteristics of these bioactive compounds. Heat pump dryer was employed by Costa *et al.* (2016) to dry spirulina sp. The results showed that drying air temperature had the biggest impact on the amount of phycocyanin.

The drying of spirulina was carried out by comparing a heat pump dryer with a conventional tray dryer (Costa *et al.*, 2015). The best preservation of Spirulina properties was found in a heat

pump dryer operating at 50 °C. The values of phycocyanin in this condition were 14% higher than in the conventional tray dryer under the same conditions.

2.3.4 Polysaccharides

The analysis of polysaccharides is particularly important because these macromolecules are involved in many different physicochemical and sensory phenomena. Radiofrequency technology was combined with a heat pump dryer to dry ganoderma lucidum by Hay *et al.* (2019). Findings indicated that after drying, more polysaccharide was retained when radio frequency power was increased. When the radio frequency power was 0, 0.65, 1.3, 1.95, and 9.18 kW, respectively, the polysaccharide content was 7.82, 9.18, 9.31, and 9.47 mg/g.

The study by Huang *et al.* (2014) compared the immunomodulatory and physicochemical properties of polysaccharide-protein complexes of litchi pulp dried by vacuum freeze, vacuum microwave, and heat pump dryer. This heat pump dryer turned out to be the best method for enhancing immunomodulatory properties.

Heat pump drying and hot air drying techniques were used to dry a fresh Gastrodia elata by Cheng *et al.* (2020). The drying temperature was 50 °C for both methods. The results show that the polysaccharides in the samples were unaffected by any of the methods of drying. The mean polysaccharide values in the heat pump and hot air dried samples were nearly equal, at 16.39 and 16.52, respectively.

Table 2: Results of nutritional content from earlier research

Author	Drying system	Country	Product dried	Vitamin C (Preserved)	Polysaccharide (Preserved)	Phycocyanin (Preserved)	Total phenolic content (Preserved)	β-carotene (mg/g) (Preserved)
Li *et al.* (2019)	Hot air drying	China	Okra	23.79% to 46.25%	73.26 to 88.27%	NA	81.85 to 96.12%	NA
	HPD	China	Okra	29.52% to 72.23%	82.78 to 94.1 %		85.44 to 97.54%	
Costa *et al.* (2016)	HPD	Brazil	Spirulina	NA	52.6%	19.6 mg/g	NA	NA
Dai and Deng (2021)	SAHPD	China	Pumpkin slice	25.682 mg/ 100 g dried sample	NA	NA	NA	10.202 mg/g
Lee *et al.* (2021)	CFAHPD	Malaysia	Lemon slices	0.00674 kg	NA	NA	10.14 ± 0.37 kg Gallic Acid/kg dry weight	NA
Liu *et al.* (2019)	UAHPD	China	Kiwifruit	When ultrasonic powers were increased, the values increased between 11.1% and 20.3% at 40°C.	NA	NA	From 220.51 to 275.23 mg/100 g	NA
Tuncer *et al.* (2019)	HPD	Turkey	Grape pomace	NA	NA	NA	55.6 ± 4.0 (mg Gallic Acid Equivalent /g dry weight)	NA
Hay *et al.* (2019)	RFAHPD	Vietnam	Ganoderma lucidum	NA	7.82, 9.18, 9.31 and 9.47, when the radio frequency power was 0, 0.65, 1.3 and 1.95, respectively.	NA	NA	NA

Author	Drying system	Country	Product dried	Vitamin C (Preserved)	Polysaccharide (Preserved)	Phycocyanin (Preserved)	Total phenolic content (Preserved)	β-carotene (mg/g) (Preserved)
Şevik (2014)	Solar-HPD	Turkey	Tomato, strawberry, mint, and parsley.	Tomato: 83% Strawberry: 65.2 %	NA	NA	Tomato: 2% Mint and parsley: from 13.5% to 18.4% Strawberry: 35%	No substantial drop
Sanpang and Tanongkankit (2022)	Heat pump, heater and hybrid systems dryer	Thailand	Kaffir lime leaves	NA	NA	NA	14.56, 17.34, and 16.71 mg/g Gallic Acid Equivalent respectively at 45, 50, and 55 °C.	1.66, 1.17 and 1.28 respectively at 55, 45 and 50 °C
Costa *et al.* (2015)	HPD	Italia	Spirulina sp.	NA	NA	14%	60%	NA
Cheng *et al.* (2020)	Hot Air Drying and Heat pump drying	China	Gastrodia elata	NA	16.39 and 16.52 respectively, in the hot air and heat pump dried samples	NA	NA	NA

2.4 Significance of heat pump dryers in maintaining color

Color has an impact on consumers' acceptance of agricultural products (Fiorentini *et al.*, 2020; Sandoval *et al.*, 2018). Heat pump dryers are better to other drying systems in terms of color improvement, based on results reported in the literature as illustrated in Table 3.

A hot air drying and heat pump dryer was compared by Haonan *et al.* (2019), by drying jujube slices. According to the findings, employing a heat pump dryer enhanced the quality of the jujube slices by raising the lightness value and lowering the overall color difference value. By drying coffee with open-loop batch heat pump dryer, Fernando *et al.* (2021) came to the conclusion that there was little change in the coffee's color. The total color difference value for coffee at 10.11% moisture content was found to be 31.65 when compared to fresh coffee.

Banana drying in closed-loop heat pump dryer system was studied by Tunckal *et al.* (2020). Results showed that the total color difference and redness color values increased as the drying temperature rose, while lightness and yellowness color values decreased. When the drying air temperature was raised from 37 °C to 43 °C, the overall color difference increased from 30.71 to 31.04.

The impact of heat pump drying on color change were investigated by Gan *et al.* (2017). It was discovered that using an intermittent heat pump dryer improves the color change. The results also showed that drying bird's nest with a heat pump at 28.6 °C decreased overall color change by 76%.

In order to assess the drying kinetics and product quality of misai kucing, solar-assisted heat pump drying was compared with solar drying (Gan *et al.,* 2017). Samples that were dried using a solar heat pump exhibited a smaller overall color change as a result of chlorophyll degradation than samples that were dried using a solar heat pump. Far infrared radiation or a heat pump dryer were used to dry yam chips at power levels of 500, 1000, and 2000 watts. In comparison to the heat pump-treated samples, the yam chips that were dried using a heat pump dryer and far infrared radiation were lighter and had more red and yellow tones. When dried in a heat pump dryer with far-infrared radiation at 1000 watts, the dried Chinese yam chips showed reduced shrinkage, better rehydration ability, lower hardness, and higher brittleness than the others (Song *et al.,* 2018).

Table 3: Results of color analysis from earlier research

Authors	Drying system	Country	Product dried	Drying temperature (°C)	Colour parameters							
					Lightness (L*)		Redness/greenness (a*)		Yellowness/blueness (b*)		Total colour difference (△E)	
					Initial	Final	Initial	Final	Initial	Final	Initial	Final
Haonan *et al.* (2019)	HPD	China	Jujube	60	44.7	38.1	13.6	15.1	24.5	20.6	0	3.7
Costa *et al.* (2016)	HPD	Brazil	Spirulina SP.	50	NA	21.9 ± 0.5	NA	−3.68 ± 0.09	NA	7.44 ± 0.09	0	5.71 ± 0.18
Gan *et al.* (2017)	HPD	Malaysia	Edible Bird's Nest	28.6	58.7 ± 2.62	59.6 ± 1.54	0.80 ± 0.21	0.80 ± 0.09	12.1 ± 2.85	16.7 ± 0.92	0	4.74 ± 5.02
Gan *et al.* (2017)	SAHPD	Malaysia	Misai Kucing leaves	33.1 ± 0.24	30.00 ± 0.26	42.30± 0.43	-5.10 ± 0.35	- 7.20 ± 0.12	3.50 ± 0.36	4.80 ± 0.38	0	18.29 ±0.11
			Misai Kucing flowers	35.3 ± 0.19	33.00 ± 0.37	33.70± 0.46	7.40 ± 0.12	8.20 ± 0.24	5.00 ± 0.42	7.80 0± .31	0	21.23 ± 0.23
			Misai Kucing stems	34.6 ± 0.14	30.00 ± 0.16	30.40 ± 0.10	-6.40 ± 0.09	-6.60 ± 0.37	11.10 ± 0.54	11.60 0± .43	0	2.72 ±0.64
			Misai Kucing mix	34.9 ± 0.09	36.00 ± 0.21	34.90 0±.24	-6.80 ± 0.36	-5.00 ± 0.19	4.90 ± 0.27	6.50 ± 0.22	0	17.26 ± 0.25
Song *et al.* (2018)	HPD	China	Chinese Yam	50	78.67	58.90 ±1.87	-3.13	5.19 ± 0.42	10.17	26.39 ± 0.90	0	26.89 ± 0.79
	HPD combined with far infrared	China	Chinese Yam	50	78.67	66.98 ±1.45	-3.13	3.98 ± 0.25	10.17	28.17 ± 0.99	0	22.61 ± 0.62

Authors	Drying system	Country	Product dried	Drying temperature (℃)	Colour parameters							
					Lightness (L*)		Redness/greenness (a*)		Yellowness/blueness (b*)		Total colour difference (△E)	
					Initial	Final	Initial	Final	Initial	Final	Initial	Final
	radiation at 1000 W											
Ferdinando *et al.* (2021)	HPD	Sri-lanka	Coffee	56.9±2.2	49.14±3.79	32.60±3.44	12.35±3.49	6.18±3.72	29.39±3.59	9.77±3.51	0	31.65
Tunckal and Doymaz (2020)	HPD	Turkey	Banana	37	88.63	62.36	2.28	2.54	32.48	28.39	0	30.71
				40	88.63	61.32	2.28	2.72	32.48	28.15	0	30.73
				43	88.63	59.87	2.28	3.06	32.48	27.48	0	31.04
Hay *et al.* (2019)	RFAHPD (Radio frequency power = 1 .95 kW)	Vietnam	Ganoderma lucidum	45	47.12	39.35	4.11	5.12	18.85	14.46	0	8.98
	RFAHPD (Radio frequency power = 1 .3 kW)	Vietnam	Ganoderma lucidum	45	47.12	39.02	4.11	5.42	18.85	14.1	0	9.48
	RFAHPD (Radio frequency power= 0. 65 kW)	Vietnam	Ganoderma lucidum	45	47.12	38.71	4.11	5.75	18.85	13.76	0	9.97

Authors	Drying system	Country	Product dried	Drying temperature (℃)	Colour parameters							
					Lightness (L*)		Redness/greenness (a*)		Yellowness/blueness (b*)		Total colour difference (△E)	
					Initial	Final	Initial	Final	Initial	Final	Initial	Final
	HPD	Vietnam	Ganoderma lucidum	45	47.12	36.5	4.11	6.94	18.85	12.52	0	12.68

2.5 Techno-economic analysis for heat pump dryers

The goal of techno-economic analysis is to assess the economic impacts of new technologies by looking at how technologies are developed and research projects are structured in terms of risks, benefits, uncertainties, costs, and time frames (Shiozawa, 2020). Numerous researchers have thoroughly investigated heat pump dryers. Moreover, Table 4 indicates that the techno-economic aspects of these systems have not received much attention in the literature. In one of the few studies on the topic, the heat pump dryer's economic analysis was compared to other heating systems by Meyer and Greyvenstein (1992), discovered that heat pump dryers' life cycle costs were more affordable. When solar assisted heat pump dryers and heat pump dryers were compared, it was discovered that although the solar assisted heat pump dryer was more expensive initially, its operating costs were lower (Singh *et al.*, 2020f).

Since the payback period is a significant techno-economic factor, numerous authors focus on it specifically, and the findings differ amongst studies. According to Yahya *et al.* (2018), the payback period for heat pump dryers can be as short as 1.6 years. The research concentrated on a solar-powered heat pump fluidized bed dryer that was combined with a biomass furnace to dry rice. This is also applies to the photovoltaic assisted-heat pump dryer developed by Koşan *et al.* (2020), which provided a 2.32-year payback period. A short payback period of 2.75 years was also reported by Singh *et al.* (2020a) using waste heat recovery-assisted heat pump dryer.

As previously mentioned, the literature pertaining to heat pump dryers has relatively few techno-economic research studies. The results of the techno-economic analysis of the aforementioned studies are compiled in Table 5. This table indicates that the payback period has drawn the greatest attention out of all the major parameters that were presented, Conversely, the return on capital and net present value have received little attention. Consequently, it is challenging to obtain a broad understanding of the financial implications linked to each type of heat pump dryer that is currently on the market.

Table 4: Results of techno-economic analysis from earlier research

Authors	Country	Drying system	Initial cost ($)	Capital cost ($)	Operating cost ($)	Production cost ($)	Installation cost ($)	Profit or benefit (yearly) in ($)	Return of capital	Payback period (years)	Net present value ($)
Singh *et al.* (2020f)	India	HPD	556.89	NA	1565	NA	138.98	NA	NA	NA	NA
		SAHPD	928.52	NA	1470	NA	166.04	95	NA	3.9	NA
Yahya *et al.* (2018)	Malaysia	SAHPD with biomass furnace	NA	2550	NA	28 902.25	NA	1528.74	NA	1.6	8563.82
Koşan *et al.* (2020)	Turkey	PVTAHPD	NA	NA	NA	NA	NA	NA	NA	2.32	NA
Singh *et al.* (2020a)	India	HPD	521.31	NA	2238	NA	NA	NA	NA	NA	NA
		HPD with WHR	864.46	NA	2112	NA	NA	NA	NA	2.75	NA

2.6 Life cycle analysis of heat pump dryers

Systems that use solar energy are less harmful to the environment than those using conventional sources of energy. The apparent trend of solar energy technologies frequently has to deal with the potential for adverse environmental effects. The effects of solar energy technologies on soil, air, and water; their effects on vegetation and animals; and their possible use in conjunction with hazardous materials are a few environmental factors to take into account (Rabaia *et al.*, 2021; Sayed *et al.*, 2021; Rahman *et al.*, 2022). For some users, these potential issues seem to be a major obstacle.

In light of this, life cycle analysis seems to be a necessary stage before releasing solar energy technologies onto the market in order to create solar systems that are more environmentally conscious. A product's overall environmental impact at every stage of its life is examined using life cycle analysis. Typically, life cycle analysis is provided in terms of greenhouse gas emissions (Lee *et al.*, 2020; Uusitalo *et al.*, 2016). It is widely acknowledged that by identifying the materials and energy used as well as environmental emissions, it provides a clearer understanding of the effect of a product on the environment. Studies that look into the life cycle assessment of a few drying technologies are displayed in Table 5.

A life cycle assessment was used to evaluate the effects of industrial solar thermal systems on the environment. Based on the results of the life cycle assessment, the most environmentally harmful stages of the assessed solar thermal systems are the manufacturing and raw material extraction phases as well as the use phase. Furthermore, the findings indicated that the system manufacturing phases and raw material extraction account for more than 85% of the total impact in the areas of ozone and element depletions, human health ecotoxicity, as well as marine and terrestrial environments (Kylili *et al.*, 2017).

A life cycle analysis of two dried seaweed productions was conducted in the study by Oirschot *et al.* (2017). The impact assessment process employed ten impact categories: photochemical oxidation, acidification, eutrophication, human toxicity, terrestrial ecotoxicity, ozone layer depletion, climate change, abiotic depletion, and freshwater and marine aquatic ecotoxicity. Based on the results, the seeding lines had minimal influence on the overall effects. Almost all impact profiles showed a contribution of less than 5% from harvesting and transportation, with the exception of eutrophication and acidification, where their contributions were 7% and 6%, respectively. Over 70% of each impact category was influenced by the infrastructure and

the drying process, though not equally. Consequently, learning about the life cycle analysis of agricultural drying systems aids in identifying the drying system component with the highest environmental load and offers opportunities to enhance its environmental efficiency (Lamidi *et al.*, 2019).

The environmental impact of the infrastructure and operation of the pilot solar drying unit was also assessed using life cycle analysis. Based on the findings, it was concluded that the solar drying unit's main environmental effects are due to the electricity it uses to operate (Abeliotis *et al.*, 2022a). The life cycle assessment was conducted by Nayanita *et al.* (2022) to compare the environmental effects of a mixed-mode dryer and a direct-mode dryer. The "Cradle-to-grave" method of life cycle analysis was used to examine the environmental effects of the Direct and Mixed-Mode Type Solar Dryers' production and recycling. The results showed that the production and recycling of Mixed-Mode Type Dryers had endpoint single score impact values on resources, ecosystems, and human health of 16.5 points, 1.22 points, and 25.99 points, respectively. In contrast, the Direct Mode Type Dryer showed endpoint single score impact scores for the same factors of 7.14, 0.599, and 15.48 points. Given that its effects are notably smaller than those of the Mixed-Mode Type Dryer, this suggests that the Direct Mode Type Dryer is a more environmentally friendly dryer. A quantitative and thorough life cycle analysis of the environmental performances of the industrial stages of apple powder production was presented in a study by De Marco *et al.* (2015). The primary factors affecting the different impact categories in the drum drying method were the heating, drying, and low-temperature storage of apples. The drying and storing phases of the multistage drying process were the ones that affect the different categories the most.

Using the Life Cycle Assessment approach, the environmental effects of a thermal electric dryer and an indirect cabinet solar dryer fitted with phase-change materials were assessed by Mirzaee *et al.* (2023). When comparing the solar dryer (3.55 mPt) and the electric thermal dryer (11.36 mPt), the results showed a significant difference in the effects of emissions for each of the four indicators. This is because solar dryers run on clean, renewable energy that comes straight from the sun. However, electric heat dryers have a detrimental effect on resources, ecosystem quality, climate change, and human health because they usually use energy from non-renewable sources. Kumar (2022) investigated, through the life cycle assessment method, the environmental impacts of the heat pump dryer and the microwave vacuum dryer. The six most significant impact categories were determined to be particulate matter formation, ionizing

radiation, human toxicity, climate change, fossil fuel depletion, and photochemical oxidant formation. The findings indicated that in terms of sustainability, the heat pump dryer was a better choice. Nevertheless, there are hardly any life cycle analysis studies on heat pump dryers, which is why it is important to contribute significantly at this point in order to have a global understanding of the consequences associated with the advancement of heat pump dryers.

Table 5: Results of life cycle assessment from earlier research

Drying method	Dried product	Boundary and Scope	Functional unit	LCI data collection	Impact assessment method	Software	Results
Solar Drying Unit (Abeliotis *et al.*, 2022a)	Food waste	The system boundary included the weighing, lifting and unloading of waste bins, sorting, conveyor system, grinding, solar drying, effluent and pet food production. The scope of the present study includes all infrastructure and equipment of the pilot solar drying unit.	The processing of 1 ton of collected food waste	Ecoinvent databases using Greek data	The CML2 baseline 2000 impact assessment method was utilized.	Simapro 5.1	Results showed that the major environmental impacts are produced during the drying operation due to the use of electricity.
Mixed-Mode Type and Direct Mode Type Solar Dryers (Nayanita *et al.*, 2022)	Ginger	The system boundary included a drying chamber, SAH, connecting pipes, and a blower. The scope of the study included a drying chamber, a SAH, and connecting pipes. The system boundary also included electricity. It was, however, excluded from the scope of the study because the scope only covered the fabrication of the dryers and not their operation.	The functional unit consists of the system boundary and scope of the study considered.	Ecoinventv3 database	ReCiPe method	Simapro 8.3	The impact on a single score point caused by the fabrication and recycling of Mixed-Mode Type Dryer was 40% to 56% higher than that of Direct Mode Type Solar Dryer.
Indirect cabinet solar dryer integrated with phase change material and electrical dryer (Mirzaee *et al.*, 2023)	Tomato	The system boundary was formed by the solar radiation energy entering the system, the solar collector, the built-in cabinet, the freshly cut tomatoes, and thin slices of dried tomatoes.	NA	Ecoinvent database	IMPACT 2002+ version 2.15	Simapro 9	Results revealed that when comparing the effects of emissions for all four indicators, there was a significant difference between the solar dryer (3.55 mPt) and the electric thermal dryer (11.36 mPt).
Heat pump and microwave vacuum dryers (Kumar *et al.*, 2022)	Tomato	The boundary chosen was ‘‘Gate-to-gate,” i.e., the emission of only the process was considered and anything precursor or post that was not, like farming, packaging, disposal, etc.	The functional unit chosen for this analysis was 1 kg of dried tomatoes.	Ecoinvent database	ReCipe MidPoint 2014	OpenLCA	Result showed that heat pump dryer was a better choice from the sustainability point of view.
Drum drying and multistage drying (Marco *et al.*, 2015)	Apple pulp	The system boundaries of this study were set from apples’ transportation to the company to apple powders’ distribution.	The functional unit is one 3-kg weight apple powder package	Ecoinvent 3.1 database	IMPACT 2002+	SimaPro 8.0.4	Results showed that the drum drying method generated higher emissions on all the impact catego-ries with respect to the multistage drying method.

2.7 Policy implications in heat pump dryers for drying agricultural products

Because of their effectiveness, heat pump drying technologies are being developed by scientists worldwide. However, the application of heat pump drying technologies is particularly challenging in developing countries because there are no clear regulations controlling their use. Consequently, there is a lack of interest among investors in drying technology. Furthermore, the fossil fuel industry is receiving support from some governments. Therefore, in order to dry their agricultural products, consumers and businesses rely on fossil electricity. Heat pump dryers are among the drying technologies that are impacted by this issue. Another issue is that some countries have environmental regulations that require permission before installing a heat pump dryer (Hasan *et al.,* 2020).

2.8 Concluding remarks

The following key observation can be drawn from this chapter:

(i) There is no literature on the use of rocks, such as soapstone, as a thermal energy storage medium for drying processes in solar-assisted heat pump systems. This subject should be emphasized in future research.

(ii) Findings of recently published research on heat pump drying indicate that little research has been done on analysing the nutritional content of agricultural products grown in Africa's climate following the heat pump drying process.

(iii) There aren't many life cycle analyses of heat pump dryers, so more research is needed in this area to get a comprehensive understanding of the effects of heat pump dryer development.

(iv) There is a need to perform techno-economic research on heat pump dryers because there are few studies on the literature.

CHAPTER THREE

MATERIALS AND METHOD

3.1 Materials and equipment

The heat pump system, the drying chamber, the solar collector, and the thermal energy storage unit which uses soapstone as the storage medium are the key parts of the developed solar-assisted heat pump dryer integrated with thermal energy storage. The novelty of the proposed dryer lies in the integration of a thermal energy storage system with soapstone as a storage medium in a solar-assisted heat pump dryer. The thermal energy storage unit efficiently absorbs and stores solar energy in the soapstone medium through the sensible heat mechanism. The air that enters the storage system is then heated by the stored energy before it reaches the heat pump's condenser. In conclusion, energy optimization and general efficiency gains are the goals of using soapstone as the system's storage material. The system can efficiently store and uses solar energy by utilizing soapstone's advantageous thermal properties. This leads to increased energy efficiency and improved performance during the drying process. Every part of the dryer was constructed separately and step-by-step before assembly. The 3.6 m^2 drying chamber was built with both inner and outer sections made of 1.5 mm galvanized steel sheets.

In order to keep heat from escaping the drying chamber, a 6 mm thick layer of fiberglass was used to fill the space between the inner and outer sections. The drying chamber's exterior was coated with 1.5 mm-thick galvanized steel sheets. A 70 cm solar chimney with a roof turbine ventilator at one end and mild steel sheeting 1.5 mm thick has also been installed in the upper section of the drying chamber. The stainless steel roof turbine ventilator measures 300 mm in thickness. The device utilizes the convection theory between air and natural wind to convert any parallel airflow into a vertical one, thereby increasing indoor ventilation and efficiently eliminating contaminants such as dust, moisture, and soot.

There were eight trays in the drying chamber. To allow hot air from the drying chamber condenser to circulate, plastic wire mesh was used in the construction of the trays. The frame assembly for the drying chamber was made of mild steel sheets. The four main parts of the heat pump system are the following: an expansion valve (3/8 ×1/2 inch), a 4-horsepower compressor, a 4-horsepower condenser, and an evaporator. The heat pump system used R-22, commonly referred to as R22 freon and HCFC-22 freon, as the refrigerant.

The thermal energy storage system and the solar collector were built as one unit. The thermal energy storage is located at the bottom, and the solar collector is positioned at the top. Glass that was 70 cm wide, 1 meter long, and 6 cm thick was used to make the solar collector. For optimal solar radiation absorption, a 0.5 mm thick black-painted aluminum sheet has been placed at the bottom of the glass. The glass above the solar collector was the same width and length as the storage unit. An 8-cm-thick layer of insulating material was positioned between the storage unit's inner and outer sections in order to reduce heat loss. Within the storage unit, three distinct tube exchangers with a counter-flow configuration and made of aluminum sheets were arranged in parallel. In order to optimize heat transfer between the cold air entering the storage unit and the soapstone inside the exchanger tubes, a counter flow configuration was employed. Soapstone was the storage material utilized in the unit.

This storage material was collected from Ngaka hill, which is situated in the village of Kikombo-Mnadani in the urban district of Dodoma, Tanzania. It was then cut into cubes with edges measuring 2 cm each, and they were inserted into all the storage spaces that the three exchanger tubes left empty instead of inside of them. Figure 11 and Table 6 describe the primary equipment and materials used in the heat pump system, respectively.

Table 6: Materials used and description

Components	Description
Drying chamber	Material: 1.5 mm Galvanized steel sheets Dimension: 3.6 m2 Insulation material: 6 mm thick Fiberglass
Solar collector	Materials: Glass, and 0.5 mm aluminum sheet Dimension:1m long X 70cm wide X 6cm thick Insulation material: 6 mm thick Fiberglass
Thermal energy storage	Materials: Soapstone, 1.5 mm mild steel sheet, and 0.5 mm aluminum sheet Dimension: 1m long X 70cm wide X 40cm thick Insulation material: 6 mm thick Fiberglass
Duct	Material: 1.5 mm mild steel sheet Dimension: 1.6m long Insulation material: 6 mm thick Fiberglass
Ventilator	Material: stainless steel Dimension: 300 mm
Trays	Materials: plastic wire mesh, Galvanized steel sheets Dimension: 43m long X 40cm wide X 3cm thick Number of trays: 08

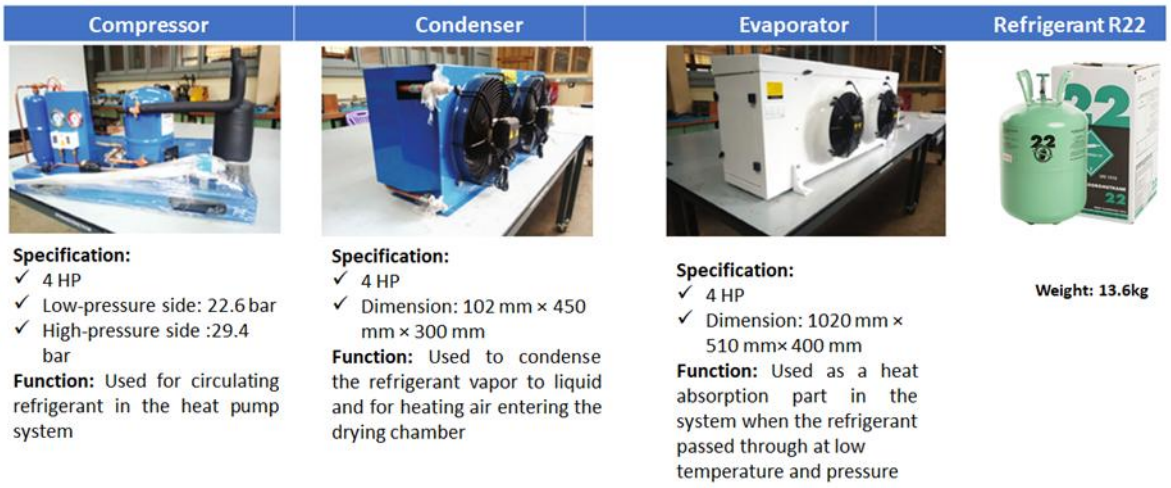

Figure 11: Equipment used in the heat pump system

3.2 Experimental setup

The experimental setup was established at Arusha Technical College (ATC) in Tanzania. Figure 12 shows a 3D diagram and the photo of the developed solar-assisted heat pump dryer (SAHPD) integrated with thermal energy storage (TES).

Figure 12: 3D diagram (on the left) and Photo (on the right) of the developed solar-assisted heat pump dryer integrated with thermal energy storage (Loemba *et al.*, 2024; Loemba *et al.*, 2023)

3.3 Experimental procedure

All of the samples used in this study (Cavendish banana fruit, Moringa *oleifera* leaves, and tomatoes) were obtained from the Kilombero market, which is one of Arusha's largest marketplaces.

After being purchased, each sample was meticulously cleaned in water, peeled (case of banana), and manually cut into slices (case of tomatoes and banana) that were between one and two millimeters thick. These slices were then placed on trays inside the drying chamber. To get a suitable average, the experiment was conducted three times for each mode of operation, as suggested by Singer *et al.* (2007).

The standard procedure of drying a sample in an oven and calculating moisture content based on the weight difference between dry and wet materials was used to determine each sample's initial moisture content. The goal of each experiment was to examine the life cycle, performance, and economic effects of the suggested dryer in different operating scenarios. Additionally, mineral and vitamin analyses as well as proximate analyses were performed.

3.4 Data measurements and uncertainty analysis

Table 7 lists the parameters that were measured, the data collection tools that were employed, and their particular features. At 30-minute intervals, both manual and automatic data collection was conducted.

The uncertainties was evaluated using equation (1) (Sundari & Veeramanipriya, 2022):

$$U_R = \sqrt{\left[\left(\frac{\partial R}{\partial x_1}U_1\right)^2 + \left(\frac{\partial R}{\partial x_2}U_2\right)^2 + \left(\frac{\partial R}{\partial x_3}U_3\right)^2 + \cdots \left(\frac{\partial R}{\partial x_n}U_n\right)^2\right]} \qquad (1)$$

The total uncertainty for the measurement of temperatures at various places such as inlet of the drying chamber (U_{TI}), outlet of the drying chamber (U_{TO}), and ambient temperature (U_{TA}) and readings ($U_{Reading}$) is calculated using equation (2):

$$U_{Temperature} = \sqrt{{U_{Measurement}}^2 + {U_{Reading}}^2}$$

$$= \sqrt{{U_{TI}}^2 + {U_{TO}}^2 + {U_{TA}}^2 + {U_{Reading}}^2} = \sqrt{(0.1)^2 + (0.1)^2 + (0.1)^2 + (0.1)^2} = 0.2\% \qquad (2)$$

The total uncertainty for the measurement of relative humidity at various places such as inlet of the drying chamber (U_{RHI}), outlet of the drying chamber (U_{RHO}), and ambient temperature (U_{RHA}) and readings ($U_{Reading}$) is calculated using equation (3):

$$U_{Humidity} = \sqrt{U_{Measurement}{}^2 + U_{Reading}{}^2}$$

$$= \sqrt{U_{RHI}{}^2 + U_{RHO}{}^2 + U_{RHA}{}^2 + U_{Reading}{}^2} = \sqrt{(0.1)^2 + (0.1)^2 + (0.1)^2 + (0.1)^2} = 0.2\% \qquad (3)$$

The total uncertainty for the measurement of weight loss is calculated using equation (4):

$$U_{Weight} = \sqrt{U_{Measurement}{}^2 + U_{Reading}{}^2} = \sqrt{(0.1)^2 + (0.1)^2} = 0.141421\% \qquad \textbf{(4)}$$

The total uncertainty for the measurement of solar radiation is calculated using equation (5):

$$U_{Radiation} = \sqrt{U_{Measurement}{}^2 + U_{Reading}{}^2} = \sqrt{(0.1)^2 + (0.1)^2} = 0.141421\% \qquad \textbf{(5)}$$

The total uncertainty for the measurement of power consumption is calculated using equation (6):

$$U_{Power} = \sqrt{U_{Measurement}{}^2 + U_{Reading}{}^2} = \sqrt{(0.1)^2 + (0.1)^2} = 0.141421\% \qquad \textbf{(6)}$$

The total uncertainty for the measurement of wind is calculated using equation (7):

$$U_{wind} = \sqrt{U_{Measurement}{}^2 + U_{Reading}{}^2} = \sqrt{(0.1)^2 + (0.1)^2} = 0.141421\% \qquad \textbf{(7)}$$

Then, the total uncertainty of the drying experiment may be calculated using equation (8):

$$U_{total} = \sqrt{U_{Temperature}{}^2 + U_{humidity}{}^2 + U_{Weight}{}^2 + U_{Radiation}{}^2 + U_{Power}{}^2 + U_{wind}{}^2}$$
$$= 0.982693\% \qquad \textbf{(8)}$$

Table 7: Measurement instruments and uncertainty

Instruments	Parameters	Range	Accuracy	Resolution	Error (%)
Anemometer	Air velocity	0 to 30 m/s	±5%	0.1 m/s	0.141421
Temperature humidity data logger (SSN-22)	Temperature and humidity	Temperature: -35 to 80	Temperature: ±3 ℃	±0.1℃	0.2
		Humidity: 0 to 100%	Humidity: ±3%	0.1RH	0.2
Thermocouple temperature data logger (SSN-61)	Temperature	-180 to 1250 ℃	±5%	±0.1℃	0.2
Digital balance (FF1976)	Weight	2 to 400 g	5g/10g	0.1g	0.141421
Solar power meter	Irradiance	2000 W/m^2	±5%	0.1w/m^2	0.141421
Temperature sensor	Temperature and humidity	Temperature: -40 to 80 ℃	Temperature: ±0.5℃	±0.1℃	0.2
		Humidity: 0 to 100%	Humidity: 2-5%	0.01RH	0.2
CT Sensor	Power consumption	10mA to 100A	± 3%	0.1	0.141421

3.5 Evaluation of the drying performance

3.5.1 Moisture content and drying rate

The moisture content and drying rate were calculated respectively using equations (9) and (10) (Aktaş *et al.*, 2017; Singh *et al.*, 2020b):

$$\boldsymbol{MC_{wb} = \frac{M_i - M_f}{M_i} \times 100} \quad \textbf{(9)}$$

$$\boldsymbol{DR = \frac{MC_{t+dt} - MC_t}{dt}} \quad \textbf{(10)}$$

3.5.2 Condenser heating capacity

Equation (11) was used to determine how much heat a condenser rejects:

$$\boldsymbol{Q_{cond} = \dot{m}_a C_{P,a}(T_{amb} - T_{cond})} \quad \textbf{(11)}$$

Where*:*

$$\boldsymbol{\dot{m}_a = \rho_a * S * v} \quad \textbf{(12)}$$

$$\boldsymbol{\rho_a = 1.292\ \frac{273.15}{Ta(K)}} \quad \textbf{(13)}$$

$$\boldsymbol{C_{P,a} = 1.0029 + 5.410^{-5} T_a} \quad \textbf{(14)}$$

Q_{cond} is the condenser heating capacity (kW), $\dot{m}_a$ is the mass flow rate of the air (kg/s), S is the surface of the drying chamber, v is the velocity of air in the drying chamber, ρ_a is the air density in drying chamber, $C_{P,a}$ is the specific heat of air (kJ/kg °C), T_{amb} is the ambient temperature (°C) and T_{cond} is the air temperature at outlet of the condenser (°C) (Mohanraj, 2014).

3.5.3 Coefficient of Performance

The coefficient of performance (COP) was determined by dividing the quantity of heat delivered by the condenser by the total energy consumed by the whole system as shown in equation (15) (Mohanraj, 2014):

$$\boldsymbol{COP_{HP}} = \frac{\boldsymbol{Q_{cond}}}{\boldsymbol{Q_{total\ consumed}}} \quad (\mathbf{15})$$

Q_{cond} is the condenser heating capacity calculated using equation 10, and $Q_{total\ consumed}$ is the total energy consumed by the whole system obtained using CT Sensor.

3.5.4 Specific moisture extraction rate

The specific moisture extraction rate (SMER) will be calculated using equation (16) (Kesavan *et al.,* 2019; Singh *et al.*, 2020b):

$$\boldsymbol{SMER} = \frac{\boldsymbol{M_w}}{\boldsymbol{Total\ energy\ input\ per\ unit\ time}} \quad \mathbf{(16)}$$

SMER is the specific moisture extraction rate(kg/kWh), M_w is the mass of water removed (kg).

Where:

$$\boldsymbol{M_w} = \frac{\boldsymbol{M_p(MC_i - MC_f)}}{\boldsymbol{(100 - MC_f)}} \quad \mathbf{(17)}$$

MC_f is the final moisture content of the product (%), M_p is the mass of fresh samples (kg) and MC_i is the initial moisture content of the product (%).

3.5.5 Efficiency of the solar collector integrated with storage material

Efficiency of solar collector integrated with soapstone as storage material was evaluated using equation (18) (energy, 2015):

$$\eta_{col} = \frac{E_{stored}}{E_{stored,max}} \times 100 \quad (18)$$

$E_{stored} = mC_P(T_{out,col} - T_{in,col})$ is the energy stored at time t. and $E_{stored,max}$ is the maximum energy stored at time t.

3.5.6 Dryer efficiency

The drying efficiency is calculated using equation (19):

$$\eta_{\boldsymbol{d}} = \frac{\boldsymbol{L_v M_w}}{\boldsymbol{Q_{totalconsumed}}} \times \mathbf{100} \quad \mathbf{(19)}$$

L_V is the latent heat of vaporization of water, M_w is the mass of water removed (kg) and $Q_{total\ consumed}$ is the total energy consumed by the whole dryer (kWh).

3.6 Determination of proximate content

3.6.1 Determination of proximate content when drying moringa oleifera leaves

(i) Preparation of Sample

Moringa leaves, both fresh and dried, were ground into fine powder using an electric blender. The fine powder was then used for the analysis.

(ii) Analysis of Sample

Proximate analysis was performed on the powdered leaves to determine the presence of moisture, protein, ether extract (fat), ash, crude fiber, and carbohydrate using standard analytical methods as described in the Official Methods of the Association of Official Analytical Chemists (AOAC Association of official analytical chemist 19th edition, 2012) (Aoac, 1990).

(iii) Chemical reagent used

These chemicals reagents include sodium hydroxide (NaOH, 2 M), hydrochloric acid (HCl, O.1 N), sulphuric acid (H_2SO_4, 0.05 N), phosphoric acid (H_3PO_4, 85%), sodium carbonate solution, gallic acid, methanol, acetonitrile solution, meta-phosphoric acid (HPO_3), acetronile solution, ammonium, molybdate, acetronile-methanol (CH_3CN), trichloroacetic acid, petroleum ether and 2.6-dicholorophenol.

(iv) Determination of moisture content

Moisture content was determined using the oven drying method. Five grams of powdered sample were accurately weighed and placed in a clean, dry Petri dish. The sample was dried in an oven at 105 0C for 24 hours until a consistent weight was achieved. The sample was then placed in the desiccator to cool for 30 minutes. After cooling, the sample was weighed again, being careful not to expose it to the atmosphere. The moisture content (%) was calculated using the following formula (AOAC Association of official analytical chemist 19th edition, 2012).

$$\boldsymbol{MC}\ (\%) = \frac{\boldsymbol{Moisture\ Weight}}{\boldsymbol{Weight\ of\ sample}\ (\boldsymbol{g})} \times \mathbf{100} \quad \textbf{(20)}$$

(v) Determination of ash content

The ash contents were determined using the dry ashing method; a clean empty crucible was placed in a muffle furnace at 550 °C for an hour to ensure that all possible impurities on the crucible surface were burned off. After cooling in the desiccator for 30 minutes, the weight of the empty crucible was measured. Five grams of sample were placed in the crucible. The crucible and its contents were placed in a muffle furnace and heated for 24 hours. After complete heating, the sample in the crucible was cooled in the desiccator. The ash content was calculated using the following formula (AOAC Association of official analytical chemist 19th edition, 2012).

$$\boldsymbol{Ash\ content}\ (\%) = \frac{\boldsymbol{Weight\ of\ Ash}(\boldsymbol{g})}{\boldsymbol{weight\ of\ sample}(\boldsymbol{g})} \times \mathbf{100} \quad \textbf{(21)}$$

(vi) Determination of crude protein

The crude Protein was determined by Kijeldahl method, as described in Association of Official Analytical Chemists (AOAC Association of official analytical chemist 19th edition, 2012). This method involved heating samples with concentrated sulfuric acid (H_2SO_4) in the presence of a Kjeldahl catalyst. The mixture was then alkalized and distilled into a boric acid solution. The borate ions formed were titrated against standard sulphuric acid 0.05 N, which was converted to total nitrogen in the sample and multiplied by a conversion factor of 6.25 to crude protein.

$$\boldsymbol{Nitrogen}(\%) = \frac{(\boldsymbol{Vs}-\boldsymbol{Vb})\times\boldsymbol{N}\times\mathbf{1.401}}{\boldsymbol{weight\ of\ sample}(\boldsymbol{g})} \times \mathbf{100} \quad \textbf{(22)}$$

$$\boldsymbol{CP}\ (\%) = \boldsymbol{Nitrogen}\ (\%) \times \mathbf{6.25} \quad \textbf{(23)}$$

(vii) Determination of fat content

Total fat was determined using Soxhlet ether extraction, which involved placing five grammes of powered sample into an extraction thimble and connecting it to the Soxhlet apparatus. The fat analyzer machine used 70 ml of petroleum ether for the extraction process in three automatic phases. Boil for 15 minutes, rinse for 30 minutes, and recover with petroleum ether for 10 minutes. The remaining petroleum ether was then evaporated in an oven. Pre-weighed cups containing fat were dried in an oven at 105 °C for 1 hour to evaporate any remaining petroleum

ether, then cooled in a desiccator for 30 minutes before reweighing. The percentage of fat was calculated using the formula (AOAC, 2012):

$$\boldsymbol{Fat\ Content}\ (\%) = \frac{\boldsymbol{Weight\ of\ crude\ fat(g)}}{\boldsymbol{Weight\ of\ samples(g)}} \quad \textbf{(24)}$$

(viii) Determination of crude fiber

This analysis involves two stages of digestion, which were acid and alkaline solutions, using the method described by the Association of Official Analytical Chemists (AOAC, 2012) and the crude fiber is calculated, thus:

$$\boldsymbol{Crude\ fiber}\ (\%) = \frac{(\boldsymbol{Weight\ of\ residual - Weight\ of\ ash})}{\boldsymbol{Weight\ of\ samples}\ (\boldsymbol{g})} \times \mathbf{100} \quad \textbf{(25)}$$

(ix) Determination of Total Carbohydrate

Total soluble carbohydrate was calculated by subtracting the sum of all the proximate compositions from 100% (Aoac, 1990).

3.6.2 Determination of proximate content when drying banana

(i) Preparation of Sample

Using an electric blender, the dried and fresh Cavendish bananas (Musa acuminata) were finely powdered. After that, the analysis made use of the fine powder.

(ii) Analysis of Sample

Proximate analysis was performed using standard analytical techniques as outlined by the Official Methods of the Association of Official Analytical Chemists on the powdered Cavendish banana (Musa acuminata) to ascertain the presence of moisture, protein, fat, ash, crude fiber, and carbohydrates (AOAC Association of official analytical chemist 19th edition, 2012) (AOAC, 1990).

(iii) Chemical reagent used

These chemicals reagents include sodium hydroxide (NaOH, 2 M), hydrochloric acid (HCl, O.1 N), sulphuric acid (H_2SO_4, 0.05 N), phosphoric acid (H_3PO_4, 85%), sodium carbonate solution, gallic acid, methanol, acetonitrile solution, meta-phosphoric acid (HPO_3), acetronile

solution, ammonium, molybdate, acetronile-methanol (CH_3CN), trichloroacetic acid, petroleum ether and 2.6-dicholorophenol.

(iv) Determination of moisture content

The oven drying method was used to determine the moisture content. A dry, spotless Petri dish was filled with five grams of the powdered sample, which had been precisely weighed. The sample was dried in an oven set to 105 degrees Celsius for a full day in order to achieve a consistent weight. After that, the sample was cooled for 30 minutes in the desiccator. It was carefully weighed once more after cooling so as not to expose the sample to air. The moisture content was calculated using equation (26) (AOAC, 2012).

$$\boldsymbol{MC}\ (\%) = \frac{\boldsymbol{Moisture\ Weight}}{\boldsymbol{Weight\ of\ sample(g)}} \times \mathbf{100} \qquad \textbf{(26)}$$

(v) Determination of ash content

The amount of ash was ascertained by dry ashing. To make sure that any potential impurities on the crucible's surface were burned off; a clean, empty crucible was placed in a muffle furnace and heated to 550 °C for an hour. After 30 minutes of cooling in the desiccator, the empty crucible's weight was recorded. A sample weighing five grams was added to the crucible. The crucible and its contents were heated for a full day in a muffle furnace. The sample in the crucible was cooled in the desiccator following full heating. The ash content (%) was calculated using equation (27) (AOAC, 2012).

$$\boldsymbol{Ash\ content}\ (\%) = \frac{\boldsymbol{Weight\ of\ Ash(g)}}{\boldsymbol{weight\ of\ sample(g)}} \times \mathbf{100} \qquad \textbf{(27)}$$

(vi) Determination of crude protein

The crude Protein was determined by Kijeldahl method, as described in Association of Official Analytical Chemists (AOAC Association of official analytical chemist 19th edition, 2012). By heating samples with concentrated sulfuric acid (H_2SO_4) in the presence of Kjeldahl catalyst, the samples were digested using this method. After turning the mixture alkaline, it was distilled into a solution containing boric acid. The generated borate ions were titrated against standard sulfuric acid (0.05 N), which is multiplied by the 6.25 conversion factor to yield crude protein and then converted to total nitrogen in the sample.

$$\boldsymbol{Nitrogen}(\%) = \frac{(\boldsymbol{Vs}-\boldsymbol{Vb})\times \boldsymbol{N}\times \mathbf{1.401}}{\boldsymbol{weight\ of\ sample}(\boldsymbol{g})} \times \mathbf{100} \quad \textbf{(28)}$$

$$\boldsymbol{CP}\ (\%) = \boldsymbol{Nitrogen}\ (\%) \times \mathbf{6.25} \quad \textbf{(29)}$$

(vii) Determination of fat content

Using Soxhlet ether extraction, which involves putting five grams of powered sample into the extraction thimble and assembling the Soxhlet apparatus, the total fat was ascertained. The fat analyzer machine's three automatic phases of the extraction process used 70 milliliters of petroleum ether. The 15-minute boiling phase, the 30-minute rinsing phase, and the 10-minute petroleum ether recovery phase. After that, the leftover petroleum ether was evaporated in an oven.

To remove any last traces of petroleum ether, pre-weighed cups containing fat were dried for an hour at 105 °C in a desiccator. After cooling for half an hour, the cups were weighed again. Percentage fat was calculated by using equation (30) (AOAC, 2012):

$$\boldsymbol{Fat\ Content}\ (\%) = \frac{\boldsymbol{Weight\ of\ crude\ fat}(\boldsymbol{g})}{\boldsymbol{Weight\ of\ sample}(\boldsymbol{g})} \quad \textbf{(30)}$$

(viii) Determination of crude fiber

This analysis used the technique outlined by the Association of Official Analytical Chemists, which involved two stages of digestion: Acid and alkaline solution (AOAC Association of official analytical chemist 19th edition, 2012) and the crude fiber is calculated, thus:

$$\boldsymbol{Crude\ fiber}\ (\%) = \frac{(\boldsymbol{Weight\ of\ residual}-\boldsymbol{Weight\ of\ ash})}{\boldsymbol{Weight\ of\ sample}(\boldsymbol{g})} \times \mathbf{100} \quad \textbf{(31)}$$

(ix) Determination of total carbohydrate

Total soluble carbohydrate was calculated as the difference between 100% and the sum of all proximate composition (AOAC, 1990).

(x) Determination of energy

The number of grams of fat, protein, and carbohydrate were multiplied by 4, 4, and 9 to get the nutritional energy value (calorie).

3.6.3 Minerals and vitamins analysis of banana

(i) Minerals

The minerals were identified by burning one gram of the homogenized sample for four hours at 450 °C in a furnace. The minerals are copper, iron, phosphorus, calcium, zinc, and manganese. Following a mixture of the sample's ashes and 10 milliliters of a 6% hydrochloric acid solution, the mixture was filtered through Whatman filter papers and diluted with 100 milliliters of distilled water. The filtrates were then read using an atomic absorption spectrophotometer (Jorhem & Engman, 2000).

(ii) Vitamin C

After the homogenized sample was ground in a mortar and pestle, five grams of it was used to measure the amount of vitamin C. Next, 25 milliliters of 10% trichloroacetic acid was added. After that, the extracted sample was placed in a 50 ml volumetric flask and the proper concentration of trichloroacetic acid solution was added. The diluted sample was then filtered through Whatman filter papers. After that, a UV/Vis spectrophotometer was used to read the filtrates (Bineesh *et al.*, 2005).

(iii) Vitamin B6

To determine vitamin B6, one gram of the material was homogenized with 50 milliliters of 0.1 N hydrochloric acid, transferred to a 125 milliliter Erlenmeyer flask, filtered, and allowed to degas for five minutes. After a 10-milliliter degassed sample was added to volumetric flasks, the sample was diluted with 0.1 N HCl, and the absorbance was measured (Ogunneye *et al.*, 2020).

3.7 Techno-economic analysis

The capital costs (CC), production costs (PC), profit (PR), return on capital (ROR), payback period (PB), and net present value (NPV) are the primary parameters that were examined. The total cost of all component purchases and installation was used to determine the system's capital costs (CC). The cost of production included the cost of raw materials (RC), labor cost(LC), electricity (EC), and additional costs (AC), which include insurance cost (IC) and maintenance costs (MI).The production cost was calculated as follows (Fudholi *et al.*, 2015):

$$PC = RC + LC + EC + AC \quad \textbf{(32)}$$

$$AC = MC + IC \quad \textbf{(33)}$$

Profit (PR) is actually the difference between total sales (TS), capital costs (CC) and cost of production (PC) and is calculated as follows (Fudholi *et al.*, 2015):

$$PR = TS - CC - PC \quad \textbf{(34)}$$

Return of capital will be calculated using equation (11) (Fudholi *et al.,* 2011):

$$ROR = \frac{PR}{CC} \quad \textbf{(35)}$$

The Payback (PB) is defined as the investment cost per average annual net income (Fudholi *et al.*, 2015):

$$PB = \frac{CC}{PR} \quad \textbf{(36)}$$

The net present value (NPV) will be calculated using equation (13) (Fudholi *et al.*, 2015):

$$NPV = \sum_{n=1}^{N} P_n(1+i)^n - CC \quad \textbf{(37)}$$

Where $P_n = S(1+i)^{-n}$ **(38)**

P_n is the discounted present value (S) to be invested in the n years.

3.8 Life cycle analysis

The goal of life cycle assessment (LCA) is to evaluate environmental impacts using data from life cycle inventories (LCI). The life cycle assessment is used in this study to evaluate the environmental impact of the drying process of tomatoes in two different operating modes, the solar-assisted heat pump dryer integrated with thermal energy storage (Mode 1) and without thermal energy storage (Mode 2). Figure 13 depicts the methodological framework for

conducting life cycle analysis, which includes four phases: goal and scope definition, inventory analysis, impact analysis, and interpretation (Saoud *et al.*, 2021).

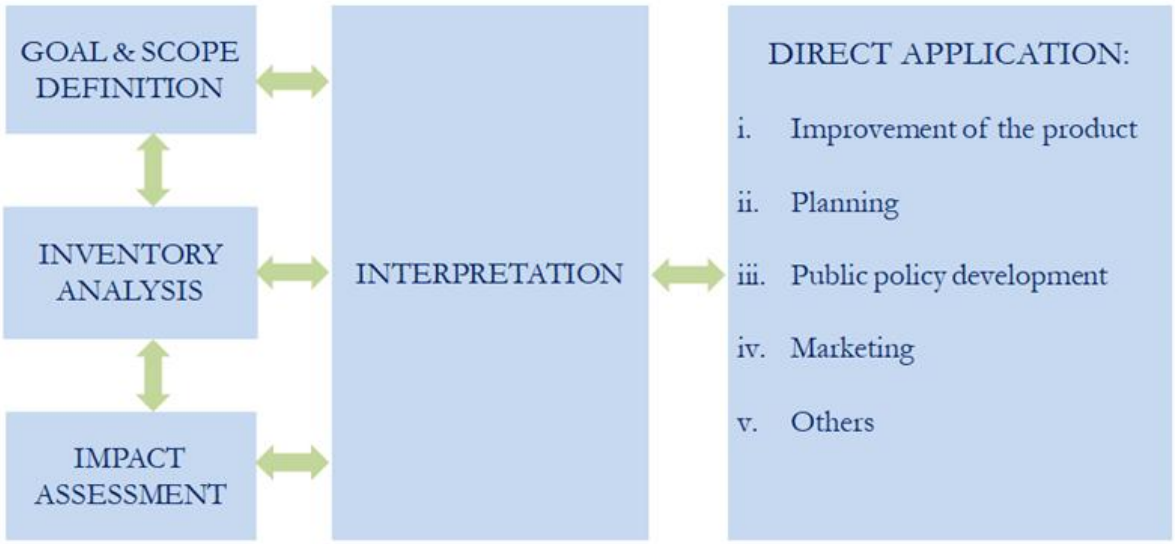

Figure 13: Life cycle assessment phases

3.8.1 Goal and scope definition

This step lays out the goals of the study, including the application to be used and the manner in which the findings will be shared. This stage additionally defines the scope of the study, including the functions of the system or product under investigation, the selected functional unit, the boundaries of the system, and the study limitations. In this study the goal of the life-cycle assessment (LCA) is to compare the environmental impact of solar-assisted heat pump dryers with and without thermal energy storage. The functional unit for this study was 1 kg of dried tomatoes. The boundary chosen was "Gate-to-Gate," which means that only the process's emission was considered.

3.8.2 Inventory analysis

This phase inventories the material and energy flows that are input and output in relation to the life cycle stages of the functional unit that was selected. The majority of the data in this study were computed or obtained experimentally, and Ecoinvent was used to model the corresponding flow of energy, materials, and emissions.

3.8.3 Life cycle impact assessment

The impact assessment method chosen for this study is ReCiPe 2016 Midpoint v.1.0 under Hierarchist, H perspective. All of the impact categories for the method are displayed in Table 8, along with descriptions of each.

Table 8: Impact categories

Impact Categories	Unit	Sahpd With Tes	Sahpd Without Tes
Terrestrial ecotoxicity	kg 1,4-DCB	4.24257	5.93522
Human non-carcinogenic toxicity	kg 1,4-DCB	3.68363	5.1542
Global warming	kg CO2 eq	2.19533	3.07116
Marine ecotoxicity	kg 1,4-DCB	0.24008	0.33596
Freshwater ecotoxicity	kg 1,4-DCB	0.18713	0.26186
Fossil resource scarcity	kg oil eq	0.15621	0.178635
Human carcinogenic toxicity	kg 1,4-DCB	0.15115	0.21128
Ionizing radiation	kBq Co-60 eq	0.114681	0.160496
Land use	m2a crop eq	0.07267	0.1017
Water consumption	m3	0.04108	0.0555
Terrestrial acidification	kg SO2 eq	0.01158	0.0162
Ozone formation, Terrestrial ecosystems	kg NOx eq	0.00426	0.00596
Ozone formation, Human health	kg NOx eq	0.00422	0.0059
Fine particulate matter formation	kg PM2.5 eq	0.00388	0.00542
Mineral resource scarcity	kg Cu eq	0.00359	0.00501
Freshwater eutrophication	kg P eq	0.00231	0.00324
Impact Categories	**Unit**	**Sahpd With Tes**	**Sahpd Without Tes**
Marine eutrophication	kg N eq	0.00016	0.00023
Stratospheric ozone depletion	Kg CFC11 eq	1.20E-06	1.68E-06

3.8.4 Interpretation of the results

In this phase, which builds on the preceding three, the results are interpreted with an emphasis on making recommendations, identifying limitations, and drawing conclusions. To that end, the results must satisfy the study's objectives

3.9 Statistical analyses

The one-way analysis of variance (ANOVA) was used in Microsoft Excel to statistically assess the proximate, minerals, and vitamins data. This means that multiple correlation analysis, standard deviations, and statistical significance ($p < 0.05$) of the data were all performed using Microsoft Excel.

CHAPTER FOUR

RESULTS AND DISCUSSION

4.1 Drying performance

4.1.1 Drying performance when drying tomatoes

The dryer's performance was evaluated by drying 1000 g of tomatoes with an initial moisture content of 92.5% (wet basis) in two drying modes. The drying process was terminated for both modes when the final moisture content reached 8.5%. This section investigates the dryer's performance by examining parameters such as drying temperature, relative humidity, moisture content, drying rate, specific moisture extraction rate, and coefficient of performance.

Figures 14 to 19 display the findings for each parameter that was examined. The averages and standard deviations are displayed in the graphs.

The drying chamber's temperature variations are depicted in Fig. 14. Using modes 1 and 2, the inlet temperature of the drying chamber was 50.5 °C and 55.12 °C, respectively. The solar-assisted heat pump dryer (SAHPD) with thermal energy storage (TES) in Mode 1 was found to have the highest temperature. The temperatures reached with the developed dryer correspond to acceptable ranges as compared to previous studies (Atalay, 2019; Coşkun *et al*., 2017; Şevik, 2014).

As seen in Fig. 16, after drying 1000 g of tomatoes for 270 and 330 minutes, respectively, using SAHPD with thermal energy storage during the day (Mode 1) and SAHPD without TES during the day (Mode 2), the final moisture content of 8.5% (wet basis) was obtained. As a result, the efficiency of the two modes in reducing moisture content is significant. When compared to Mode 2, Mode 1 has the best performance, as evidenced by its significantly shorter drying time of 270 minutes. The importance of including a TES in a SAHPD is underscored by these findings. In comparison to other studies that have been published (Atalay, 2019; Coşkun *et al.*, 2017; Şevik, 2014), the dryer that was investigated in this study showed more favorable drying times and was able to achieve significantly lower final moisture content. The performance of a heat pump dryer was also investigated by Atalay (2019). On the first day, 2 kg of tomatoes were dried, followed by 4 kg on the second day and 7kg on the third day. The drying was done

at a fixed temperature of 50 °C. The average drying time was 5.15 hours, from an initial moisture content of 94.5% to a final moisture content of 10%.

These results confirm the exceptional efficiency of the developed SAHPD in both operating modes based on the results of all thermal performances analyzed. Using Mode 1 and 2, the study's average drying rates were 0.31 and 0.25% per minute, respectively. An average coefficient of performance (COP) of 4.42 and 2.72, respectively, was determined for modes 1 and 2. The energy-efficient operation of the dryer in both tested modes is once again highlighted by these findings. The highest COP was obtained in Mode 1. This result can be attributed to lower energy requirements as a result of the shorter drying time required for 1000 g of tomatoes. These findings highlight the significant potential for energy savings and the SAHPD system's favorable performance, particularly in Mode 1. The high COP attained in Mode 1 illustrates the importance of using thermal energy storage in the current dryer. The variation of the specific moisture extraction rate is shown in Fig. 17. This graph demonstrates how the specific moisture extraction rate rapidly decreased with drying time due to a decrease in moisture content. For Mode 1 and 2, the average specific moisture extraction rate was 0.22 kg/kWh and 0.15 kg/kWh, respectively. Their respective energy consumptions of 4.88 and 6.83 kWh can be used to explain these differences. When compared with previous experimental studies on tomato drying, the COPs obtained in this study were superior to 1.96 obtained by Coşkun *et al.* (2017) and 2.7 obtained by Şevik (2014)

Consequently, this mode produced higher coefficients of performance (COP) and shorter drying times. Given the paucity of studies investigating the use of heat pump dryers for this particular application, these results highlight the significance of carrying out more research in tomato drying.

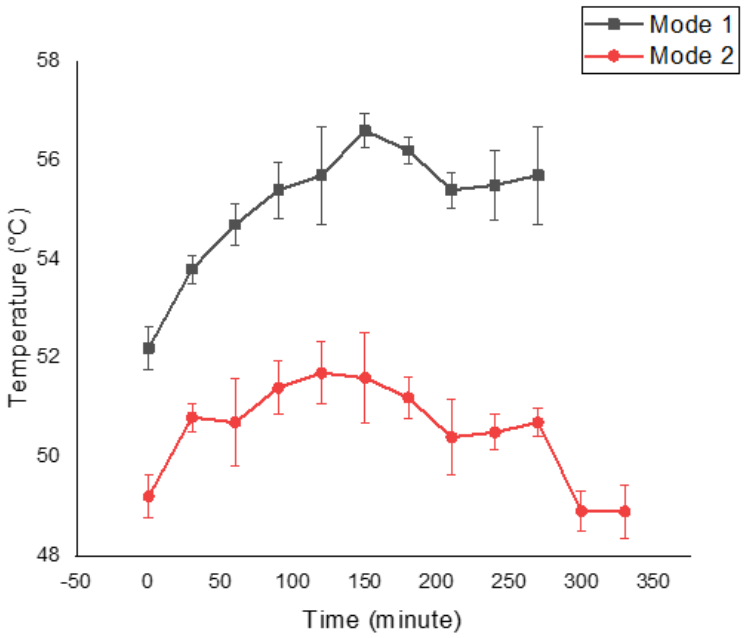

Figure 14: Variation of temperature in the drying chamber

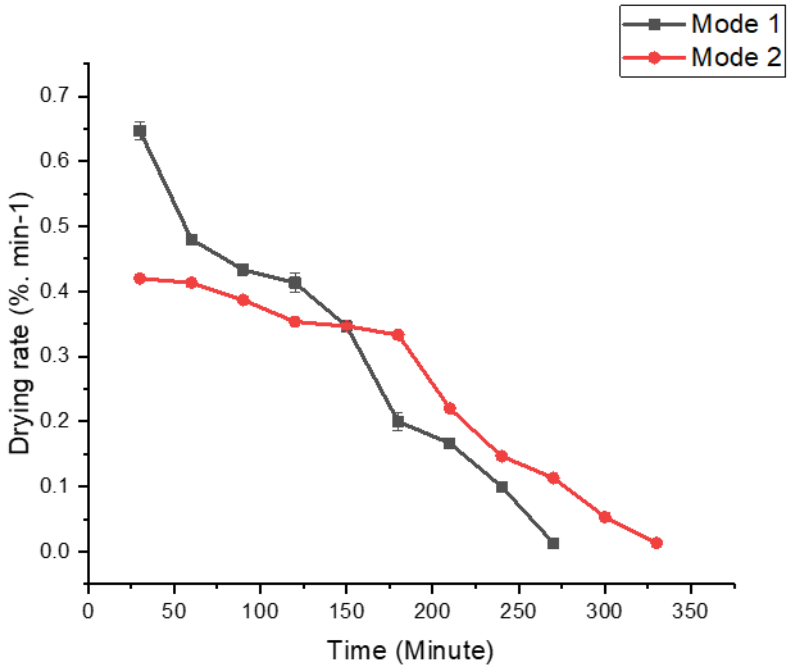

Figure 15: Variation of the drying rate

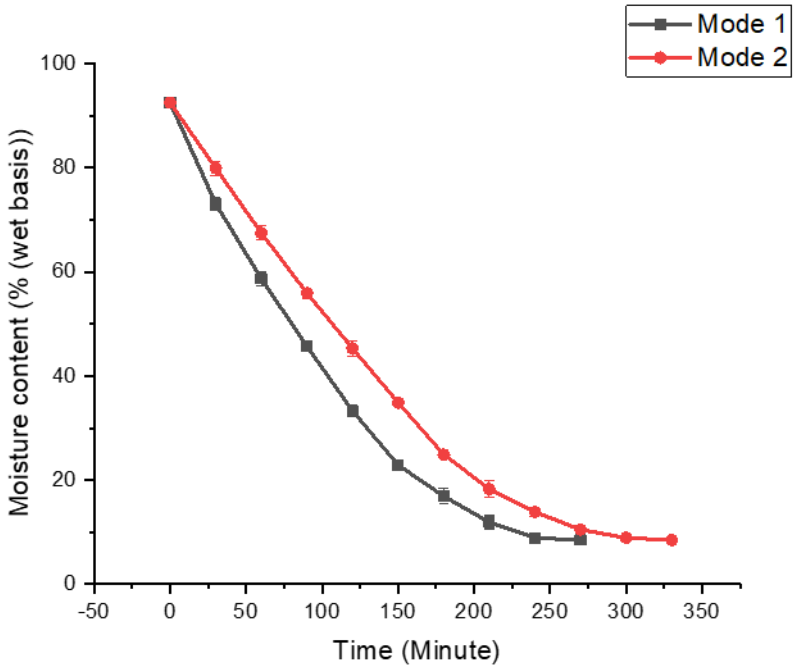

Figure 16: Variation of the moisture content

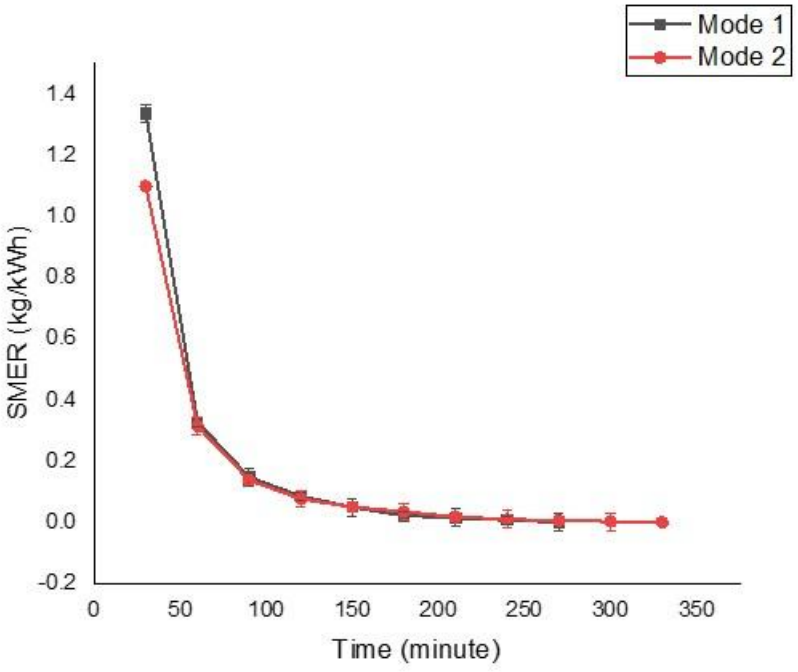

Figure 17: Variation of SMER

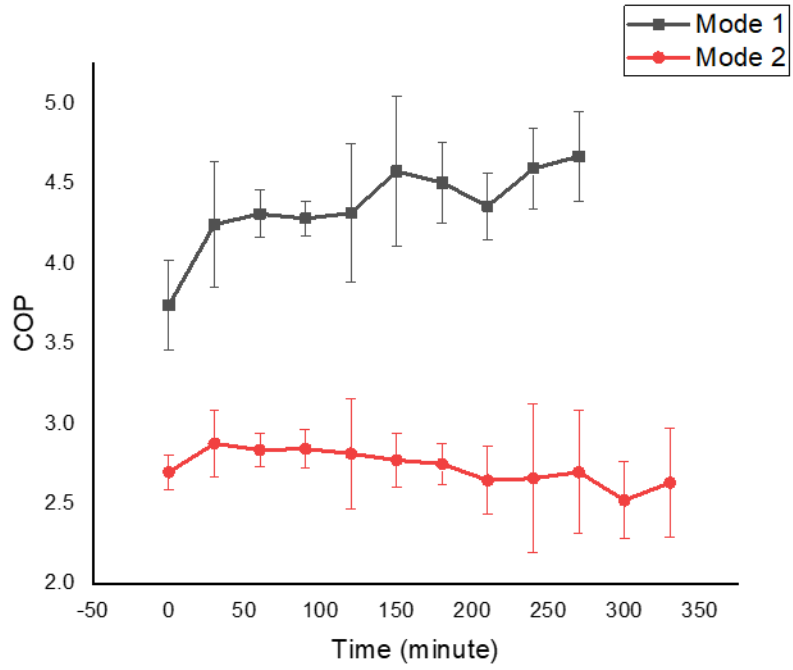

Figure 18: Variation of coefficient of performance

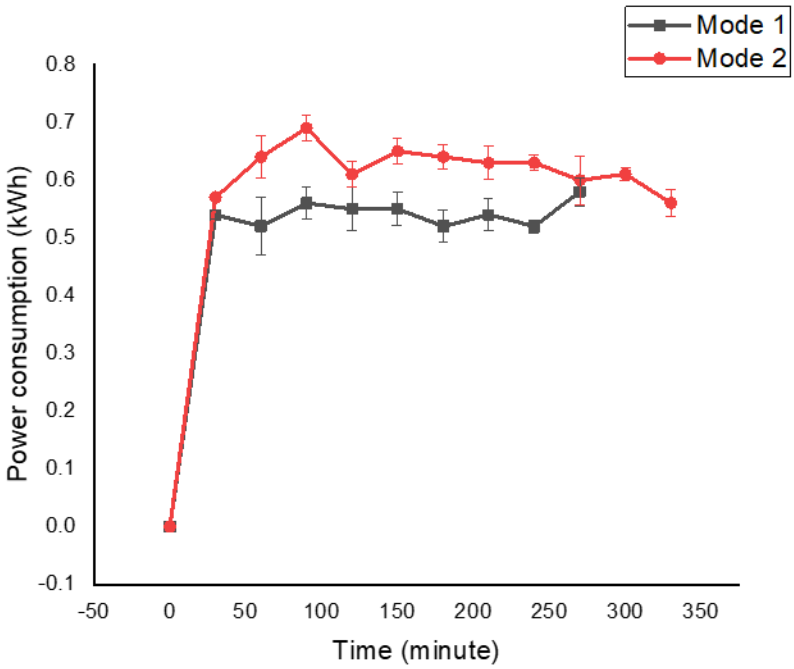

Figure 19: Variation of power consumption

4.1.2 Drying performance when drying moringa oleifera leaves

The moisture content, drying rate, and coefficient of performance (COP) were used to assess the drying system's performance. The average outcomes from three replicates for each parameter taken into account are shown in Figs. 20 to 22. Figure 20 illustrates how the moisture content of Moringa *oleifera* leaves dropped over the course of the five-hour drying process, from 75.7 to 3.3% in wet basis.

The drying rate as a function of drying time is shown in Fig. 21. The figure illustrates how the product's loss of moisture causes the drying rate to drop. Figure 22 illustrates the dryer's low energy consumption with an average COP value of 3.36. When employing a vacuum heat pump dryer to dry Moringa *oleifera* leaves, findings reported by Kumar *et al.* (2021) are mostly in agreement with these results. It was found that high temperatures greatly accelerated the rate of moisture removal. The drying air temperature averaged 50.12 °C, which is within an acceptable range when compared to the previously released results, as demonstrated by the study conducted by Ali *et al.* (2014), who dried Moringa *Oleifera* leaves at temperatures ranging from 40 to 60 °C. It is true that variations in solar radiation had an impact on this temperature. In every experiment, the average solar radiation was 740.9 W/m^2. The average relative ambient humidity was 46.12%, and the average ambient temperature was 25.10 °C. The average temperature and relative humidity at the drying chamber's inlet were 50.12 °C and 16.28%, respectively, while at the chamber's outlet they were 39.56 °C and 26.37%, respectively. Air enters the drying chamber at a high temperature with low relative humidity and exits at a low temperature with higher relative humidity, according to the differences in temperature or humidity between the inlet and outlet. This indicates that as more moisture evaporates from Moringa *oleifera* leaves, moisture is absorbed by the air moving through the drying chamber, resulting in a drop in temperature and an increase in relative humidity.

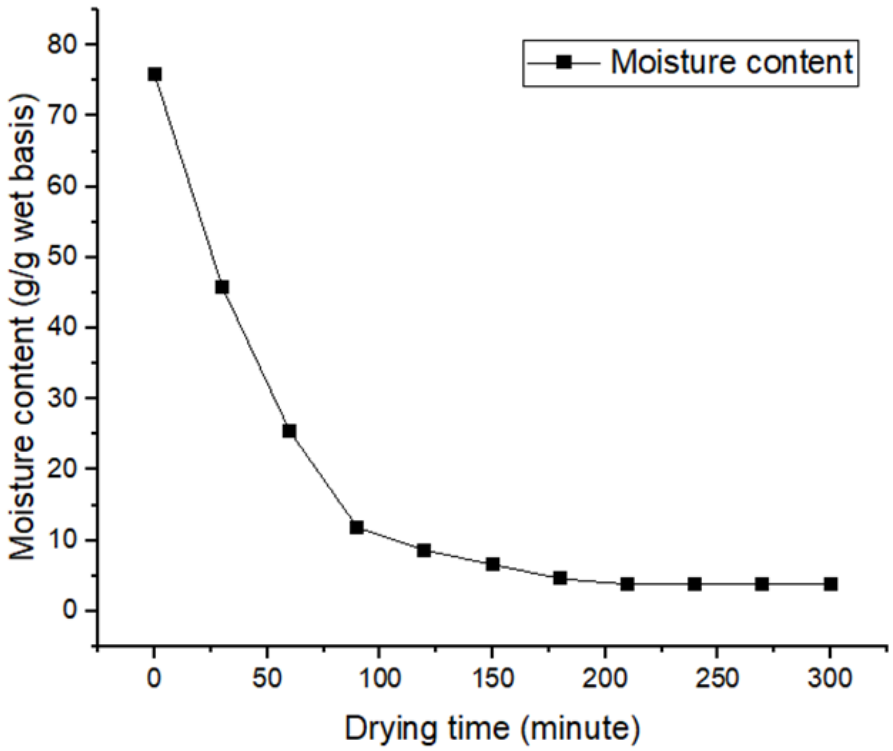

Figure 20: Variation of moisture content

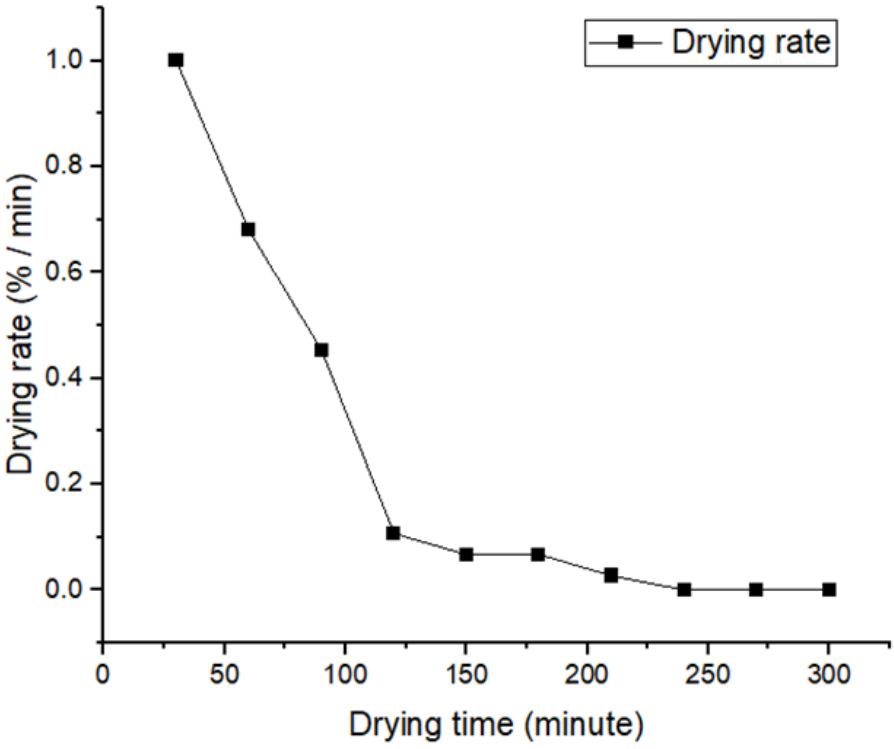

Figure 21: Variation of drying rate

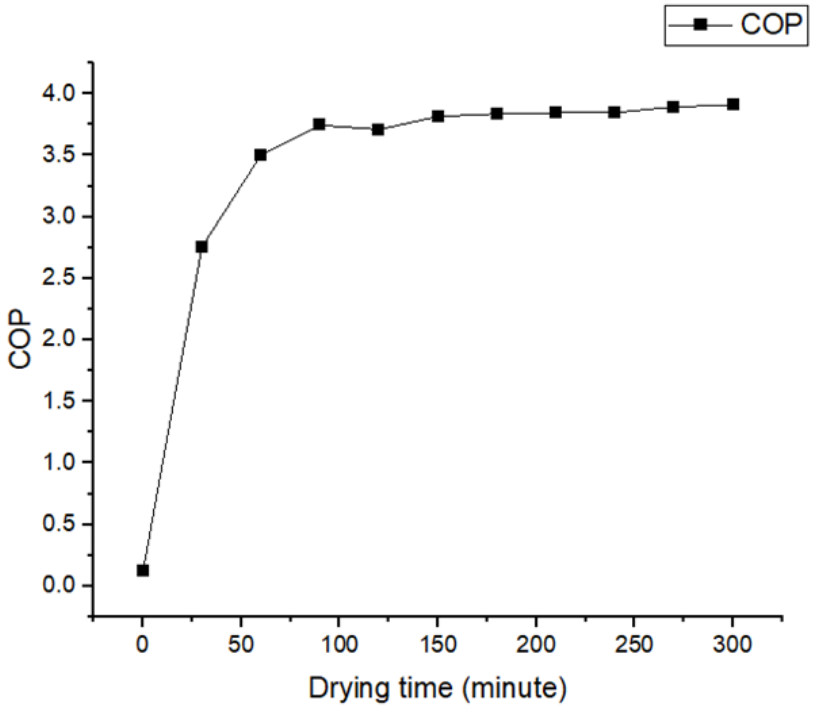

Figure 22: Variation of the coefficient of performance

4.1.3 Drying performance when drying banana

Using the three drying modes, 500 g of Cavendish bananas with an initial moisture content of 74.4% (wet basis) were dried in order to assess the overall performance of the dryer. When the final moisture content for each of the three modes reached 9.6%, the drying process was completed. The performance of the dryer is examined in this section by going over a number of different parameters, including the drying temperature variation, relative humidity, moisture content, drying rate, specific moisture extraction rate, coefficient of performance, and dryer efficiency.

The variation of all the parameters that were examined as a function of time is displayed in Figs. 23 to 30. The means and standard deviations are displayed in the graphs. Figure 23 illustrates the final moisture content (wet basis) of 9.6% that was achieved after 270, 390, and 360 minutes of drying 500 g of Cavendish bananas using SAHPD with TES during the day (Mode 1), SAHPD without TES during the night (Mode 2), and SAHPD without TES during the day (Mode 3). As a result, the three modes' effectiveness in lowering moisture content is noteworthy.

In comparison to Mode 2 and 3, Mode 1 performs significantly better, as seen by the significantly shorter drying time of 270 minutes. In contrast to the projections made by Kuan

et al. (2019) based on the simulation of banana drying using SAHPD, Using modes 1, 2, and 3, the drying times obtained in this study are 3.2, 3.5, and 5.25 times shorter, respectively. These striking outcomes bear witness to the extraordinary effectiveness exhibited by the developed SAHPD in all of its operational modes. The primary variables that are observed to have an effect on the decrease in moisture content during the drying process are the average drying temperature and the humidity in the drying chamber, as shown in Figure 30. The drying rate increases as the dryer's inlet temperature rises over time, reaching a maximum value before moisture loss from the product starts to reduce the drying rate, as seen in Figure 24.

In this study, 500 g of Cavendish bananas were dried at the average drying rates of 0.24%, 0.16%, and 0.18% per minute utilizing modes 1, 2, and 3. When compared to earlier research that looked into comparable drying techniques, these findings show encouraging and positive results. The findings demonstrate the potential of the employed modes to improve the drying process for Cavendish bananas in addition to validating the efficacy of the present study (Singh, *et al.*, 2020d)

The variation in solar radiation is shown in Fig. 27. This figure demonstrates that, in contrast to modes 1 and 2, when Mode 3 was utilized for drying, the sun's radiation entirely vanished within the first drying hour. This demonstrates unequivocally that, when utilizing Mode 3, the drying process began after sunset and continued into the night without the presence of sunlight. This demonstrates that using modes 1 and 2 resulted in extremely high temperatures in the drying chamber.

The variation of the coefficient of performance (COP) with drying time is depicted in Figure 25. The average coefficient of performance (COP) values were 3.69, 2.57, and 2.54 for modes 1, 2, and 3, respectively. These outcomes highlight the dryer's energy-efficient functioning and excellent performance in all three of the tested modes. Interestingly, the solar-assisted heat pump dryer (SAHPD) with thermal energy storage (TES) in Mode 1 during the day produced the highest coefficient of performance (COP).

This result can be explained by the lower energy needs brought about by the 500 g of Cavendish bananas requiring less time to dry. These results demonstrate the SAHPD system's good performance and significant energy-saving potential, especially in Mode 1.

This mode's optimization of energy consumption highlights the system's capacity to produce drying results that are both effective and sustainable while also improving overall operational

efficiency. The outcomes of COP in modes 1 and 2 closely resemble the forecasts made by Kuan *et al.* (2019), when drying banana using SAHPD without thermal energy storage. Consequently, the high COP attained in Mode 1 compared to modes 2 and 3 indicates the significance of incorporating storage in this particular dryer. In comparison to earlier studies on the SAHPD method of banana drying, the COP values obtained are deemed acceptable (A. Loemba *et al.*, 2022; Singh *et al.*, 2020d)

The variation of the specific moisture extraction rate is shown in Fig. 26. This graph demonstrates how the specific moisture extraction rate rapidly decreased with drying time due to a decrease in moisture content. For 500 g of Cavendish bananas dried in modes 1, 2, and 3, the average specific moisture extraction rate was 0.13 kg/kWh, 0.11 kg/kWh, and 0.12 kg/kWh, respectively. This slight variation can be attributed to the energy consumption of 5.67, 7.52, and 7.43 kWh for each mode.

Evaluation of the thermal efficiency of the solar collector integrated with the thermal storage material (soapstone) was also conducted using the data collected during the drying process of Cavendish bananas using modes 1 and 2. When operating in Mode 1, Fig. 28 illustrates how the solar collector's thermal efficiency changes over time. The average thermal efficiency of the solar collector, according to the results, was 80.48%. Moreover, drying efficiency i.e. a measure of how well the drying air extracts moisture from the product in the drying chamber was computed using the experimental data.

Figure 29 displays the drying efficiency results. Mode 1 performed better in terms of drying efficiency than modes 2 and 3, primarily because its average inlet temperature and humidity were higher and lower, respectively, than those of the other modes. The three modes of drying 500 g of Cavendish bananas are shown in Fig. 30, along with changes in the surrounding temperature and relative humidity as well as at the drying chamber's inlet and outlet. This figure shows the results for all temperatures in the upper part and all relative humidities in the lower part. During experiments, 500 g of Cavendish bananas were dried using modes 1, 2, and 3. The average ambient temperature, relative humidity, and temperature were found to be 30.22 °C, 26.21 °C, and 29.17 °C, respectively, and 37.39 °C, 39.10 °C, and 44.43%, respectively. Using modes 1, 2, and 3, the drying chamber's inlet temperatures were 54.17 °C, 48.03 °C, and 50.63 °C, in that order. The outlet temperatures of the drying chamber were 48.71 °C, 38.40 °C, and 47.11 °C, in that order.

The average relative humidity for the three modes was 17.21, 22.07, and 20.58% at the drying chamber's outlet for Mode 1, 2, and 3, and 14.83, 14.67, and 18.33% at the chamber's inlet. These results show that air has a high temperature and low relative humidity when it enters the drying chamber and a low temperature and high relative humidity when it leaves. We can conclude that the temperature decreases as more moisture is removed from the banana. The air that passes through the drying chamber absorbs moisture from the banana samples, which causes the relative humidity of the air to rise.

The results of the three tested modes were all positive, but Mode 1, which used a solar-assisted heat pump dryer (SAHPD) with thermal energy storage (TES) during the day, was found to have the lowest humidity and the highest temperature in the drying chamber. This mode consequently produced faster drying times and greater coefficients of performance (COP). These results demonstrate how important it is to include TES in the drying process and show that changes in solar irradiance have a direct effect on temperature changes in the drying chamber. To sum up, the proposed dryer demonstrated good drying times, high temperature, and a significantly low final moisture content. These results highlight the need for more research in the area of Cavendish banana drying, especially considering the dearth of studies investigating the use of heat pump dryers for this particular use.

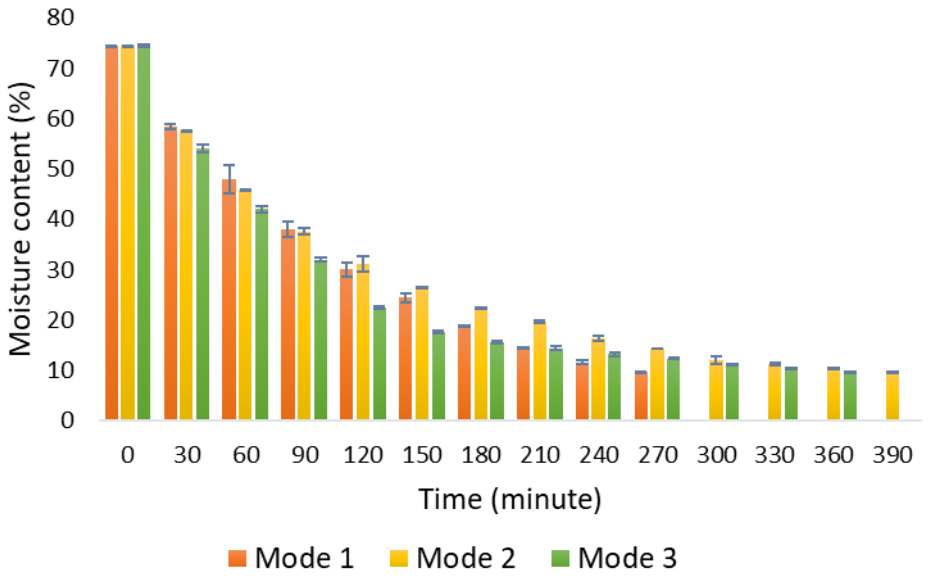

Figure 23: Variation of moisture content

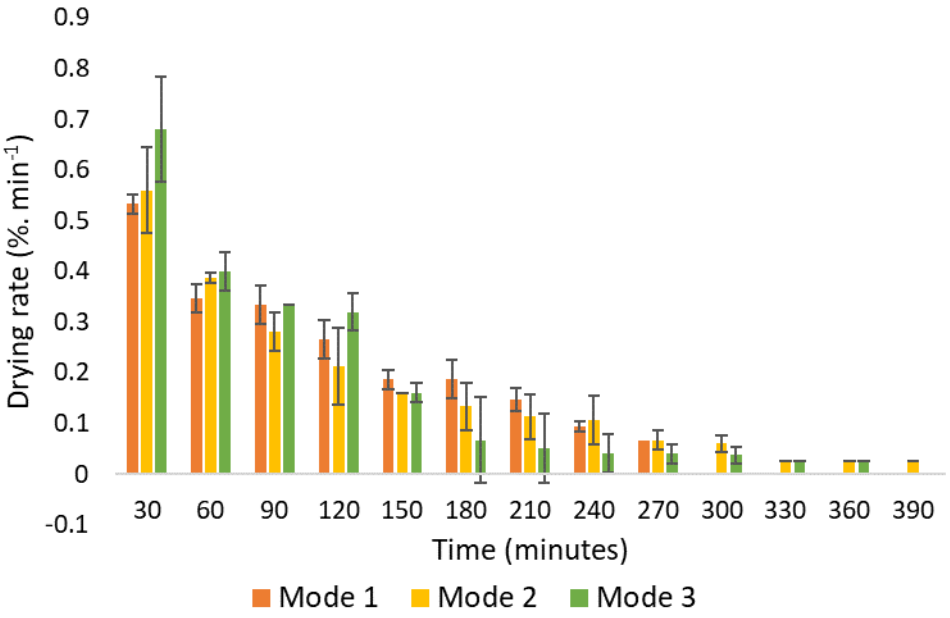

Figure 24: Variation of drying rate

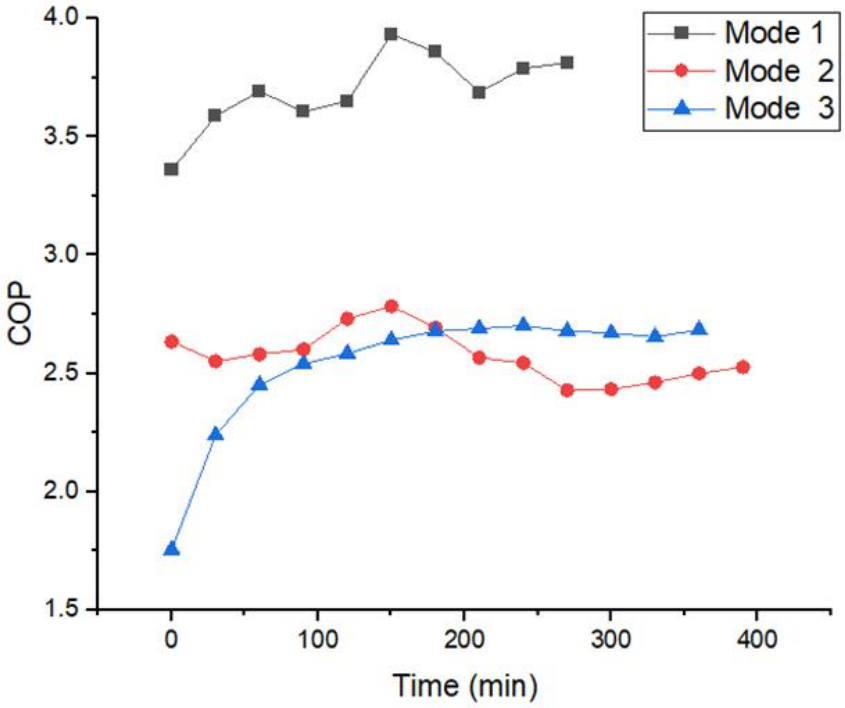

Figure 25: Variation of coefficient of performance

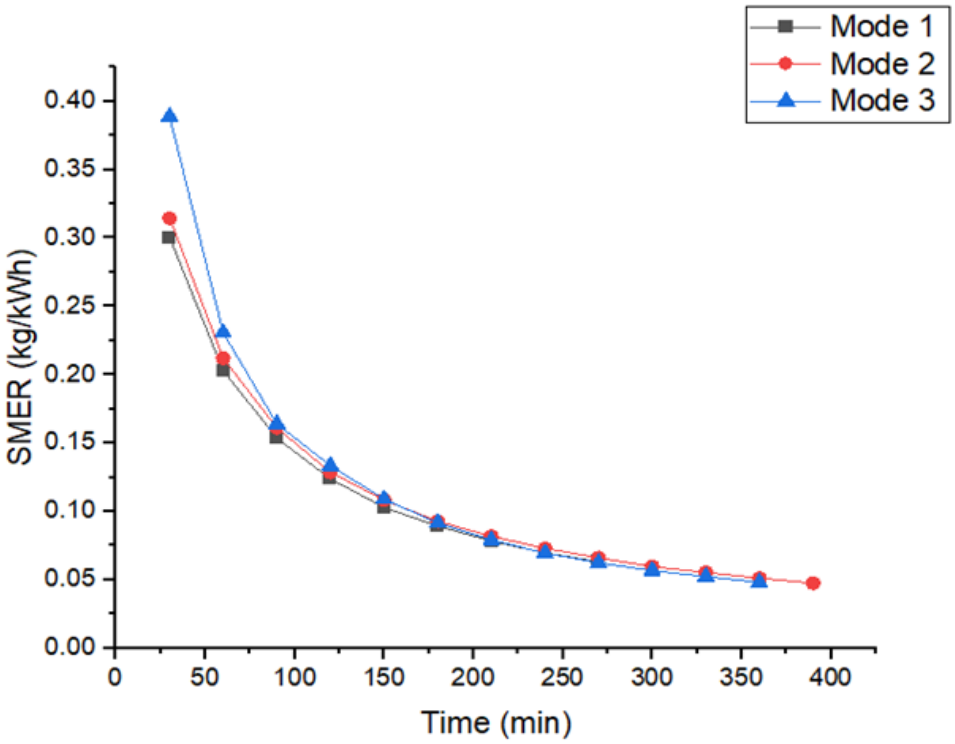

Figure 26: Variation of SMER

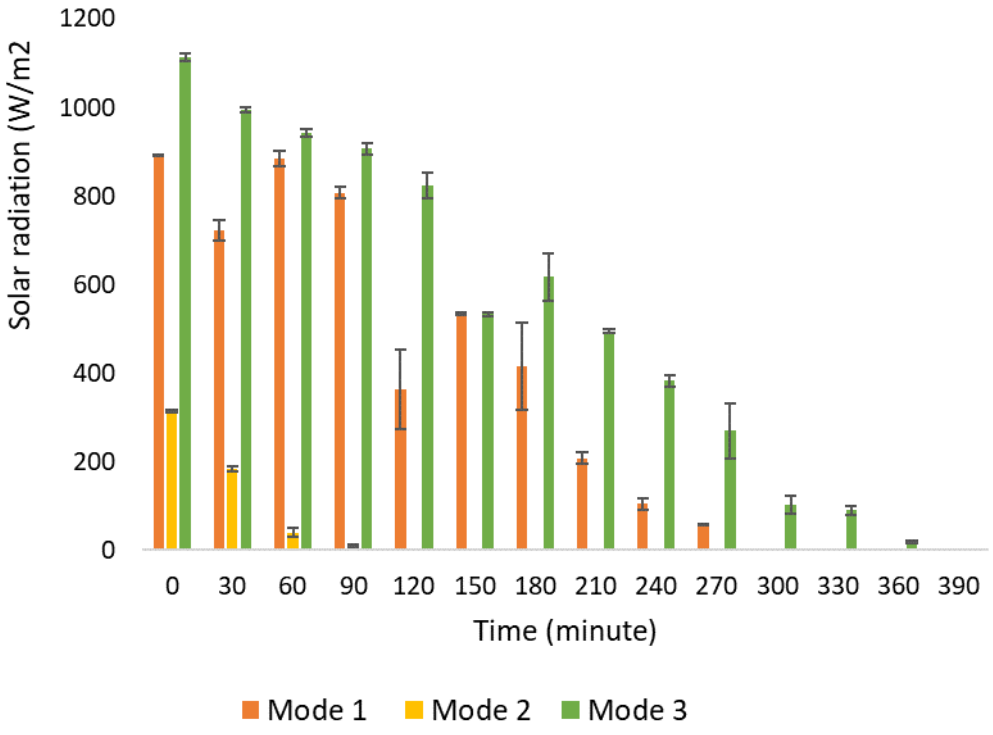

Figure 27: Variation of solar radiance

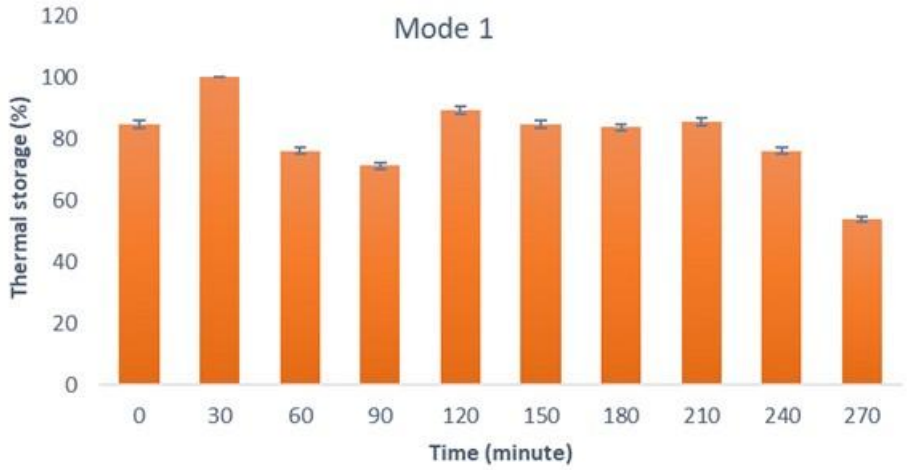

Figure 28: Variation of thermal storage efficiency

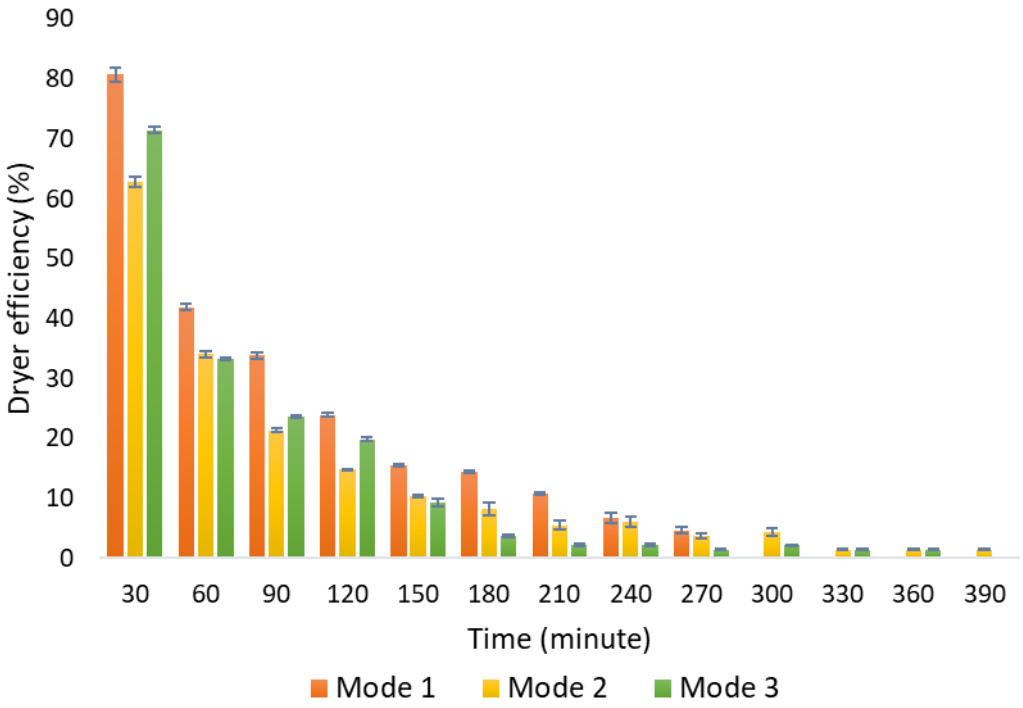

Figure 29: Variation of the dryer efficiency

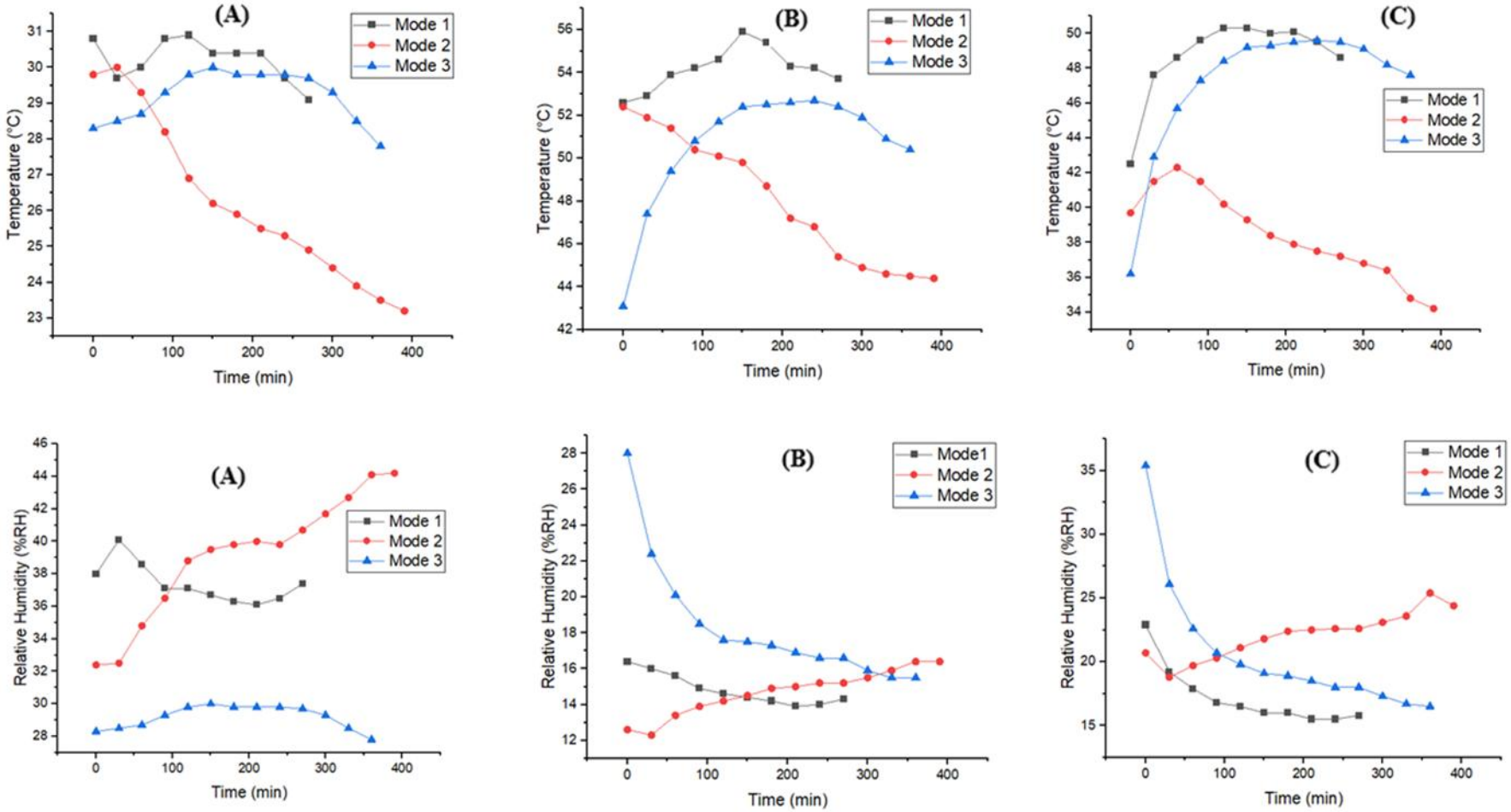

Figure 30: Variation of temperature and relative humidity [ambient air (A), Inlet (B) and outlet (C) of the drying chamber)]

4.2 Effect of the proposed dryer on proximate content

4.2.1 Proximate content of moringa leaves

Using proximate analysis, the nutritional value of Moringa *oleifera* leaves was assessed both before and after they were dried in a solar-assisted heat pump dryer integrated with thermal energy storage. The results obtained in duplicate are shown in Fig. 31. Other studies have shown that Moringa *Oleifera* leaves contain significant amounts of crude fat, crude ash, crude protein, crude fiber, crude carbohydrates, and moisture (Ogbe *et al.*, 2011; Olabode *et al.*, 2015). Of all the nutrients looked at in dried Moringa *Oleifera* leaves, carbohydrates constituted the largest percentage (45.6%). Because of water evaporation, the moisture content of dried Moringa *oleifera* leaves was much lower than that of fresh leaves. Figure 31 illustrates the higher fat content of dried Moringa *Oleifera* leaves when compared to fresh leaves.

The results also show that dried Moringa *oleifera* leaves have a significant protein content, averaging 23.37%, confirming that the leaves' increased nutrient density was caused by moisture loss (Sharaf-Eldin *et al.*, 2019). It was found that 9.49% of the dried powder crude fiber was present. The ash content of dried Moringa *oleifera* leaves increased significantly in comparison to fresh leaves, which may also be related to the moisture loss that tends to increase nutrient concentration.

The results of drying Moringa *Oleifera* leaves in solar-assisted heat pump dryers with thermal energy storage showed an increase in the overall content of protein, carbohydrate, fat, fiber, and ash. Comparable results were found for the following: proteins (31.33%), fat (2.66%), ash (3.56%), and carbohydrates (35.99%) by Olabode *et al.* (2015) when drying Moringa *Oleifera* leaves at 60 ℃. These findings show that the dried Moringa *oleifera* leaves contain a noteworthy concentration of macronutrients, including proteins, carbs, fats, fibers, and ash. On the other hand, a number of investigations have discovered that Moringa *oleifera* leaves also include micronutrients such as magnesium, calcium, potassium, zinc, iron, copper, manganese, and potassium (Alakali *et al.,* 2015; Offor *et al.*, 2014; Olabode *et al.*, 2015).

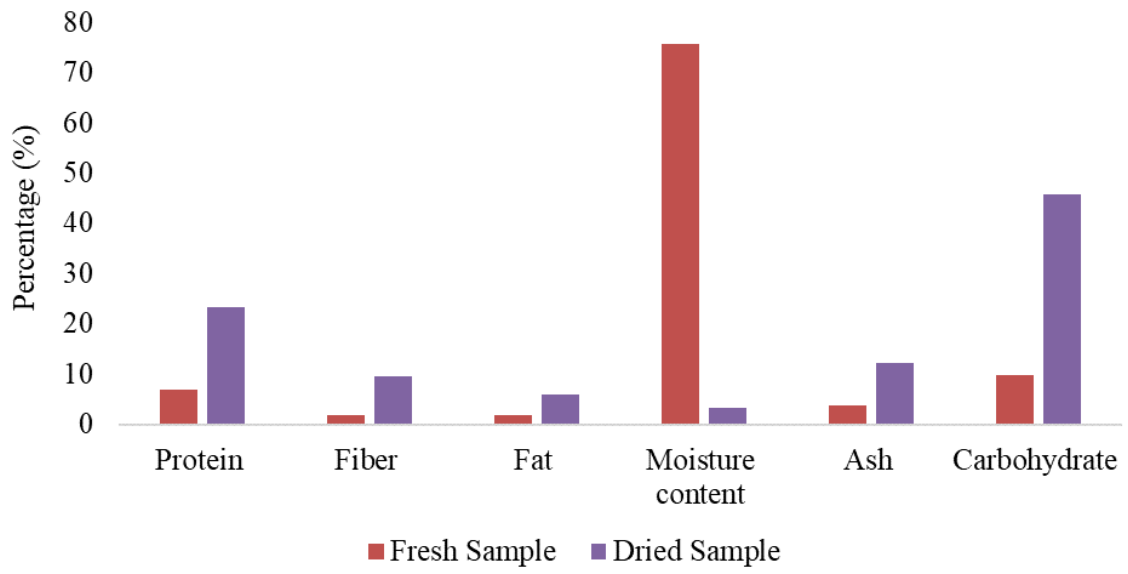

Figure 31: Proximate composition of Moringa oleifera leaves

4.2.2 Proximate, minerals and vitamins content of banana

Proximate, mineral, and vitamin analyses were used to assess the nutritional value of Cavendish bananas both before and after drying in each of the three operating modes. The means and standard deviations are displayed in the graphs. Figure 32 displays the outcomes of the proximate parameter analysis for crude fat, crude ash, crude protein, crude fiber, crude carbohydrates, and moisture. Figure 33 shows the results of the calorific value analysis, and Fig. 34 shows the results of the mineral parameter analysis (copper, iron, calcium, manganese, phosphorus, and zinc). Furthermore, Fig. 35 displays the vitamin B6 and vitamin C concentrations.

The levels of the proximate parameters i.e. crude fat, crude ash, crude protein, crude fiber, crude carbohydrates, and moisture in the dried Cavendish banana showed statistically insignificant differences ($p>0.05$) among the three modes that were examined. This is an important finding. This implies that the various operating modes used throughout the drying process had no appreciable effect on the dried Cavendish banana's proximate composition.

These results suggest that the nutritional makeup of the banana samples was not significantly altered by the drying modes chosen. Regardless of the particular operating modes used, the observed lack of significant variations provides confidence in the drying process's consistency and stability. Compared to fresh Cavendish bananas, the dried banana exhibited a significantly higher concentration of proximate parameters ($p<0.05$).

With values of 80.1, 80.8, and 81.1% for modes 1, 2, and 3, respectively, carbohydrates were found to have the highest proportion of all nutrients evaluated in dried Cavendish bananas, compared to fresh Cavendish bananas (21.6%).

The moisture content of dried Cavendish banana was lower than that of fresh Cavendish banana due to evaporation of water. For each of the three modes, the final moisture content value was 9.6%. Food products' moisture content gives an indication of their freshness and shelf life. Higher moisture content foods have a shorter shelf life and are more vulnerable to microbiological damage, which can result in decomposition (Dotto *et al.*, 2019). The dried Cavendish banana showed higher fat content values of 0.201, 0.174, and 0.208% using modes 1, 2, and 3, respectively, compared to the fresh Cavendish banana's 0.008%. Fats are rich in fat-soluble vitamins (Dotto *et al.*, 2019).

With average values of 2.604, 2.782, and 2.704% using Mode 1, Mode 2, and Mode 3, respectively, the results also show that dried Cavendish bananas had higher protein content than fresh Cavendish bananas, confirming that moisture loss of dried bananas improved nutrient density. Numerous studies have shown that proteins have a variety of structural and functional roles in the human body.

Sufficient protein intake maintains the proper development and functioning of the body (Ranjha *et al.*, 2022). After drying, the crude fiber was also found to be significant compared to the fresh Cavendish banana (0.048%), with values of 3.738, 3.297, and 3.218% using modes 1, 2, and 3, respectively. Fiber has a significant role in nutrition. It has been associated with increased clearance of possible mutagens, blood sugar control, preservation of intestinal health, and decreased cholesterol (Dotto *et al.*, 2019). When compared to fresh Cavendish banana, the ash content of dried Cavendish banana increased with values of 3.8, 3.36, and 3.15% using modes 1, 2, and 3, respectively (2.95). Moisture loss, which tends to increase nutritional concentration, may be the cause of this rise. These values for the ash content indicate that the dried Cavendish banana has a good mineral concentration (Dotto *et al.*, 2019).

With values of 332.5, 335.9, and 337.1 Kcal/100 g utilizing modes 1, 2, and 3, respectively, the energy value of the dried banana also increased significantly in comparison to the fresh Cavendish banana (90.2 kcal/100 g). The obtained results are consistent with those published by Carughi (2013), demonstrating the high content of potein (1.09 g), ash (0.82 g), fiber (2.6 g), fat (0.33 g), carbohydrates (22.84 g), and calories (89 kcal) in fresh Cavendish bananas.

Protein (2.30 g), ash (1.4 g), fiber (7.7 g), fat (33.60 g), carbohydrate (58.40 g), and energy value (519 kcal) all increased significantly after drying.

These results suggest that the Cavendish banana's nutritional content was improved through the drying process, resulting in higher concentrations of important elements. Additionally, when comparing the dried Cavendish banana to its fresh counterpart, the results showed a significant ($p<0.05$) increase in mineral concentration.

This suggests that the concentration of minerals was enhanced by the drying process, and that dried Cavendish bananas may be a more nutrient-dense option than fresh ones. The dried samples' higher concentrations of protein, ash, fiber, fat, carbohydrate, energy value, and minerals demonstrate the possible health advantages of eating dried Cavendish bananas.

These results offer important new information about the nutritional alterations that take place in Cavendish bananas during the drying process. They add to our understanding of the nutritional makeup of Cavendish bananas and stress the significance of taking drying techniques into account when assessing their nutritional composition. To maximize the nutritional value and health benefits of dried Cavendish bananas and encourage their consumption as a convenient and nutrient-dense snack, it is imperative to comprehend these changes.

Minerals are vital components of our food. They carry out a variety of functions, such as forming the building blocks of our bones, influencing the activity of muscles and nerves, and maintaining the proper balance of water in the body (Kim & Choi, 2013; Weyh *et al.*, 2022). The findings demonstrated that a significant amount of calcium and phosphorus are present in both fresh and dried Cavendish bananas. Of all the minerals examined, copper and zinc were found to be present in relatively small amounts. All three modes resulted in an increase in the concentration of vitamin B6, which is essential for the development of the immune system and the brain. Vitamin B6 also facilitates metabolism. The three modes of drying that were tested led to notable drops in vitamin C concentrations ($p<0.05$). This is likely because vitamin C is heat sensitive.

Similar findings were reported by Carughi (2013), who also observed that fresh Cavendish bananas had high concentrations of minerals, such as calcium (5 mg), zinc (0.15 mg), manganese (0.27 mg), phosphorus (22 mg), copper (0.08 mg), iron (0.26 mg), and magnesium (27 mg). Calcium (18 mg), copper (0.21 mg), iron (1.25 mg), magnesium (76 mg), manganese

(1.56 mg), phosphorus (56 mg), and zinc (0.75 mg) concentrations all rose after the drying process. Additionally, Carughi (2013) showed that fresh Cavendish bananas have a vitamin C content of 8.7 mg; however, the drying process reduced the concentration of vitamin C, resulting in a value of 6.3 mg.

These results highlight how drying affects the nutritional makeup of Cavendish bananas, especially the vitamin C's sensitivity to heat. The dried Cavendish banana showed higher mineral concentrations, including calcium, copper, iron, magnesium, manganese, phosphorus, and zinc, even though its vitamin C content had decreased. These alterations show that even though the drying process might cause some nutrient loss, the dried Cavendish banana keeps important minerals that add to its nutritional value.

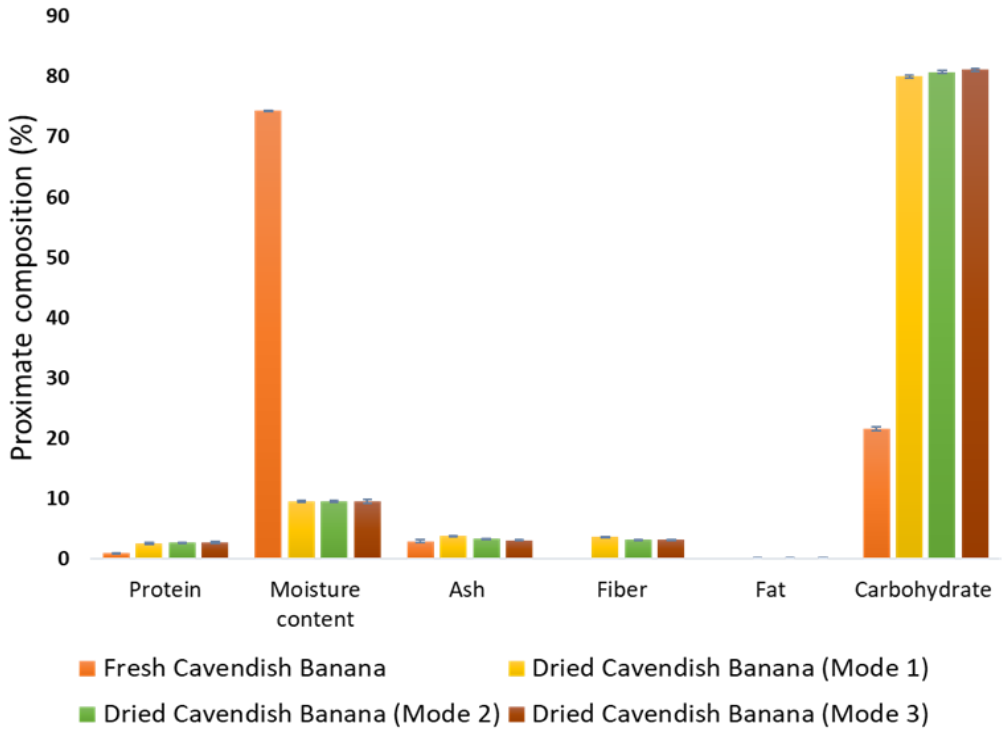

Figure 32: Proximate composition of Cavendish Banana

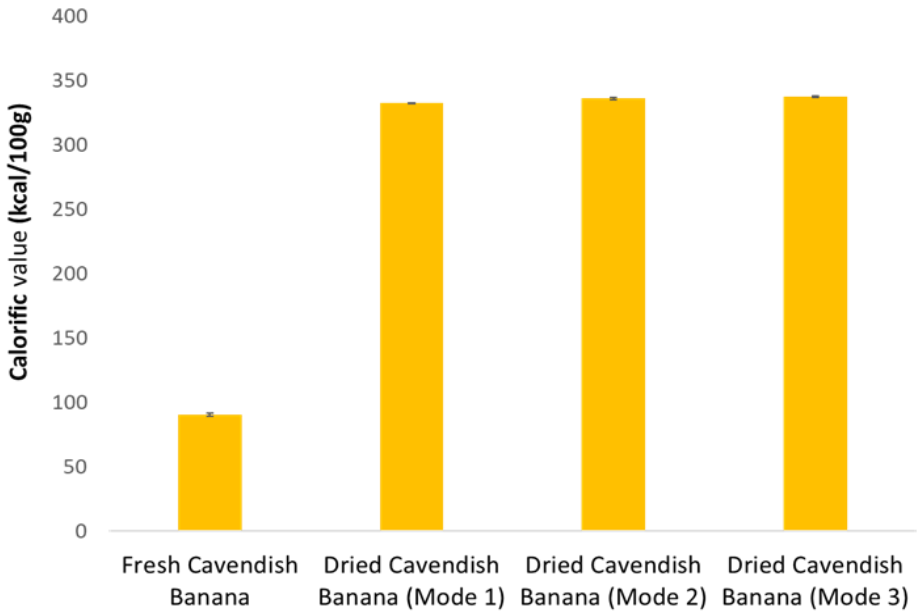

Figure 33: Calorific value of Cavendish Banana

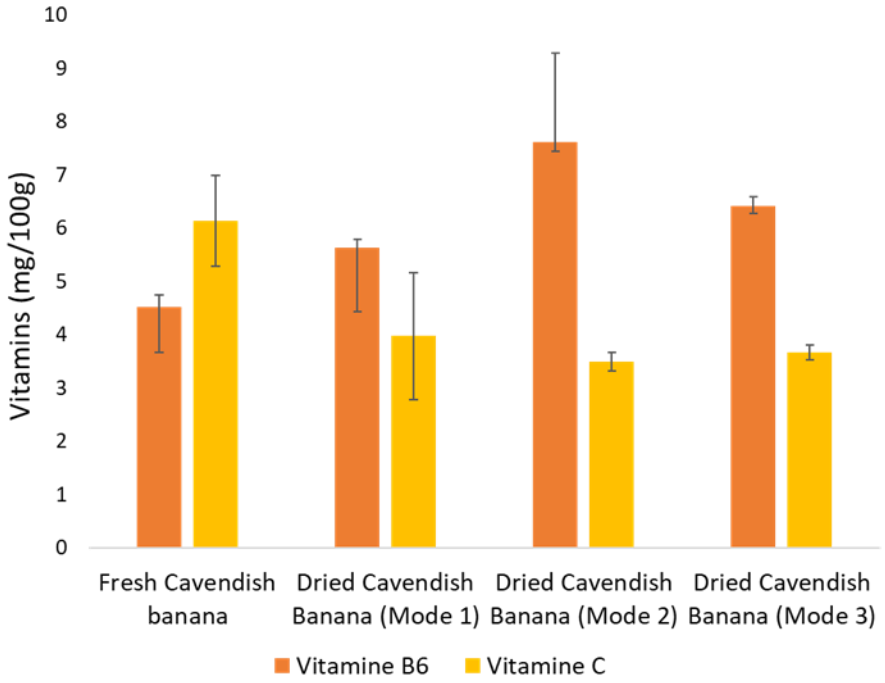

Figure 34: Composition in Vitamin B6 and C of Cavendish Banana

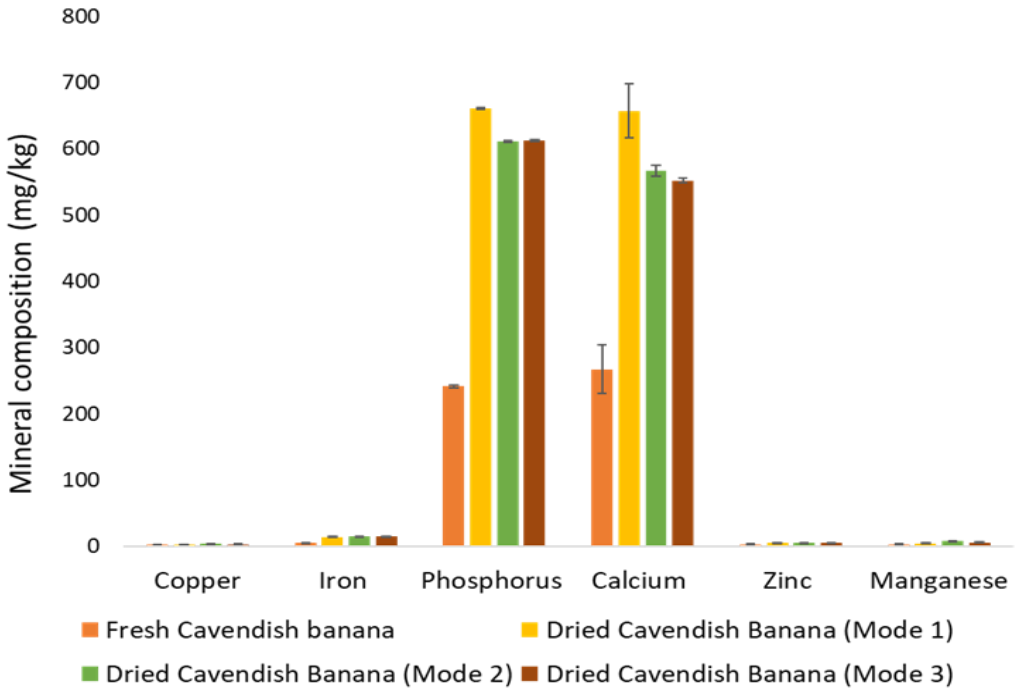

Figure 35: Mineral composition of Cavendish Banana

4.3 Techno-economic analysis result of the proposed dryer

Using Mode 1's capital expenditures, operating costs, approximation profitability measures based on payback periods, return on investment, and annual net cash flow as well as a rigorous profitability measure using the net present value as an indicator, the economic viability of the SAHPD with TES was evaluated. The Tanzanian economy in 2023 served as the basis for the economic analysis (Bank of Tanzania [BOT], 2023).

The results every calculation made and every assumption made for the economic analysis of drying Cavendish bananas are compiled in Tables 9 to 13. As demonstrated in Table 9, equipment and labor costs incurred during manufacturing were factored into the calculation of CapEX. As indicated in Table 10, the annual cost of fresh bananas, the annual cost of electricity, the annual operating labor charge, and depreciation were all included in the computation of OpEX.

It was found that CapEX and OpEX were, respectively, $4647 and $11680.5. These CapEX and OpEX values represent the expenses required to produce the developed dryer and make money, respectively. Table 11 illustrates the estimated production of 4200 kg of dried bananas per year for 300 working days using SAHPD with TES (Mode 1), with a $3.5/kg price tag. Table 12 shows the expected yearly cash flow that result from this, which is $3019.5. This

income, in comparison to the OpEX, is extremely reasonable. Table 12's results also indicated that the payback period is 1.5 years.

This implies that after 1.5 years, the cash flows will be sufficient to cover the expense of the investment. The return on investment is found to be 65% in Table 12. This substantial return on investment suggests that there is little risk associated with investing in the developed dryer and that it is profitable. As Table 13 shows, the net present value is $13906.6.

This outcome supports the developed dryer's profitability in addition to the payback period and ROI since it shows that investments with larger net present values are viewed as more desirable. Therefore, the SAHPD that was developed with TES is a financially feasible option for drying bananas.

Table 9: CapEX (Capital costs)

Indicators	**Value ($)**
Cost of manufacturing materials	2 142.88
Cost of insulation materials	47.24
Labor cost associated with production	257.29
Cost of purchasing the heat pump system	3859.14
Cost of purchasing the wiring apparatus	99.49
Cost of labor to install the heat pump system	257.29
Cost of purchasing the refrigerant	126.5
Total	**4646.95**

Table 10: OpEX (Operating cost)

Indicators	**Value ($)**
Annual cost of fresh bananas	8400
Annual cost of electricity	415.8
Annual labor charge	2400
Depreciation	464.695
Total	**11680.495**

Table 11: Annual sale estimation

Indicators	Value ($)
The cost of a kilogram of dried bananas	3.5
Total amount of dried bananas annually	4200
Annual sales of the dried banana	14700

Table 12: Approximate profitability measures

Indicators	Value
Net cash-flow	$3019.5
Payback period	1.5 years
Return on Investment	65%

Table 13: Rigorous profitability measure (calculation of NPV)

Year	Net cash flow	10 % Discount rate	Present value	Unit
1	3019.505	0.90909091	2745.004545	
2	3019.505	0.82644628	2495.458678	
3	3019.505	0.7513148	2268.598798	
4	3019.505	0.68301346	2062.362544	
5	3019.505	0.62092132	1874.87504	
6	3019.505	0.56447393	1704.431854	
7	3019.505	0.51315812	1549.483504	
8	3019.505	0.46650738	1408.621367	
9	3019.505	0.42409762	1280.564879	
10	3019.505	0.38554329	1164.14989	
Cumulative present value			**18553.5511**	**$**
Net present value (NPV)			**13906.6**	**$**

4.4 Life cycle assessment results of the proposed dryer

ReCiPe 2016 Midpoint v.1.0 under Hierarchist, H perspective was used to compute the impact assessment data in this life cycle assessment, which examined the environmental impacts of the drying process of tomato using both Solar-Assisted Heat Pump Dryer with and without thermal energy storage. Using OpenLCA software tool, the midpoint characterization impact on the 18 midpoint categories was computed. Ionizing radiation, land use, marine ecotoxicity, marine eutrophication, mineral resource scarcity, stratospheric ozone depletion, terrestrial

acidification, terrestrial ecotoxicity, fine particulate matter formation, freshwater ecotoxicity, freshwater eutrophication, global warming, human carcinogenic toxicity, human non-carcinogenic toxicity, and ionizing radiation are among the 18 impact categories. These are the impact categories that are examined the most often.

Each of those impact categories classifies various emissions according to their environmental impact. Fine particulate matter formation refers to suspended extremely small particles produced by anthropogenic processes that have a negative impact on human health. Global warming is defined as the change of global temperature caused by greenhouse gases. Human carcinogenic toxicity and human non-carcinogenic toxicity describe the effects of toxic substances released into the environment on humans. Ionizing radiation is the type of radiation made up of particles with enough energy to liberate an electron from an atom or molecule. Land use describes the effects of agriculture, human settlement, and resource extraction on the land. Marine ecotoxicity, terrestrial ecotoxicity, and freshwater ecotoxicity are the toxic effects of chemicals on an ecosystem.

Marine and freshwater eutrophication refer to the accumulation of nutrients in aquatic systems. Mineral and fossil resource scarcity refer to the decrease in the availability of non-biological resources as a result of their excessive use. Ozone formation-Human health and Ozone formation-Terrestrial ecosystems stand for photochemical ozone formation, which is caused by the release of volatile organic compounds that are meta-stable. When these compounds are exposed to UV light and NOx, they initiate a sequence of photochemical reactions that eventually result in the formation of ozone and other secondary pollutants at the ground level. These can have a negative impact on human health. The term "stratospheric ozone depletion" describes the reduction of the stratosphere's ozone layer as a result of human emissions of substances that deplete the ozone layer. The term Terrestrial acidification describes the decrease of pH as a result of human-caused acidification. Finally, water consumption measures the water withdrawal-to-availability ratio of the system under consideration. Withdrawal corresponds to all off-stream water use, excluding water extracted and subsequently returned to the environment unpolluted, such as cooling water (Abdou *et al.*, 2020; Abeliotis *et al.*, 2022b; Pelletier *et al.*, 2007).

The results of the 18 impact categories analyzed are displayed in Table 14. According to the results, the impact of SAHPD in the category of terrestrial ecotoxicity was 5.93522 kg 1,4-DCB without thermal energy storage and 4.24257 kg 1,4-DCB with thermal energy storage.

The findings indicate that the non-carcinogenic toxicity to humans was 3.68363 kg for SAHPD with thermal energy storage and 5.1542 kg 1,4-DCB without storage. With thermal energy storage, SAHPD experienced 2.19533 kg CO2 equivalent of global warming, while without it, 3.07116 kg CO2 equivalent. The marine ecotoxicity values for SAHPD with thermal energy storage and 1,4-DCB without thermal energy storage were 0.24008 and 0.33596 kg, respectively. For SAHPD with and without thermal energy storage, the observed values of the impact of freshwater ecotoxicity were 0.18713 and 0.26186 kg 1,4-DCB, respectively. For SAHPD with thermal energy storage, the fossil resource scarcity was 0.15621, whereas for SAHPD without thermal energy storage, it is 0.178635 kg NOx eq. In terms of human carcinogenic toxicity, SAHPD has an impact of 0.21128 without thermal energy storage and 0.15115 with thermal energy storage. Furthermore, the effect of SAHPD on ionizing radiation was 0.114681 with thermal energy storage, and 0.160496 kBq Co-60 eq without syorage. Regarding land use, the impact results were 0.07267 with thermal energy storage and 0.1017 m2a crop eq for SAHPD without thermal energy storage.

However, in all other categories, the impacts of SAHPD without storage are found to be in general higher than those of SAHPD with storage. This is partly because the SAHPD uses more energy when it doesn't have thermal energy storage. The findings of this investigation are consistent with those of Kumar *et al.* (2022), who came to the conclusion that, in terms of sustainability, using a heat pump dryer for the drying process is a better option. Kumar *et al.* (2022) used the life cycle assessment to analyze and quantify the environmental impacts of two dryers, namely the heat pump dryer and the microwave vacuum dryer. Comparing the results of the current study to those of Kumar *et al.* (2022), the results show higher values for both the formation of fine particle matter and human carcinogenic toxicity. The overall results of Kumar *et al.* (2022) indicated that a heat pump dryer is a better choice in terms of environmental sustainability. The results of the current study agree with those obtained by Kumar *et al.* (2022). Table 14 presents in detail and in ascending order the results of all impact categories examined.

Figures 36 to 45 present results of the first ten impact factors separately. Figure 46 shows the relative indicator results of the respective project variants. For each indicator, the maximum result is set to 100% and the results of the other variants are displayed in relation to this result.

Table 14: Impacts categories results

Impact categories	Unit	Sahpd with tes	Sahpd without tes
Terrestrial ecotoxicity	kg 1,4-DCB	4.24257	5.93522
Human non-carcinogenic toxicity	kg 1,4-DCB	3.68363	5.1542
Global warming	kg CO2 eq	2.19533	3.07116
Marine ecotoxicity	kg 1,4-DCB	0.24008	0.33596
Freshwater ecotoxicity	kg 1,4-DCB	0.18713	0.26186
Fossil resource scarcity	kg oil eq	0.15621	0.178635
Human carcinogenic toxicity	kg 1,4-DCB	0.15115	0.21128
Ionizing radiation	kBq Co-60 eq	0.114681	0.160496
Land use	m2a crop eq	0.07267	0.1017
Water consumption	m3	0.04108	0.0555
Terrestrial acidification	kg SO2 eq	0.01158	0.0162
Ozone formation, Terrestrial ecosystems	kg NOx eq	0.00426	0.00596
Ozone formation, Human health	kg NOx eq	0.00422	0.0059
Fine particulate matter formation	kg PM2.5 eq	0.00388	0.00542
Mineral resource scarcity	kg Cu eq	0.00359	0.00501
Freshwater eutrophication	kg P eq	0.00231	0.00324
Marine eutrophication	kg N eq	0.00016	0.00023
Stratospheric ozone depletion	kg CFC11 eq	1.20E-06	1.68E-06

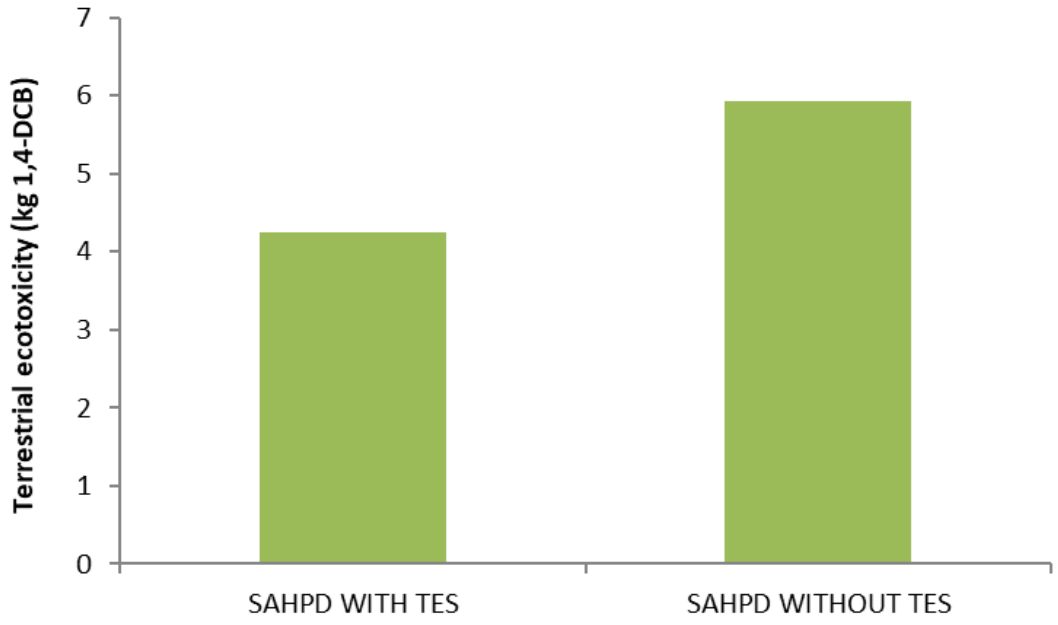

Figure 36: Life cycle assessment results of Terrestrial ecotoxicity

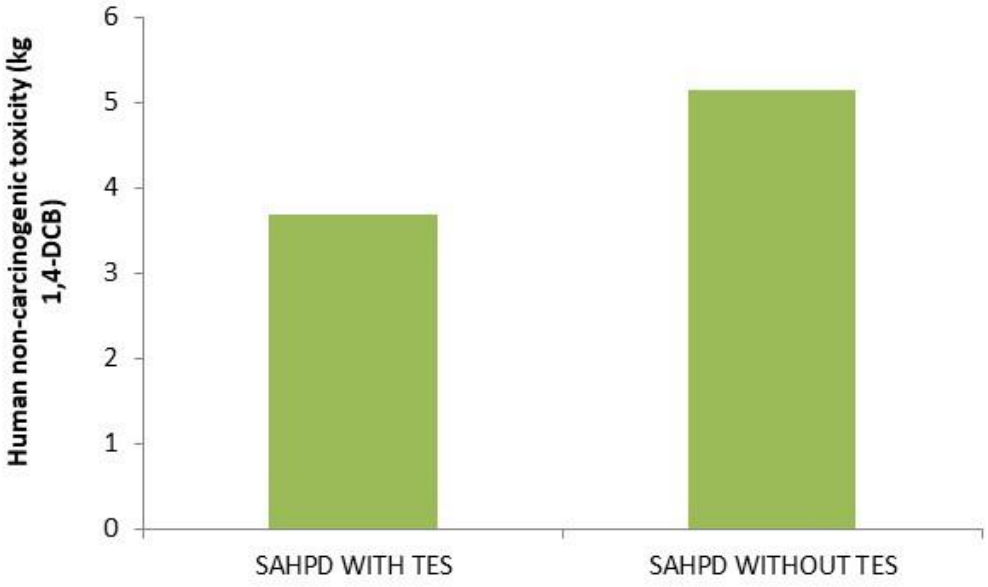

Figure 37: Life cycle assessment results of human non-carcinogenic toxicity

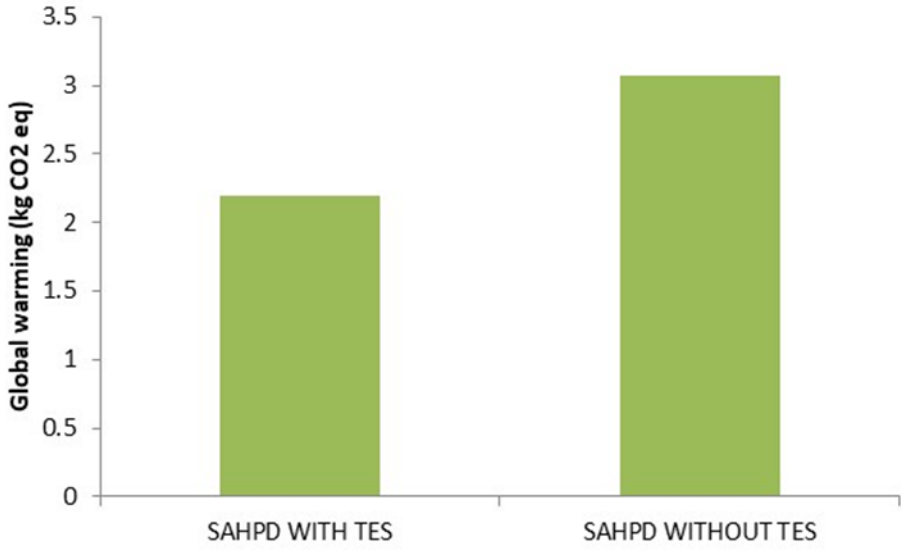

Figure 38: Life cycle assessment results of global warming

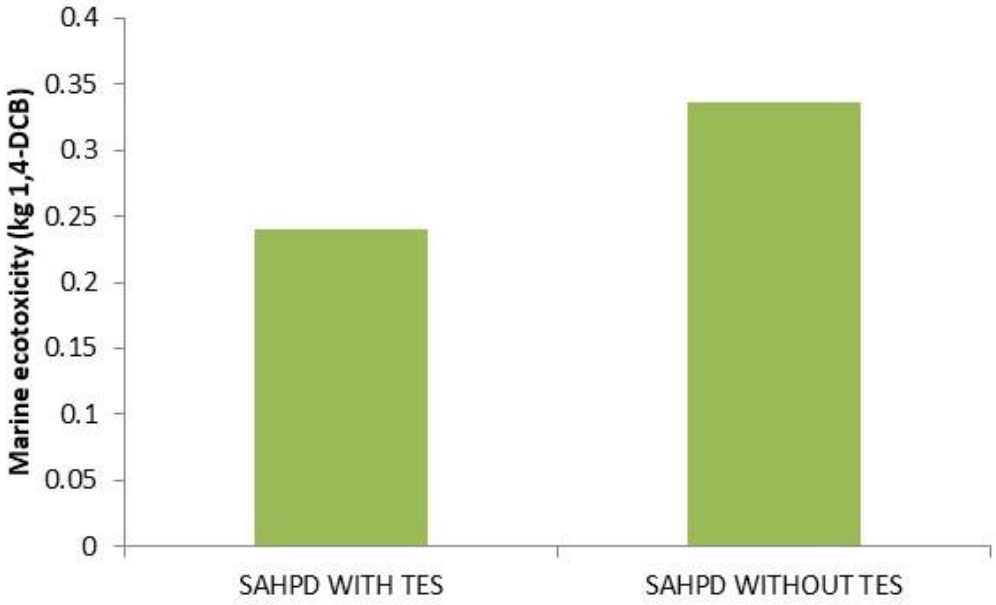

Figure 39: Life cycle assessment results of marine ecotoxicity

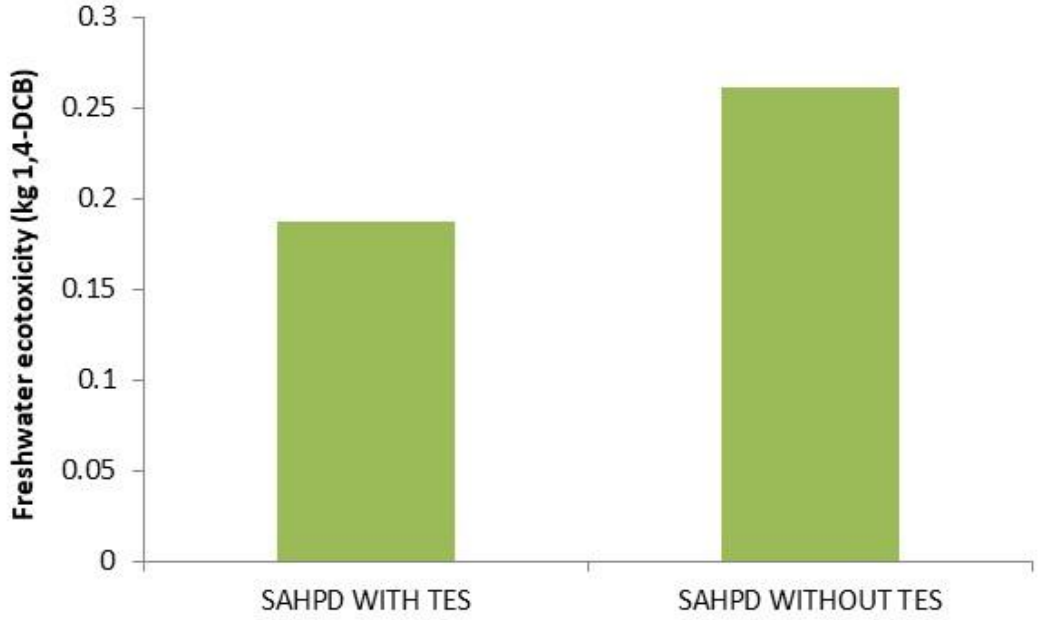

Figure 40: Life cycle assessment results of freshwater ecotoxicity

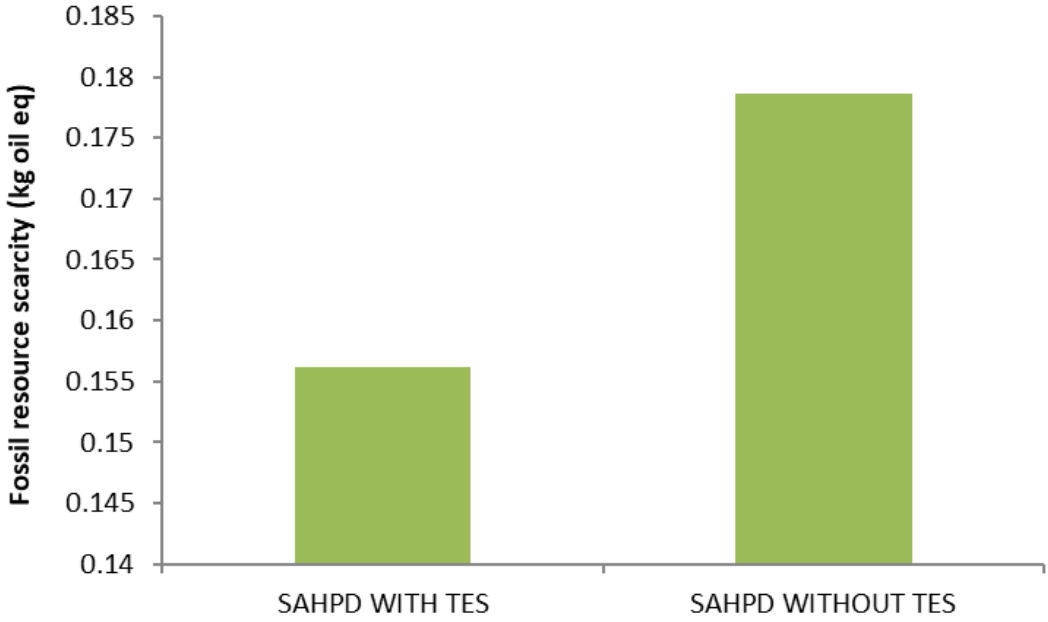

Figure 41: Life cycle assessment results of fossil resource scarcity

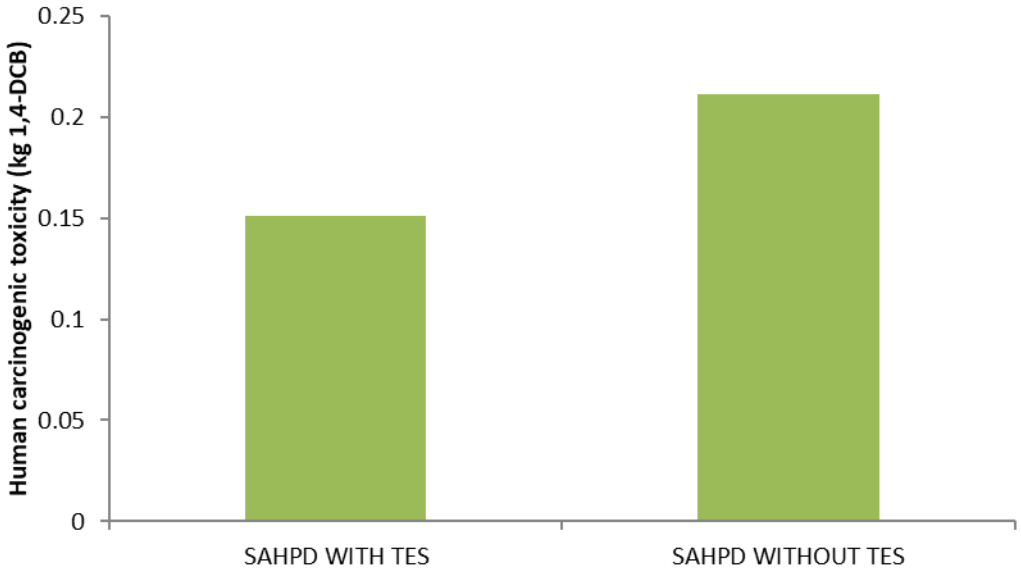

Figure 42: Life cycle assessment results of human carcinogenic toxicity

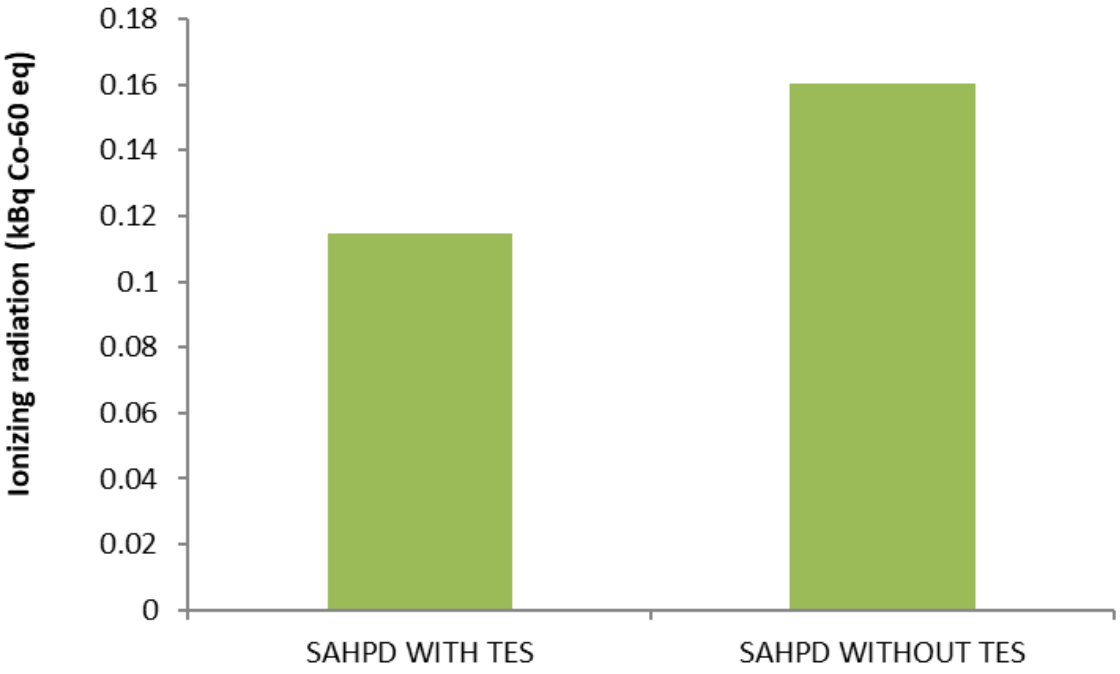

Figure 43: Life cycle assessment results of ionizing radiation

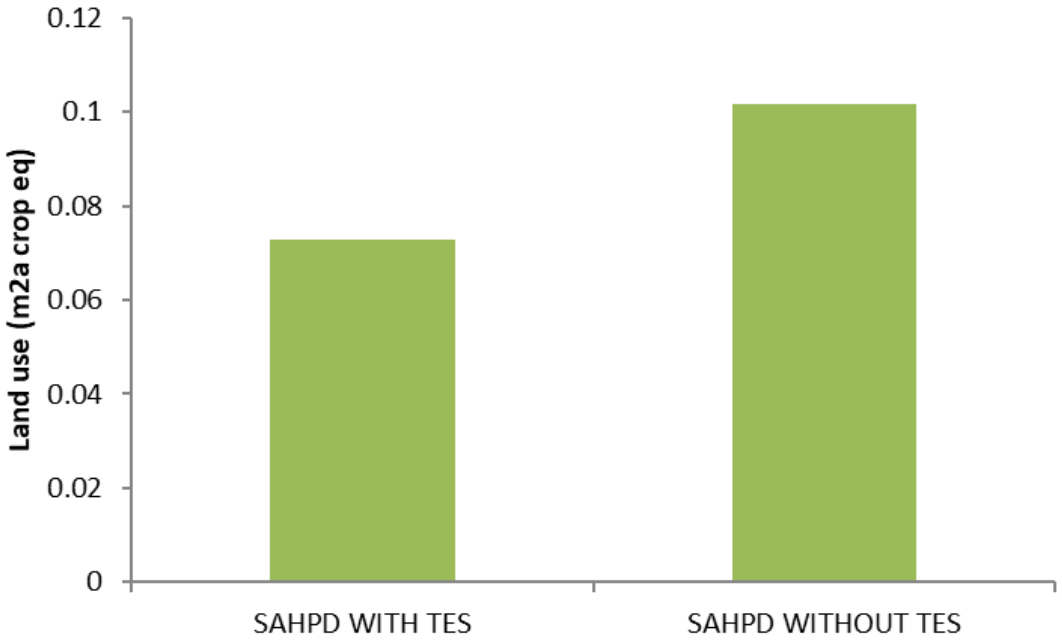

Figure 44: Life cycle assessment results of land use

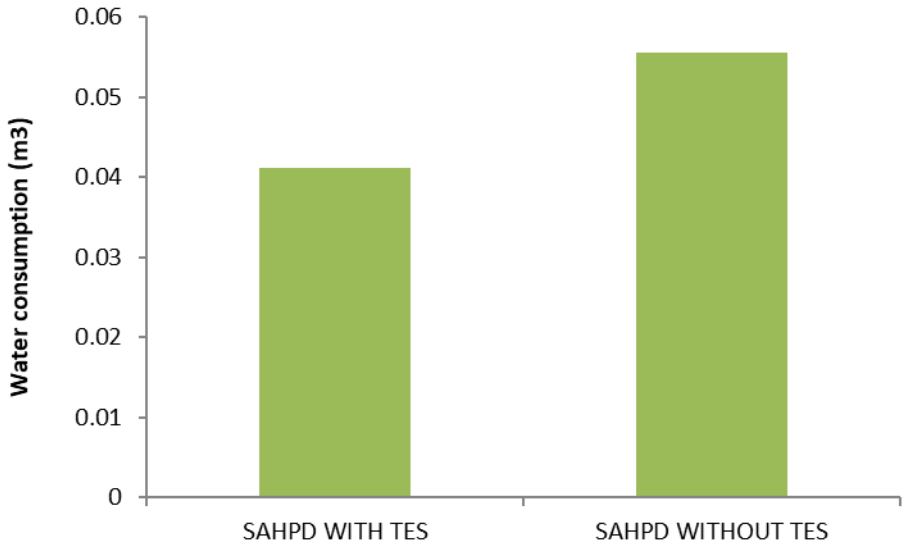

Figure 45: Life cycle assessment results of water consumption

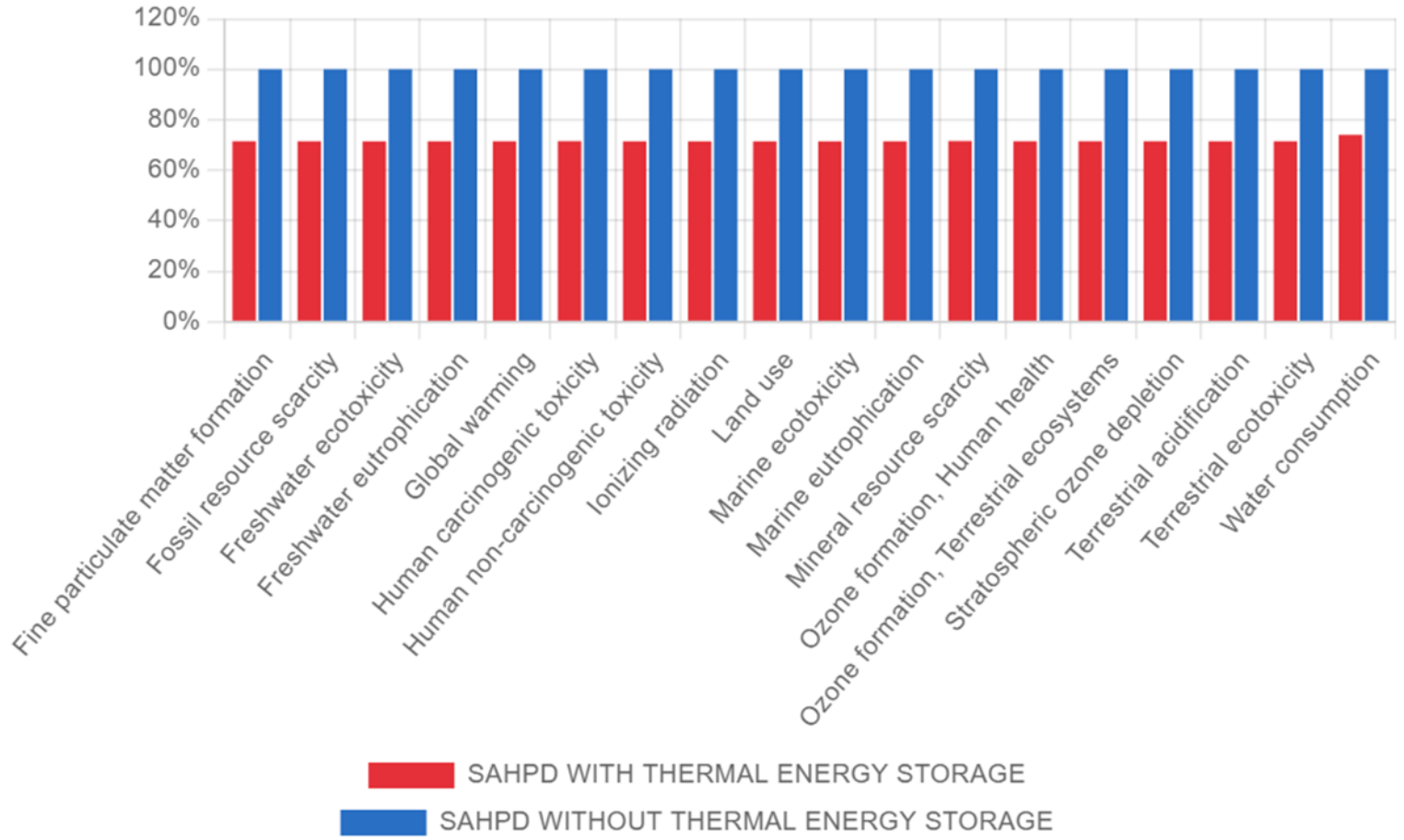

Figure 46: Life cycle assessment results

CHAPTER FIVE

CONCLUSION AND RECOMMENDATIONS

5.1 Conclusion

In this study a novel solar-assisted heat pump dryer integrated with thermal energy storage has been developed and tested for drying moringa *oleifera* leaves, banana and tomatoes. Thermal performance analysis, nutritional composition, as well as techno-economic and life cycle assessment were examined. Results showed that, when drying moringa aleifera leaves using one operating mode i.e "solar-assisted heat pump dryer integrated with thermal energy storage during the day", the proposed dryer preserved nutrients such as fat, ash, protein, fiber, and carbohydrates, the moisture content was reduced from 75.7 to 3.3%, in five hours of the drying process. The average COP value was 3.36, confirming the dryer's low energy consumption.

Additionally, when drying tomatoes in Mode 1 (with thermal energy storage during the day) and Mode 2 (without thermal energy storage during the day), using the proposed dryer, the initial moisture content was found to have significantly decreased from 92.5% to 8.5%, as per the results. This reduction was reached in 270 minutes for Mode 1 and 330 minutes for Mode 2, respectively. For modes 1 and 2, the average specific moisture extraction rates were 0.22 and 0.15 kg/kWh, respectively. The average drying rates for modes 1 and 2 were 0.31 and $0.25\%.min^{-1}$, respectively. The coefficient of performance for modes 1 and 2 was 2.72 and 4.42, respectively.

Nevertheless, the dryer was tested in three different operating modes when drying bananas using the proposed dryer: Mode 1 with thermal energy storage during the day, Mode 2 without thermal energy storage during the night, and Mode 3 without thermal energy storage during the day. Consistent results from three replicates of the experiment demonstrated a noteworthy decrease in the initial sample's moisture content from 74.4% to 9.6% following various drying times. This reduction was accomplished in 270 minutes by Mode 1, 390 minutes by Mode 2, and 360 minutes by Mode 3. For modes 1, 2, and 3, the corresponding average specific moisture extraction rates were 0.13, 0.11, and 0.12 kg/kWh. The drying rate varied concurrently from 0.16 to 0.24% per minute. Among the tested modes, the drying efficiency varied, with Mode 1 obtaining the highest efficiency at 23.23%. Mode 1, Mode 2, and Mode 3 showed coefficient of performance values of 3.69, 2.57, and 2.54, in that order. Furthermore, a p value less than 0.05 demonstrated that the dried Cavendish banana had substantially greater concentrations of

proximate parameters and minerals than the fresh banana. The techno-economic analysis carried out especially for Mode 1 showed that the payback period i.e. the amount of time needed to recover the initial investment, was 1.5 years.

Results of the life cycle assessment revealed that the drying process using the proposed dryer has less environmental effects. According to the results, the impact of SAHPD in the category of terrestrial ecotoxicity was 5.93522 kg 1,4-DCB without thermal energy storage and 4.24257 kg 1,4-DCB with thermal energy storage. The findings also indicate that the non-carcinogenic toxicity to humans was 3.68363 kg for SAHPD with thermal energy storage and 5.1542 kg 1,4-DCB without storage. Furthermore with thermal energy storage, SAHPD experienced 2.19533 kg CO2 equivalent of global warming, while without it, 3.07116 kg CO2 equivalent. However, in all other categories, the impacts of SAHPD without storage are found to be in general higher than those of SAHPD with storage. This is partly because the SAHPD uses more energy when it doesn't have thermal energy storage. To sum up, the findings highlight the importance of incorporating a thermal energy storage unit with soapstone to improve the performance and efficiency of the solar-assisted heat pump dryer in agricultural product drying. The high COP value obtained indicates efficient energy consumption relative to achieved drying output, which not only leads to cost-effectiveness but also diminishes the ecological footprint linked to industrial drying processes.

Concluding, these results underline the need for careful consideration of drying parameters, including drying time and mode selection, to optimize the performance of SAHPD systems. Additionally, practical applications of SAHPD technology in various industries, such as food processing and agriculture, could benefit from tailored drying protocols based on these findings. In addition, the findings align closely with the research objectives of developing an energy-efficient and sustainable drying solution for agricultural products, demonstrating the feasibility and potential impact of solar-assisted heat pump dryer technology.

These results are in line with earlier studies. Consequently, the proposed dryer is a viable method to dry agricultural goods. The results emphasize how important it is to use thermal energy storage materials to further improve the performance and efficiency of solar-assisted heat pump dryers for drying agricultural products. Future research should look into alternative storage materials to improve the operation of solar-assisted heat pump dryers.

5.2 Recommendations

Following are our recommendations for future research on heat pump dryers. Implementing the recommended research directions would not only advance our understanding of heat pump dryer technology but also contribute to the broader goal of sustainable agricultural development:

(i) Develop simple and energy-efficient heat pump dryer designs to lower production costs, electricity consumption, and maintenance requirements.

(ii) Propose an in-depth investigation of heat pump dryers that includes all of the kinetic, energy, and exergy assessment parameters in order to more clearly demonstrate their efficiency.

(iii) Conduct comprehensive studies on the life cycle, techno-economic, and exergoeconomic analyses of heat pump dryers, which may provide a global view of the environmental and economic consequences of heat pump dryers and assist in determining the components to be optimized in the system.

REFERENCES

Abdou, K., Le Loc'h, F., Gascuel, D., Romdhane, M. S., Aubin, J., & Ben Rais Lasram, F. (2020). Combining ecosystem indicators and life cycle assessment for environmental assessment of demersal trawling in Tunisia. *The International Journal of Life Cycle Assessment, 25*(1), 105-119.

Abeliotis, K., Chroni, C., Lasaridi, K., Terzis, E., Galliou, F., & Manios, T. (2022a). Environmental impact assessment of a solar drying unit for the transformation of food waste into animal feed. *Resources, 11*(12), 1-12. https://doi.org/10.3390/resources 11120117

Abeliotis, K., Chroni, C., Lasaridi, K., Terzis, E., Galliou, F., & Manios, T. (2022b). Environmental impact assessment of a solar drying unit for the transformation of food waste into animal feed. *Resources, 11*(12), 1-12. https://doi.org/10.3390/resources 11120117

Aktaş, M., Khanlari, A., Amini, A., & Şevik, S. (2017). Performance analysis of heat pump and infrared–heat pump drying of grated carrot using energy-exergy methodology. *Energy Conversion and Management, 132*, 327–338.

Alakali, J. S., Kucha, C. T., & Rabiu, I. A. (2015). Effect of drying temperature on the nutritional quality of Moringa oleifera leaves. *African Journal of Food Science*, *9*(7), 395-399.

Alfaifi, B., Tang, J., Rasco, B., Wang, S., & Sablani, S. (2016). Computer simulation analyses to improve radio frequency (RF) heating uniformity in dried fruits for insect control. *Innovative Food Science and Emerging Technologies*, *37*, 125-137.

Ali, M. A., Yusof, Y. A., Chin, N. L., Ibrahim, M. N., & Basra, S. M. A. (2014). Drying kinetics and colour analysis of Moringa oleifera leaves. *Agriculture and Agricultural Science Procedia*, *2*, 394-400.

AOAC. (1990). *Official methods of analysis of the association of official analytical chemists. Vitamin C (Ascorbic acid) method 43.051, I&II.* chrome-extension://efaidnbmnnnibpcajpcglclefindmkaj/https://law.resource.org/pub/us/cfr/ibr/002/aoac.methods.1.1990.pdf

AOAC. (2012). *Official methods of analysis*. https://law.resource.org/pub/us/cfr/ibr/002/aoac.methods.1.1990.pdf

Atalay, H. (2019). Comparative assessment of solar and heat pump dryers with regards to exergy and exergoeconomic performance. *Energy, 189*, 116180. https://doi.org/10.1016/j.energy.2019.116180

Badiei, A., Golizadeh Akhlaghi, Y., Zhao, X., Shittu, S., Xiao, X., Li, J., Fan, Y., & Li, G. (2020). A chronological review of advances in solar assisted heat pump technology in 21st century. *Renewable and Sustainable Energy Reviews, 132*, 1-55. doi:https:// doi.org /10.1016/j.rser.2020.110132

Balana, B. B., Aghadi, C. N., & Ogunniyi, A. (2022). Improving livelihoods through postharvest loss management: Evidence from Nigeria. *Food security, 14*(1), 249-265.

Barbosa, J., & Teixeira, P. (2017). Development of probiotic fruit juice powders by spray-drying: A review. *Food Reviews International*, *33*(4), 335-358.

Bhardwaj, A. K., Kumar, R., & Chauhan, R. (2019). Experimental investigation of the performance of a novel solar dryer for drying medicinal plants in Western Himalayan region. *Solar Energy, 177*, 395-407.

Bineesh, N. P., Singhal, R. S., & Pandit, A. B. (2005). A study on degradation kinetics of ascorbic acid in drumstick (Moringa olifera) leaves during cooking. *Journal of the Science of Food Agriculture, 85*(11), 1953-1958.

BOT. (2023). *Monthly Economic Review*. https://www.bot.go.tz/Publications/Regular/Monthly%20Economic%20Review/en/2023120611573901.pdf

Budžaki, S., Leko, J., Jovanović, K., Viszmeg, J., & Koški, I. (2019). Air source heat pump assisted drying for food applications: A mini review. *Croatian Journal of Food Science, 11*(1), 122-130.

Candan, D., Oktay, Z., & Coskun, C. (2021). Design and an instantaneous experimental analysis of photovoltaic-assisted heat pump dryer for agricultural applications using banana chips. *Journal of Food Process Engineering*, *44*(10), 1-24.

Carughi, A. (2013). Bananas, dried bananas, and banana chips: Nutritional characteristics, phytochemicals, and health effects. *Dried Fruits*, *2013,* 414-427.

Catherine, B. (2016). *Prédiction de la dégradation de la vitamine C en conditions de traitement thermique: Etude en milieu modèle liquide entre 50 et 90° C.* Paris, AgroParisTech.chrome-extension://efaidnbmnnnibpcajpcglclefindmkaj/https:// pastel. hal.science/tel-03001158v1/file/44072_GOMEZRUIZ_2016_archivage.pdf

Chen, Q. H., Wu, B. K., Pan, D., Sang, L. X., & Chang, B. (2021). Beta-carotene and its protective effect on gastric cancer. *World Journal of Clinical Cases, 9*(23), 6591–6607

Cheng, B., Tan, C., Tang, X., Chu, Z., Min, J., & Luo, Y. (2020). *Study on quality influence of hot air drying and heat pump drying of Xiaocaoba Gastrodia elata. In Journal of Physics: Conference Series*. IOP Publishing. https://iopscience.iop.org/article/10. 1088/1742-6596/1601/4/042009/pdf

Coşkun, S., Doymaz, İ., Tunçkal, C., & Erdoğan, S. (2017). Investigation of drying kinetics of tomato slices dried by using a closed loop heat pump dryer. *Heat and Mass Transfer, 53*(6), 1863-1871. doi:10.1007/s00231-016-1946-7

Costa, B. R., Rodrigues, M. C., Rocha, S. F., Pohndorf, R. S., Larrosa, A. P., & Pinto, L. A. (2016). Optimization of Spirulina sp. drying in heat pump: Effects on the physicochemical properties and color parameters. *Journal of Food Processing and Preservation*, *40*(5), 934-942.

Costa, B. R., Rocha, S. F., Rodrigues, M. C., Pohndorf, R. S., Larrosa, A. P., & Pinto, L. (2015). Physicochemical characteristics of the Spirulina sp. dried in heat pump and conventional tray dryers. *The International Journal of Food Science & Technology, 50*(12), 2614-2620.

Costa, B. R., Rodrigues, M. C., Rocha, S. F., Pohndorf, R. S., Larrosa, A. P., & Pinto, L. A. (2016). Optimization of Spirulina sp. drying in heat pump: Effects on the physicochemical properties and color parameters. *Journal of Food Processing and Preservation, 40*(5), 934-942.

Daghigh, R., Ruslan, M. H., Sulaiman, M. Y., & Sopian, K. (2010). Review of solar assisted heat pump drying systems for agricultural and marine products. *Renewable and Sustainable Energy Reviews, 14*(9), 2564-2579.

Dai, Y., & Deng, K. (2021). Modeling and optimization of solar-assisted heat pump drying of pumpkin slice. *British Food Journal*, *123*(12), 4383-4401.

De Marco, I., Miranda, S., Riemma, S., & Iannone, R. (2015). Environmental assessment of drying methods for the production of apple powders. *The International Journal of Life Cycle Assessment, 20*, 1659-1672.

Dotto, J., Matemu, A. O., & Ndakidemi, P. A. (2019). Nutrient composition and selected physicochemical properties of fifteen Mchare cooking bananas: A study conducted in northern Tanzania. *Scientific African, 6*, 1-9. https://doi.org/10.1016/j.sciaf.2019.e00150

European Association for Storage of Energy [EASE]. (2015). *Storage Efficiency Calculation Methods.* chrome-extension://efaidnbmnnnibpcajpcglclefindmkaj/https://ease-storage.eu/wp-content/uploads/2016/03/Storage_efficiencies_EASE_Final.pdf

Fan, Y., Zhao, X., Han, Z., Li, J., Badiei, A., Akhlaghi, Y. G., & Liu, Z. J. E. (2021). Scientific and technological progress and future perspectives of the solar assisted heat pump (SAHP) system. *Energy, 229*, 1-32 http://creativecommons.org/licenses/by-nc-nd/4.0/

Fayose, F., & Huan, Z. (2016). Heat Pump Drying of Fruits and Vegetables: Principles and Potentials for Sub-Saharan Africa. *International Journal of Food Science, 2016*, 1-8.

Fernando, J., Amaratunga, K. S., Madhushanka, H. T., & Jayaweera, H. R. Y. (2021). "Drying performance of coffee in a batch-type heat pump dryer." *The American Society of Agricultural and Biological Engineers,* In 64 (4): 1237-1245, vol. 64, no. 4, pp. 1237-1245.

Fernando, J., Amaratunga, K. S., Madhushanka, H. T., & Jayaweera, H. R. Y. (2020). *Drying performance of coffee in a batch-type heat pump dryer. The American Society of Agricultural and Biological Engineers,* In 2020 ASABE Annual International Virtual Meeting (p. 1)

Fiorentini, M., Kinchla, A. J., & Nolden, A. (2020). Role of sensory evaluation in consumer acceptance of plant-based meat analogs and meat extenders: A scoping review. *Food, 9*(9), 1-15. https://doi.org/10.3390/foods9091334

Fudholi, A. H. M. A. D., Othman, M. Y., Ruslan, M. H., Yahya, M., Zaharim, A., & Sopian, K. (2011). Techno-economic analysis of solar drying system for seaweed in Malaysia. In *Proc. of the 7th IASME/WSEAS Int. Conf. on Energy, Environment, Ecosystems and Sustainable Development (EEESD)*. https://citeseerx.ist.psu.edu/document?repid =rep1 &type=pdf&doi=df078b33bab95181c70344b5ea11a5e5320383ac

Fudholi, A., Sopian, K., Gabbasa, M., Bakhtyar, B., Yahya, M., Ruslan, M. H., & Mat, S. (2015). Techno-economic of solar drying systems with water based solar collectors in Malaysia: A review. *Renewable and Sustainable Energy Reviews, 51*, 809-820. https://doi.org/10.1016/j.rser.2015.06.059

Gan, S., Chua, L. S., Aziz, R., Baba, M., Luqman Chuah, A., Ong, S. P., & Law, C. (2017). Drying characteristics of orthosiphon stamineus benth by solar assisted heat pump drying. *Drying Technology, 35*(14), 1755-1764.

Gan, S. H., Ong, S. P., Chin, N. L., & Law, C. L. (2017). A comparative quality study and energy saving on intermittent heat pump drying of Malaysian edible bird's nest. *Drying Technology, 35*(1), 4-14. doi:10.1080/07373937.2016.1155053

Gao, S., Wang, Y., Yu, S., Huang, Y., Liu, H., Chen, W., & He, X. (2020). Effects of drought stress on growth, physiology and secondary metabolites of two adonis species in Northeast China. *Scientia Horticulturae*, *259*, 108795. https://doi.org/10.1016/j. scienta.2019.108795

Goh, L. J., Othman, M. Y., Mat, S., Ruslan, H., & Sopian, K. (2011). Review of heat pump systems for drying application. *Renewable and Sustainable Energy Reviews, 15*(9), 4788-4796. https://doi.org/10.1016/j.rser.2011.07.072

Grassi, W. (2017). *Heat pumps: fundamentals and applications*. Springer. https://link. springer.com/book/10.1007/978-3-319-62199-9

Ha, N. M., & Tung, H. A. (2021). Experimental study of infrared–assisted heat pump drying of lime slices. *The Journal of Technical Education Science, 66,* 1-10.

Hao, W., Zhang, H., Liu, S., Mi, B., & Lai, Y. J. R. E. (2021). Mathematical modeling and performance analysis of direct expansion heat pump assisted solar drying system. *Renewable Energy, 165*, 77-87.

Haonan, H., Chen, Q., Bi, J., Wu, X., Jin, X., Li, X., Qiao-YeNing, Q. Y., & Lyu, Y. (2019). *Understanding appearance quality improvement of jujube slices during heat pump drying via water state and glass transition.* https://www.cabidigitallibrary.org/ doi/full/ 10.5555/20203111202

Hasan-Masud, M., Karim, A., Ananno, A. A., Karim, A., & Ahmed, A. (2020). *Challenges in implementing proposed sustainable food drying techniques. Sustainable food drying techniques in developing countries: Prospects and challenges.* https://link.springer. com/book/10.1007/978-3-030-42476-3

Hay, N., & Van Kien, P. (2019). *Study on designing and manufacturing a radio-frequency generator used in drying technology and efficiency of a radio frequency-assisted heat pump dryer in drying of Ganoderma lucidum. In Innovation in Global Green Technologies 2020.* IntechOpen. http://dx.doi.org/10.5772/intechopen. 88825

Hay, N., Van Kien, P., & Le Duc, A. (2018). *Study on Designing and Manufacturing a Radio Frequency Generator Using in Drying Technology. Paper presented at the 2018 4th International Conference on Green Technology and Sustainable Development (GTSD).* https://doi.org/10.1109/GTSD.2018.8595618

Hnin, K. K., Zhang, M., Mujumdar, A. S., & Zhu, Y. (2018). Emerging food drying technologies with energy-saving characteristics: A review. *Drying Technology*, *2019,* 1465-1480.

Houhou, H., Yuan, W., & Wang, G. (2017). *Simulation of Solar Heat Pump Dryer Directly Driven by Photovoltaic Panels. IOP Conference Series: Earth and Environmental Science.* http://dx.doi.org/10.1088/1755-1315/63/1/012007

Hu, Z., Zhang, S., Chu, W., He, W., Yu, C., & Yu, H. (2020). Numerical Analysis and Preliminary Experiment of a Solar Assisted Heat Pump Drying System for Chinese Wolfberry. *Energies, 13*(17), 1-16.

Huang, F., Guo, Y., Zhang, R., Yi, Y., Deng, Y., Su, D., & Zhang, M. J. M. (2014). Effects of drying methods on physicochemical and immunomodulatory properties of polysaccharide-protein complexes from litchi pulp. *Molecules, 19*(8), 12760-12776.

Ismaeel, H. H., & Yumrutaş, R. (2020). Thermal performance of a solar-assisted heat pump drying system with thermal energy storage tank and heat recovery unit. *International Journal of Energy Research*, *44*(5), 3426-3445.

Jabari, F., Mohammadi-Ivatloo, B., Li, G., & Mehrjerdi, H. (2018). Design and performance investigation of a novel absorption ice-making system using waste heat recovery from flue gases of air to air heat pump. *Applied Thermal Engineering*, *130*, 782-792.

Jarman, A., Thompson, J., McGuire, E., Reid, M., Rubsam, S., Becker, K., & Mitcham, E. (2023). Postharvest technologies for small-scale farmers in low- and middle-income countries: A call to action. *Postharvest Biology and Technology, 206*, 1-14. https://doi.org/10.1016/j.postharvbio.2023.112491

Jayaraman, K., & Gupta, D. D. (2020). *Drying of fruits and vegetables. In Handbook of industrial drying:* CRC Press. https://www.taylorfrancis.com/chapters/edit/10.1201/9780429289774-21/drying-fruits-vegetables-jayaraman-das-gupta

Jorhem, L., & Engman, J. (2000). Determination of lead, cadmium, zinc, copper, and iron in foods by atomic absorption spectrometry after microwave digestion: NMKL1 collaborative study. *Journal of AOAC International, 83*(5), 1189-1203.

Kakoko, L. D., Jande, Y. A. C., & Kivevele, T. (2023). Experimental Investigation of Soapstone and Granite Rocks as Energy-Storage Materials for Concentrated Solar Power Generation and Solar Drying Technology. *ACS Omega, 8*(21), 18554-18565.

Kesavan, S., Arjunan, T. V., & Vijayan, S. (2019). Thermodynamic analysis of a triple-pass solar dryer for drying potato slices. *Journal of Thermal Analysis and Calorimetry, 136*(1), 159-171. doi:10.1007/s10973-018-7747-0

Kien, P., Son, D., & Sang, N. (2021). *The optimization of radiofrequency assisted heat pump drying of Ganoderma lucidum*. https://doi.org/10.1063/5.0066669

Kim, M. H., & Choi, M. K. (2013). Seven Dietary Minerals (Ca, P, Mg, Fe, Zn, Cu, and Mn) and Their Relationship with Blood Pressure and Blood Lipids in Healthy Adults with Self-Selected Diet. *Biological Trace Element Research, 153*(1), 69-75.

Koşan, M., Demirtaş, M., Aktaş, M., & Dişli, E. (2020). Performance analyses of sustainable PV/T assisted heat pump drying system. *Solar Energy, 199*, 657-672.

Kuan, M., Shakir, Y., Mohanraj, M., Belyayev, Y., Jayaraj, S., & Kaltayev, A. (2019). Numerical simulation of a heat pump assisted solar dryer for continental climates. *Renewable Energy, 143*, 214-225. https://doi.org/10.1016/j.renene.2019.04.119

Kumar, M. A., Kumaresan, G., & Rajakarunakaran, S. (2021). Experimental study of moisture removal rate in Moringa leaves under vacuum pressure in closed-loop heat pump dryer. *Materials Today: Proceedings*, *45*, 1205-1210.

Kumar, S., Jadhav, S. V., & Thorat, B. N. (2022). Life cycle assessment of tomato drying in heat pump and microwave vacuum dryers. *Materials Today: Proceedings, 57*, 1700-1705. https://doi.org/10.1016/j.matpr.2021.12.333

Kylili, A., Fokaides, P. A., Ioannides, A., & Kalogirou, S. (2018). Environmental assessment of solar thermal systems for the industrial sector. *Journal of Cleaner Production*, *176*, 99-109.

Lamidi, R. O., Jiang, L., Pathare, P. B., Wang, Y., & Roskilly, A. J. A. E. (2019). Recent advances in sustainable drying of agricultural produce: A review. *Applied Energy, 233*, 367-385.

Lee, U., Benavides, P. T., & Wang, M. (2020). Chapter 8-Life cycle analysis of waste-to-energy pathways. *Waste-to-Energy*, *2020,* 213-233.

Lee, Y. H., Chin, S. K., & Chung, B. K. (2021). Drying characteristics and quality of lemon slices dried under Coulomb force-assisted heat pump drying. *Drying Technology*, *39*(6), 765-776.

Lee, Y. H., Chin, S. K., & Chung, B. K. (2015). Drying characteristics and product quality of lemon slices dried with hot air circulation oven and hybrid heatpump dryers. *International Journal of Science and Engineering*, *8*(1), 69-74.

Li, H., Xie, L., Ma, Y., Zhang, M., Zhao, Y., & Zhao, X. (2019). Effects of drying methods on drying characteristics, physicochemical properties and antioxidant capacity of okra. *Food Science and Technology, 101*, 630-638. https://doi.org/10.1016/j.lwt. 2018.11. 076

Liu, H., Yousaf, K., Chen, K., Fan, R., Liu, J., & Soomro, S. (2018). Design and Thermal Analysis of an Air Source Heat Pump Dryer for Food Drying. *Sustainability, 10*, (9) 1-17. https://doi.org/10.3390/su10093216

Liu, S., Li, X., Song, M., Hailong, L. I., & Sun, Z. (2017). Experimental investigation on drying performance of an existed enclosed fixed frequency air source heat pump drying system. *Applied Thermal Engineering, 130*, 375-744

Liu, Y., Zeng, Y., Guo, L., & Sun, X. (2019). Drying process and quality characteristics of contact ultrasound reinforced heat pump drying on kiwifruit slices. *Journal of Food Processing and Preservation, 43*(10), e14162. https://doi.org/10.1111/jfpp.14162

Loemba, A. B., Kichonge, B., & Kivevele, T. (2023). Comprehensive assessment of heat pump dryers for drying agricultural products. *Energy Science and Engineering*, *11*(8), 2985-3014.

Loemba, A. B. T., Kichonge, B., & Kivevele, T. (2024). Thermal Performance and Technoeconomic Analysis of Solar-Assisted Heat Pump Dryer Integrated with Energy Storage Materials for Drying Cavendish Banana (Musa acuminata). *Journal of Food Processing and Preservation*, *2024*(1), 1-21.

Loemba, A. B. T., Kichonge, B., Selemani, J. R., & Kivevele, T. (2023). Performance evaluation of solar-assisted heat pump dryer integrated with thermal energy storage for drying Moringa oleifera leaves. *MRS Advances*, *8*(12), 698-702.

Mahiuddin, M., Khan, M. I. H., Kumar, C., Rahman, M. M., & Karim, M. A. (2018). Shrinkage of food materials during drying: Current status and challenges. *Comprehensive Reviews in Food Science and Food Safety*, *17*(5), 1113-1126.

Majid, Z. A. A., Othman, M. Y., Ruslan, M. H., Mat, S., Ali, B., Zaharim, A., & Sopian, K. (2009). *Multifunctional solar thermal collector for heat pump application. Paper presented at the Proceedings of the 3rd WSEAS international conference on renewable energy sources.* chrome-extension://efaidnbmnnnibpcajpcglclefindmkaj/https://solarthermalworld.org/sites/default/files/EPREWA53_1.pdf

Mao, Y., & Wang, S. (2023). Recent developments in radio frequency drying for food and agricultural products using a multi-stage strategy: A review. *Critical Reviews in Food Science and Nutrition*, *63*(16), 2654-2671.

Masud, M. H., Karim, A., Ananno, A. A., & Ahmed, A. (2020). *Sustainable food drying techniques in developing countries: Prospects and challenges* Switzerland: Springer. https://link.springer.com/book/10.1007/978-3-030-42476-3

Menon, A., Stojceska, V., & Tassou, S. A. (2020). A systematic review on the recent advances of the energy efficiency improvements in non-conventional food drying technologies. *Trends in Food Science and Technology*, *100*, 67-76.

Meyer, J. P., & Greyvenstein, G. P. (1992). The drying of grain with heat pumps in South Africa: A techno-economic analysis. *International Journal of Energy Research, 16*(1), 13-20.

Mirzaee, P., Salami, P., Akhijahani, H. S., & Zareei, S. (2023). Life cycle assessment, energy and exergy analysis in an indirect cabinet solar dryer equipped with phase change materials. *Journal of Energy Storage, 61*, 106760. https://doi.org/10.1016/j.est.2023.106760

Mohanraj, M. (2014). Performance of a solar-ambient hybrid source heat pump drier for copra drying under hot-humid weather conditions. *Energy for Sustainable Development*, *23*, 165-169. https://doi.org/10.1016/j.esd.2014.09.001

Montaigne, I. (2019). *Énergie solaire en Afrique: Un avenir rayonnant?* https://www.institutmontaigne.org/publications/energie-solaire-en-afrique-un-avenir-rayonnant

Mothibe, K. J., Zhang, M., Nsor-atindana, J., & Wang, Y. C. (2011). Use of ultrasound pretreatment in drying of fruits: Drying rates, quality attributes, and shelf life extension. *Drying Technology*, *29*(14), 1611-1621.

Naikwade, P. (2015). Effect of drying methods on nutritional value of some vegetables. *Proceeding of the National Conference on Conservation of Natural Resources and Biodiversity for Sustainable Development. Bioscience Discovery.* https://www.ejfood.org/index.php/ejfood/article/view/247

Nayanita, K., Shaik, S. R., & Muthukumar, P. (2022). Comparative study of mixed-mode type and direct mode type solar dryers using life cycle assessment. *Sustainable Energy Technologies and Assessments, 53*, 102680. https://doi.org/10.1016/j.seta.2022.102680

Niroula, A., Khatri, S., Khadka, D., & Timilsina, R. (2019). Total phenolic contents and antioxidant activity profile of selected cereal sprouts and grasses. *International Journal of Food Properties, 22*(1), 427-437.

Offor, I. F., Ehiri, R. C., & Njoku, C. N. (2014). Proximate nutritional analysis and heavy metal composition of dried Moringa oleifera leaves from Oshiri Onicha LGA, Ebonyi State, Nigeria. *Journal of Environmental Science, Toxicology and Food Techno- logy*, *8*(1), 57-62.

Ogbe, A. O., & Affiku, J. P. (2011). Proximate study, mineral and anti-nutrient composition of Moringa oleifera leaves harvested from Lafia, Nigeria: Potential benefits in poultry nutrition and health. *Journal of Microbiology, Biotechnology and Food Sciences*, *1*(3), 296-308.

Ogunneye, A., Banjoko, O., Gbadamosi, M., Falegbe, O., Moberuagba, K., & Badejo, O. (2020). Spectrophotometic Determination of Caffeine and Vitamin B6 in Selected Beverages, Energy/Soft Drinks and Herbal Products. *Nigerian Journal of Basic Applied Sciences, 28*(1), 22-29.

Oirschot, R., Thomas, J. B., Gröndahl, F., Fortuin, K., Brandenburg, W., & Potting, J. (2017). Explorative environmental life cycle assessment for system design of seaweed cultivation and drying. *Algal Research, 27*, 43-54. doi:10.1016/j.algal.2017.07.025

Olabode, Z., Akanbi, C., Olunlade, B., & Adeola, A. (2015). Effects of Drying Temperature on the Nutrients of Moringa (Moringa oleifera) Leaves and Sensory Attributes of Dried Leaves Infusion. *Direct Journal of Agriculture and Food Science, 3*, 117-122.

Pelletier, N. L., Ayer, N. W., Tyedmers, P. H., Kruse, S. A., Flysjo, A., Robillard, G., Ziegler, F., Scholz, A. J., & Sonesson, U. (2007). Impact categories for life cycle assessment research of seafood production systems: Review and prospectus. *The International Journal of Life Cycle Assessment*, *12*, 414-421.

Qu, H., Masud, M. H., Islam, M., Khan, M. I. H., Ananno, A. A., & Karim, A. (2022). Sustainable food drying technologies based on renewable energy sources. *Critical Reviews in Food Science and Nutrition*, 62(25), 6872-6886.

Rabaia, M. K. H., Abdelkareem, M. A., Sayed, E. T., Elsaid, K., Chae, K. J., Wilberforce, T., & Olabi, A. G. (2021). Environmental impacts of solar energy systems: A review. *Science of the Total Environment*, *754*, 141989. https://doi.org/10.1016/j.scitotenv.2020.141989

Rahman, A., Farrok, O., Haque, M. M. J. R., & Reviews, S. E. (2022). Environmental impact of renewable energy source based electrical power plants: Solar, wind, hydroelectric, biomass, geothermal, tidal, ocean, and osmotic. *Renewable and Sustainable Energy Reviews, 161*, 112279. https://doi.org/10.1016/j.rser.2022.112279

Ranjha, M. M. A. N., Irfan, S., Nadeem, M., & Mahmood, S. (2022). A comprehensive review on nutritional value, medicinal uses, and processing of banana. *Food Reviews International, 38*(2), 199-225.

Rasskazova, E., Ivanova, T., & Sheldon, K. (2016). Comparing the effects of low-level and high-level worker need-satisfaction: A synthesis of the self-determination and Maslow need theories. *Motivation and Emotion*, *40*, 541-555.

Rocha, R. P., Melo, E. C., & Radünz, L. L. (2011). Influence of drying process on the quality of medicinal plants: A review. *Journal of Medicinal Plants Research*, *5*(33), 7076-7084.

Sagar, V. R., & Suresh Kumar, P. (2010). Recent advances in drying and dehydration of fruits and vegetables: A review. *Journal of Food Science and Technology*, *47*, 15-26.

Sandoval, J. R. M., Rosas, M. E. M., Sandoval, E. M., Velasco, M. M. M., & De Ávila, H. C. (2018). *Color analysis and image processing applied in agriculture*. Rijeka: InTech. https://www.intechopen.com/chapters/57543

Sanpang, P., & Tanongkankit, Y. (2022). *Effects of drying with heat pump, heater and hybrid systems on quality of kaffir lime leaves and energy consumption* [Doctoral dissertation, Maejo University]. http://202.28.38.45/dspace/handle/123456789/822

Saoud, A., Harajli, H., & Manneh, R. (2021). Cradle-to-grave life cycle assessment of an air to water heat pump: Case study for the Lebanese context and comparison with solar and conventional electric water heaters for residential application. *Journal of Building Engineering,* 44, 103253. https://doi.org/10.1016/j.jobe.2021.103253

Sayed, E. T., Wilberforce, T., Elsaid, K., Rabaia, M. K. H., Abdelkareem, M. A., Chae, K. J., & Olabi, A. G. (2021). A critical review on environmental impacts of renewable energy systems and mitigation strategies: Wind, hydro, biomass and geothermal. *Science of the Total Environment*, 766, 144505.

Şevik, S. (2014). Experimental investigation of a new design solar-heat pump dryer under the different climatic conditions and drying behavior of selected products. *Solar Energy, 105*, 190-205. https://doi.org/10.1016/j.solener.2014.03.037

Sharaf-Eldin, M. A., Pravej-Alam, P. A., Elkholy, S. F., Abdul-Samad, A. S., Aftab-Alam, A. A., & Palada, M. C. (2019). Impact of different drying methods on nutritional value, flavonoid content and antioxidant activity of Moringa oleifera*. Zeitschrift für Arznei- & Gewürzpflanzen*, Vol. 24, No. 1, 22-27

Shen, J., Guo, T., Tian, Y., & Xing, Z. (2018). Design and experimental study of an air source heat pump for drying with dual modes of single stage and cascade cycle. *Applied Thermal Engineering*, 129, 280-289

Shiozawa, Y. (2020). A new framework for analyzing technological change. *Journal of Evolutionary Economics*, *30*(4), 989-1034.

Singer, J. M., Pedroso-de-Lima, A. C., Tanaka, N. I., & González-López, V. A. (2007). To triplicate or not to triplicate? *Chemometrics Intelligent Laboratory Systems, 86*(1), 82-85.

Singh, A., Sarkar, J., & Sahoo, R. R. (2020a). Experiment on waste heat recovery-assisted heat pump drying of food chips: Performance, economic, and exergoeconomic

analyses. *Journal of Food Processing and Preservation*, *44*(9), e14699. https://doi.org/10.1111/jfpp.14699

Singh, A., Sarkar, J., & Sahoo, R. R. (2020b). Experimental energy-exergy performance and kinetics analyses of compact dual-mode heat pump drying of food chips. *Journal of Food Process Engineering, 43*(6), e13404. http://dx.doi.org/10.1111/jfpe.13404

Singh, A., Sarkar, J., & Sahoo, R. R. (2020c). Experimental performance analysis of novel indirect-expansion solar-infrared assisted heat pump dryer for agricultural products. *Solar Energy, 206*, 907-917. https://doi.org/10.1016/j.solener.2020.06.065

Singh, A., Sarkar, J., & Sahoo, R. R. (2020d). Experimentation on solar-assisted heat pump dryer: Thermodynamic, economic and exergoeconomic assessments. *Solar Energy, 208*, 150-159. http://dx.doi.org/10.1016/j.solener.2020.07.081

Singh, A., Sarkar, J., & Sahoo, R. R. (2021). Experimentation and Performance Analysis of Solar-Assisted Heat Pump Dryer for Intermittent Drying of Food Chips. *Journal of Solar Energy Engineering, 144*(2), 1-10. https://doi.org/10.1115/1.4052549

Singh, A., Sarkar, J., & Sahoo, R. R. (2020e). Experimental energy-exergy performance and kinetics analyses of compact dual-mode heat pump drying of food chips. *Journal of Food Process Engineering, 43*(6), e13404. https://doi.org/10.1111/jfpe.13404

Singh, A., Sarkar, J., & Sahoo, R. R. (2020f). Experimentation on solar-assisted heat pump dryer: Thermodynamic, economic and exergoeconomic assessments. *Solar Energy, 208*, 150-159. https://doi.org/10.1016/j.solener.2020.07.081

Song, X., Hu, H., & Zhang, B. (2018). Drying characteristics of Chinese Yam (Dioscorea opposita Thunb.) by far-infrared radiation and heat pump. *Journal of the Saudi Society of Agricultural Sciences*, *17*(3), 290-296.

Sundari, A. U., & Veeramanipriya, E. (2022). Performance evaluation, morphological properties and drying kinetics of untreated Carica Papaya using solar hybrid dryer integrated with heat storage material. *Journal of Energy Storage, 55*, 105679. https://doi.org/10.1016/j.est.2022.105679

Taşeri, L., Aktaş, M., Şevik, S., Gülcü, M., Seckin, G. U., & Aktekeli, B. (2018). Determination of drying kinetics and quality parameters of grape pomace dried with a heat pump dryer. *Food Chemistry, 260*, 152-159.

Teferra, T. F. (2022). The cost of postharvest losses in Ethiopia: Economic and food security implications. *Heliyon*, *8*(3), 1-8.

Tuncer, A. D., Mavuş, R., Gökçe, C., Koşan, M., & Aktaş, M. J. T. J. (2019). Efficient Energy Systems Models for Sustainable Food Processing. *Turkish Journal of Agriculture - Food Science and Technology, 7*(8), 1138-1145.

Tunckal, C., & Doymaz, İ. (2020). Performance analysis and mathematical modelling of banana slices in a heat pump drying system. *Renewable Energy, 150*, 918-923. https://doi.org/10.1016/j.renene.2020.01.040

Uusitalo, A., Uusitalo, V., Grönman, A., Luoranen, M., & Jaatinen-Värri, A. (2016). Greenhouse gas reduction potential by producing electricity from biogas engine waste heat using organic Rankine cycle. *Journal of Cleaner Production, 127*, 399-405. doi:https://doi.org/10.1016/j.jclepro.2016.03.125

Wang, Y., Li, M., Qiu, Y., Yu, Q., Luo, X., Li, G., & Ma, X. (2019). Performance analysis of a secondary heat recovery solar-assisted heat pump drying system for mango. *Energy Exploration and Exploitation*, *37*(4), 1377-1387.

Weyh, C., Krüger, K., Peeling, P., & Castell, L. (2022). The Role of Minerals in the Optimal Functioning of the Immune System. *Nutrients, 14*(3), 1-15.

Wu, H., Liu, W., & Qi, W. (2021). *Theoretical analysis of open-circuit ground source heat pump drying system. Paper presented at the IOP Conference Series: Earth and Environmental Science.* https://iopscience.iop.org/article/10.1088/1755-1315/680/1/012053/pdf

Xu, B., Wang, D., Li, Z., & Chen, Z. J. R. E. (2021). Drying and dynamic performance of well-adapted solar assisted heat pump drying system. *Renewable Energy, 164*, 1290-1305.

Yahya, M. (2016). Design and Performance Evaluation of a Solar Assisted Heat Pump Dryer Integrated with Biomass Furnace for Red Chilli. International Journal of Photoenergy, 2016, 1-14. https://onlinelibrary.wiley.com/doi/pdf/10.1155/2016/8763947

Yahya, M., Fahmi, H., Fudholi, A., & Sopian, K. (2018). Performance and economic analyses on solar-assisted heat pump fluidised bed dryer integrated with biomass furnace for drying, *Solar Energy*, 174, 1058-1067.

Yahya, M., Fudholi, A., Hafizh, H., & Sopian, K. (2016). Comparison of solar dryer and solar-assisted heat pump dryer for cassava. *Solar Energy*, *136*, 606-613.

Yang, Z., Li, X., Tao, Z., Luo, N., & Yu, F. (2018). Ultrasound-assisted heat pump drying of pea seed. *Drying Technology, 36*, 1-12. doi:10.1080/07373937.2018.1430041

Yang, Z., Yang, Z., Yu, F., & Tao, Z. (2020). Ultrasound-assisted heat pump intermittent drying of adzuki bean seeds: Drying characteristics and parameter optimization. *Journal of Food Process Engineering*, *43*(10), e13501. https://doi.org-/10. 1111/jfpe.13501

Yitayew, T., & Fenta, T. (2021). T*he Effect of Drying Method on the Texture, Color, Vitamin C and β-Carotene Content of Dried Mango Slices (Cv. Apple and Kent). In: Delele, M. A., Bitew, M. A., Beyene, A. A., Fanta, S. W., Ali, A. N. (Eds.) Advances of Science and Technology. ICAST 2020. Lecture Notes of the Institute for Computer Sciences, Social Informatics and Telecommunications Engineering.* Springer, Cham. https://doi.org/10. 1007/978-3-030-80621-7_7

Zhang, X., Bian, Z., Li, S., Chen, X., & Lu, C. (2019). Comparative analysis of phenolic compound profiles, antioxidant capacities, and expressions of phenolic biosynthesis-related genes in soybean microgreens grown under different light spectra. *Journal of Agricultural and Food Chemistry, 67*(49), 13577-13588.

Zhou, X., & Wang, S. J. D. T. (2019). Recent developments in radio frequency drying of food and agricultural products: A review. *Drying Technology, 37*(3), 271-286.

Zhou, X., Xu, R., Zhang, B., Pei, S., Liu, Q., Ramaswamy, H. S., & Wang, S. (2018). Radio frequency-vacuum drying of kiwifruits: Kinetics, uniformity, and product quality. *Food and Bioprocess Technology*, *11*, 2094-2109.

APPENDICES

Appendix 1: Detailed engineering drawing of the solar assisted heat pump dryer integrated with thermal energy storage

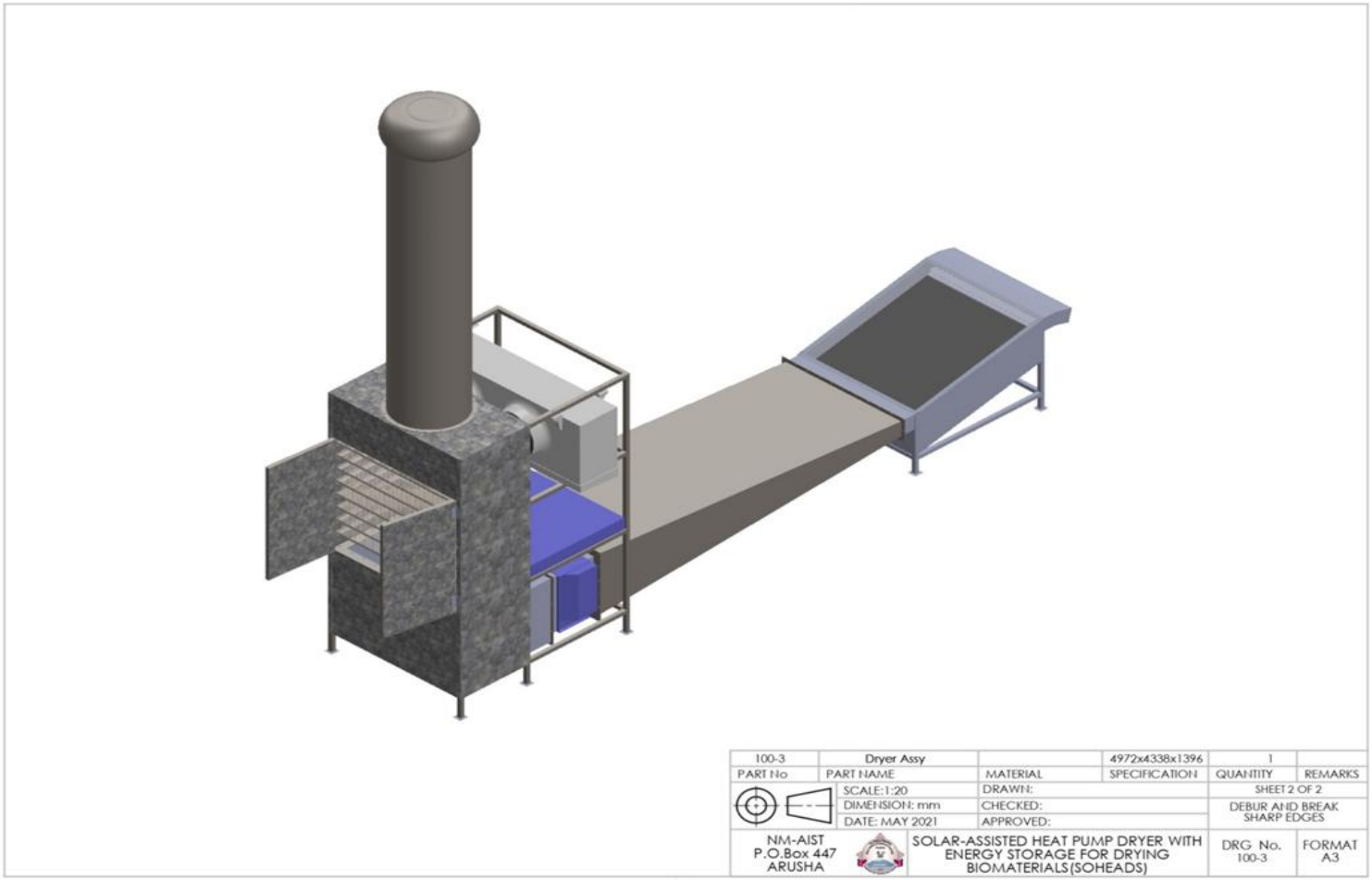

100-3	Dryer Assy		4972x4338x1396	1	
PART No	PART NAME	MATERIAL	SPECIFICATION	QUANTITY	REMARKS
	SCALE:1:20	DRAWN:		SHEET 2 OF 2	
	DIMENSION: mm	CHECKED:		DEBUR AND BREAK SHARP EDGES	
	DATE: MAY 2021	APPROVED:			
NM-AIST P.O.Box 447 ARUSHA	SOLAR-ASSISTED HEAT PUMP DRYER WITH ENERGY STORAGE FOR DRYING BIOMATERIALS(SOHEADS)			DRG No. 100-3	FORMAT A3

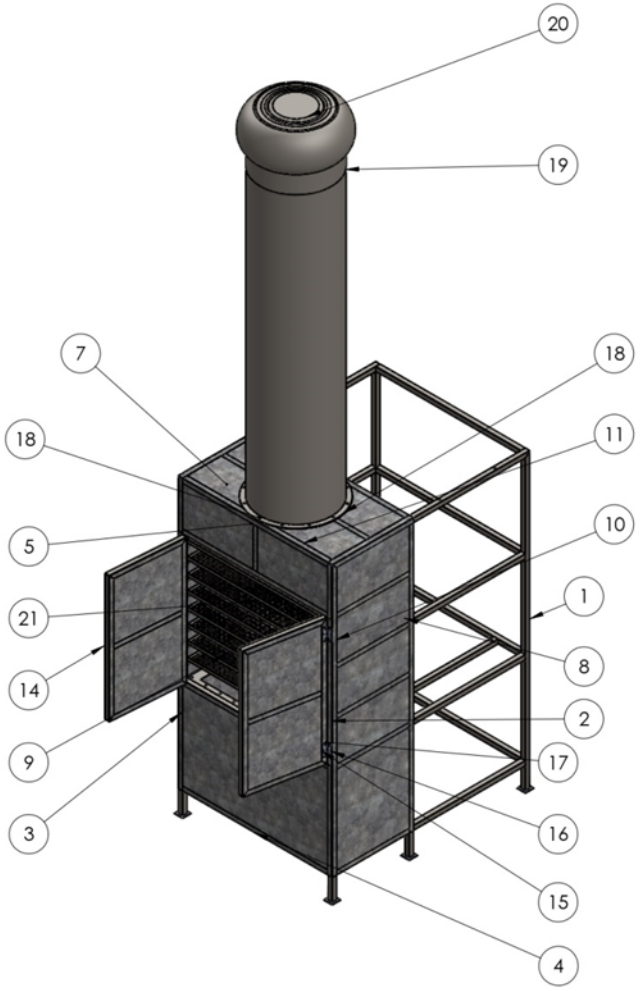

ITEM NO.	PART NUMBER	DESCRIPTION	QTY.
1	150-3	Chamber Frame Assy	1
2	160-4	Chamber Outside Sheet	1
3	161-4	Chamber Outside Sheet	1
4	163-4	Chamber Outside Sheet	1
5	162-4	Chamber Outside Sheet	1
6	164-4	Chamber Outside Sheet	1
7	165-4	Chamber Outside Sheet	1
8	169-4	Chamber Inside Sheet	1
9	168-4	Chamber Inside sheet	1
10	170-4	Chamber Inside Sheet	1
11	171-4	Chamber Inside Sheet	1
12	172-4	Chamber Outside Sheet	1
13	173-4	Tray Support	16
14	340-4	Feeding Door Assy	2
15	101-4	Door Hinge	4
16	102-4	Door Hinge	4
17	103-4	Hinge Pin	4
18	175-4	Ring Flange	1
19	174-4	Ventilator Duct	1
20	178-4	Ventilator	1
21	104-4	Tray	8

149-3	Chamber Assy		4338x1390x1090	1	
PART No	PART NAME	MATERIAL	SPECIFICATION	QUANTITY	REMARKS
	SCALE:1:20	DRAWN:		SHEET 1 OF 2	
	DIMENSION: mm	CHECKED:		DEBUR AND BREAK SHARP EDGES	
	DATE: MAY 2021	APPROVED:			
NM-AIST P.O.Box 447 ARUSHA		SOLAR-ASSISTED HEAT PUMP DRYER WITH ENERGY STORAGE FOR DRYING BIOMATERIALS(SOHEADS)		DRG No. 149-3	FORMAT A3

ITEM NO.	PART NUMBER	DESCRIPTION	QTY.
1	155-4	Hollow Section	4
2	154-4	Hollow Section	14
3	152-4	Hollow Section	10
4	158-4	Hollow Section	1
5	159-4	Hollow Section	2
6	156-4	Hollow Section	5
7	153-4	Hollow Section	6
8	157-4	Hollow Section	2
9	150-4	Hollow Section	2
10	151-4	Hollow Section	2
11	315-4	Hollow Section End Cap	6
12	166-4	Chamber Base Flange	1

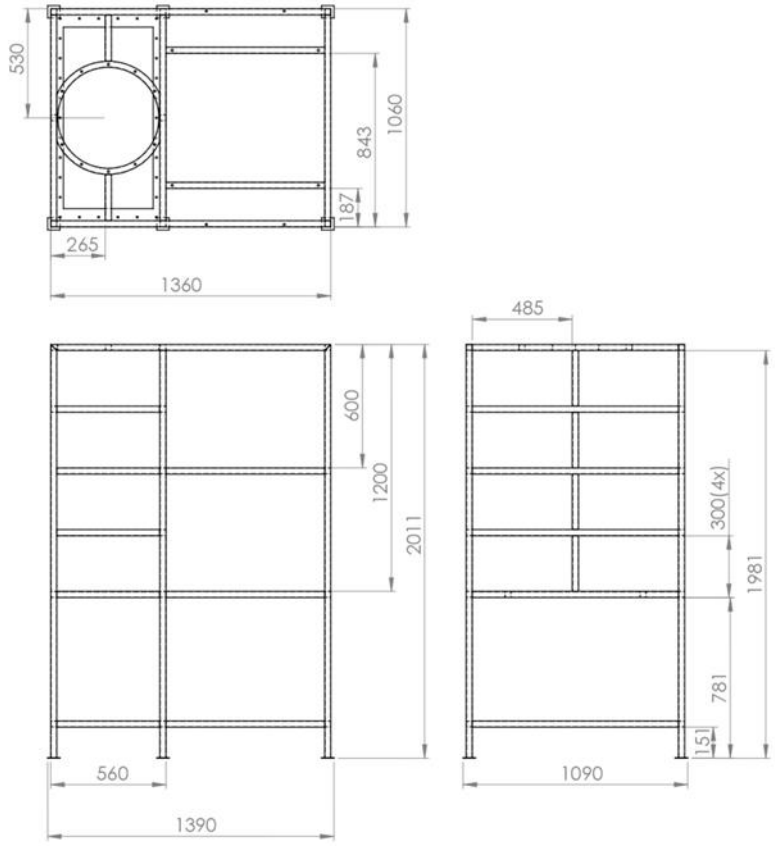

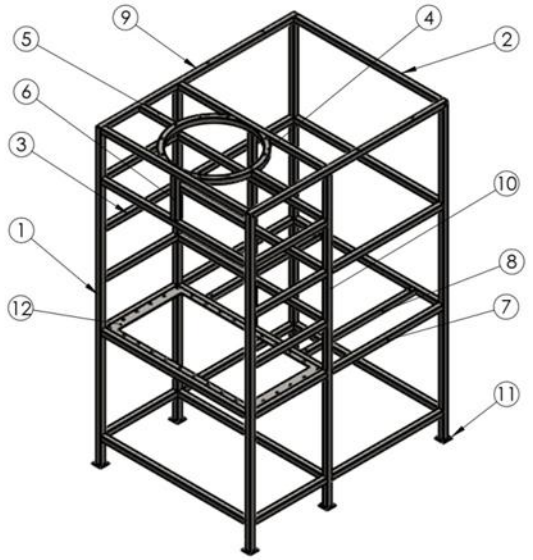

150-3	Chamber Frame Assy	Mild Steel	2011x1390x1090	1	
PART No	PART NAME	MATERIAL	SPECIFICATION	QUANTITY	REMARKS
	SCALE:1:20	DRAWN:		SHEET 1 OF 1	
	DIMENSION: mm	CHECKED:		DEBUR AND BREAK SHARP EDGES	
	DATE: MAY 2021	APPROVED:			

NM-AIST P.O.Box 447 ARUSHA	SOLAR-ASSISTED HEAT PUMP DRYER WITH ENERGY STORAGE FOR DRYING BIOMATERIALS(SOHEADS)	DRG No. 150-3	FORMAT A3

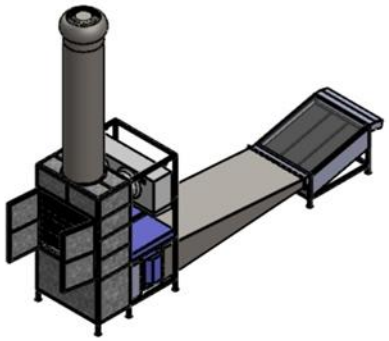

ITEM NO.	PART NUMBER	DESCRIPTION	QTY.
1	149-3	Chamber Assy	1
2	323-4	Connector Assy	1
3	200-3	Intermediate Duct	1
4	300-3	Solar Collector Assy	1
5	350-4	Condensor Assy	1
6	351-4	Evaporator	1
7	352-4	Compressor	1

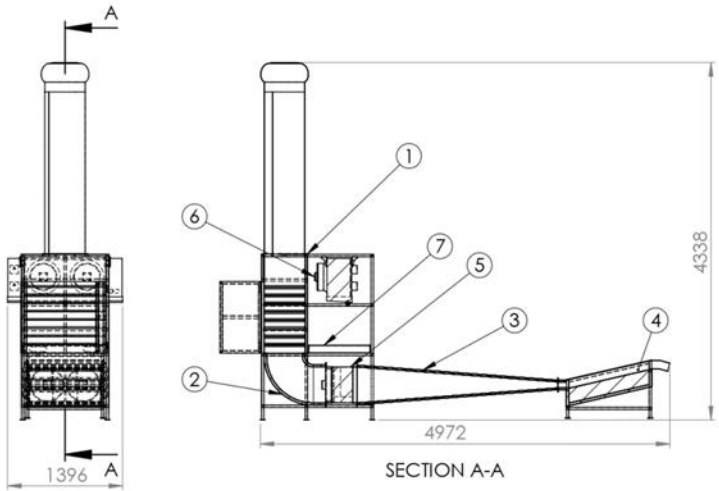

SECTION A-A

100-3	Dryer Assy		4972x4338x1396	1	
PART No	PART NAME	MATERIAL	SPECIFICATION	QUANTITY	REMARKS
	SCALE:1:50	DRAWN:		SHEET 1 OF 2	
	DIMENSION: mm	CHECKED:		DEBUR AND BREAK SHARP EDGES	
	DATE: MAY 2021	APPROVED:			
NM-AIST P.O.Box 447 ARUSHA		SOLAR-ASSISTED HEAT PUMP DRYER WITH ENERGY STORAGE FOR DRYING BIOMATERIALS(SOHEADS)		DRG No. 100-3	FORMAT A3

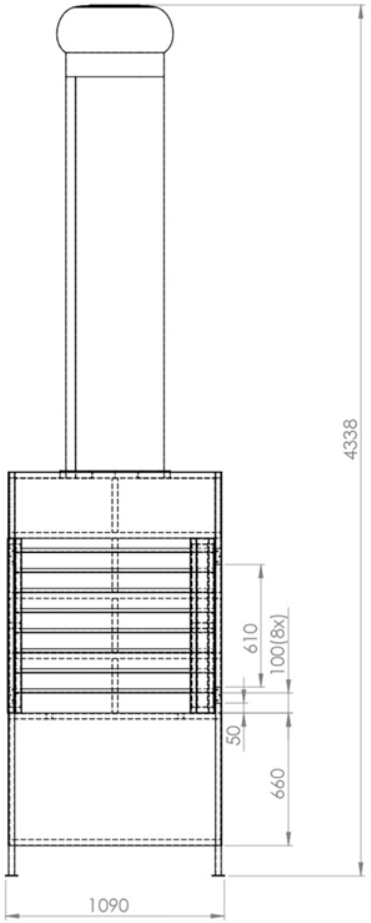

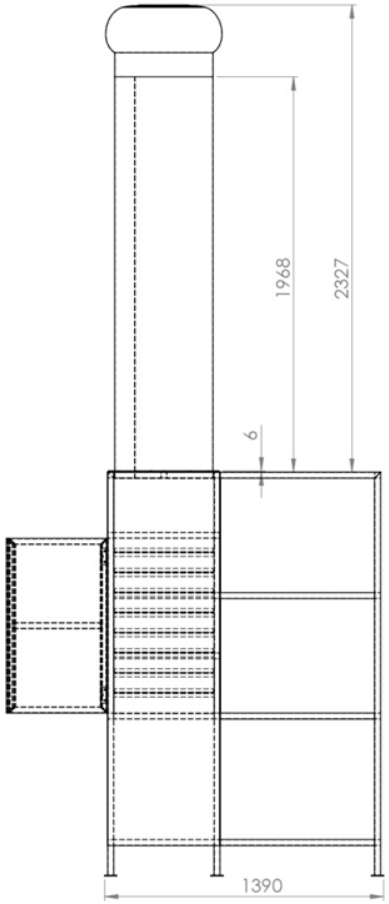

149-3	Chamber Assy		4338x1390x1090	1	
PART No	PART NAME	MATERIAL	SPECIFICATION	QUANTITY	REMARKS
	SCALE:1:20	DRAWN:		SHEET 2 OF 2	
	DIMENSION: mm	CHECKED:		DEBUR AND BREAK SHARP EDGES	
	DATE: MAY 2021	APPROVED:			
NM-AIST P.O.Box 447 ARUSHA		SOLAR-ASSISTED HEAT PUMP DRYER WITH ENERGY STORAGE FOR DRYING BIOMATERIALS(SOHEADS)		DRG No. 149-3	FORMAT A3

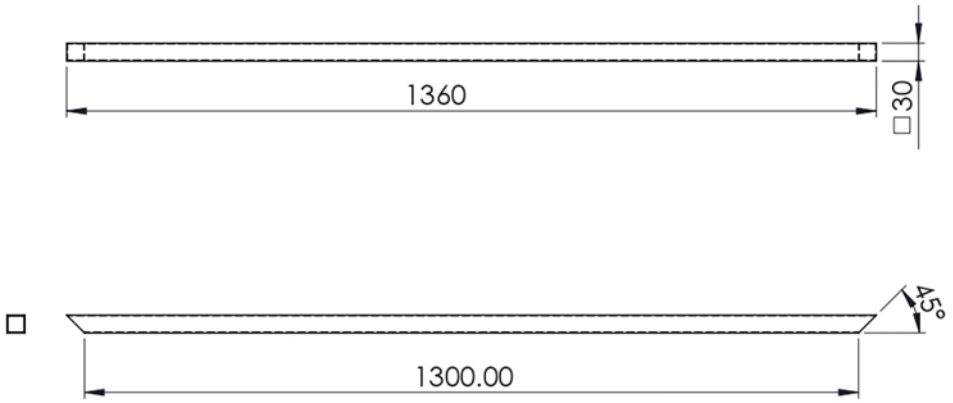

150-4	Hollow Section	Mild Steel	1360x30x1.5	2	
PART No	PART NAME	MATERIAL	SPECIFICATION	QUANTITY	REMARKS
	SCALE:1:10	DRAWN:		SHEET 1 OF 1	
	DIMENSION: mm	CHECKED:		DEBUR AND BREAK SHARP EDGES	
	DATE: MAY 2021	APPROVED:			
NM-AIST P.O.Box 447 ARUSHA		SOLAR-ASSISTED HEAT PUMP DRYER WITH ENERGY STORAGE FOR DRYING BIOMATERIALS(SOHEADS)		DRG No. 150-4	FORMAT A4

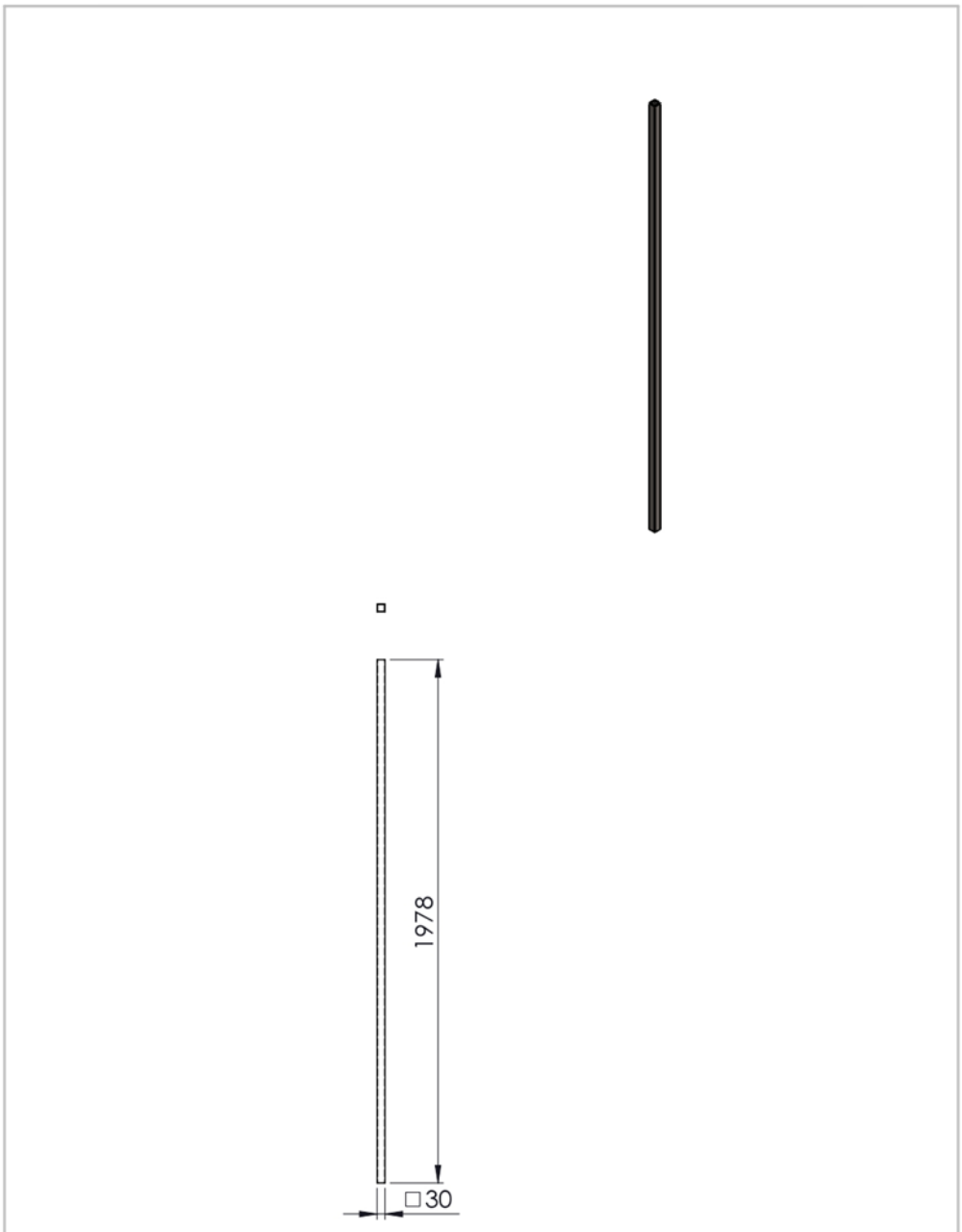

151-4	Hollow Section	Mild Steel	30x30x1.5x1978	2	
PART No	PART NAME	MATERIAL	SPECIFICATION	QUANTITY	REMARKS
	SCALE:1:20	DRAWN:		SHEET 1 OF 1	
	DIMENSION: mm	CHECKED:		DEBUR AND BREAK SHARP EDGES	
	DATE: MAY 2021	APPROVED:			
NM-AIST P.O.Box 447 ARUSHA		SOLAR-ASSISTED HEAT PUMP DRYER WITH ENERGY STORAGE FOR DRYING BIOMATERIALS(SOHEADS)		DRG No. 151-4	FORMAT A4

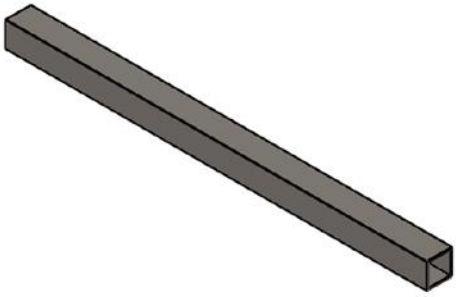

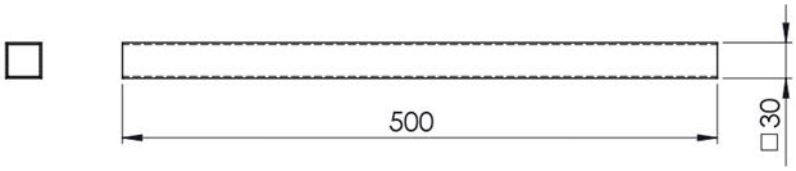

152-4	Hollow Section	Mild Steel	30x30x1.5x500	10	
PART No	PART NAME	MATERIAL	SPECIFICATION	QUANTITY	REMARKS
	SCALE:1:5	DRAWN:		SHEET 1 OF 1	
	DIMENSION: mm	CHECKED:		DEBUR AND BREAK SHARP EDGES	
	DATE: MAY 2021	APPROVED:			
NM-AIST P.O.Box 447 ARUSHA		SOLAR-ASSISTED HEAT PUMP DRYER WITH ENERGY STORAGE FOR DRYING BIOMATERIALS(SOHEADS)		DRG No. 152-4	FORMAT A4

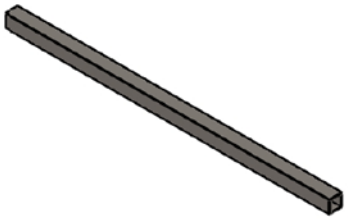

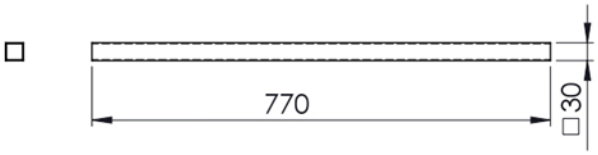

153-4	Hollow Section	Mild Steel	30x30x1.5x770	6	
PART No	PART NAME	MATERIAL	SPECIFICATION	QUANTITY	REMARKS
	SCALE:1:10	DRAWN:		SHEET 1 OF 1	
	DIMENSION: mm	CHECKED:		DEBUR AND BREAK SHARP EDGES	
	DATE: MAY 2021	APPROVED:			
NM-AIST P.O.Box 447 ARUSHA		SOLAR-ASSISTED HEAT PUMP DRYER WITH ENERGY STORAGE FOR DRYING BIOMATERIALS(SOHEADS)		DRG No. 153-4	FORMAT A4

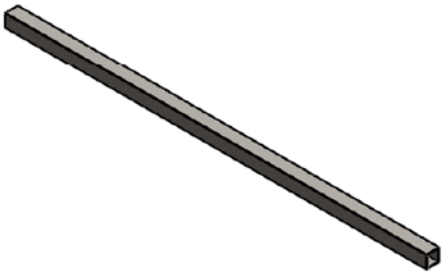

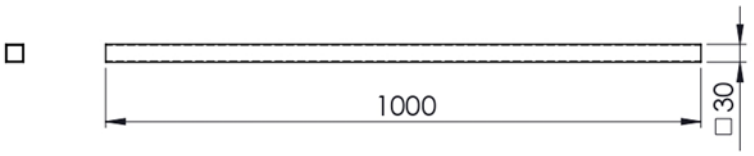

154-4	Hollow Section	Mild Steel	30x30x1.5x1000	14	
PART No	PART NAME	MATERIAL	SPECIFICATION	QUANTITY	REMARKS
	SCALE:1:10	DRAWN:		SHEET 1 OF 1	
	DIMENSION: mm	CHECKED:		DEBUR AND BREAK SHARP EDGES	
	DATE: MAY 2021	APPROVED:			
NM-AIST P.O.Box 447 ARUSHA		SOLAR-ASSISTED HEAT PUMP DRYER WITH ENERGY STORAGE FOR DRYING BIOMATERIALS(SOHEADS)		DRG No. 154-4	FORMAT A4

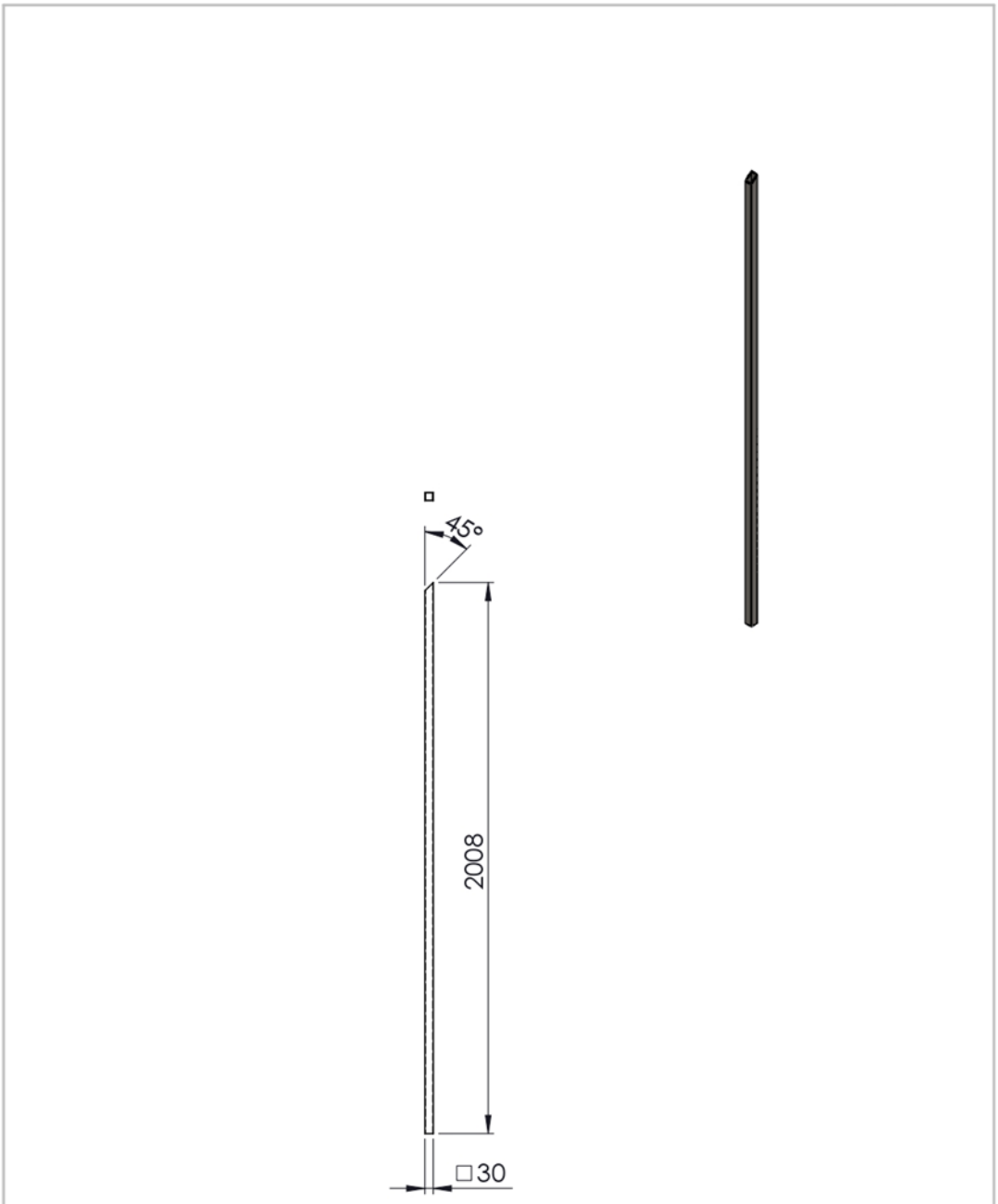

155-4	Hollow Section	Mild Steel	30x30x1.5x2008	4	
PART No	PART NAME	MATERIAL	SPECIFICATION	QUANTITY	REMARKS
	SCALE:1:20	DRAWN:		SHEET 1 OF 1	
	DIMENSION: mm	CHECKED:		DEBUR AND BREAK SHARP EDGES	
	DATE: MAY 2021	APPROVED:			
NM-AIST P.O.Box 447 ARUSHA		SOLAR-ASSISTED HEAT PUMP DRYER WITH ENERGY STORAGE FOR DRYING BIOMATERIALS(SOHEADS)		DRG No. 155-4	FORMAT A4

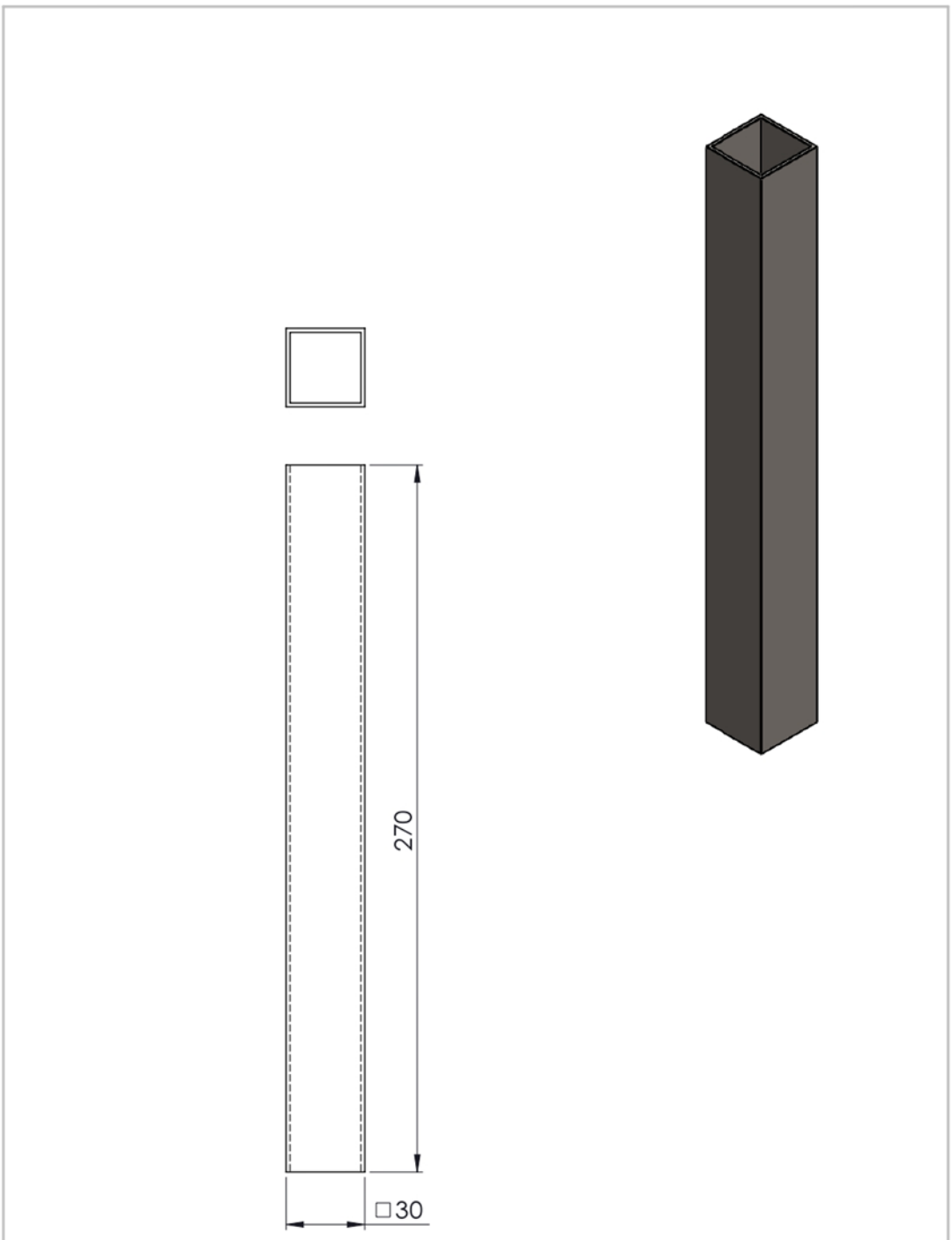

156-4	Hollow Section	Mild Steel	30x30x1.5x270	5	
PART No	PART NAME	MATERIAL	SPECIFICATION	QUANTITY	REMARKS
	SCALE:1:2	DRAWN:		SHEET 1 OF 1	
	DIMENSION: mm	CHECKED:		DEBUR AND BREAK SHARP EDGES	
	DATE: MAY 2021	APPROVED:			
NM-AIST P.O.Box 447 ARUSHA		SOLAR-ASSISTED HEAT PUMP DRYER WITH ENERGY STORAGE FOR DRYING BIOMATERIALS(SOHEADS)		DRG No. 156-4	FORMAT A4

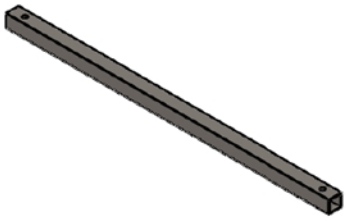

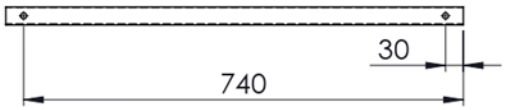

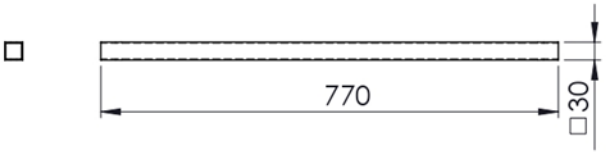

157-4	Hollow Section	Mild Steel	30x30x1.5x770	2	
PART No	PART NAME	MATERIAL	SPECIFICATION	QUANTITY	REMARKS
	SCALE:1:10	DRAWN:		SHEET 1 OF 1	
	DIMENSION: mm	CHECKED:		DEBUR AND BREAK SHARP EDGES	
	DATE: MAY 2021	APPROVED:			
NM-AIST P.O.Box 447 ARUSHA		SOLAR-ASSISTED HEAT PUMP DRYER WITH ENERGY STORAGE FOR DRYING BIOMATERIALS(SOHEADS)		DRG No. 157-4	FORMAT A4

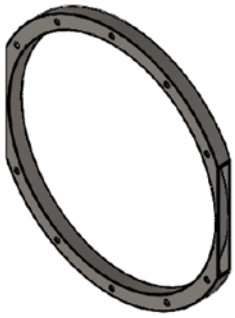

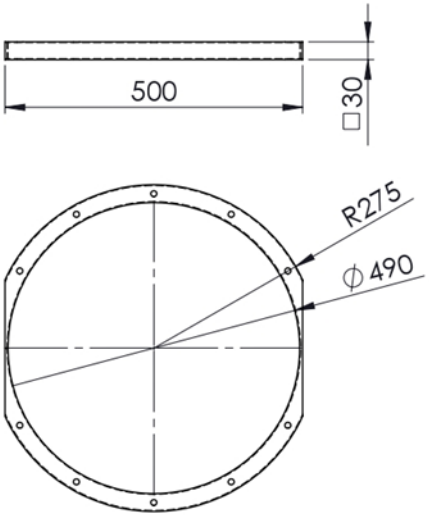

158-4	Hollow Section	Mild Steel	30x30x1.5x500	1	
PART No	PART NAME	MATERIAL	SPECIFICATION	QUANTITY	REMARKS
	SCALE:1:10	DRAWN:		SHEET 1 OF 1	
	DIMENSION: mm	CHECKED:		DEBUR AND BREAK SHARP EDGES	
	DATE: MAY 2021	APPROVED:			

NM-AIST P.O.Box 447 ARUSHA	SOLAR-ASSISTED HEAT PUMP DRYER WITH ENERGY STORAGE FOR DRYING BIOMATERIALS(SOHEADS)	DRG No. 158-4	FORMAT A4

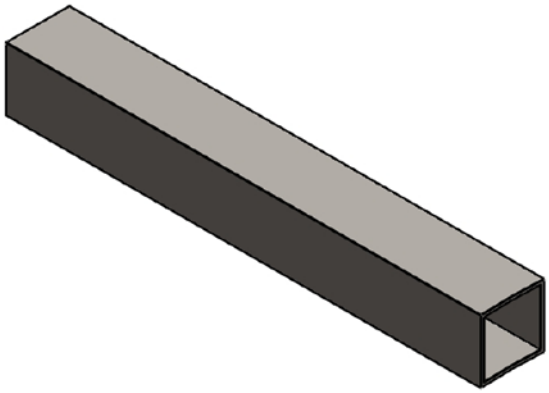

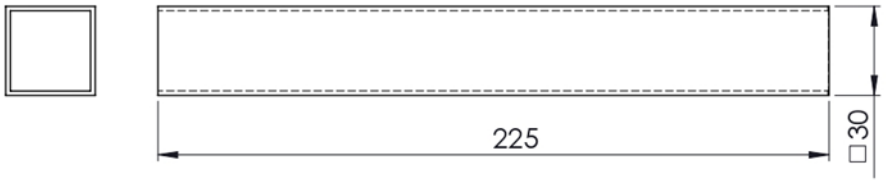

159-4	Hollow Section	Mild Steel	30x30x1.5x225	2	
PART No	PART NAME	MATERIAL	SPECIFICATION	QUANTITY	REMARKS
	SCALE:1:2	DRAWN:		SHEET 1 OF 1	
	DIMENSION: mm	CHECKED:		DEBUR AND BREAK SHARP EDGES	
	DATE: MAY 2021	APPROVED:			
NM-AIST P.O.Box 447 ARUSHA		SOLAR-ASSISTED HEAT PUMP DRYER WITH ENERGY STORAGE FOR DRYING BIOMATERIALS(SOHEADS)		DRG No. 159-4	FORMAT A4

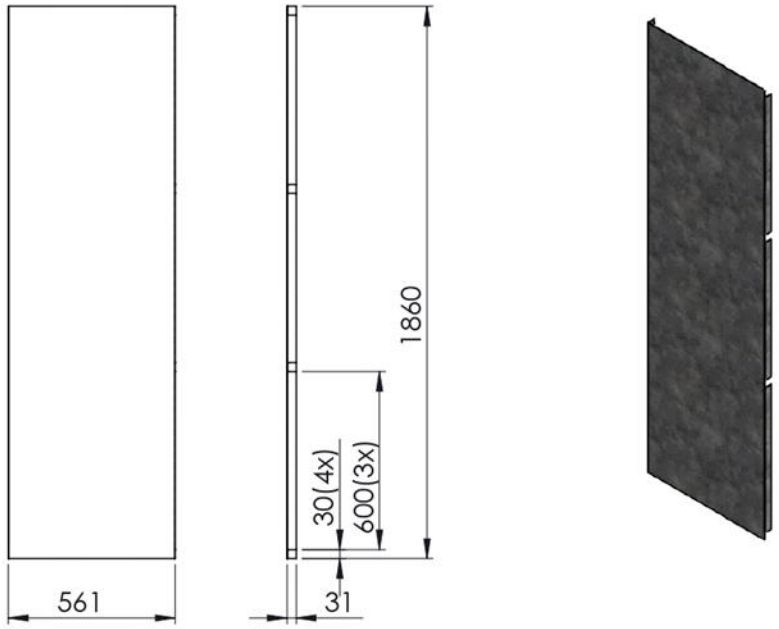

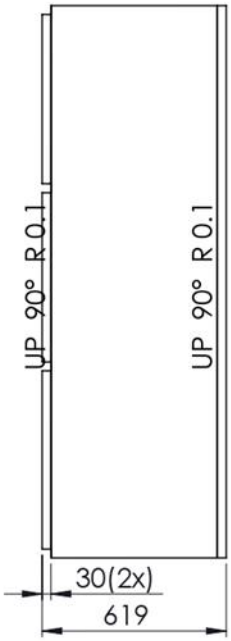

DEVELOPMENT

160-4	Chamber Outside Sheet	Galvanized Steel	1860x561x31x0.8	2	L & R
PART No	PART NAME	MATERIAL	SPECIFICATION	QUANTITY	REMARKS
	SCALE:1:20	DRAWN:		SHEET 1 OF 1	
	DIMENSION: mm	CHECKED:		DEBUR AND BREAK SHARP EDGES	
	DATE: MAY 2021	APPROVED:			
NM-AIST P.O.Box 447 ARUSHA		SOLAR-ASSISTED HEAT PUMP DRYER WITH ENERGY STORAGE FOR DRYING BIOMATERIALS(SOHEADS)		DRG No. 160-4	FORMAT A4

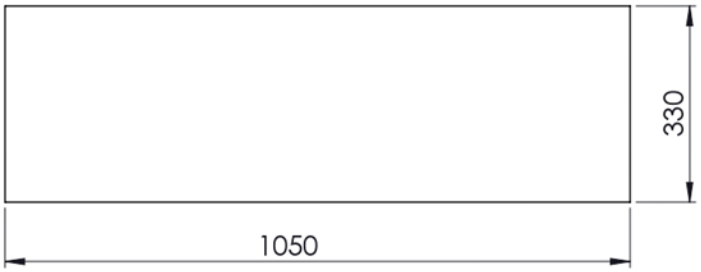

162-4	Chamber Outside Sheet	Galvanized Steel	1050 x 330 x 0.8	1	
PART No	PART NAME	MATERIAL	SPECIFICATION	QUANTITY	REMARKS
	SCALE:1:10	DRAWN:		SHEET 1 OF 1	
	DIMENSION: mm	CHECKED:		DEBUR AND BREAK SHARP EDGES	
	DATE: MAY 2021	APPROVED:			
NM-AIST P.O.Box 447 ARUSHA		SOLAR-ASSISTED HEAT PUMP DRYER WITH ENERGY STORAGE FOR DRYING BIOMATERIALS(SOHEADS)		DRG No. 162-4	FORMAT A4

163-4	Chamber Outside Sheet	Galvanized Steel	1050 x 660 x 0.8	1	
PART No	PART NAME	MATERIAL	SPECIFICATION	QUANTITY	REMARKS
	SCALE:1:10	DRAWN:		SHEET 1 OF 1	
	DIMENSION: mm	CHECKED:		DEBUR AND BREAK SHARP EDGES	
	DATE: MAY 2021	APPROVED:			
NM-AIST P.O.Box 447 ARUSHA		SOLAR-ASSISTED HEAT PUMP DRYER WITH ENERGY STORAGE FOR DRYING BIOMATERIALS(SOHEADS)		DRG No. 163-4	FORMAT A4

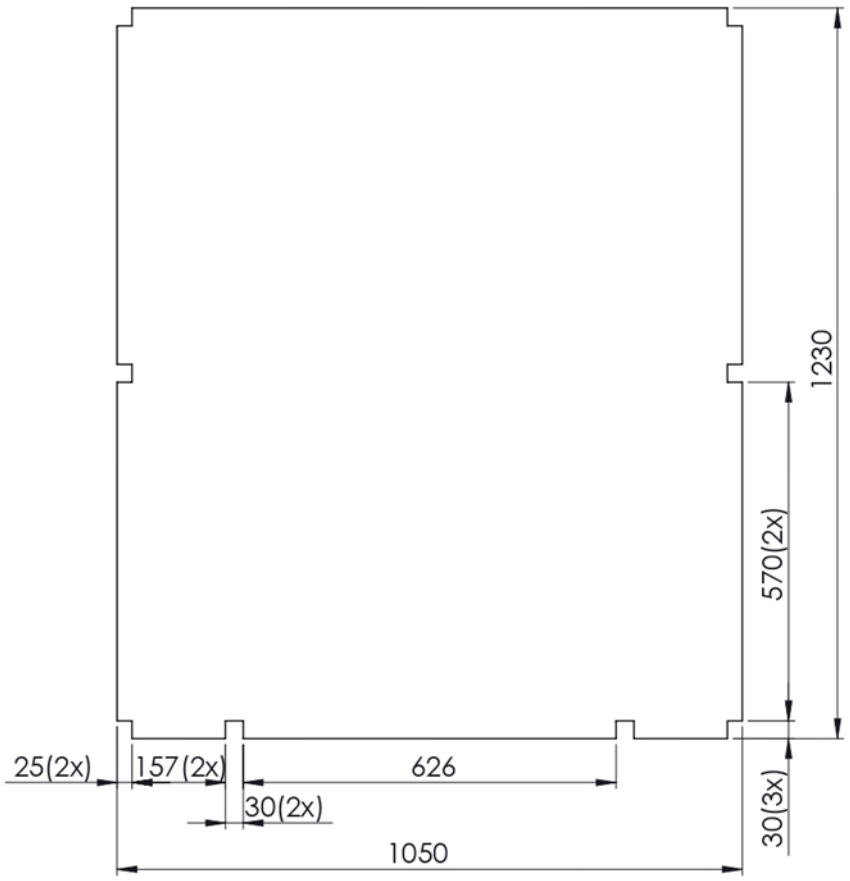

164-4	Chamber Outside Sheet	Galvanized Steel	1050 x 1230 x 0.8	1	
PART No	PART NAME	MATERIAL	SPECIFICATION	QUANTITY	REMARKS
	SCALE:1:10	DRAWN:		SHEET 1 OF 1	
	DIMENSION: mm	CHECKED:		DEBUR AND BREAK SHARP EDGES	
	DATE: MAY 2021	APPROVED:			
NM-AIST P.O.Box 447 ARUSHA		SOLAR-ASSISTED HEAT PUMP DRYER WITH ENERGY STORAGE FOR DRYING BIOMATERIALS(SOHEADS)		DRG No. 164-4	FORMAT A4

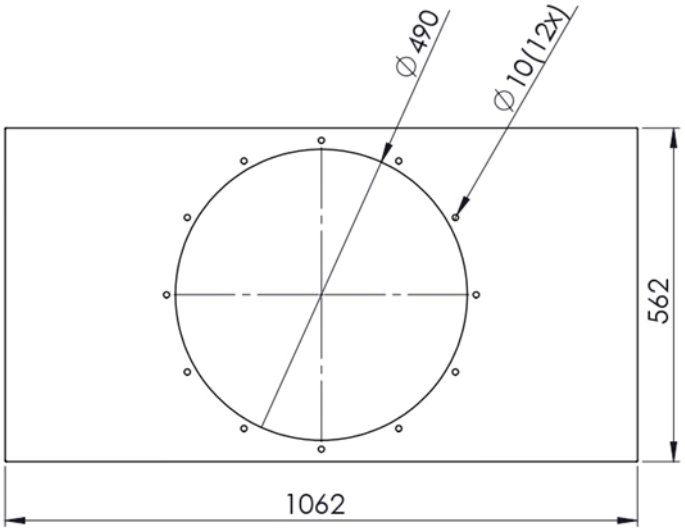

165-4	Chamber Outside Sheet	Galvanized Steel	1062x562x0.8	1	
PART No	PART NAME	MATERIAL	SPECIFICATION	QUANTITY	REMARKS
	SCALE:1:10	DRAWN:		SHEET 1 OF 1	
	DIMENSION: mm	CHECKED:		DEBUR AND BREAK SHARP EDGES	
	DATE: MAY 2021	APPROVED:			

NM-AIST P.O.Box 447 ARUSHA	SOLAR-ASSISTED HEAT PUMP DRYER WITH ENERGY STORAGE FOR DRYING BIOMATERIALS(SOHEADS)	DRG No. 165-4	FORMAT A4

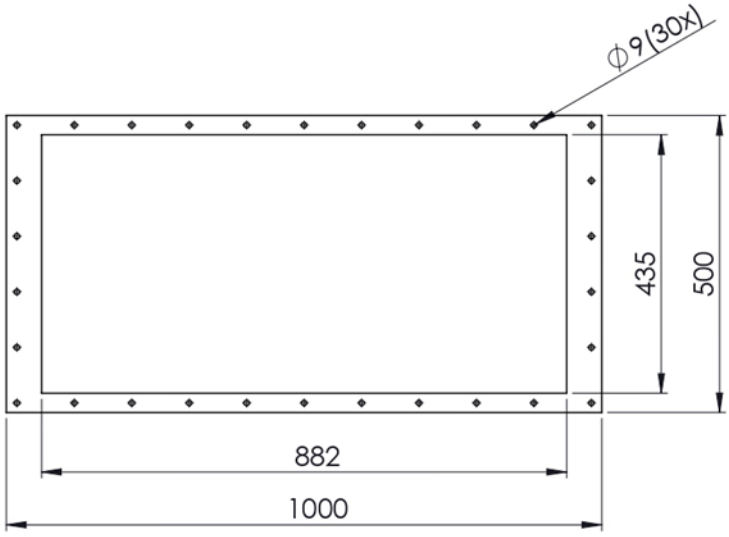

166-4	Chamber Base Flange	Mild Steel	1000 x 500 x 3	1	
PART No	PART NAME	MATERIAL	SPECIFICATION	QUANTITY	REMARKS
	SCALE:1:10	DRAWN:		SHEET 1 OF 1	
	DIMENSION: mm	CHECKED:		DEBUR AND BREAK SHARP EDGES	
	DATE: MAY 2021	APPROVED:			
NM-AIST P.O.Box 447 ARUSHA		SOLAR-ASSISTED HEAT PUMP DRYER WITH ENERGY STORAGE FOR DRYING BIOMATERIALS(SOHEADS)		DRG No. 166-4	FORMAT A4

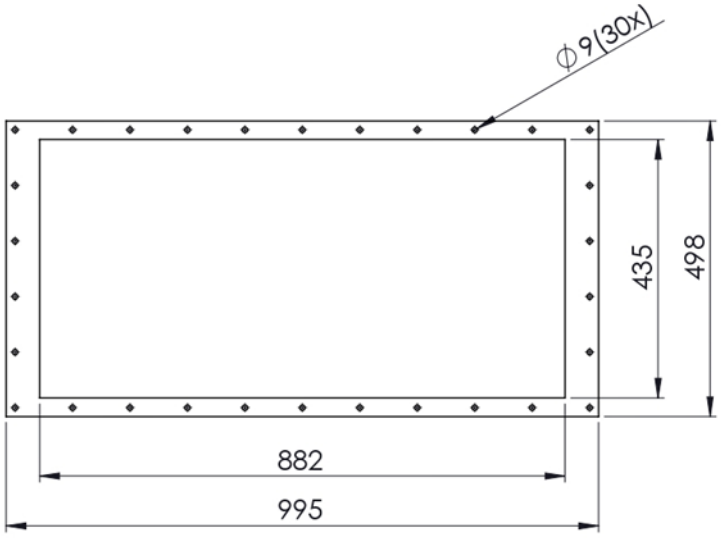

167-4	Chamber Base Flange	Mild Steel	995 x 498 x 3	1	
PART No	PART NAME	MATERIAL	SPECIFICATION	QUANTITY	REMARKS
	SCALE:1:10	DRAWN:		SHEET 1 OF 1	
	DIMENSION: mm	CHECKED:		DEBUR AND BREAK SHARP EDGES	
	DATE: MAY 2021	APPROVED:			
NM-AIST P.O.Box 447 ARUSHA		SOLAR-ASSISTED HEAT PUMP DRYER WITH ENERGY STORAGE FOR DRYING BIOMATERIALS(SOHEADS)		DRG No. 167-4	FORMAT A4

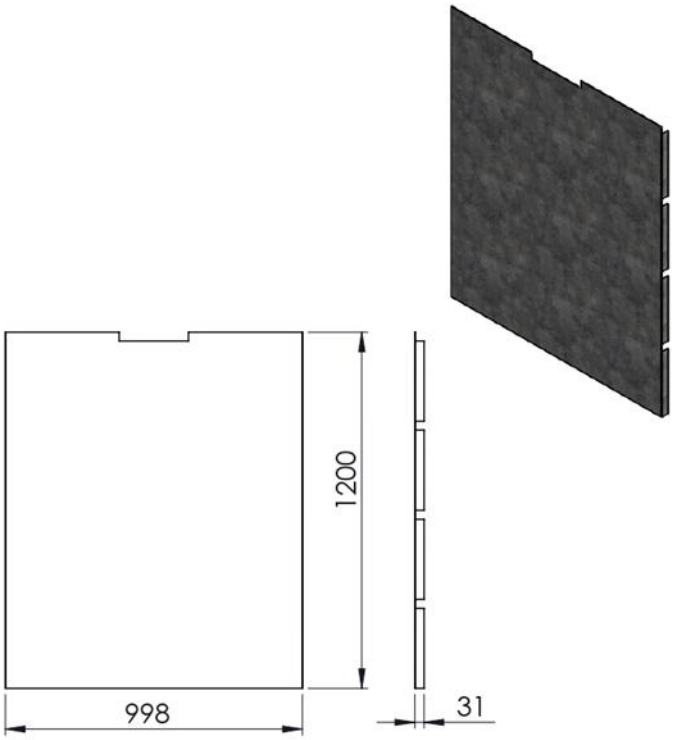

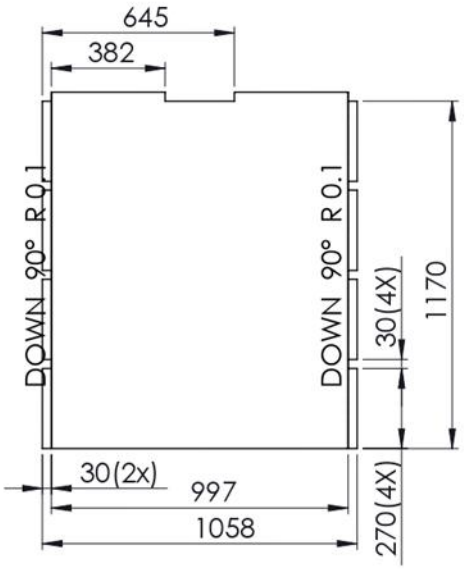

DEVELOPMENT

169-4	Chamber Inside Sheet	Galvanized Steel	1200x998x31x0.8	1	
PART No	PART NAME	MATERIAL	SPECIFICATION	QUANTITY	REMARKS
	SCALE:1:20	DRAWN:		SHEET 1 OF 1	
	DIMENSION: mm	CHECKED:		DEBUR AND BREAK SHARP EDGES	
	DATE: MAY 2021	APPROVED:			

NM-AIST P.O.Box 447 ARUSHA	SOLAR-ASSISTED HEAT PUMP DRYER WITH ENERGY STORAGE FOR DRYING BIOMATERIALS(SOHEADS)	DRG No. 169-4	FORMAT A4

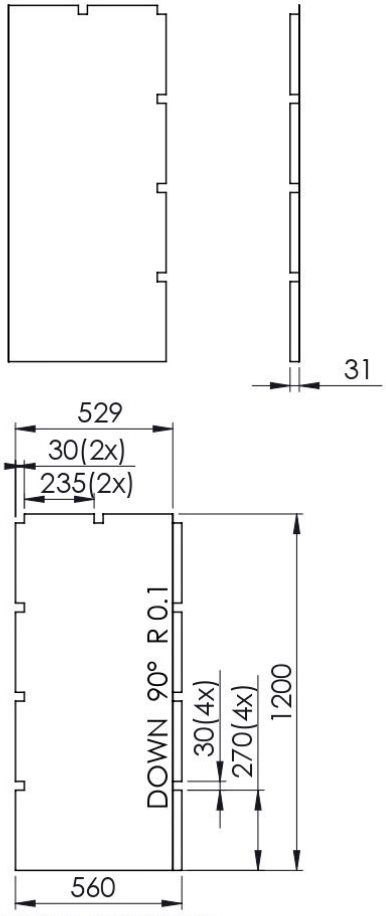

DEVELOPMENT

170-4	Chamber Inside Sheet	Galvanized Steel	1200x529x31x0.8	2	L & R
PART No	PART NAME	MATERIAL	SPECIFICATION	QUANTITY	REMARKS
	SCALE:1:20	DRAWN:		SHEET 1 OF 1	
	DIMENSION: mm	CHECKED:		DEBUR AND BREAK SHARP EDGES	
	DATE: MAY 2021	APPROVED:			
NM-AIST P.O.Box 447 ARUSHA		SOLAR-ASSISTED HEAT PUMP DRYER WITH ENERGY STORAGE FOR DRYING BIOMATERIALS(SOHEADS)		DRG No. 170-4	FORMAT A4

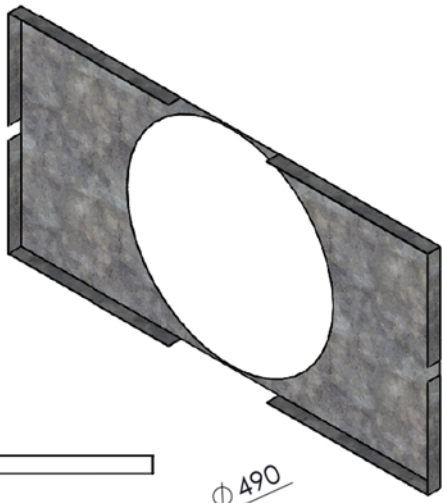

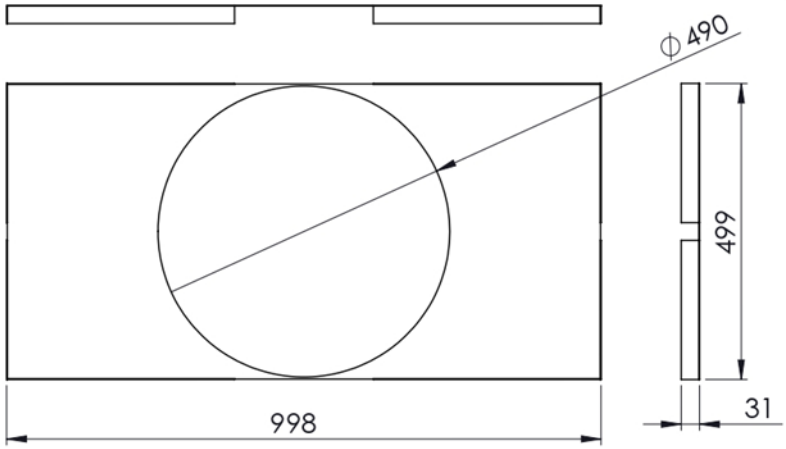

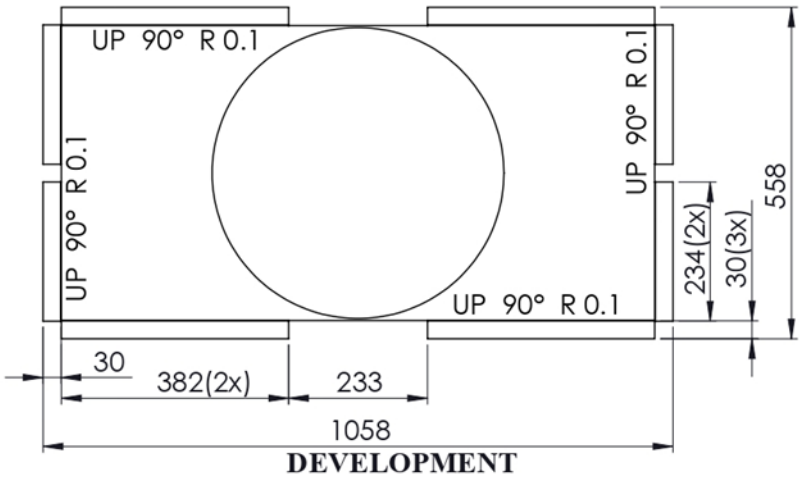

DEVELOPMENT

171-4	Chamber Inside Sheet	Galvinized Steel	998 x 499 x 0.8	1	
PART No	PART NAME	MATERIAL	SPECIFICATION	QUANTITY	REMARKS
	SCALE:1:10	DRAWN:		SHEET 1 OF 1	
	DIMENSION: mm	CHECKED:		DEBUR AND BREAK SHARP EDGES	
	DATE: MAY 2021	APPROVED:			
NM-AIST P.O.Box 447 ARUSHA		SOLAR-ASSISTED HEAT PUMP DRYER WITH ENERGY STORAGE FOR DRYING BIOMATERIALS(SOHEADS)		DRG No. 171-4	FORMAT A4

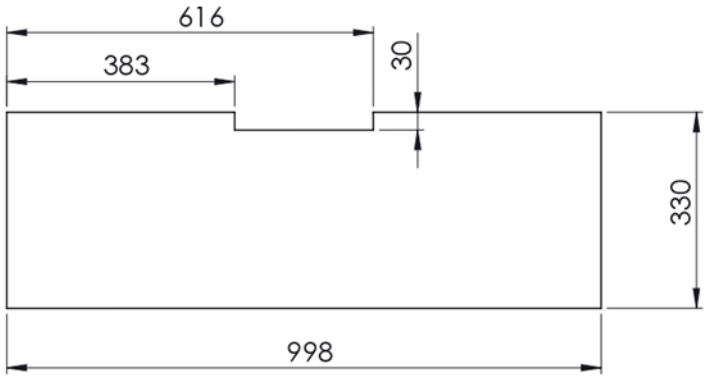

172-4	Chamber Outside Sheet	Galvanized Steel	998 x 330 x 0.8	1	
PART No	PART NAME	MATERIAL	SPECIFICATION	QUANTITY	REMARKS
	SCALE:1:10	DRAWN:		SHEET 1 OF 1	
	DIMENSION: mm	CHECKED:		DEBUR AND BREAK SHARP EDGES	
	DATE: MAY 2021	APPROVED:			
NM-AIST P.O.Box 447 ARUSHA		SOLAR-ASSISTED HEAT PUMP DRYER WITH ENERGY STORAGE FOR DRYING BIOMATERIALS(SOHEADS)		DRG No. 172-4	FORMAT A4

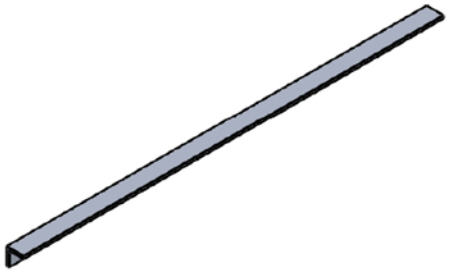

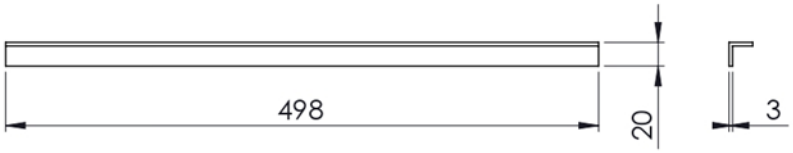

173-4	Tray Support	Aluminium	20x20x3x498	16	
PART No	PART NAME	MATERIAL	SPECIFICATION	QUANTITY	REMARKS
	SCALE:1:5	DRAWN:		SHEET 1 OF 1	
	DIMENSION: mm	CHECKED:		DEBUR AND BREAK SHARP EDGES	
	DATE: MAY 2021	APPROVED:			
NM-AIST P.O.Box 447 ARUSHA		SOLAR-ASSISTED HEAT PUMP DRYER WITH ENERGY STORAGE FOR DRYING BIOMATERIALS(SOHEADS)		DRG No. 173-4	FORMAT A4

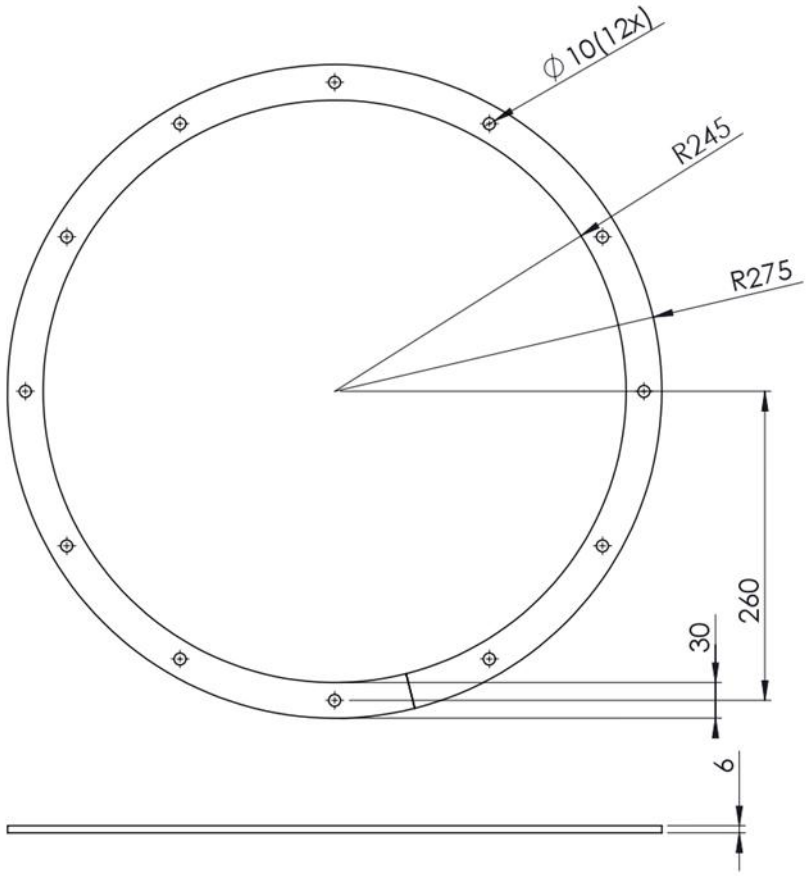

175-4	Ring Flange	Mild Steel	550 x 30 x 6	1	
PART No	PART NAME	MATERIAL	SPECIFICATION	QUANTITY	REMARKS
	SCALE:1:5	DRAWN:		SHEET 1 OF 1	
	DIMENSION: mm	CHECKED:		DEBUR AND BREAK SHARP EDGES	
	DATE: MAY 2021	APPROVED:			

NM-AIST P.O.Box 447 ARUSHA	SOLAR-ASSISTED HEAT PUMP DRYER WITH ENERGY STORAGE FOR DRYING BIOMATERIALS(SOHEADS)	DRG No. 175-4	FORMAT A4

ITEM NO.	PART NUMBER	DESCRIPTION	QTY.
1	202-3	Inside Duct Sheet	1
2	201-3	Outside Duct Sheet	1
3	200-4	Duct/Condenser Flange	1
4	201-4	Duct/Collector Flange	1
5	203-3	Duct Insulation	1

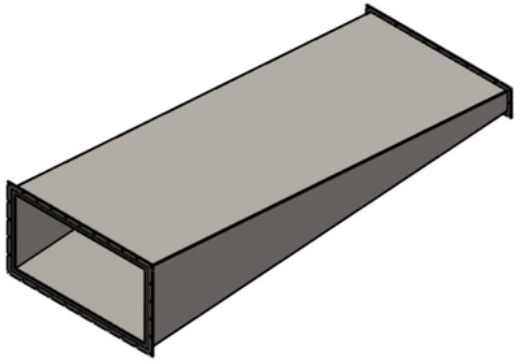

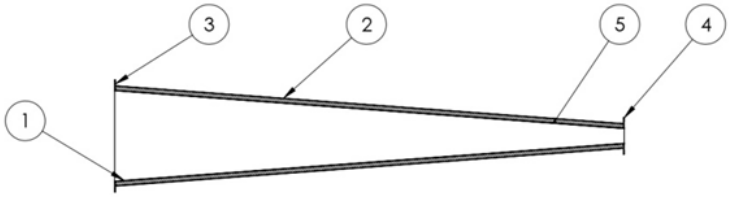

SECTION A-A

200-3	Intermediate Duct		985 X 538 X 2440	1	
PART No	PART NAME	MATERIAL	SPECIFICATION	QUANTITY	REMARKS
	SCALE:1:20	DRAWN:		SHEET 1 OF 1	
	DIMENSION: mm	CHECKED:		DEBUR AND BREAK SHARP EDGES	
	DATE: MAY 2021	APPROVED:			
NM-AIST P.O.Box 447 ARUSHA		SOLAR-ASSISTED HEAT PUMP DRYER WITH ENERGY STORAGE FOR DRYING BIOMATERIALS(SOHEADS)		DRG No. 200-3	FORMAT A3

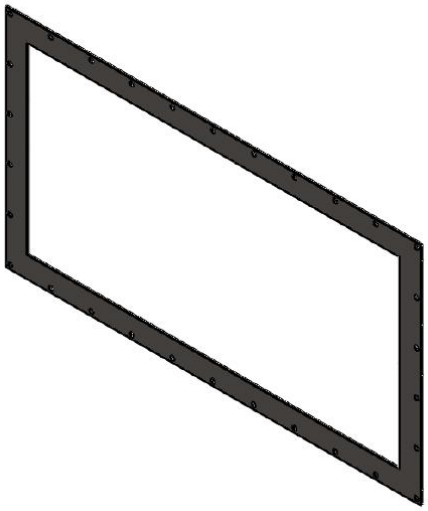

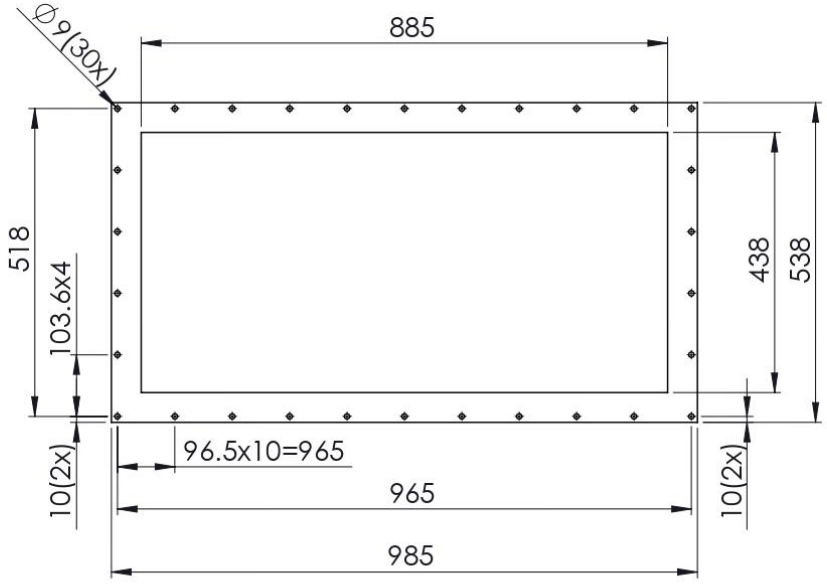

200-4	Duct/Condenser Flange	Mild Steel Sheet	985 x 538 x 3	2	
PART No	PART NAME	MATERIAL	SPECIFICATION	QUANTITY	REMARKS
	SCALE:1:10	DRAWN:		SHEET 1 OF 1	
	DIMENSION: mm	CHECKED:		DEBUR AND BREAK SHARP EDGES	
	DATE: MAY 2021	APPROVED:			
NM-AIST P.O.Box 447 ARUSHA		SOLAR-ASSISTED HEAT PUMP DRYER WITH ENERGY STORAGE FOR DRYING BIOMATERIALS(SOHEADS)		DRG No. 200-4	FORMAT A4

.

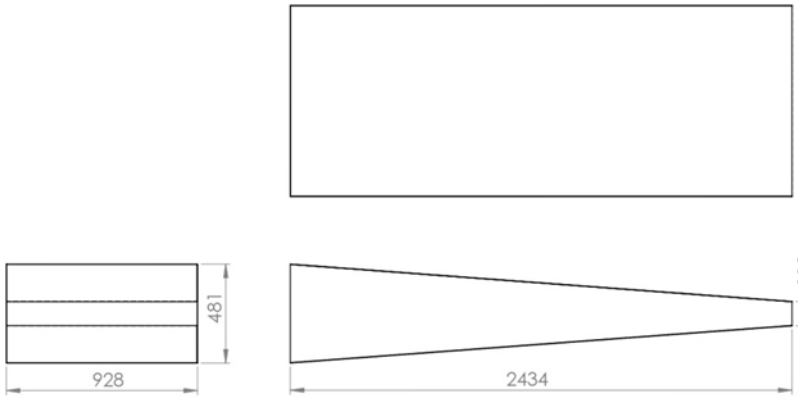

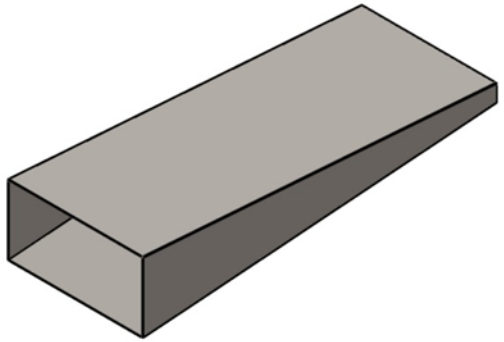

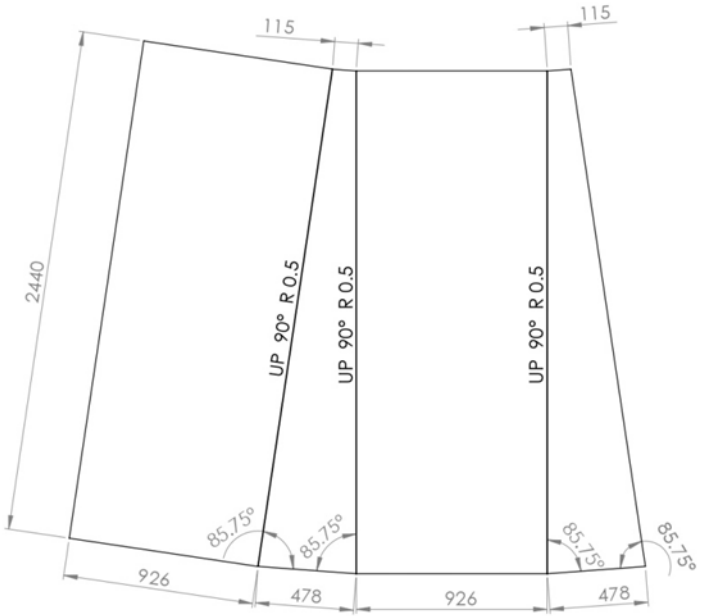

DEVELOPMENT

201-3	Outside Duct Sheet	Mild Steel	2434x928x481x1.5	1	
PART No	PART NAME	MATERIAL	SPECIFICATION	QUANTITY	REMARKS
	SCALE:1:20	DRAWN:		SHEET 1 OF 1	
	DIMENSION: mm	CHECKED:		DEBUR AND BREAK SHARP EDGES	
	DATE: MAY 2021	APPROVED:			
NM-AIST P.O.Box 447 ARUSHA		SOLAR-ASSISTED HEAT PUMP DRYER WITH ENERGY STORAGE FOR DRYING BIOMATERIALS(SOHEADS)		DRG No. 201-3	FORMAT A3

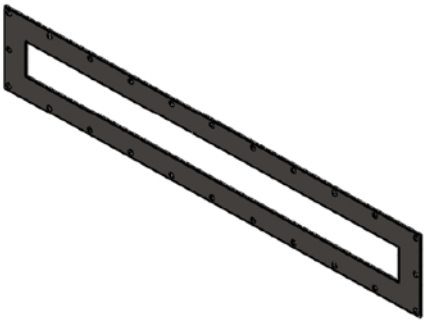

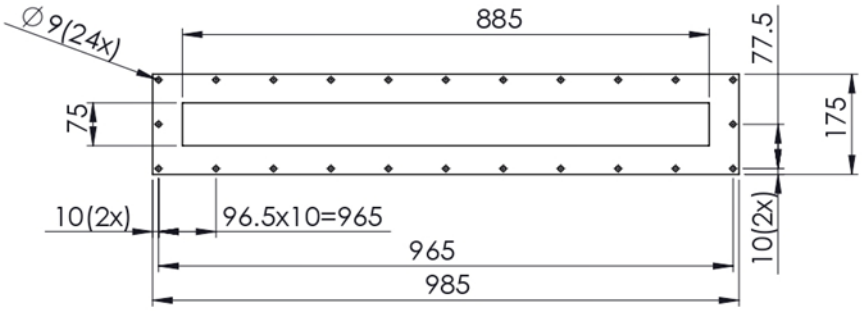

201-4	Duct/Collector Flange	Mild Steel	985 x 175 x 3	2	
PART No	PART NAME	MATERIAL	SPECIFICATION	QUANTITY	REMARKS
	SCALE:1:10	DRAWN:		SHEET 1 OF 1	
	DIMENSION: mm	CHECKED:		DEBUR AND BREAK SHARP EDGES	
	DATE: MAY 2021	APPROVED:			
NM-AIST P.O.Box 447 ARUSHA		SOLAR-ASSISTED HEAT PUMP DRYER WITH ENERGY STORAGE FOR DRYING BIOMATERIALS(SOHEADS)		DRG No. 201-4	FORMAT A4

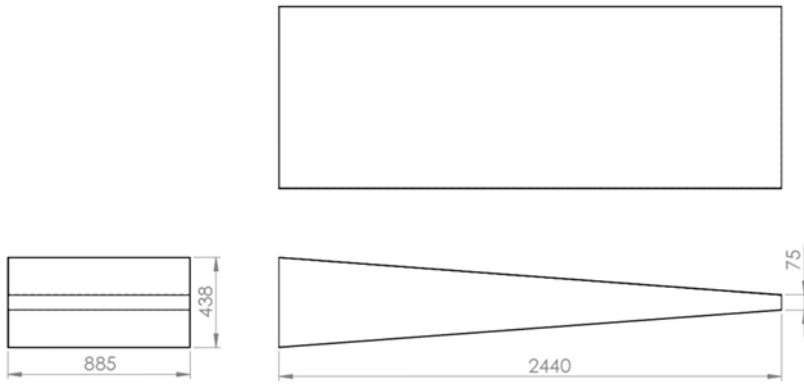

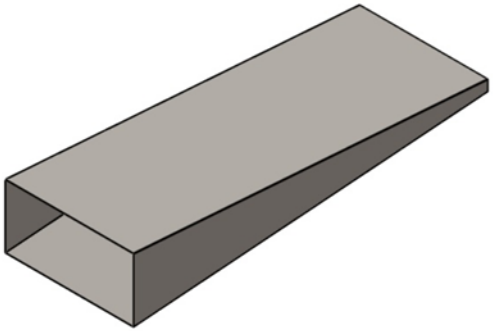

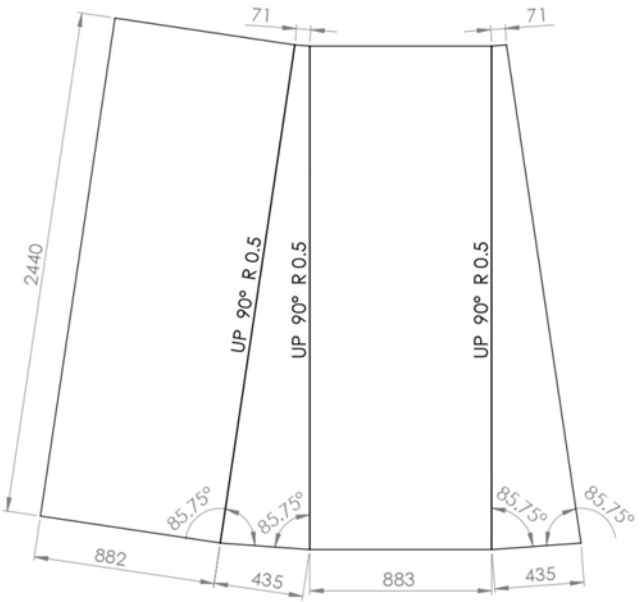

DEVELOPMENT

202-3	Inside Duct Sheet	Mild Steel	2440x885x438x1.5	1	
PART No	PART NAME	MATERIAL	SPECIFICATION	QUANTITY	REMARKS
	SCALE:1:20	DRAWN:		SHEET 1 OF 1	
	DIMENSION: mm	CHECKED:		DEBUR AND BREAK SHARP EDGES	
	DATE: MAY 2021	APPROVED:			
NM-AIST P.O.Box 447 ARUSHA		SOLAR-ASSISTED HEAT PUMP DRYER WITH ENERGY STORAGE FOR DRYING BIOMATERIALS(SOHEADS)		DRG No. 202-3	FORMAT A3

ITEM NO.	PART NUMBER	DESCRIPTION	QTY.
1	320-4	Collector Inside Sheet	1
2	318-4	Granite Partition Sheet	2
3	316-4	Granite Chamber Cover	1
4	317-4	Collector Glass	1
5	309-4	Collector Air Outlet Assy	1
6	305-4	Collector Air Inlet	1
7	321-4	Fibre Insulation	1
8	322-4	Granite Particles	1
9	314-4	Solar Collector Frame	1
10	319-3	Collector Outside Sheet	1

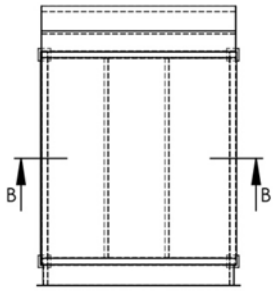

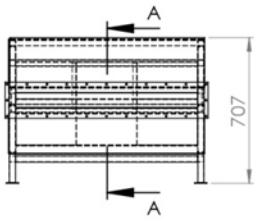

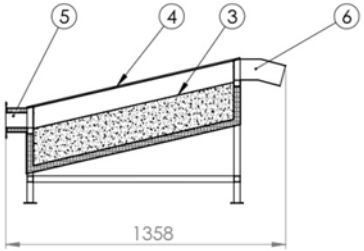

SECTION A-A

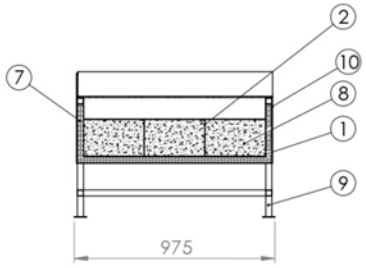

SECTION B-B

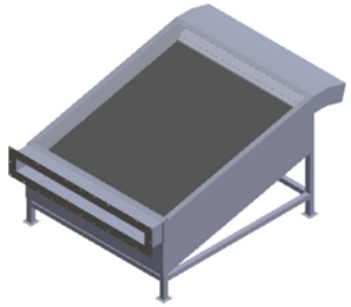

300-3	Solar Collector Assy		1358x975x707	1	
PART No	PART NAME	MATERIAL	SPECIFICATION	QUANTITY	REMARKS
	SCALE:1:20	DRAWN:		SHEET 1 OF 2	
	DIMENSION: mm	CHECKED:		DEBUR AND BREAK SHARP EDGES	
	DATE: MAY 2021	APPROVED:			
NM-AIST P.O.Box 447 ARUSHA		SOLAR-ASSISTED HEAT PUMP DRYER WITH ENERGY STORAGE FOR DRYING BIOMATERIALS(SOHEADS)		DRG No. 300-3	FORMAT A3

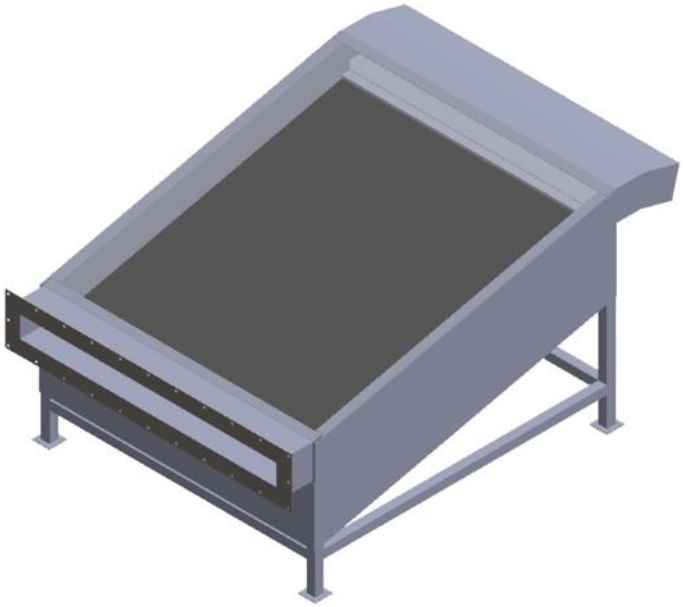

300-3	Solar Collector Assy		1358x975x707	1	
PART No	PART NAME	MATERIAL	SPECIFICATION	QUANTITY	REMARKS
	SCALE:1:10	DRAWN:		SHEET 2 OF 2	
	DIMENSION: mm	CHECKED:		DEBUR AND BREAK SHARP EDGES	
	DATE: MAY 2021	APPROVED:			

NM-AIST P.O.Box 447 ARUSHA	SOLAR-ASSISTED HEAT PUMP DRYER WITH ENERGY STORAGE FOR DRYING BIOMATERIALS(SOHEADS)	DRG No. 300-3	FORMAT A3

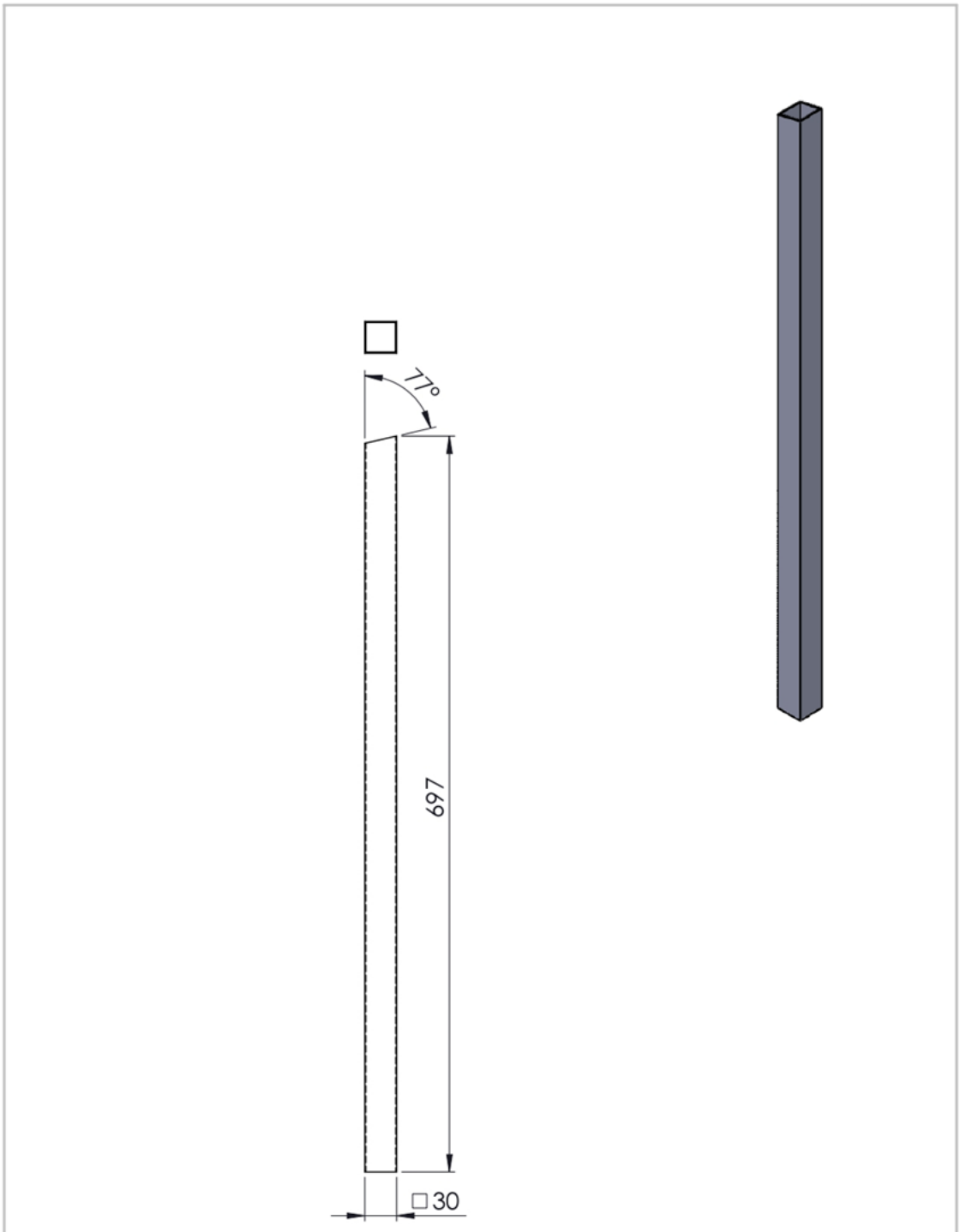

300-4	Hollow Section	Mild Steel	30x30x1.5x697	2	
PART No	PART NAME	MATERIAL	SPECIFICATION	QUANTITY	REMARKS
	SCALE:1:5	DRAWN:		SHEET 1 OF 1	
	DIMENSION: mm	CHECKED:		DEBUR AND BREAK SHARP EDGES	
	DATE: MAY 2021	APPROVED:			
NM-AIST P.O.Box 447 ARUSHA		SOLAR-ASSISTED HEAT PUMP DRYER WITH ENERGY STORAGE FOR DRYING BIOMATERIALS(SOHEADS)		DRG No. 300-4	FORMAT A4

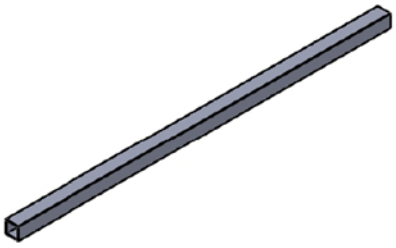

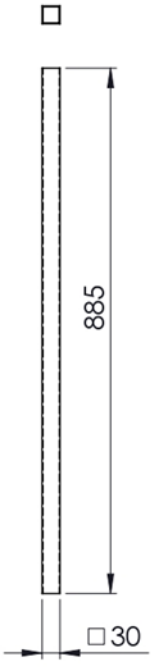

302-4	Hollow Section	Mild Steel	30x30x1.5x885	4	
PART No	PART NAME	MATERIAL	SPECIFICATION	QUANTITY	REMARKS
	SCALE:1:10	DRAWN:		SHEET 1 OF 1	
	DIMENSION: mm	CHECKED:		DEBUR AND BREAK SHARP EDGES	
	DATE: MAY 2021	APPROVED:			
NM-AIST P.O.Box 447 ARUSHA		SOLAR-ASSISTED HEAT PUMP DRYER WITH ENERGY STORAGE FOR DRYING BIOMATERIALS(SOHEADS)		DRG No. 302-4	FORMAT A4

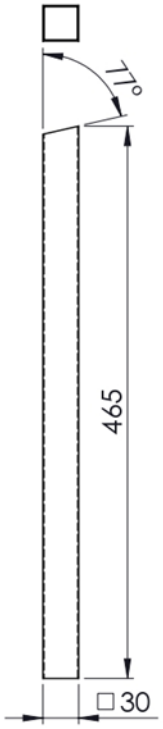

301-4	Hollow Section	Mild Steel	30x30x1.5x465	2	
PART No	PART NAME	MATERIAL	SPECIFICATION	QUANTITY	REMARKS
	SCALE:1:5	DRAWN:		SHEET 1 OF 1	
	DIMENSION: mm	CHECKED:		DEBUR AND BREAK SHARP EDGES	
	DATE: MAY 2021	APPROVED:			
NM-AIST P.O.Box 447 ARUSHA		SOLAR-ASSISTED HEAT PUMP DRYER WITH ENERGY STORAGE FOR DRYING BIOMATERIALS(SOHEADS)		DRG No. 301-4	FORMAT A4

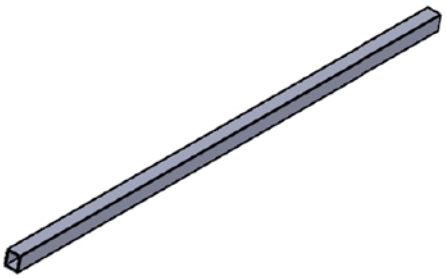

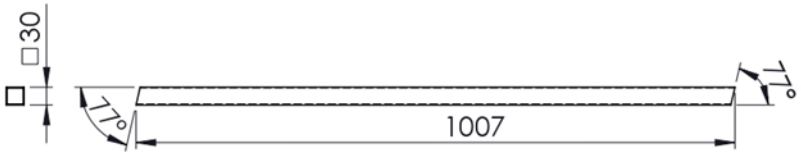

303-4	Hollow section	Mild Steel	30x30x1.5x1007	2	
PART No	PART NAME	MATERIAL	SPECIFICATION	QUANTITY	REMARKS
	SCALE:1:10	DRAWN:		SHEET 1 OF 1	
	DIMENSION: mm	CHECKED:		DEBUR AND BREAK SHARP EDGES	
	DATE: MAY 2021	APPROVED:			
NM-AIST P.O.Box 447 ARUSHA		SOLAR-ASSISTED HEAT PUMP DRYER WITH ENERGY STORAGE FOR DRYING BIOMATERIALS(SOHEADS)		DRG No. 303-4	FORMAT A4

ITEM NO.	PART NUMBER	DESCRIPTION	QTY.
1	306-4	Collector Air Inlet Sheet	1
2	307-4	Collector Air Inlet Sheet	2
3	308-4	Collector Air Inlet Sheet	1

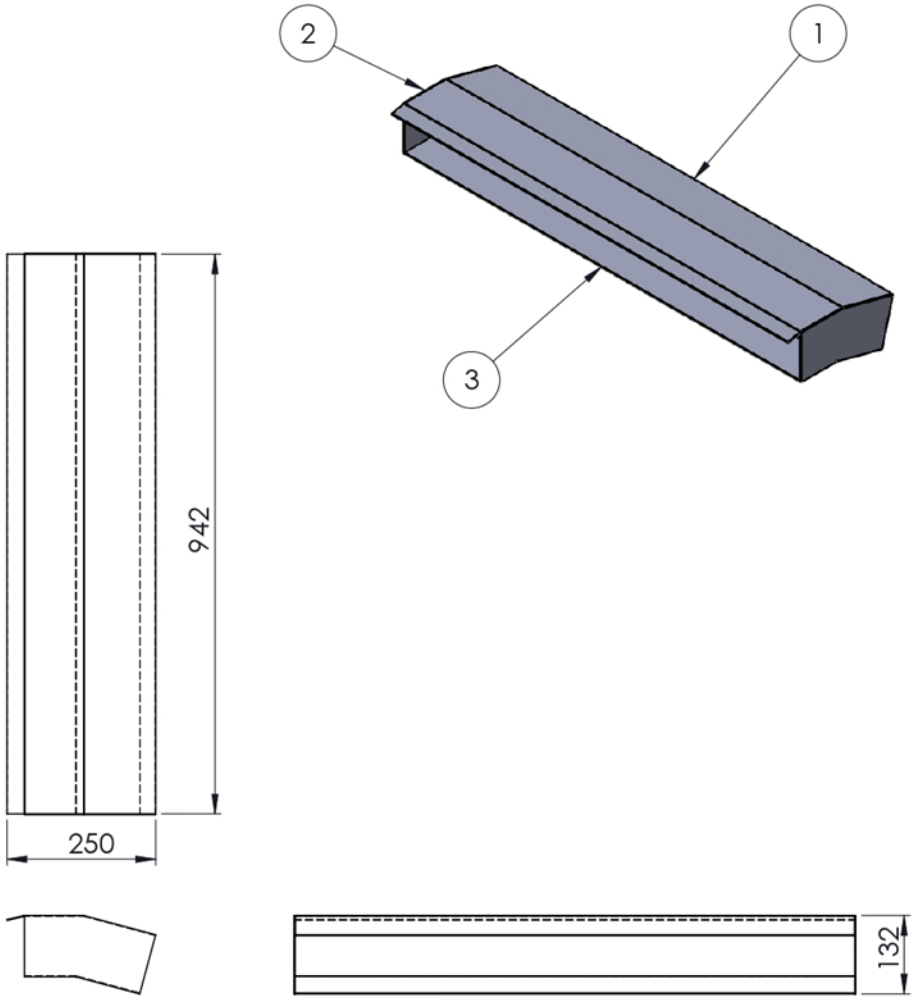

305-4	Collector Air Inlet	Mild Steel	942 x 250 x 132	1	
PART No	PART NAME	MATERIAL	SPECIFICATION	QUANTITY	REMARKS
	SCALE:1:10	DRAWN:		SHEET 1 OF 1	
	DIMENSION: mm	CHECKED:		DEBUR AND BREAK SHARP EDGES	
	DATE: MAY 2021	APPROVED:			
NM-AIST P.O.Box 447 ARUSHA		SOLAR-ASSISTED HEAT PUMP DRYER WITH ENERGY STORAGE FOR DRYING BIOMATERIALS(SOHEADS)		DRG No. 305-4	FORMAT A4

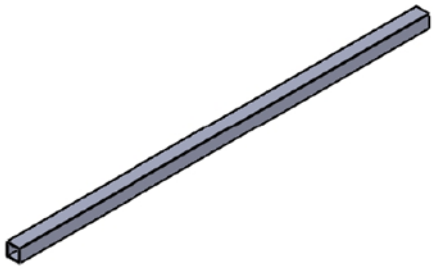

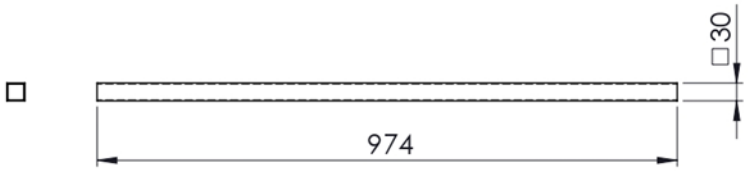

304-4	Hollow Section	Mild Steel	30x30x1.5x974	2	
PART No	PART NAME	MATERIAL	SPECIFICATION	QUANTITY	REMARKS
	SCALE:1:10	DRAWN:		SHEET 1 OF 1	
	DIMENSION: mm	CHECKED:		DEBUR AND BREAK SHARP EDGES	
	DATE: MAY 2021	APPROVED:			
NM-AIST P.O.Box 447 ARUSHA		SOLAR-ASSISTED HEAT PUMP DRYER WITH ENERGY STORAGE FOR DRYING BIOMATERIALS(SOHEADS)		DRG No. 304-4	FORMAT A4

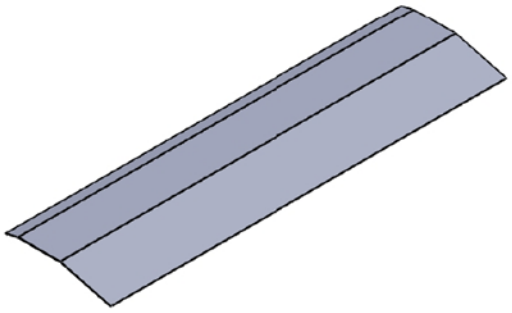

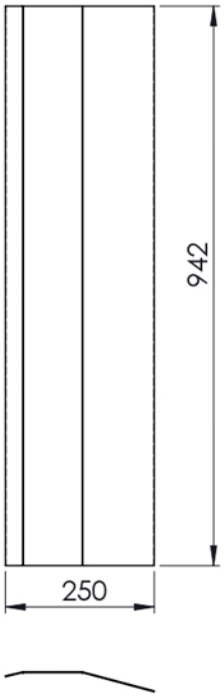

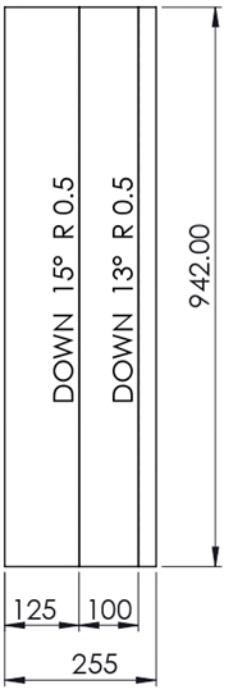

DEVELOPMENT

306-4	Collector Air Inlet Sheet	Mild Steel	942x250x34x1.5	1	
PART No	PART NAME	MATERIAL	SPECIFICATION	QUANTITY	REMARKS
	SCALE:1:10	DRAWN:		SHEET 1 OF 1	
	DIMENSION: mm	CHECKED:		DEBUR AND BREAK SHARP EDGES	
	DATE: MAY 2021	APPROVED:			
NM-AIST P.O.Box 447 ARUSHA		SOLAR-ASSISTED HEAT PUMP DRYER WITH ENERGY STORAGE FOR DRYING BIOMATERIALS(SOHEADS)		DRG No. 306-4	FORMAT A4

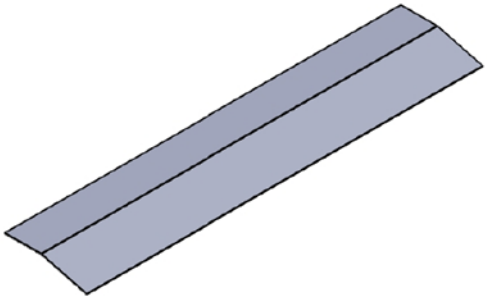

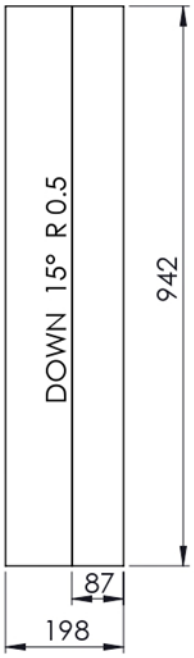

DEVELOPMENT

308-4	Collector Air Inlet Sheet	Mild Steel	942x194x30x1.5	1	
PART No	PART NAME	MATERIAL	SPECIFICATION	QUANTITY	REMARKS
	SCALE:1:10	DRAWN:		SHEET 1 OF 1	
	DIMENSION: mm	CHECKED:		DEBUR AND BREAK SHARP EDGES	
	DATE: MAY 2021	APPROVED:			
NM-AIST P.O.Box 447 ARUSHA		SOLAR-ASSISTED HEAT PUMP DRYER WITH ENERGY STORAGE FOR DRYING BIOMATERIALS(SOHEADS)		DRG No. 308-4	FORMAT A4

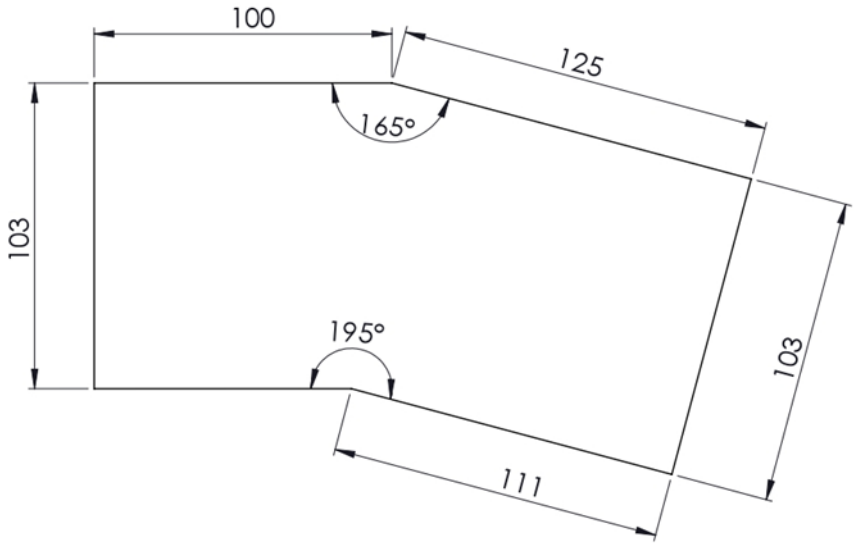

307-4	Collector Air Inlet Sheet	Mild Steel	221 x 132 x 1.5	2	
PART No	PART NAME	MATERIAL	SPECIFICATION	QUANTITY	REMARKS
	SCALE:1:2	DRAWN:		SHEET 1 OF 1	
	DIMENSION: mm	CHECKED:		DEBUR AND BREAK SHARP EDGES	
	DATE: MAY 2021	APPROVED:			

NM-AIST P.O.Box 447 ARUSHA	SOLAR-ASSISTED HEAT PUMP DRYER WITH ENERGY STORAGE FOR DRYING BIOMATERIALS(SOHEADS)	DRG No. 307-4	FORMAT A4

ITEM NO.	PART NUMBER	DESCRIPTION	QTY.
1	310-4	Collector Air Outlet	1
2	311-3	Collector Air Outlet	1
3	201-4	Duct/Collector Flange	1
4	313-4	Fibre Insulation	1

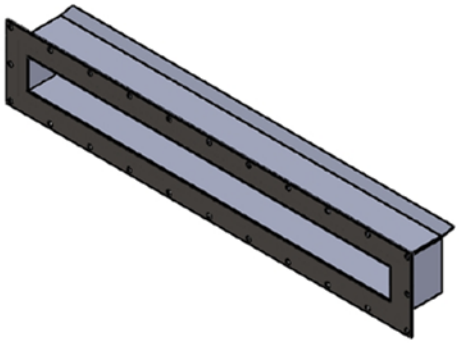

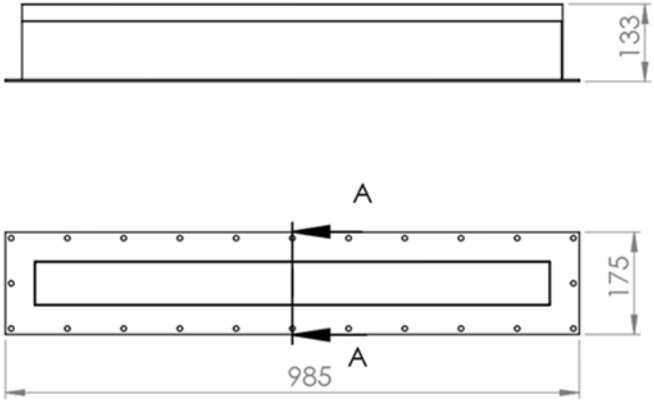

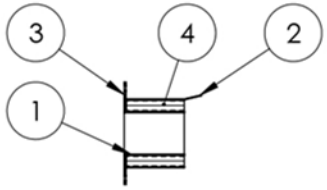

SECTION A-A

309-4	Collector Air Outlet Assy		985 x 175 x 133	1	
PART No	PART NAME	MATERIAL	SPECIFICATION	QUANTITY	REMARKS
	SCALE:1:10	DRAWN:		SHEET 1 OF 1	
	DIMENSION: mm	CHECKED:		DEBUR AND BREAK SHARP EDGES	
	DATE: MAY 2021	APPROVED:			
NM-AIST P.O.Box 447 ARUSHA		SOLAR-ASSISTED HEAT PUMP DRYER WITH ENERGY STORAGE FOR DRYING BIOMATERIALS(SOHEADS)		DRG No. 309-4	FORMAT A4

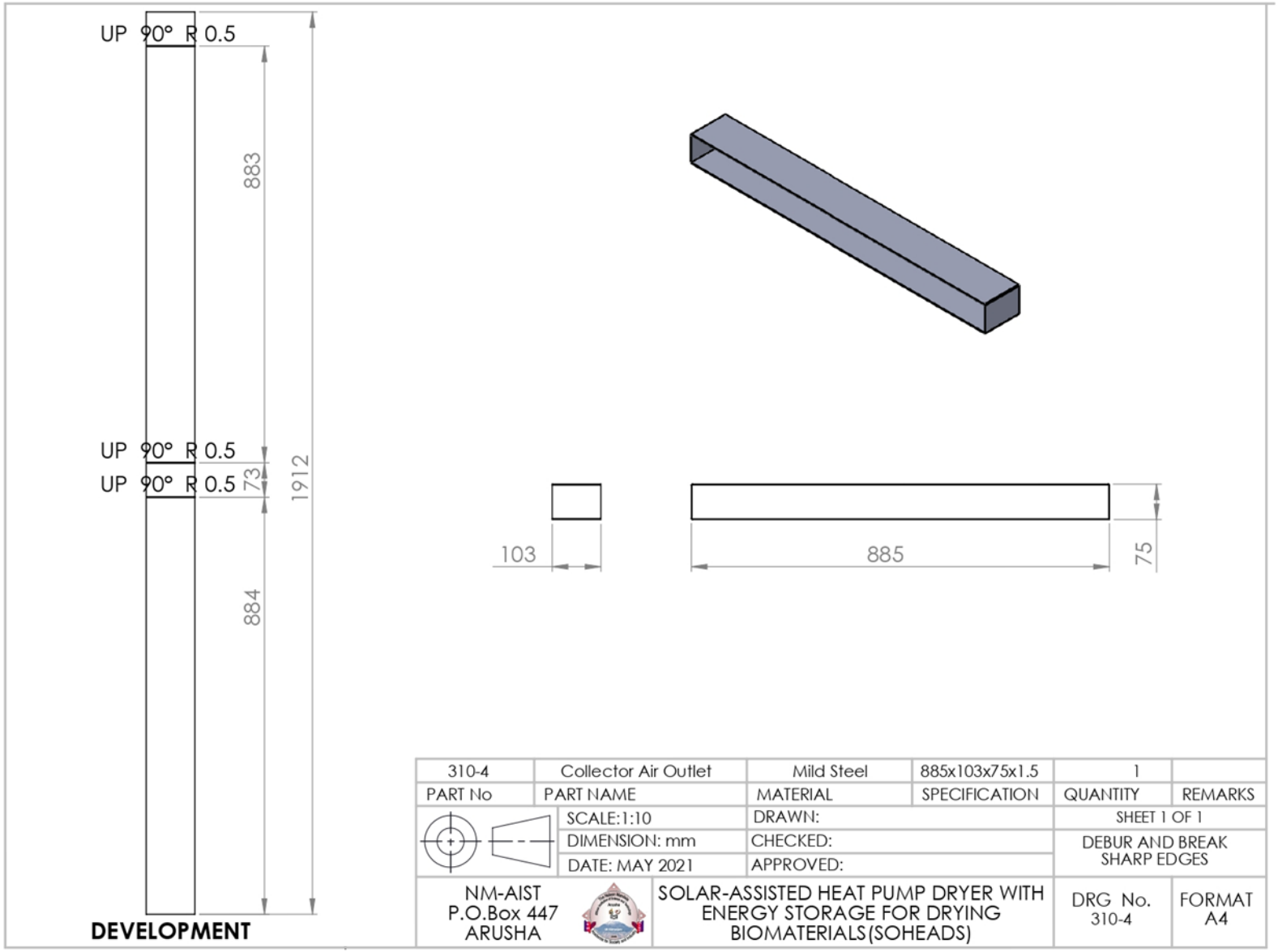

310-4	Collector Air Outlet	Mild Steel	885x103x75x1.5	1	
PART No	PART NAME	MATERIAL	SPECIFICATION	QUANTITY	REMARKS
	SCALE:1:10	DRAWN:		SHEET 1 OF 1	
	DIMENSION: mm	CHECKED:		DEBUR AND BREAK SHARP EDGES	
	DATE: MAY 2021	APPROVED:			
NM-AIST P.O.Box 447 ARUSHA		SOLAR-ASSISTED HEAT PUMP DRYER WITH ENERGY STORAGE FOR DRYING BIOMATERIALS(SOHEADS)		DRG No. 310-4	FORMAT A4

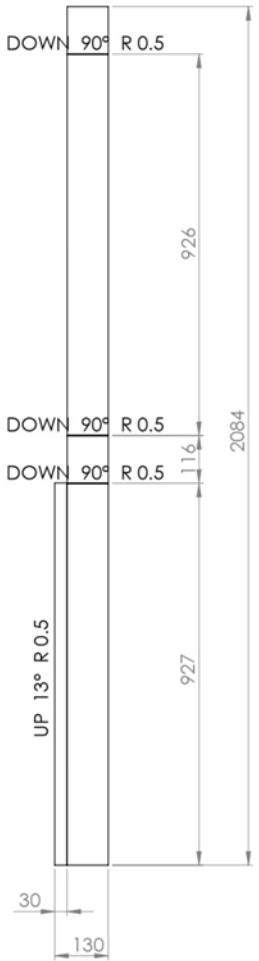

DEVELOPMENT

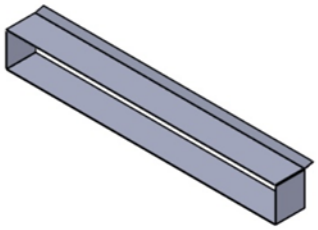

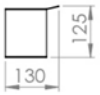

311-3	Collector Air Outlet	Mild Steel	928x130x125x1.5	1	
PART No	PART NAME	MATERIAL	SPECIFICATION	QUANTITY	REMARKS
	SCALE:1:10	DRAWN:		SHEET 1 OF 1	
	DIMENSION: mm	CHECKED:		DEBUR AND BREAK SHARP EDGES	
	DATE: MAY 2021	APPROVED:			
NM-AIST P.O.Box 447 ARUSHA		SOLAR-ASSISTED HEAT PUMP DRYER WITH ENERGY STORAGE FOR DRYING BIOMATERIALS(SOHEADS)		DRG No. 311-3	FORMAT A3

ITEM NO.	PART NUMBER	DESCRIPTION	QTY.
1	300-4	Hollow Section	2
2	301-4	Hollow Section	2
3	302-4	Hollow Section	4
4	304-4	Hollow Section	2
5	303-4	Hollow section	2
6	315-4	Hollow Section End Cap	4

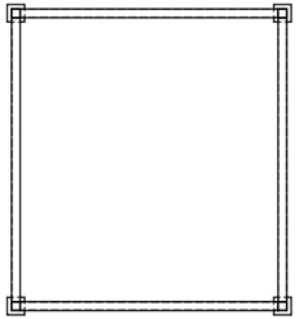

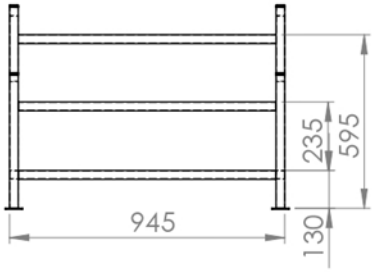

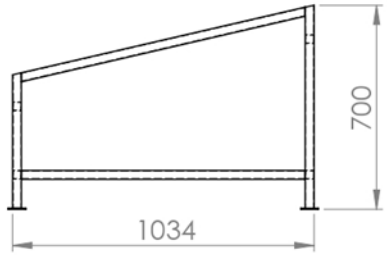

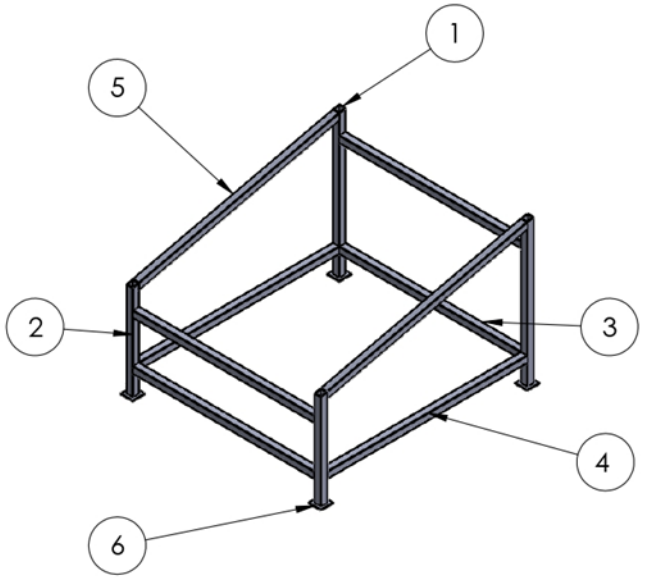

314-4	Solar Collector Frame	Mild Steel	1034x945x700	1	
PART No	PART NAME	MATERIAL	SPECIFICATION	QUANTITY	REMARKS
	SCALE:1:20	DRAWN:		SHEET 1 OF 1	
	DIMENSION: mm	CHECKED:		DEBUR AND BREAK SHARP EDGES	
	DATE: MAY 2021	APPROVED:			
NM-AIST P.O.Box 447 ARUSHA		SOLAR-ASSISTED HEAT PUMP DRYER WITH ENERGY STORAGE FOR DRYING BIOMATERIALS(SOHEADS)		DRG No. 314-4	FORMAT A4

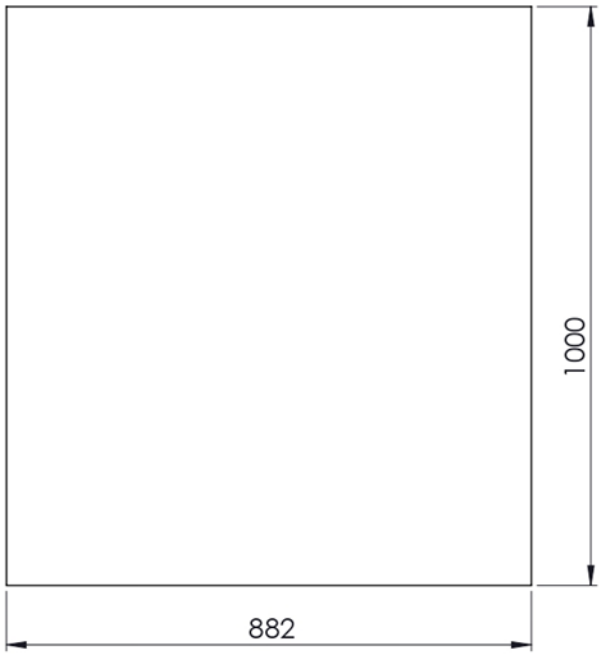

316-4	Granite Chamber Cover	Aluminium	1000 x 882 x 0.8	1	
PART No	PART NAME	MATERIAL	SPECIFICATION	QUANTITY	REMARKS
	SCALE:1:10	DRAWN:		SHEET 1 OF 1	
	DIMENSION: mm	CHECKED:		DEBUR AND BREAK SHARP EDGES	
	DATE: MAY 2021	APPROVED:			
NM-AIST P.O.Box 447 ARUSHA		SOLAR-ASSISTED HEAT PUMP DRYER WITH ENERGY STORAGE FOR DRYING BIOMATERIALS(SOHEADS)		DRG No. 316-4	FORMAT A4

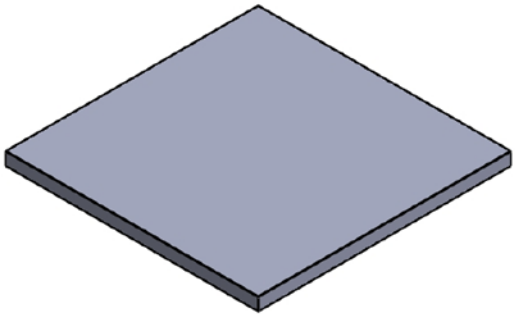

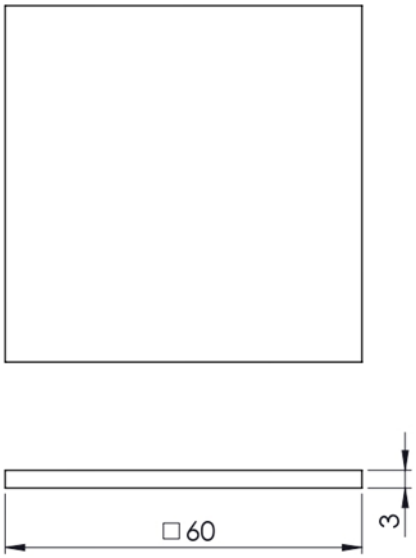

315-4	Hollow Section End Cap	Mild Steel	60 x 60 x 3	10	
PART No	PART NAME	MATERIAL	SPECIFICATION	QUANTITY	REMARKS
	SCALE:1:2	DRAWN:		SHEET 1 OF 1	
	DIMENSION: mm	CHECKED:		DEBUR AND BREAK SHARP EDGES	
	DATE: MAY 2021	APPROVED:			

NM-AIST P.O.Box 447 ARUSHA	SOLAR-ASSISTED HEAT PUMP DRYER WITH ENERGY STORAGE FOR DRYING BIOMATERIALS(SOHEADS)	DRG No. 315-4	FORMAT A4

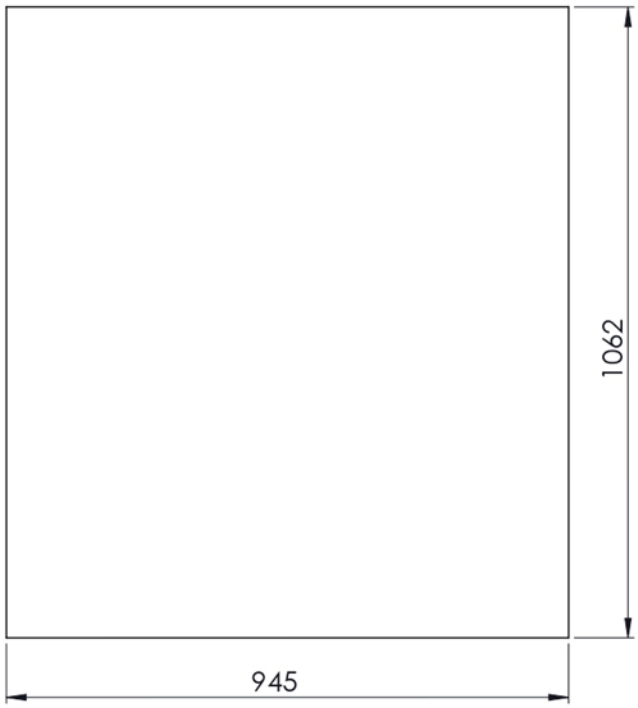

317-4	Collector Glass	Glass	1063 x 945 x 6	1	
PART No	PART NAME	MATERIAL	SPECIFICATION	QUANTITY	REMARKS
	SCALE:1:20	DRAWN:		SHEET 1 OF 1	
	DIMENSION: mm	CHECKED:		DEBUR AND BREAK SHARP EDGES	
	DATE: MAY 2021	APPROVED:			
NM-AIST P.O.Box 447 ARUSHA		SOLAR-ASSISTED HEAT PUMP DRYER WITH ENERGY STORAGE FOR DRYING BIOMATERIALS(SOHEADS)		DRG No. 317-4	FORMAT A4

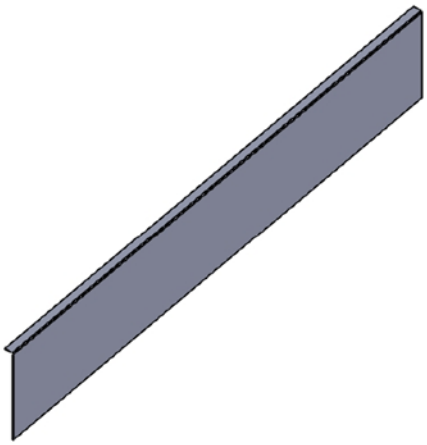

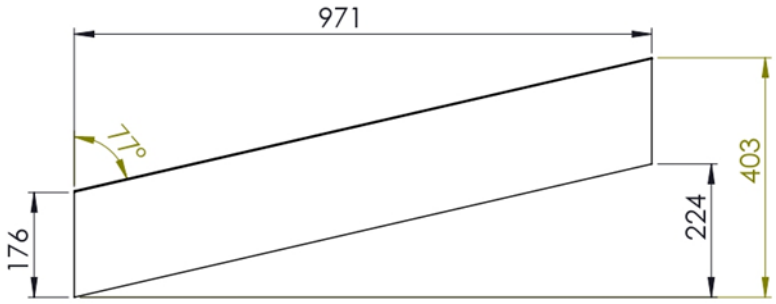

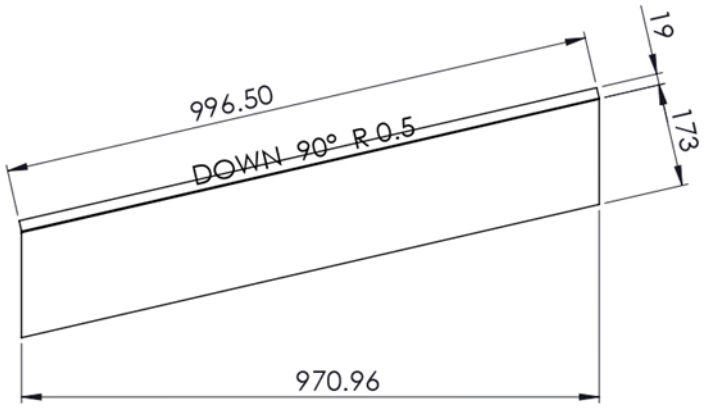

DEVELOPMENT

318-4	Granite Partition Sheet	Mild Steel	971 x 403 x 1.5	2	
PART No	PART NAME	MATERIAL	SPECIFICATION	QUANTITY	REMARKS
	SCALE:1:10	DRAWN:		SHEET 1 OF 1	
	DIMENSION: mm	CHECKED:		DEBUR AND BREAK SHARP EDGES	
	DATE: MAY 2021	APPROVED:			
NM-AIST P.O.Box 447 ARUSHA		SOLAR-ASSISTED HEAT PUMP DRYER WITH ENERGY STORAGE FOR DRYING BIOMATERIALS(SOHEADS)		DRG No. 318-4	FORMAT A4

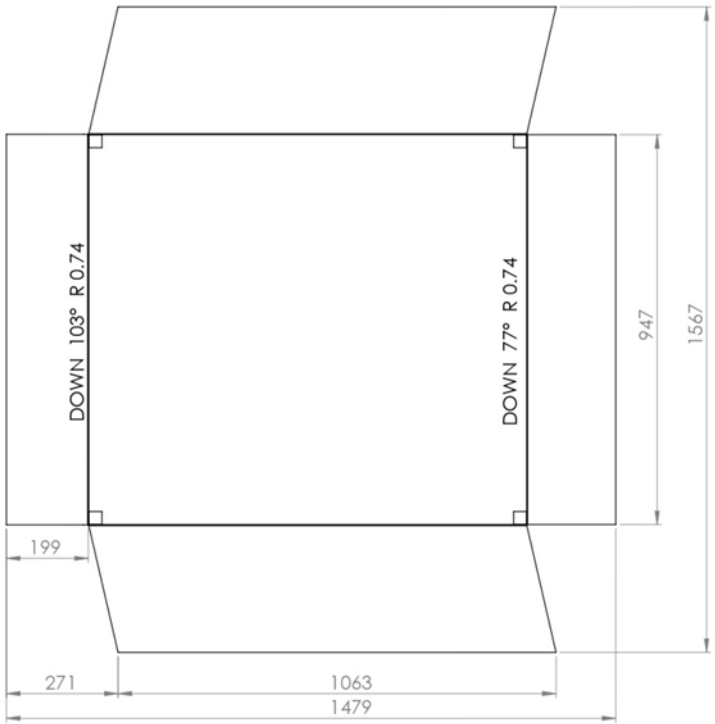

DEVELOPMENT

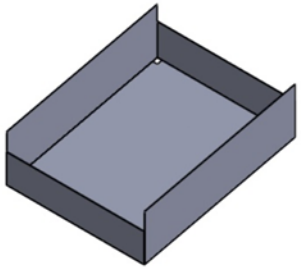

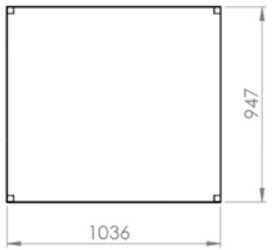

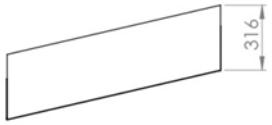

319-3	Collector Outside Sheet	Mild Steel	1036x947x316x1.5	1	
PART No	PART NAME	MATERIAL	SPECIFICATION	QUANTITY	REMARKS
	SCALE:1:20	DRAWN:		SHEET 1 OF 1	
	DIMENSION: mm	CHECKED:		DEBUR AND BREAK SHARP EDGES	
	DATE: MAY 2021	APPROVED:			
NM-AIST P.O.Box 447 ARUSHA		SOLAR-ASSISTED HEAT PUMP DRYER WITH ENERGY STORAGE FOR DRYING BIOMATERIALS(SOHEADS)		DRG No. 319-3	FORMAT A3

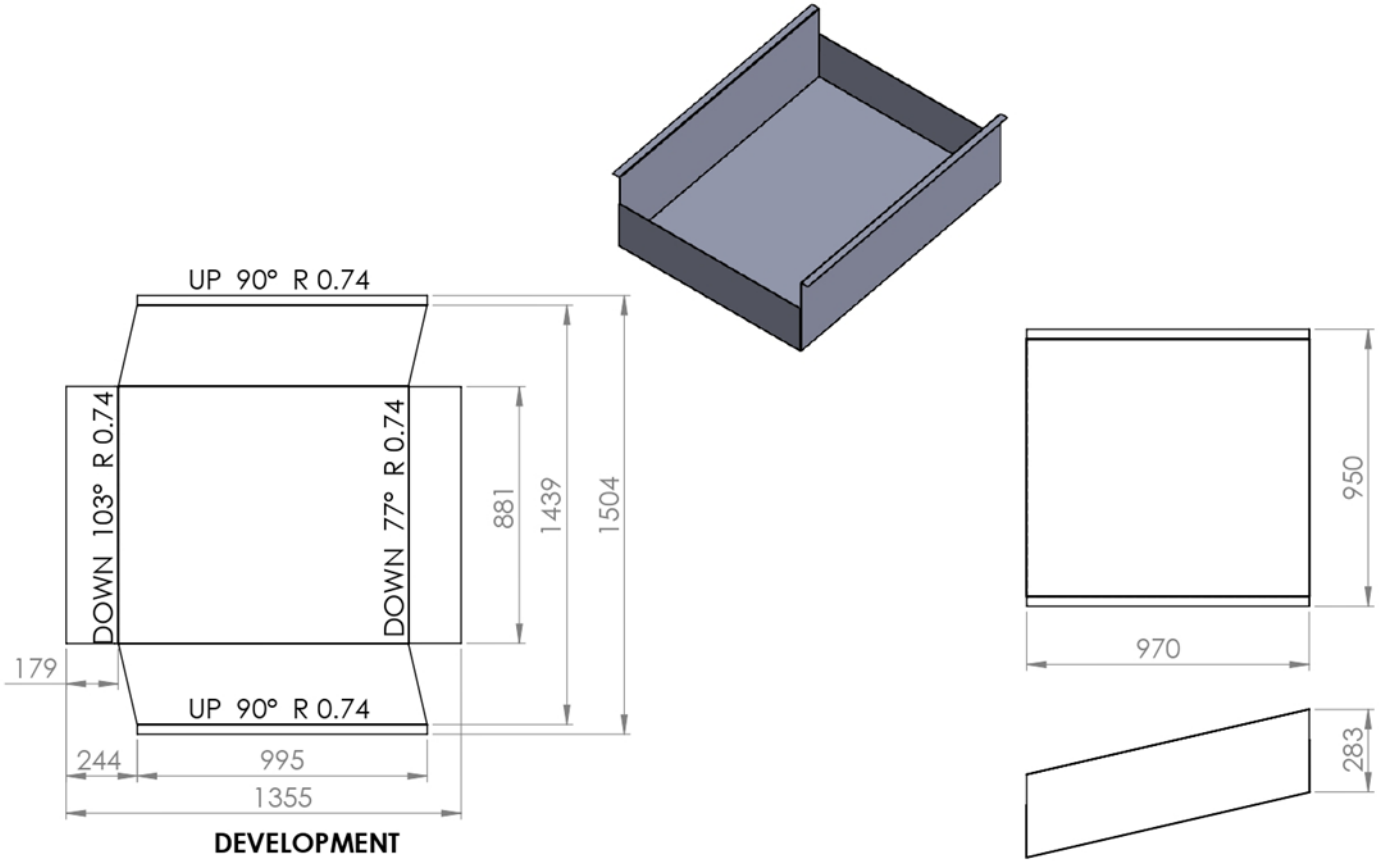

320-4	Collector Inside Sheet	Mild Steel	970x950x283x1.5	1	
PART No	PART NAME	MATERIAL	SPECIFICATION	QUANTITY	REMARKS
	SCALE:1:20	DRAWN:		SHEET 1 OF 1	
	DIMENSION: mm	CHECKED:		DEBUR AND BREAK SHARP EDGES	
	DATE: MAY 2021	APPROVED:			
NM-AIST P.O.Box 447 ARUSHA		SOLAR-ASSISTED HEAT PUMP DRYER WITH ENERGY STORAGE FOR DRYING BIOMATERIALS(SOHEADS)		DRG No. 320-4	FORMAT A4

ITEM NO.	PART NUMBER	DESCRIPTION	QTY.
1	327-4	Connector Outside Assy	1
2	331-4	Connector Inside Assy	1
3	324-4	Fibre Insulation	1
4	335-4	Connector Flange	1
5	167-4	Chamber Base Flange	1

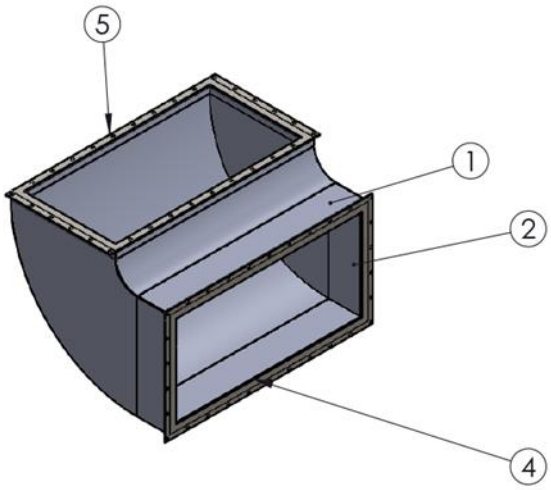

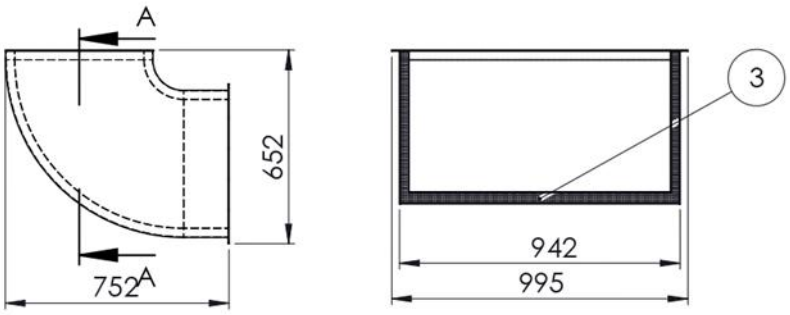

SECTION A-A

323-4	Connector Assy		995 x 772 x 625	1	
PART No	PART NAME	MATERIAL	SPECIFICATION	QUANTITY	REMARKS
	SCALE:1:20	DRAWN:		SHEET 1 OF 1	
	DIMENSION: mm	CHECKED:		DEBUR AND BREAK SHARP EDGES	
	DATE: MAY 2021	APPROVED:			
NM-AIST P.O.Box 447 ARUSHA		SOLAR-ASSISTED HEAT PUMP DRYER WITH ENERGY STORAGE FOR DRYING BIOMATERIALS(SOHEADS)		DRG No. 323-4	FORMAT A4

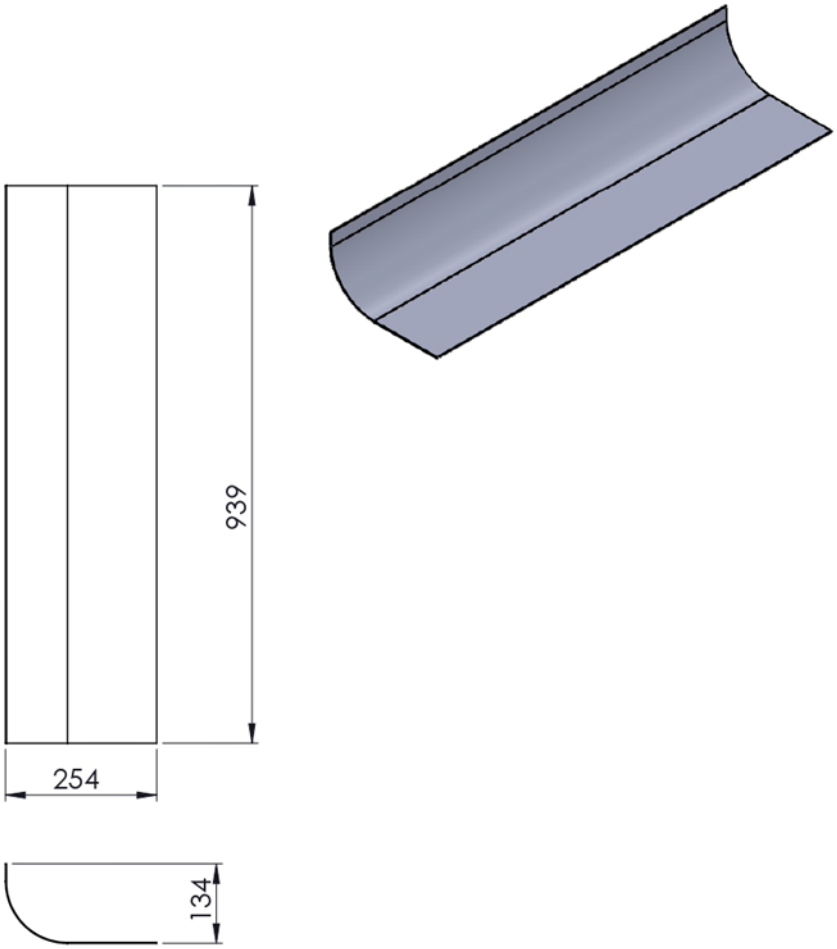

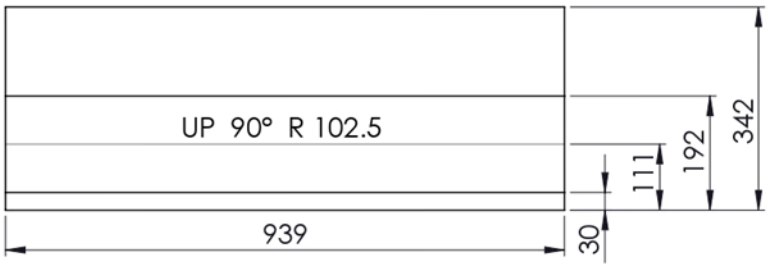

DEVELOPMENT

328-4	Connector Outside Sheet	Mild Steel	939x254x134x1.5	1	
PART No	PART NAME	MATERIAL	SPECIFICATION	QUANTITY	REMARKS
	SCALE:1:10	DRAWN:		SHEET 1 OF 1	
	DIMENSION: mm	CHECKED:		DEBUR AND BREAK SHARP EDGES	
	DATE: MAY 2021	APPROVED:			
NM-AIST P.O.Box 447 ARUSHA		SOLAR-ASSISTED HEAT PUMP DRYER WITH ENERGY STORAGE FOR DRYING BIOMATERIALS(SOHEADS)		DRG No. 328-4	FORMAT A4

ITEM NO.	PART NUMBER	DESCRIPTION	QTY.
1	330-4	Connector Outside Sheet	2
2	328-4	Connector Outside Sheet	1
3	329-4	Connector Outside Sheet	1

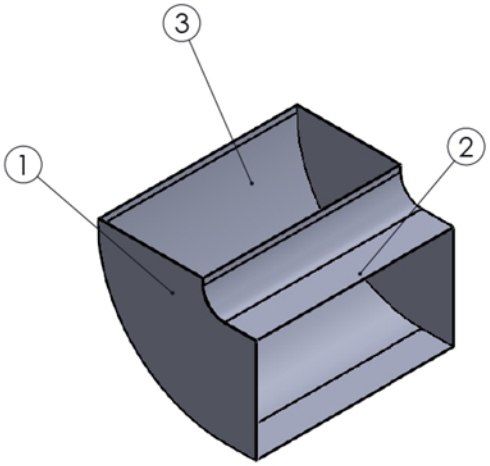

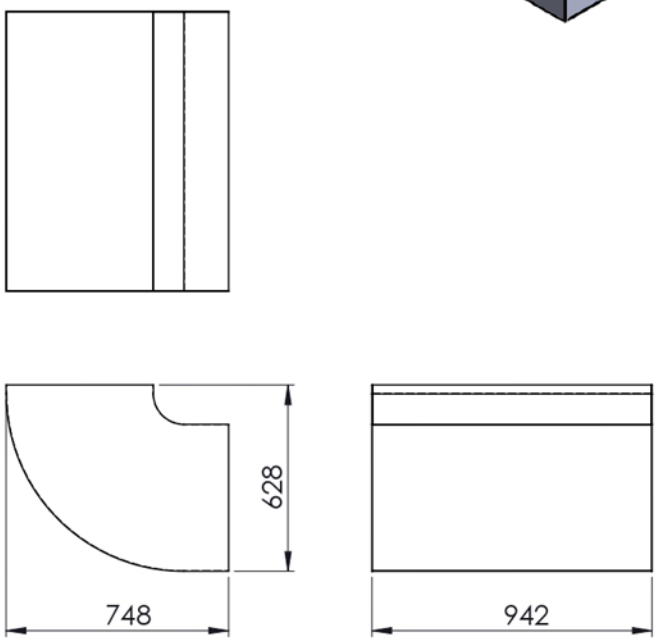

327-4	Connector Outside Assy	Mild Steel	942x748x628x1.5	1	
PART No	PART NAME	MATERIAL	SPECIFICATION	QUANTITY	REMARKS
	SCALE:1:20	DRAWN:		SHEET 1 OF 1	
	DIMENSION: mm	CHECKED:		DEBUR AND BREAK SHARP EDGES	
	DATE: MAY 2021	APPROVED:			

NM-AIST P.O.Box 447 ARUSHA	SOLAR-ASSISTED HEAT PUMP DRYER WITH ENERGY STORAGE FOR DRYING BIOMATERIALS(SOHEADS)	DRG No. 327-4	FORMAT A4

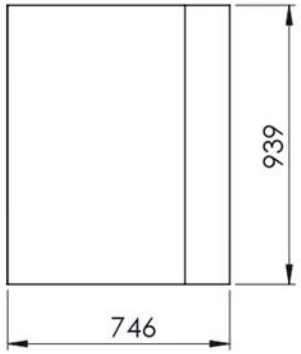

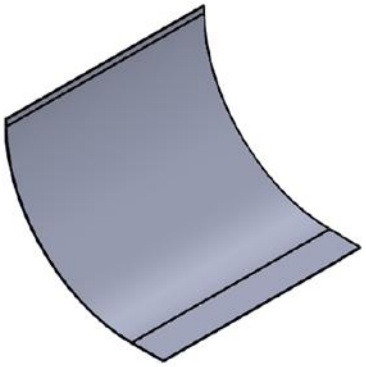

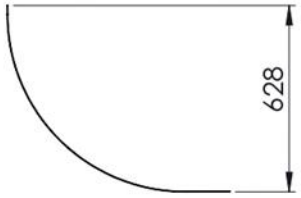

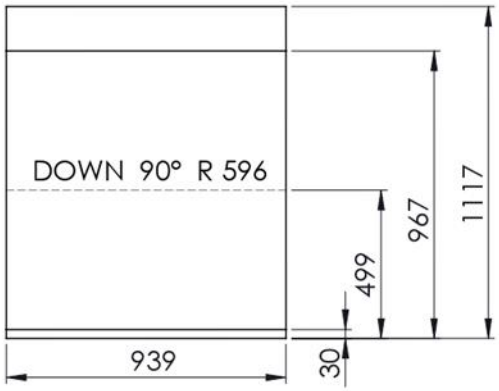

DEVELOPMENT

329-4	Connector Outside Sheet	Mild Steel	939x746x628x1.5	1	
PART No	PART NAME	MATERIAL	SPECIFICATION	QUANTITY	REMARKS
	SCALE:1:20	DRAWN:		SHEET 1 OF 1	
	DIMENSION: mm	CHECKED:		DEBUR AND BREAK SHARP EDGES	
	DATE: MAY 2021	APPROVED:			
NM-AIST P.O.Box 447 ARUSHA		SOLAR-ASSISTED HEAT PUMP DRYER WITH ENERGY STORAGE FOR DRYING BIOMATERIALS(SOHEADS)		DRG No. 329-4	FORMAT A4

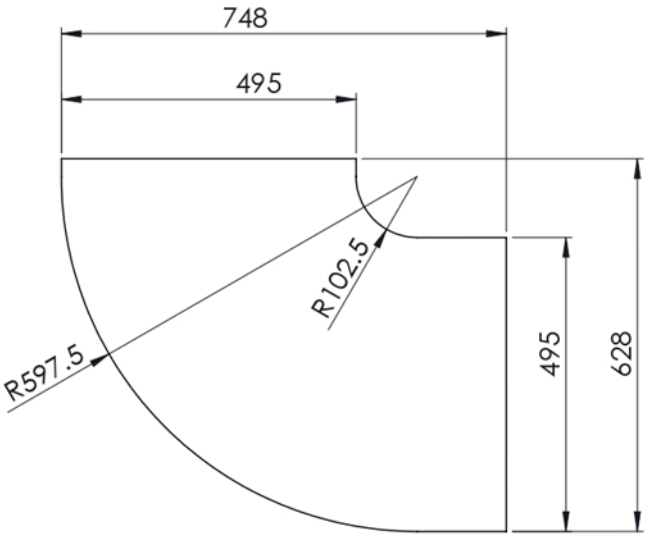

330-4	Connector Outside Sheet	Mild Steel	748 x 628 x 1.5	2	
PART No	PART NAME	MATERIAL	SPECIFICATION	QUANTITY	REMARKS
	SCALE:1:10	DRAWN:		SHEET 1 OF 1	
	DIMENSION: mm	CHECKED:		DEBUR AND BREAK SHARP EDGES	
	DATE: MAY 2021	APPROVED:			

NM-AIST P.O.Box 447 ARUSHA	SOLAR-ASSISTED HEAT PUMP DRYER WITH ENERGY STORAGE FOR DRYING BIOMATERIALS(SOHEADS)	DRG No. 330-4	FORMAT A4

ITEM NO.	PART NUMBER	DESCRIPTION	QTY.
1	332-4	Connector Inside Sheet	1
2	334-4	Connector Inside Sheet	2
3	333-4	Connector Inside Sheet	1

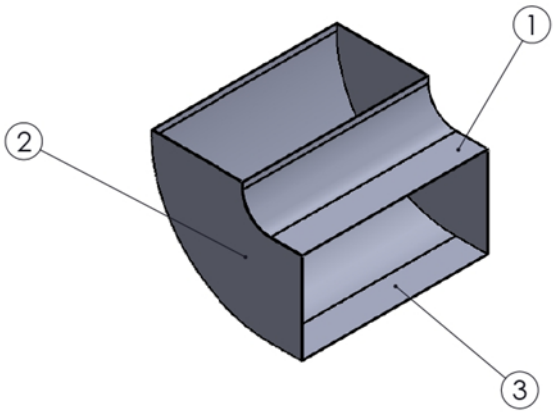

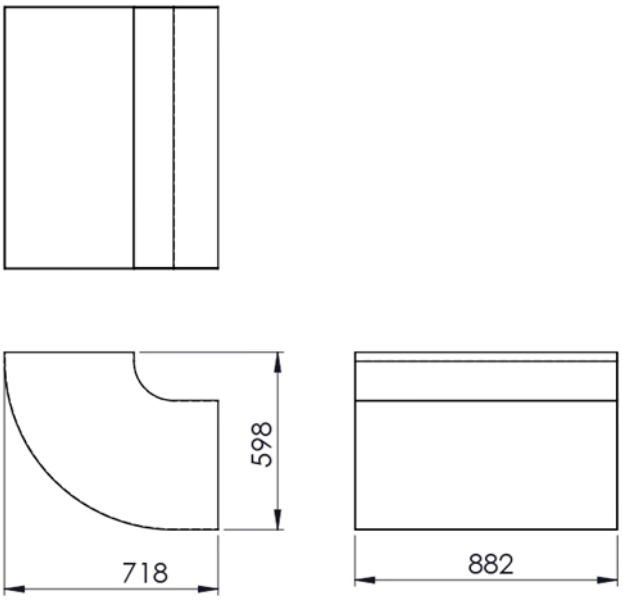

331-4	Connector Inside Assy	Mild Steel	882x718x598x1.5	1	
PART No	PART NAME	MATERIAL	SPECIFICATION	QUANTITY	REMARKS
	SCALE:1:20	DRAWN:		SHEET 1 OF 1	
	DIMENSION: mm	CHECKED:		DEBUR AND BREAK SHARP EDGES	
	DATE: MAY 2021	APPROVED:			
NM-AIST P.O.Box 447 ARUSHA		SOLAR-ASSISTED HEAT PUMP DRYER WITH ENERGY STORAGE FOR DRYING BIOMATERIALS(SOHEADS)		DRG No. 331-4	FORMAT A4

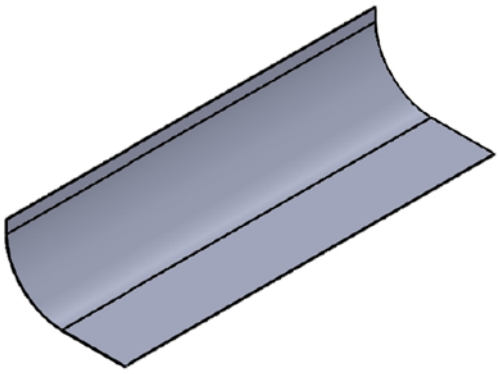

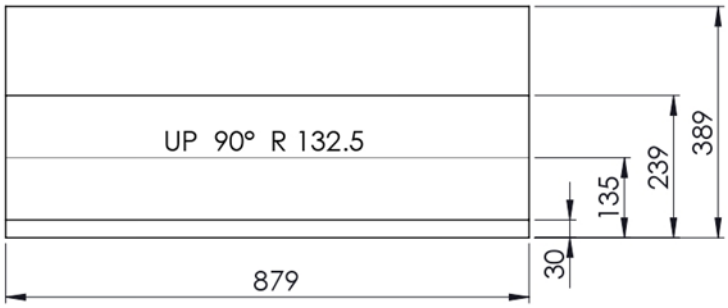

DEVELOPMENT

332-4	Connector Inside Sheet	Mild Steel	879x284x164x1.5	1	
PART No	PART NAME	MATERIAL	SPECIFICATION	QUANTITY	REMARKS
	SCALE:1:10	DRAWN:		SHEET 1 OF 1	
	DIMENSION: mm	CHECKED:		DEBUR AND BREAK SHARP EDGES	
	DATE: MAY 2021	APPROVED:			
NM-AIST P.O.Box 447 ARUSHA		SOLAR-ASSISTED HEAT PUMP DRYER WITH ENERGY STORAGE FOR DRYING BIOMATERIALS(SOHEADS)		DRG No. 332-4	FORMAT A4

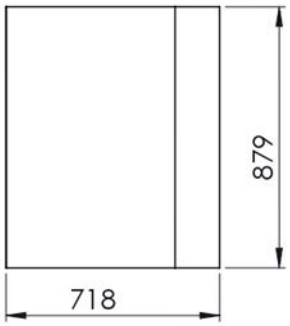

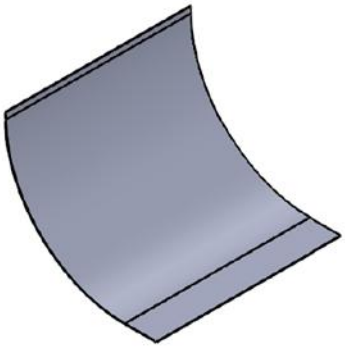

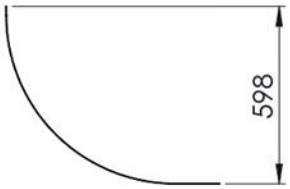

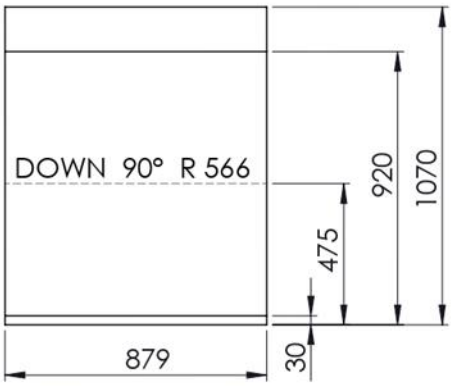

DEVELOPMENT

333-4	Connector Inside Sheet	Mild Steel	879x718x598x1.5	1	
PART No	PART NAME	MATERIAL	SPECIFICATION	QUANTITY	REMARKS
	SCALE:1:20	DRAWN:		SHEET 1 OF 1	
	DIMENSION: mm	CHECKED:		DEBUR AND BREAK SHARP EDGES	
	DATE: MAY 2021	APPROVED:			
NM-AIST P.O.Box 447 ARUSHA		SOLAR-ASSISTED HEAT PUMP DRYER WITH ENERGY STORAGE FOR DRYING BIOMATERIALS(SOHEADS)		DRG No. 333-4	FORMAT A4

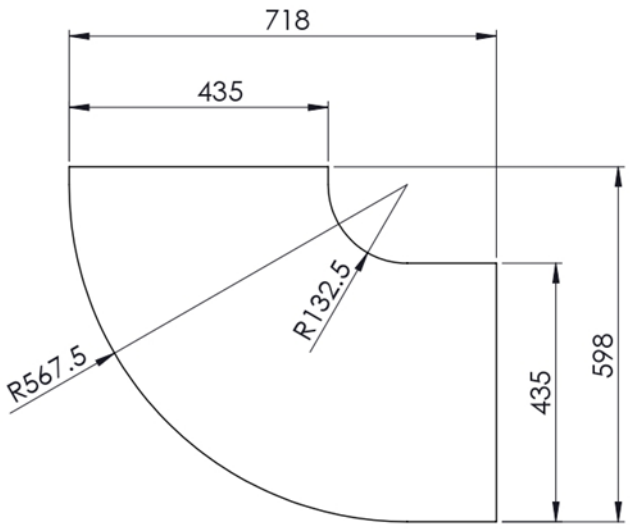

334-4	Connector Inside Sheet	Mild Steel	718 x 598 x 1.5	2	
PART No	PART NAME	MATERIAL	SPECIFICATION	QUANTITY	REMARKS
	SCALE:1:10	DRAWN:		SHEET 1 OF 1	
	DIMENSION: mm	CHECKED:		DEBUR AND BREAK SHARP EDGES	
	DATE: MAY 2021	APPROVED:			

NM-AIST P.O.Box 447 ARUSHA	SOLAR-ASSISTED HEAT PUMP DRYER WITH ENERGY STORAGE FOR DRYING BIOMATERIALS(SOHEADS)	DRG No. 334-4	FORMAT A4

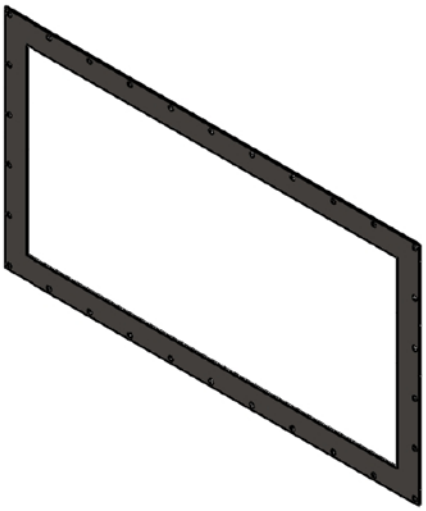

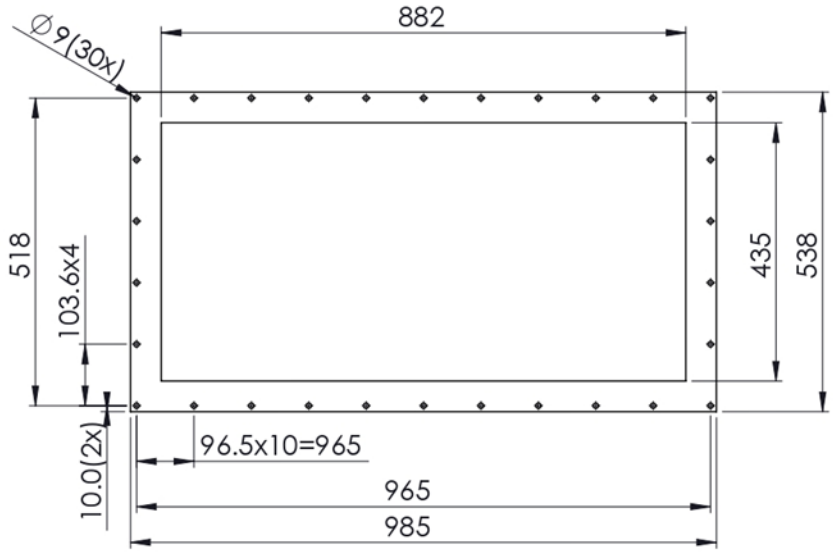

335-4	Connector Flange	Mild Steel Sheet	985 x 538 x 3	3	
PART No	PART NAME	MATERIAL	SPECIFICATION	QUANTITY	REMARKS
	SCALE:1:10	DRAWN:		SHEET 1 OF 1	
	DIMENSION: mm	CHECKED:		DEBUR AND BREAK SHARP EDGES	
	DATE: MAY 2021	APPROVED:			
NM-AIST P.O.Box 447 ARUSHA		SOLAR-ASSISTED HEAT PUMP DRYER WITH ENERGY STORAGE FOR DRYING BIOMATERIALS(SOHEADS)		DRG No. 335-4	FORMAT A4

ITEM NO.	PART NUMBER	DESCRIPTION	QTY.
1	343-4	Door Frame	1
2	341-4	Door Sheet	2
3	342-4	Fibre Insulaton	1

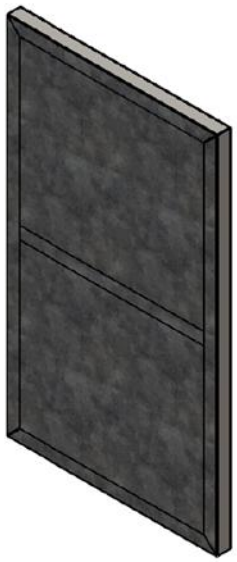

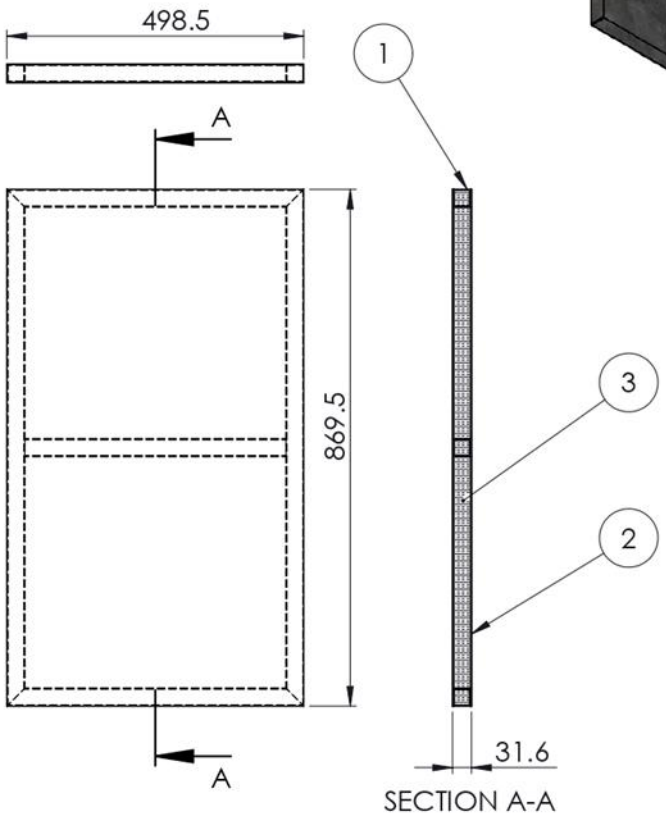

SECTION A-A

340-4	Feeding Door Assy		869.5x498.5x31.6	2	
PART No	PART NAME	MATERIAL	SPECIFICATION	QUANTITY	REMARKS
	SCALE:1:10	DRAWN:		SHEET 1 OF 1	
	DIMENSION: mm	CHECKED:		DEBUR AND BREAK SHARP EDGES	
	DATE: MAY 2021	APPROVED:			

NM-AIST P.O.Box 447 ARUSHA	SOLAR-ASSISTED HEAT PUMP DRYER WITH ENERGY STORAGE FOR DRYING BIOMATERIALS(SOHEADS)	DRG No. 340-4	FORMAT A4

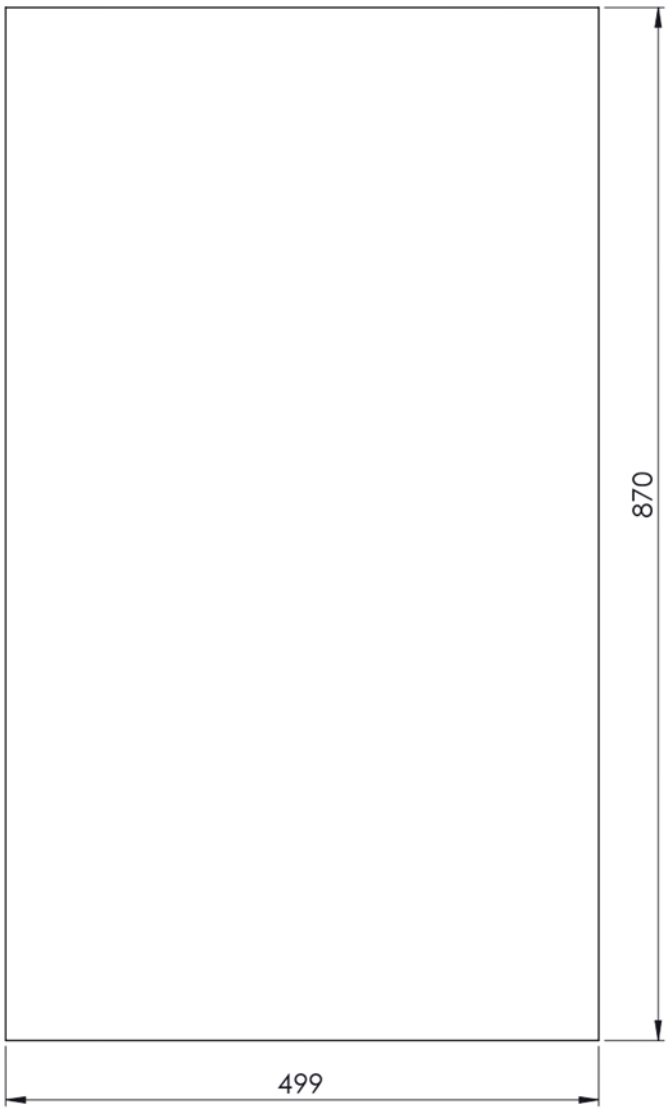

341-4	Door Sheet	Galvanised Sheet	870x499x0.8	2	
PART No	PART NAME	MATERIAL	SPECIFICATION	QUANTITY	REMARKS
	SCALE:1:5	DRAWN:		SHEET 1 OF 1	
	DIMENSION: mm	CHECKED:		DEBUR AND BREAK SHARP EDGES	
	DATE: MAY 2021	APPROVED:			
NM-AIST P.O.Box 447 ARUSHA		SOLAR-ASSISTED HEAT PUMP DRYER WITH ENERGY STORAGE FOR DRYING BIOMATERIALS(SOHEADS)		DRG No. 341-4	FORMAT A4

ITEM NO.	PART NUMBER	DESCRIPTION	QTY.
1	344-4	Hollow Section	2
2	345-4	Hollow Section	2
3	346-4	Hollow Section	1

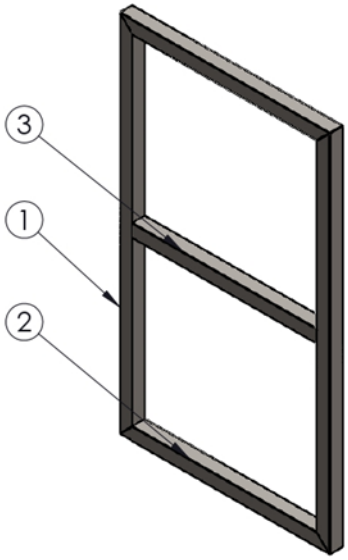

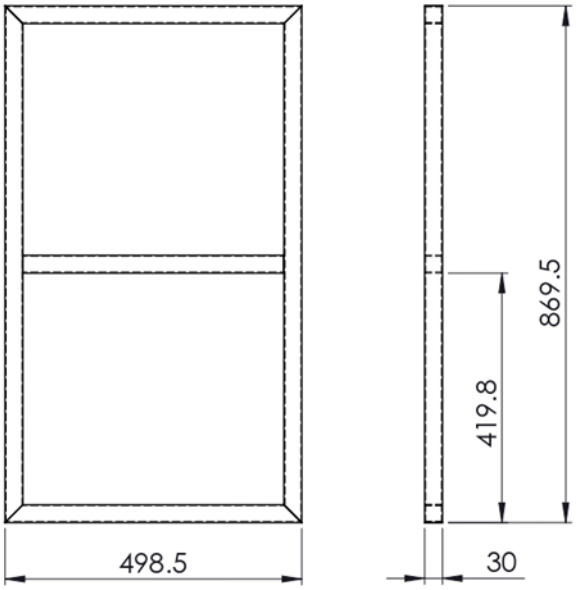

343-4	Door Frame	Mild Steel	869.5x498.5x30	2	
PART No	PART NAME	MATERIAL	SPECIFICATION	QUANTITY	REMARKS
	SCALE:1:10	DRAWN:		SHEET 1 OF 1	
	DIMENSION: mm	CHECKED:		DEBUR AND BREAK SHARP EDGES	
	DATE: MAY 2021	APPROVED:			
NM-AIST P.O.Box 447 ARUSHA		SOLAR-ASSISTED HEAT PUMP DRYER WITH ENERGY STORAGE FOR DRYING BIOMATERIALS(SOHEADS)		DRG No. 343-4	FORMAT A4

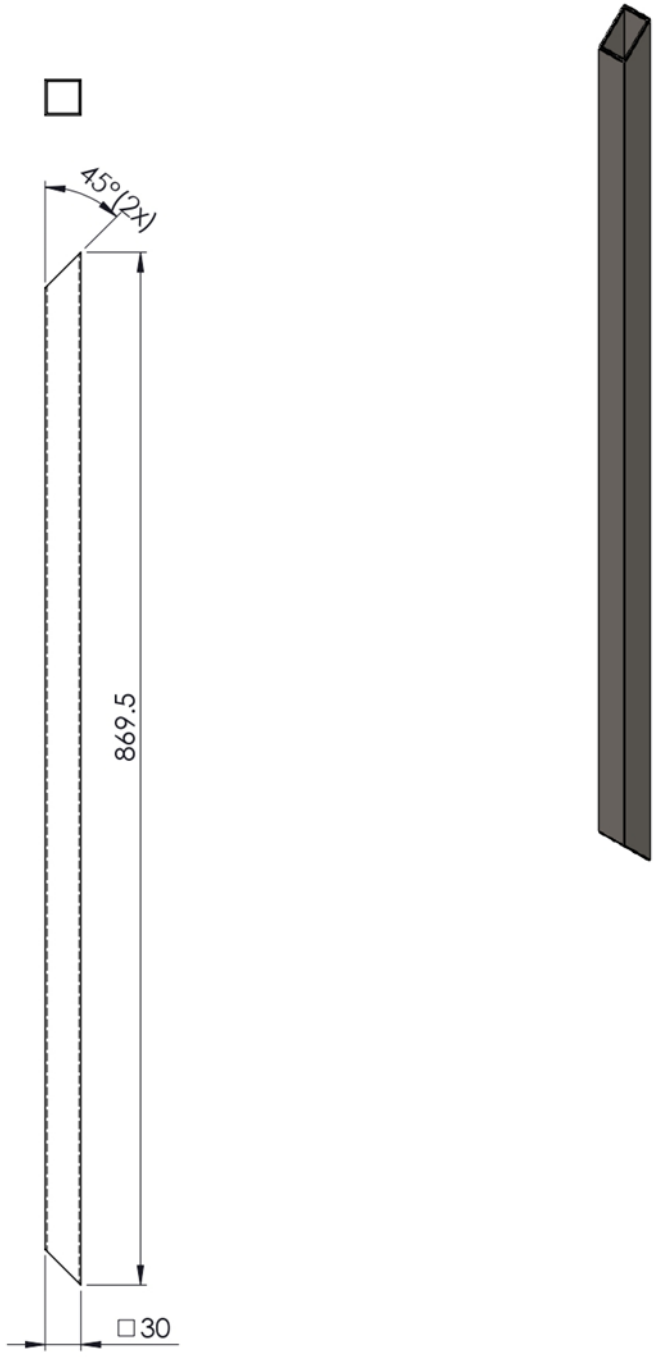

344-4	Hollow Section	Mild steel	30x30x1.5x869.5	2	
PART No	PART NAME	MATERIAL	SPECIFICATION	QUANTITY	REMARKS
	SCALE:1:5	DRAWN:		SHEET 1 OF 1	
	DIMENSION: mm	CHECKED:		DEBUR AND BREAK SHARP EDGES	
	DATE: MAY 2021	APPROVED:			
NM-AIST P.O.Box 447 ARUSHA		SOLAR-ASSISTED HEAT PUMP DRYER WITH ENERGY STORAGE FOR DRYING BIOMATERIALS(SOHEADS)		DRG No. 344-4	FORMAT A4

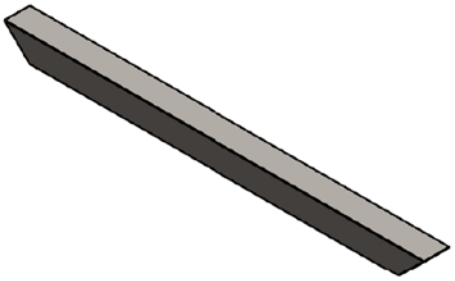

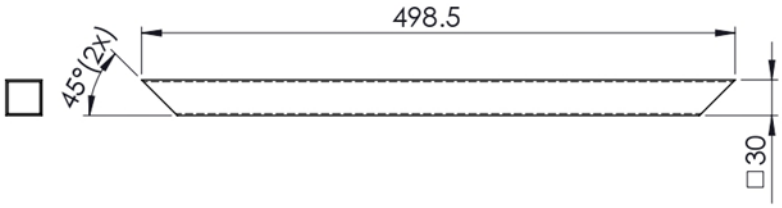

345-4	Hollow Section	Mild Steel	30x30x1.5x498.5	2	
PART No	PART NAME	MATERIAL	SPECIFICATION	QUANTITY	REMARKS
	SCALE:1:5	DRAWN:		SHEET 1 OF 1	
	DIMENSION: mm	CHECKED:		DEBUR AND BREAK SHARP EDGES	
	DATE: MAY 2021	APPROVED:			
NM-AIST P.O.Box 447 ARUSHA		SOLAR-ASSISTED HEAT PUMP DRYER WITH ENERGY STORAGE FOR DRYING BIOMATERIALS(SOHEADS)		DRG No. 345-4	FORMAT A4

RESEARCH OUTPUTS

(i) Published papers

Loemba, A. B., Kichonge, B., & Kivevele, T. (2023). Comprehensive assessment of heat pump dryers for drying agricultural products. *Energy Science & Engineering*, *11*(8), 2985-3014.

Loemba, A. B. T., Kichonge, B., & Kivevele, T. (2024). Thermal Performance and Technoeconomic Analysis of Solar-Assisted Heat Pump Dryer Integrated with Energy Storage Materials for Drying Cavendish Banana (Musa acuminata). *Journal of Food Processing and Preservation*, *2024*(1), 7496826.

Loemba, A. B. T., Kichonge, B., Selemani, J. R., & Kivevele, T. (2023). Performance evaluation of solar-assisted heat pump dryer integrated with thermal energy storage for drying Moringa oleifera leaves. *MRS Advances*, *8*(12), 698-702.

Aldé Belgard Tchicaya Loemba, Baraka Kichonge, Thomas Kivevele, Life cycle assessment and experimental investigation of a solar-assisted heat pump dryer integrated with thermal energy storage (*to be submitted soon*)

(ii) Patent

Patent number: TZ/P/2023/000093 Solar Assisted Heat Pump Dryer with Thermal Energy Storage, TANZANIA, https://ors.brela.go.tz/ors/searchjournalpublic

(iii) Conference attended

The 11th International Conference of the African Materials Research Society (AMRS2022), Université Cheikh Anta Diop, Dakar, Senegal 12-15 December 2022.